SYNTHESIS, ANALYSIS AND BIOLOGICAL EVALUATION OF NOVEL INDOLOQUINOLINE CRYPTOLEPINE ANALOGUES AS POTENTIAL ANTITUMOUR AGENTS

THESIS
SUBMITTED FOR THE DEGREE OF
DOCTOR OF PHILOSOPHY

BY

VENKATESWARA RAO GUDIVAKA

School of Pharmacy and Chemistry
Kingston University

JULY 2014

ALL MISSING PAGES ARE BLANK IN THE ORIGINAL

I dedicate this doctoral thesis to my parents

Seshagiri Rao Gudivaka and Varalakshmi Gudivaka

and my brother Sivanagaraju Gudivaka

Contents

Acknowledgements

I would like to thank my supervisors: Dr. Simon Carrington, Prof. John E Brown, Prof. Andy Jewell and Dr. Adam Le Gresley for giving me such a great opportunity to work under the excellent guidance provided by them. I am deeply grateful for their continuous share of skills. This work has really benefited by greatly detailed and perceptive reviews provided by them.

I should thank Dr. Jean-Marie Peron who was always helpful in using the NMR fecility.

A special thanks goes to Julian Swinden for his help with mass spectrometry

I would like to extend a special appreciation to the students and research community of School of Pharmacy and Chemistry, for their continuous support in the lab.

I would also like express my sincere thanks to BPSRG, Kingston University for the financial support.

Abstract

This project investigated the development of novel anticancer agents with good efficacy and selectivity. Cryptolepine is an alkaloid found in the roots of West African climbing shrub species including *Cryptolepis triangularis and Cryptolepis sanguinolenta*. Cryptolepine is 5-methyl-10*H*-indolo [3, 2-b]quinolone, and was first identified as an antimalarial agent, but also acts as an anti-cancer agent by intercalating into DNA and also inhibiting topoisomerase II and other key enzymes. Studies elsewhere have shown the mode of action of cryptolepine *in vitro* appears to be unaffected by drug resistance mechanisms identified. In this project a number Cryptolepine analogues have been made, modifying key positions in order to enhance DNA binding. The aim of this study was to attach halogens (F, Cl, Br and I) and alkyl amino or amido side chains at the 11-position and then test these molecules for anticancer activity. It was anticipated that these nitrogen containing side chains might interact with the sugar-phosphate backbone of DNA to give improved binding and hence interfering with topoisomerase II and related enzymes such as helicase and hence enhancing cytotoxicity. Fluorescence microscopy was used to investigate whether the derivatives reach the cell nucleus.

In conclusion, these studies have shown that novel amino- and halogenated cryptolepine analogues have greater *in vitro* cytotoxicity than the parent compound and are important lead compounds in the development of novel potent and selective indoloquinone anti-neoplastic agents.

Abbreviations

DNA	Deoxyribonucleic acid
DHFR	Dihydrofolate reductase
Å	Angstrom
^{1}H NMR	Proton nuclear magnetic resonance
ATP	Adenosine triphosphate
pK_a	Ionisation Constant
THF	Tetrahydrofuran
MeOTf	Methyl triflate
XANTPHOS	9,9-dimethyl-4,5-bis(diphenylphosphino-9*H*-xanthene
DBA	Dibenzylidene acetone
DMA	Dimethyl amine
Hrs	Hours
Min	Minutes
RT	Room temperature
ppm	Parts per million
TLC	Thin layer chromatography
R_f	Rentention factor
^{13}C NMR	Carbon NMR
IR	Infrared
MS	Mass spectra
v/v	Volume to volume
NOE	Nuclear Overhauser Effect
FAB	Fast atom bombardment
λ_{max}	Wavelength where maximum absorption occurs

UV	Ultraviolet
CT-DNA	Calf thymus deoxyribonucleic acid
Tris-HCl	Tris(hydroxymethyl)aminomethane hydrochloride
EDTA	Ethylenediaminetetraacetic acid
K_a	Affinity constant of a drug
T_m	Melting temperature
ΔT_m	Change in melting temperature
KDNA	Kinetoplast deoxyribonucleic acid
MIC	Minimun inhibition concentration
MTT	3-(4,5-Dimethylthiazol-2-yl)-2,5-diphenyltetrazolium bromide
PBS	Phosphate buffered saline
DMEM	Dulbecco's modified eagle's medium
RPMI	Roswell park memorial institute
FBS	Foetal bovine serum
IC_{50}	Measure of the extent a particular drug inhibits a biological process by half
mp	Melting point
DCM	Dichloromethane
DMSO	Dimethylsulfoxide
δ	Chemical shift
ν	Wave number
CD_3OD	Deutrated methanol
$CDCl_3$	Deutrated chloroform
RT	Reaction time

Chapter 1 Introduction

1.1 Cancer

Cancer is a widespread disease occurring throughout the world causing millions to die. According to recent cancer statistical reports, to date more than 200 different types of cancer have been identified along with disease specific causes, symptoms and therapies.

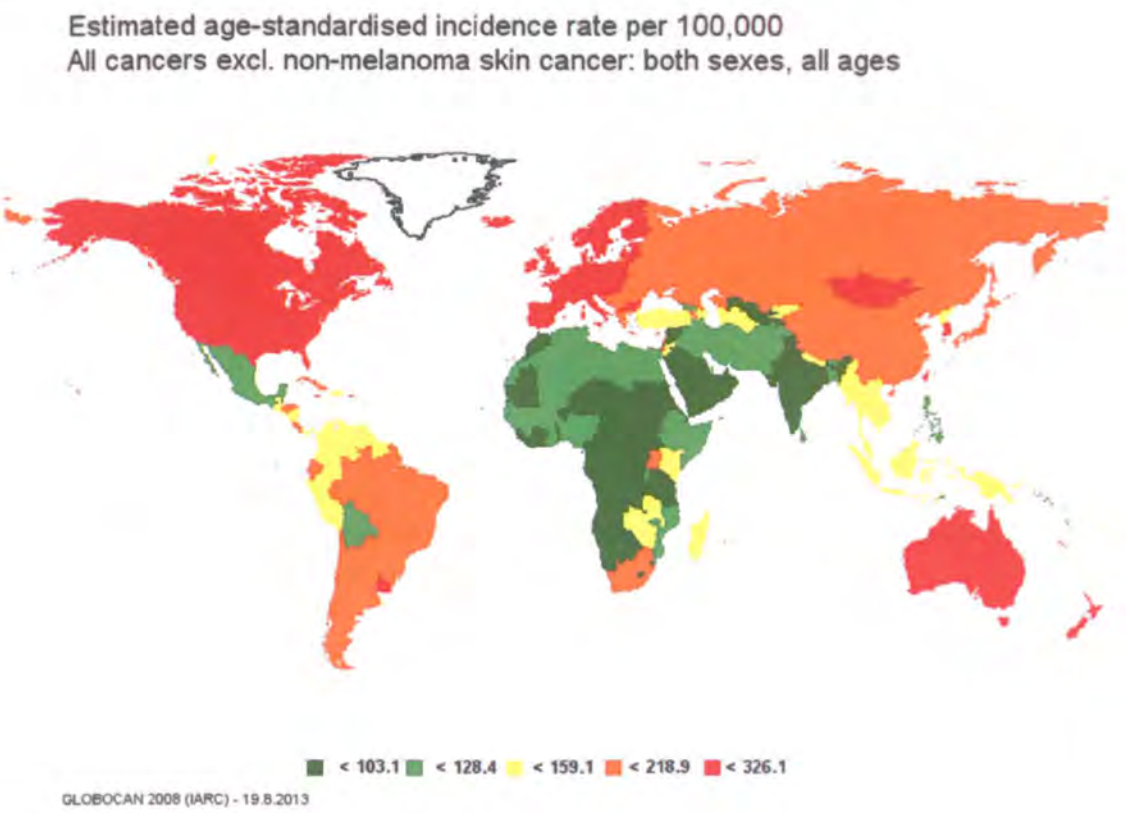

Figure 1.1 Cancer incidence in men and women worldwide (The International Agency for Research on Cancer GLOBOCAN, 2008)

According to the International Agency for Research on Cancer, the incidence is higher in developed countries including the UK, USA, and Australia than in

developing countries for example the Indian subcontinent and in Africa (Figure 1.1) (The International Agency for Research on Cancer GLOBOCAN, 2008).When it comes to overall number of cancer deaths, it is higher in developed countries. Across the world more men die than women (Figure 1.2).

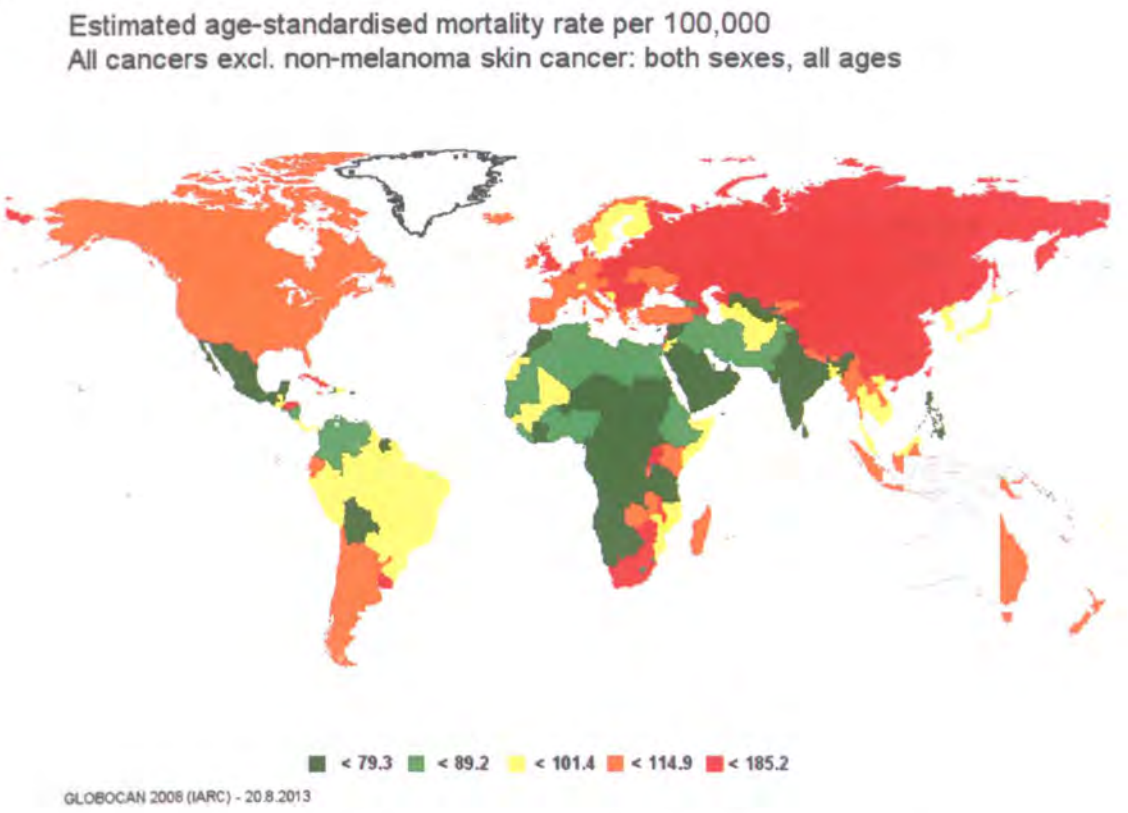

Figure 1.2 Death rates from cancer per 100,000 population worldwide, sex: both men and women, (The International Agency for Research on Cancer GLOBOCAN, 2008)

According to the WHO, in 2008, 7.6 million people died of cancer which is 13% of all deaths worldwide. Cancer deaths are likely to continue increasing with an estimate of 13.1 million worldwide by 2030. 70% of all cancer deaths worldwide are from economically poor countries.

In the UK, 156 000 cancer deaths were recorded in 2008 rising to 157 275 in 2010. These account for one in four of all deaths (Cancer Research UK statistical reports, 2008 and 2010). According to Cancer Research UK, males

are more prone to developing cancer than females and men are 37% more likely to die from the disease. Recent data shows that a new-born male's life time risk of cancer is expected to reach 50% by the year 2027, whereas for females it is expected to be only 40-44%. Of particular note, data from May 2014 shows that over the past 35 years, incidence of prostate cancer has tripled in the UK (Cancer research UK, May 2014). In females more deaths are occurring from breast, lung and colorectal cancer (Figure 1.3).

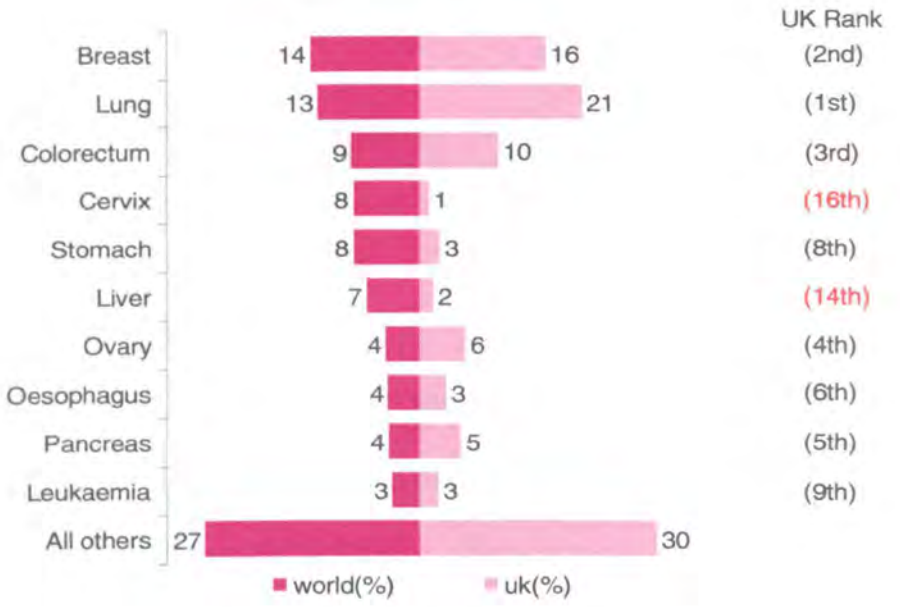

Figure 1.3 The top most common female cancer deaths worldwide compared to UK (The International Agency for Research on Cancer GLOBOCAN, 2008)

Whereas men are more prone to die from lung, liver and stomach cancer (Figure 1.4) (The International Agency for Research on Cancer GLOBOCAN, 2008). Interestingly, because of recent advancements in cancer therapies and treatment options, the total number of deaths from cancer are likely to fall by 17% by 2030 (Cancer Research UK statistical reports, 2012).

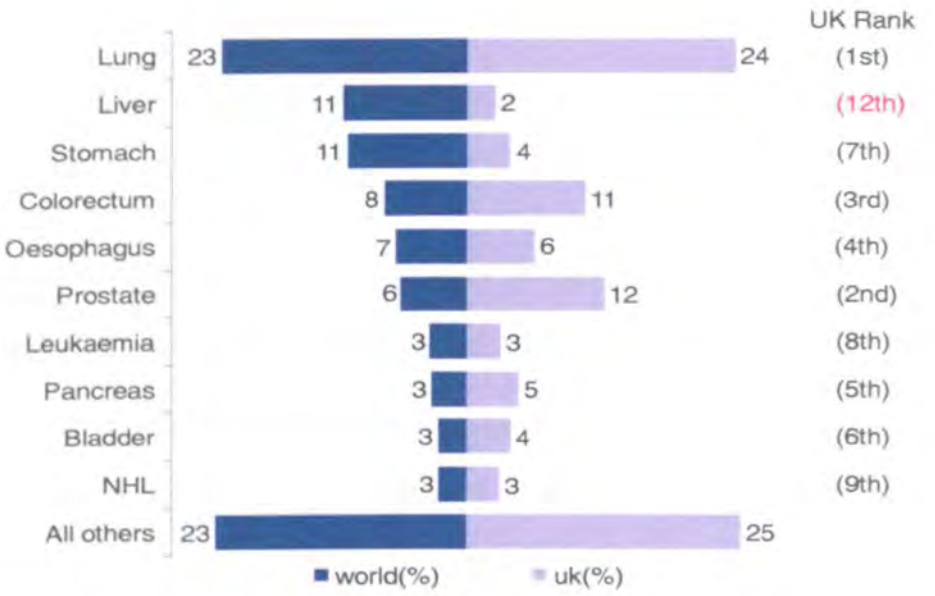

Figure 1.4 The top most common male cancer deaths worldwide compared to UK (The International Agency for Research on Cancer GLOBOCAN, 2008)

1.2 Treatment options

The ultimate aims of cancer treatments are a complete cure or increasing the survival time for patients suffering from advanced stage disease. There are three main ways of treating cancer.

1.2.1 Surgery

Surgery has the most prominent role in the treatment of cancer (King and Primrose, 2003). In terms of curing the disease, it is the most effective treatment. There are several clinical conditions which are closely associated with development of malignancy for example ulcerative colitis or cryptorchidism. Surgery will be the first line treatment of such conditions thus limiting the chances of cancers forming (King and Primrose, 2003).

In recent years surgical procedures have been developed in such a way that the normal appearance and functioning of the affected organ can be pre-

served. This has led to an increase in the number of patients undergoing surgery for cancer (King and Primrose, 2003).

1.2.2 Radiation therapy

The effectiveness of radiation therapy is linked to its action on DNA. Applied gamma radiation introduces DNA strand breaks in cancer cells. The radiation absorbed by the cells immediately ionises atoms and raises them to excited states, these in turn form highly reactive free radicals which interact with cellular contents, including nucleic acids. It is important that the planning of the radiation therapy is done carefully. This is based on the tumour volume and the uniform dose of radiation required for the treatment so that the normal tissue damage will be minimised (Falk, 2006). In radiation therapy, along with the cancer cells, normal cells also absorb radiation so damage occurs to both. However cancer cells lack control when it comes to division and do not maintain the essential cell cycle check points. Whereas normal cells would not divide under these circumstances, the cancer cells continue to do so and eventually many of them undergo apoptosis due to the DNA damage done by the radiation (Palayoor *et al.*, 1995). Radiation therapy can be used both internally (brachy therapy) and externally (external beam radiation therapy) (Falk, 2006).

Despite the developments in surgical and chemotherapies, radiation therapy is still a valuable choice for anticancer treatment. Up to a 50% of all cancer patients will receive radiation therapy at some stage of the disease (Falk, 2006).

1.2.3 Chemotherapy

As well as treatments by surgery and radiation, chemotherapy also has a major role to play in the cure and control of a wide range of cancerous malignancies. Some cancers are chemo-sensitive and can be cured using chemotherapy (Falk, 2006).

However, a complete cure will only be achieved when the tumours are treated with a combination of chemotherapeutic agents. For example the gemcitabine-cisplatin combination is used to treat pancreatic and ovarian cancers (Parnell and Woll, 2003).

Despite the number of chemotherapeutic drugs available, due to resistance mechanisms in cancer cells and a lack of efficacy, there is always a need to develop new anticancer therapies. Most commercially available potent anticancer agents are targeted directly to DNA or its associated enzymes responsible for replication such as topoisomerase II (Louvet *et al.*, 2002).

In the past two decades, more research has been focussed on developing cytotoxic agents which selectively target cancer cells and do not affect healthy cells. The major disadvantages of chemotherapy include bone marrow suppression, nervous system damage, hair loss and infertility (Palchaudhuri and Hergenrother, 2007a).

1.3 Structure of DNA

Nucleic acids, key targets for chemotherapies, include DNA and RNA which are long thread-like polymer structures made up of a sequence of monomers called nucleotides. The number of nucleotides present in a nucleic acid va-

ries from 80 in tRNA to 10^8 in one eukaryotic chromosome. Nucleotides are made up of phosphate esters of nucleosides.

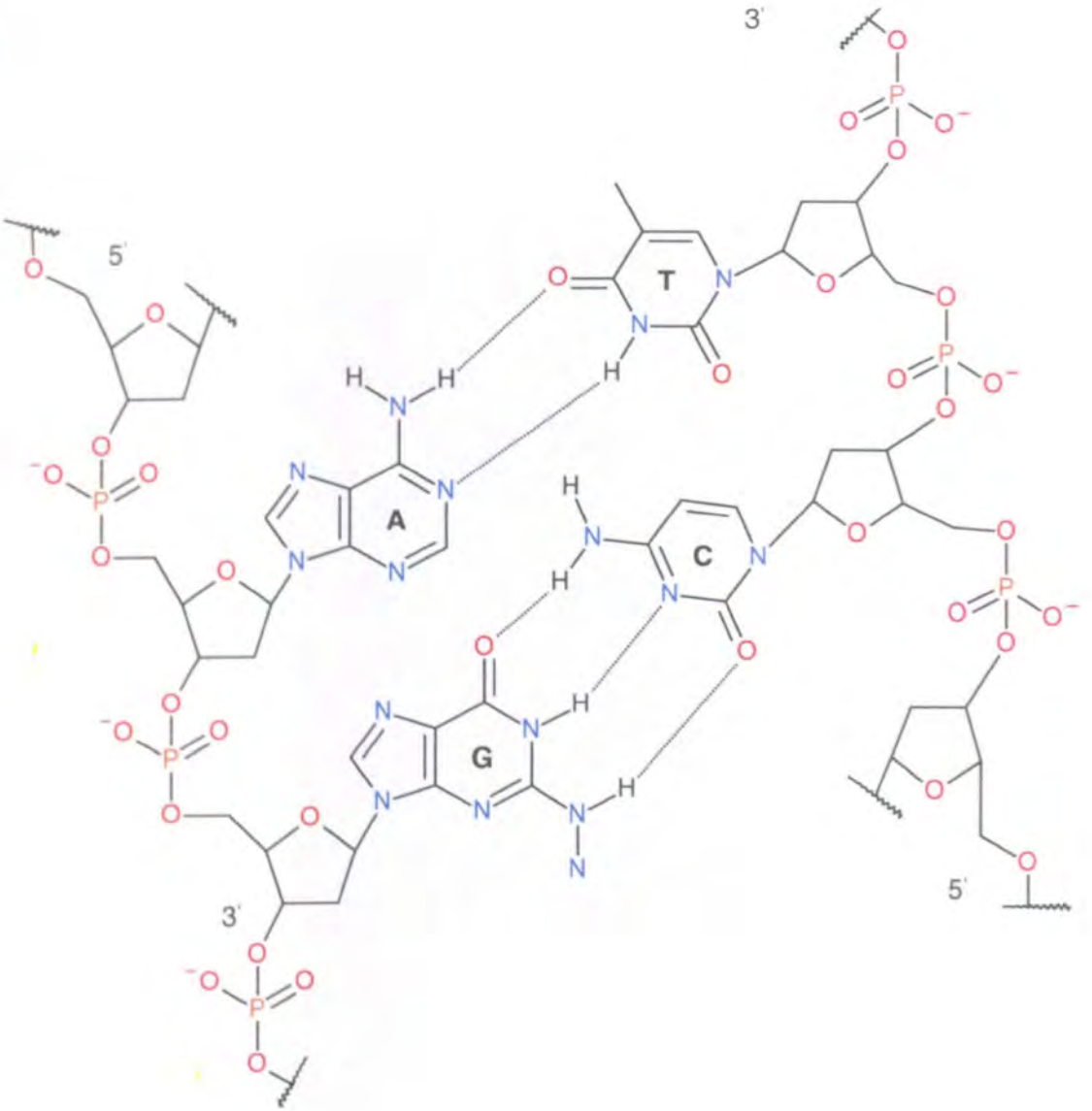

Figure 1.5 Showing how the nucleotides are linked via their phosphate groups to form nucleic acid strands. The strands are then held together by hydrogen bonds (dotted in the structure) (Blackburn, 2006).

The latter contain two fundamental components: a heterocyclic base and a sugar (pentose). Usually the purines: adenine (A) and guanine (G) and the pyrimidines; cytosine (C), thiamine (T) and uracil (U) are the bases, deoxyri-

bose or ribose is the sugar. In DNA these bases recognise each other and exist as pairs joined by hydrogen bonding. Adenine pairs with thymine and guanine joins with cytosine to establish structure of DNA (Figure 1.5) (Blackburn, 2006).

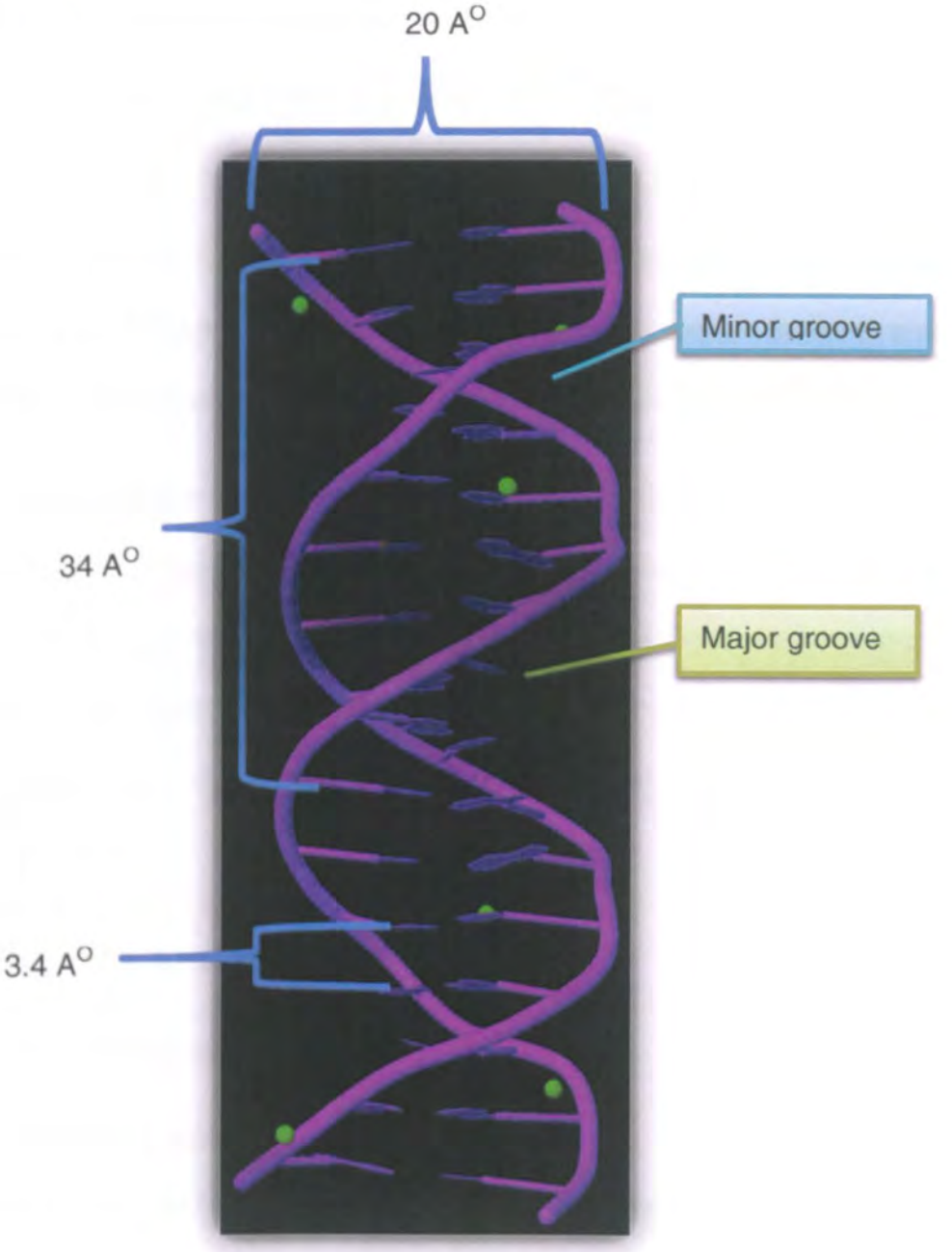

Figure 1.6 Showing minor and major grooves of DNA redrawn from (Narayana and Weiss, 2009)

In DNA two chains of nucleotides are joined in antiparallel fashion with hydrogen bonds between bases and twisted as a helix. This gives raise to the formation of grooves. Where the phosphate backbones of two stands are far apart, the space inside the groove is larger so it is named the major groove whereas, the minor grove arises where the phosphate backbones are closer in the DNA double helix (Figure 1.6) (Blackburn, 2006; Narayana and Weiss, 2009).

As the major groove has more open space it offers access to more functional groups on the DNA bases. Generally DNA binding proteins interact in a sequence-specific fashion in this groove (Blackburn, 2006).

On the other hand the minor groove allows the binding of small molecules. as it offers better Van der Waals interactions. Generally, apart from intercalators which prefer GC rich sequences, ligands which bind at the minor groove prefer AT rich sequences. Major and minor groves have distinct hydrogen bonding potential, size, shape, electrostatic potential and degrees of hydration (Blackburn, 2006).

1.4 Anticancer drugs

1.4.1 Drugs acting on DNA

1.4.1.1 Alkylating agents

Alkylating agents are highly electrophilic molecules that are capable of covalently binding with electron rich nucleophilic groups on biological molecules such as DNA bases. Various groups of organic molecules which include nitrogen mustards, ethylene imines and methanesulfonates come under this category. These compounds are mostly simple structures with high reactivity

towards nucleic acids, a key cancer target; which makes them suitable candidates as cytotoxic agents (Brookes and Lawley, 1964). Compounds with two alkylating functional groups (Figure 1.7 and 1.8) can cause cross linking of DNA which affects its replication and transcription and hence causes cytotoxicity.

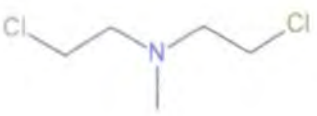

Figure 1.7 Mechlorethamine

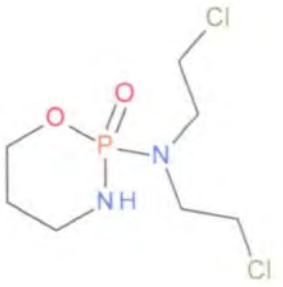

Figure 1.8 Cyclophosphamide

The major drawback of alkylating drugs is that they themselves are carcinogens and can affect healthy tissues (Brookes and Lawley, 1961). Nitrogen mustards have a common bis(2-chloroethyl)amino moiety. At physiological pH, the strong negative inductive effect caused by the two chlorine atoms decreases the basic strength of the nitrogen dramatically; which enables the intramolecular displacement of chlorine to form an aziridinium by the lone pair of electrons present on the nitrogen (Figure 1.9).

This electrophilic species establishes a covalent link, usually with the nucleophilic N7 position of guanine which leads to mispairing of bases and hence to mutagenesis. In addition, the other chloro group can make another aziridine and then can react with the next nearest guanine to form inter- or intra-strand cross links (guanine-guanine) resulting in disruption of DNA replication and transcription. This causes cells to undergo apoptosis. Nitrogen mustards are

used in the treatment of haematological malignancies, ovarian cancers and refractory prostate cancers (Brookes and Lawley, 1964).

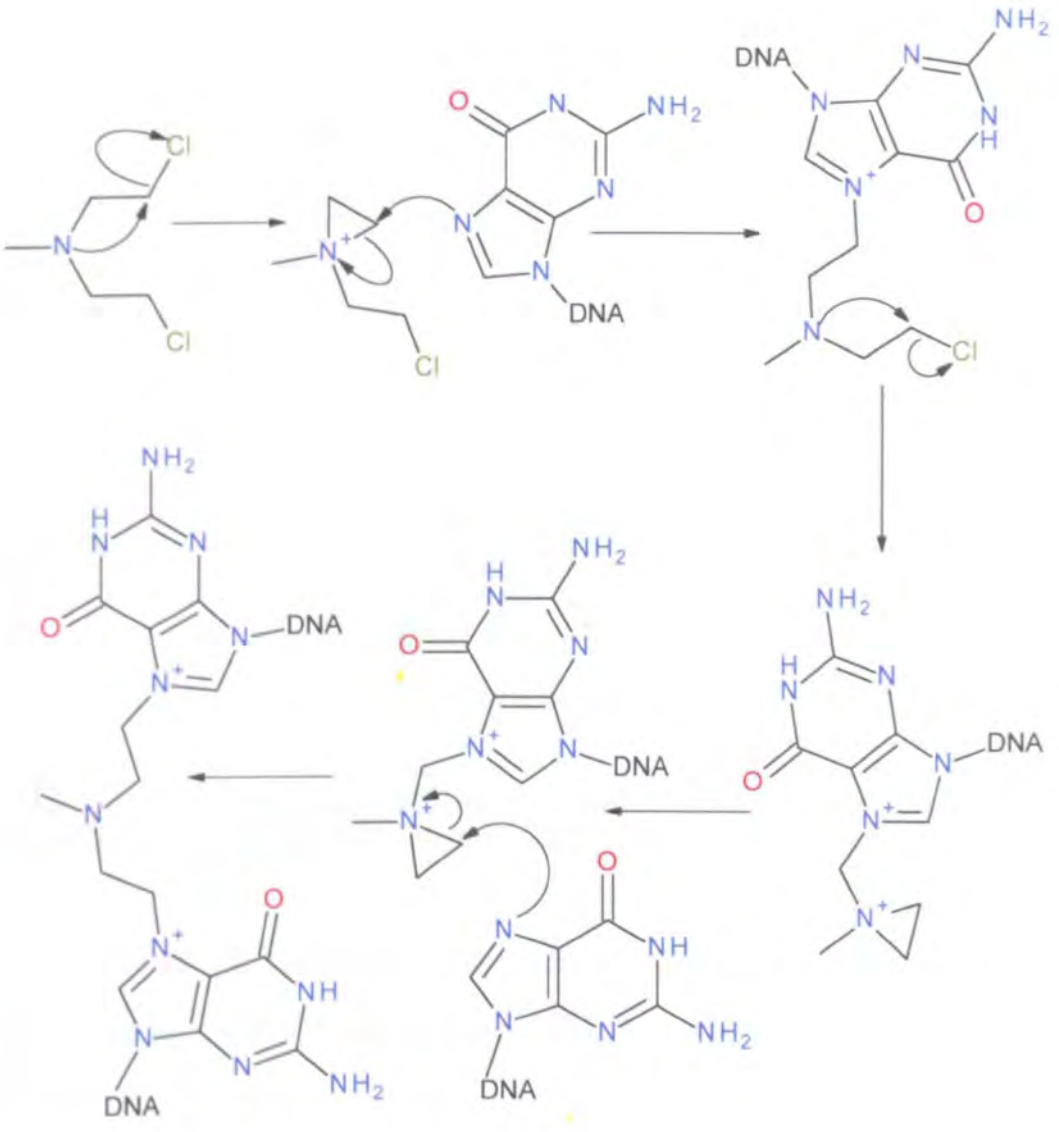

Figure 1.9 DNA alkylation by mechlorethamine (Hubbard and Fidanze, 2007)

Cyclophosphamide (Figure 1.8) is a pro-drug activated by CYP450, a liver oxidase enzyme and then the metabolites produced reach the tumour cells via the blood-stream. The two metabolites, phosphoramide and acrolein, are produced in an equimolar ratio (Figure 1.10).

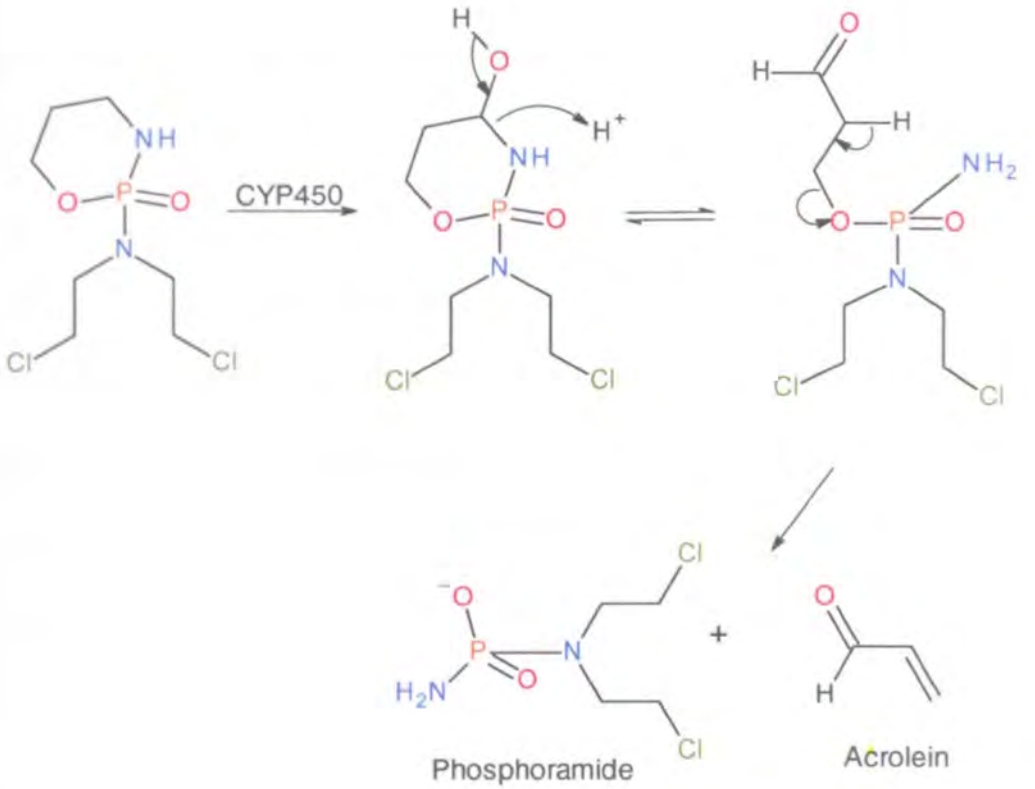

Figure 1.10 Generation of the active alkylating agents from cyclophosphamide (Hubbard and Fidanze, 2007)

Cyclophosphamide itself is inactive because of the electron withdrawing effect caused by the P=O bond preventing the formation of the aziridinium. Later, once it is converted to phosphoramide, the negative charge on the oxygen balances the electron withdrawing effect of P=O which allows the activation to aziridinium ion (Avendaño and Menendez, 2008).

In addition, the nucleophilicity of nitrogen on this active metabolite is hindered by the phosphoramide, which make it less reactive than mechlorethamine, hence it is less likely to be hydrolysed and can only react with stronger nucleophiles such as guanine.

Phosphoramide is the main anticancer mustard whereas acrolein is thought to be to the reason for the toxic side effects including hematuria, syndrome of inappropriate antidiuretic hormone and slow-healing of existing wounds (Anderson *et al.*, 1995).

1.4.1.1.1 Carbazines

These drugs produce an intermediate methyldiazonium ion and/or a methyl free radical which can alkylate DNA or RNA which then leads to their disintegration. This action was first reported in 1960 which led to synthesis of a range of prodrugs of the methyldiazonium ion. Procarbazine (Figure 1.11) and dacarbazine (Figure 1.112) belong to this class.

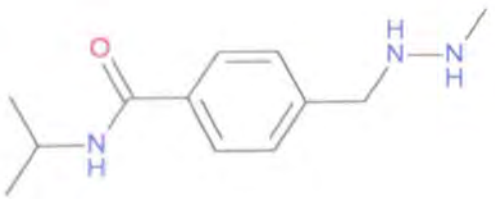

Figure 1.11 Procarbazine

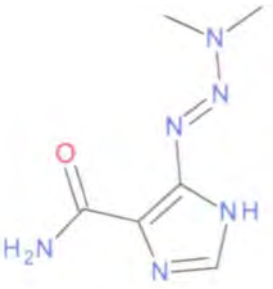

Figure 1.12 Dacarbazine

Alkylation occurs at the O6, C8 or N7-positions of guanine, and then this pairs up with thymine causing mismatched pairs which ultimately leads to cell death through gene mutations. Of particular note, patients who are able to repair this mispairing by transferring the methyl group to a cysteine residue may show resistance to these drugs. Whereas those who underexpress alkyltransferase will respond well to the treatment with carbazines (Foye, Lemke and Williams, 2008).

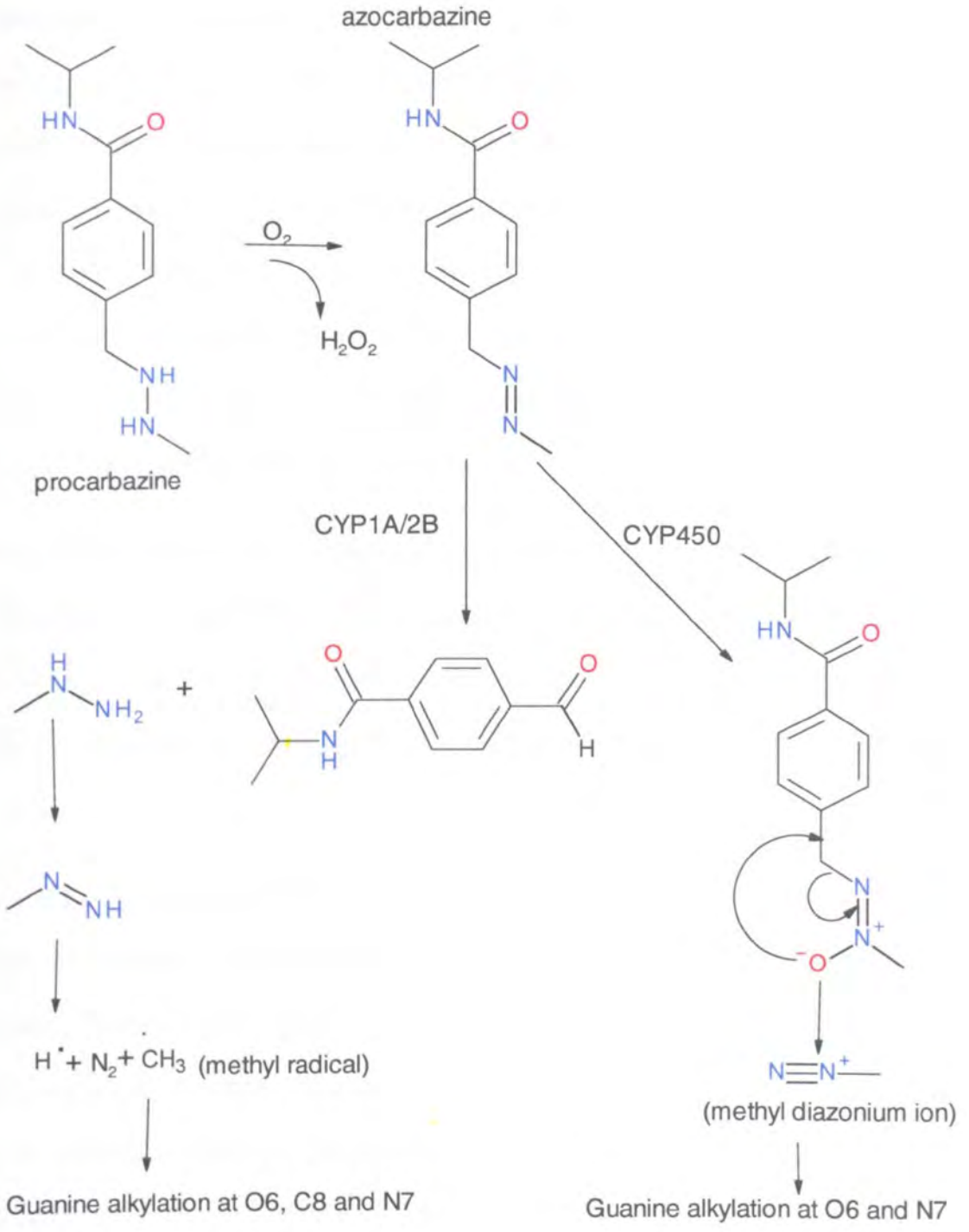

Figure 1.13 Generation of the active alkylating agent from procarbazine (Anderson *et al.*, 1995) (Avendaño and Menendez, 2008; Foye, Lemke and Williams, 2008)

Metabolism of procarbazine, involves the enzymes CYP1A or CYP2B. Once the procarbazine is converted to azoprocarbazine, these liver enzymes come in to action to produce methyhydrazine from azoprocarbazine by benzylic oxidation which then forms a methyl radical via a methyldiazine intermediate. This radical then alkylates guanine at the O6, C8 and N7-positions. On the other hand, a methydiazonium ion is formed via CYP450 which can also alkylate the DNA (Figure 1.13) (Avendaño and Menendez, 2008; Foye, Lemke and Williams, 2008; Sullivan and Wong, 1977).

In contrast triazines including dacabazine methylate DNA predominantly via diazomethane formation. Their metabolic activation is dependent on CYP1A1, CYP1A2 and CYP2E1. These drugs mainly alkylate guanine at the O6 and N7-positions (Foye, Lemke and Williams, 2008; Sullivan and Wong, 1977).

1.4.1.1.2 Platinum derivatives

Cisplatin (Figure 1.14) alkylates DNA irreversibly and forms adducts. In response, cells activate signal transduction pathways that arrest the cell cycle and cause apoptosis (Eastman, 1990). It platinates the DNA via intra-strand cross linking at d(ApG), d(GpNpG), d(GpG) and inter-strand cross linking at d(GpG) sites of DNA (Figure 1.15) (Valentini *et al.*, 2006). The adducts formed stop the action of DNA polymerase when they are present in the lagging strand (Fedier and Fink, 2004). Cells have a defence mechanism which repairs the DNA by removing the platinum-DNA adducts with the help of the nucleotide excision repair mechanism (NER) (Eastman, 1990).

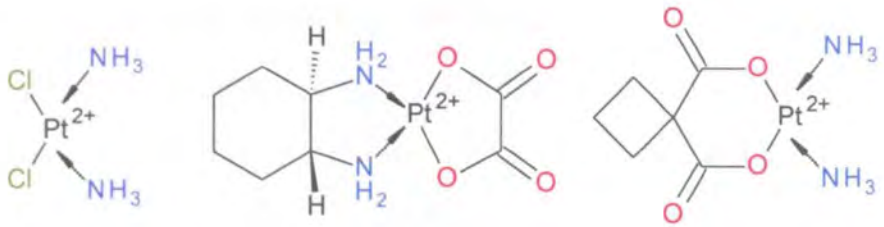

Cisplatin oxaliplatin Carboplatin

Figure 1.14 Showing different platinum compounds

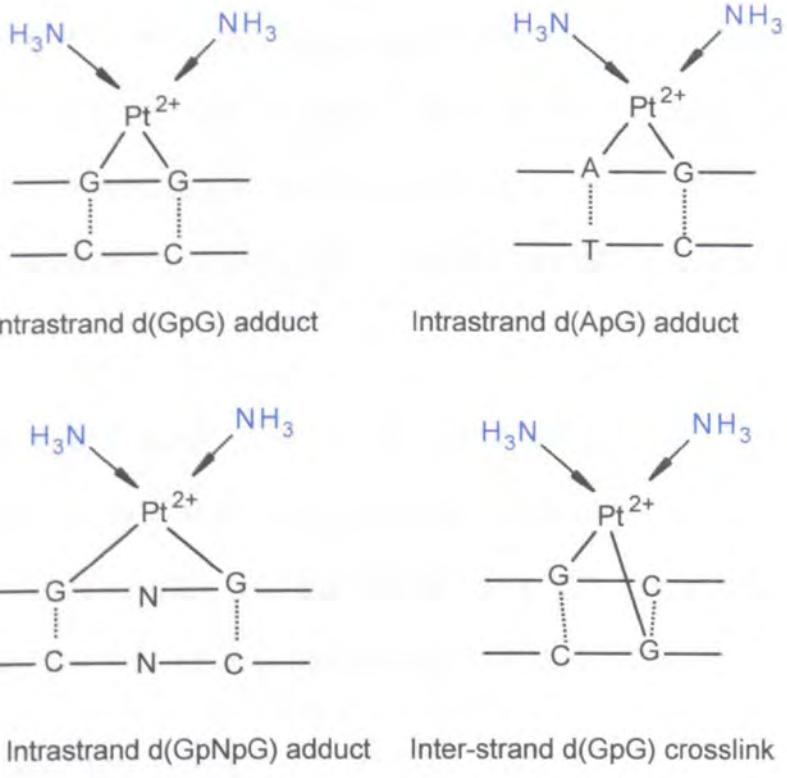

Figure 1.15 Showing interactions of cisplatin with DNA (where p is phosphate group and N is any DNA base)

It has also been demonstrated that increased activity of NER may lead to the decreased sensitivity of tumours to cisplatin (Zamble *et al.*, 1996).

Oxaliplatin (Figure 1.14) is a more recent platinum containing anticancer agent that is more potent than cisplatin. This is due to the presence of the

diaminocyclohexane group which interacts at the major groove of DNA to form d(GpTpG) intra-strand cross links (Figure 1.15, where N is T) (Valentini *et al.*, 2006).

Mode of action of carboplatin is same as cisplatin, forming cross links with Guanine in DNA but it causes lower nephrotoxicity because of the dicarboxylate ligands, which enables its excretion (Avendaño and Menendez, 2008).

The main advantage of oxaplatin is that the DNA adducts will not be recognised by the DNA mismatch repair system (MMR). The protiens involved in this repair mechanism only recognise the 1, 2 intra-strand d(GpG) adducts but not the 1,3 intra-strand adducts. This is the main reason for its use against cisplatin resistant tumours (Valentini *et al.*, 2006; Sergent *et al.*, 2002).

1.4.2 Antimetabolites

These drugs act by inhibiting the enzymes responsible for the synthesis of DNA or its bases. This leads to the disruption of DNA functioning or synthesis of abnormal DNA structures which causes apoptosis of the cell to occur.

1.4.2.1 Folate antagonists

These drugs inhibit the enzyme dihydrofolate reductase (DHFR) which is responsible for the maintenance of the enzyme-cofactor tetrahydrofolate (TH_4) (Figure 1.16) which is a single carbon carrier for the biosynthesis of DNA (Figure 1.17) (Patrick, 2009). In the absence of TH_4, DNA synthesis will slow down which in turn leads to slow proliferation of tumour cells (Rubino, 2001). Methotrexate (Figure 1.18) is an example of this class.

Methotrexate (Figure 1.18) resembles the structure of folic acid; the only difference is the presence of amino group at the C4 position instead of OH. It binds to dihydrofolatereductase (DHFR) and hence prevents the conversion of folic acid to dihydrofolate (TH_2) and then to tetrahydrofolate (TH_4) (Figure 1.16).

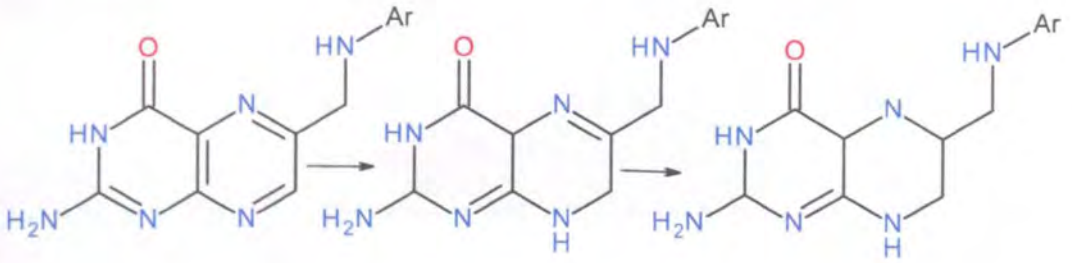

Folic acid Dihydrofolate(TH_2) Tetrahydrofolate(TH_4)

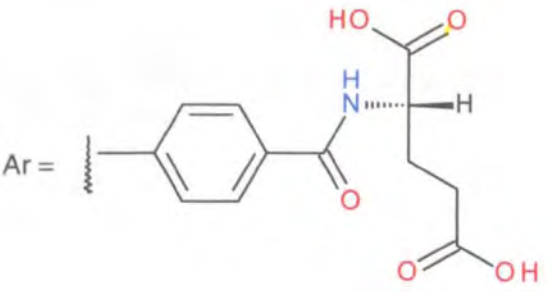

Figure 1.16 Showing conversion of folic acid to tetrahydrofolate

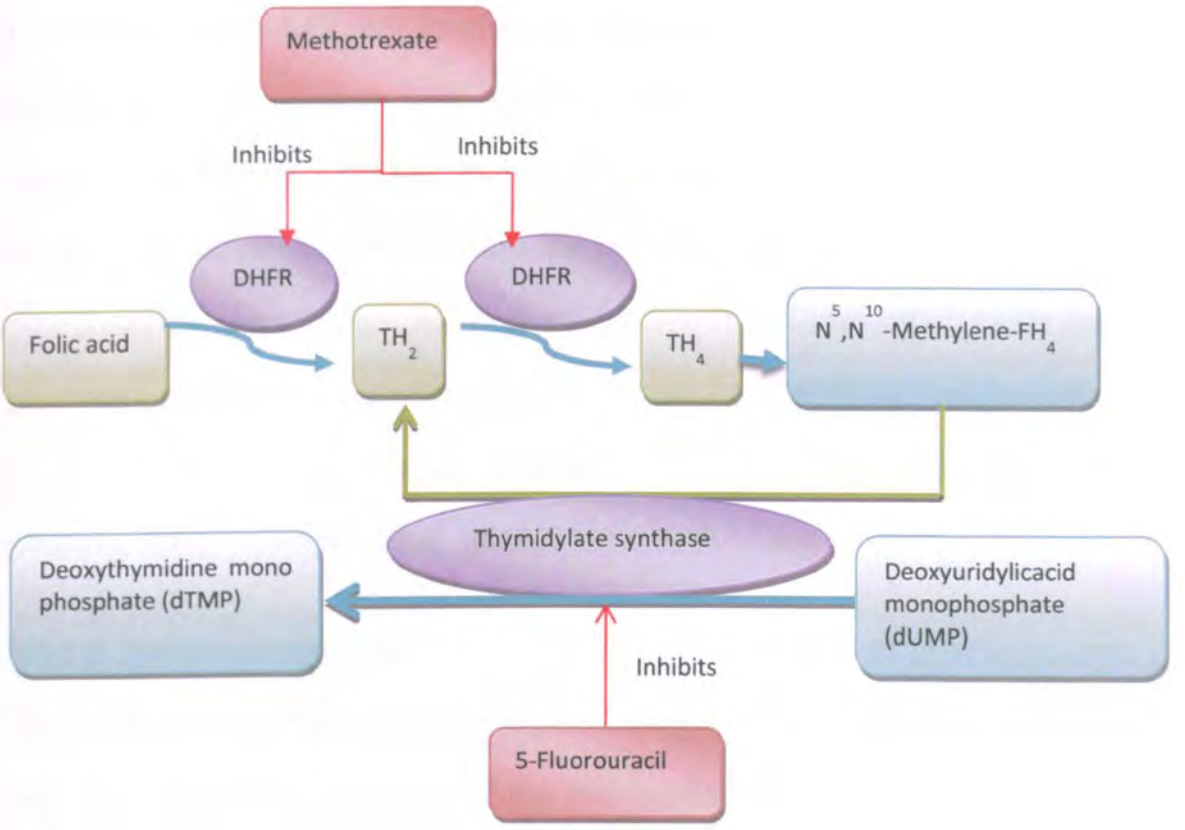

Figure 1.17 Showing mode of action of methotrexate

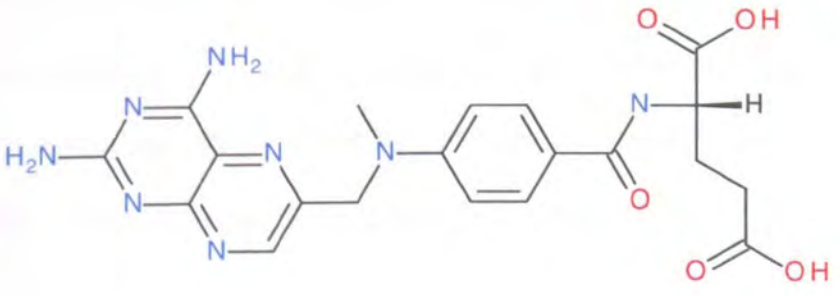

Figure 1.18 Methotrexate

This inhibition of a critical enzyme leads to the reduction of DNA synthesis and hence impaired tumour growth. Methotrexate is selective towards cancer cells over normal cells becuse halting DNA synthesis has more effect on rapidly dividing cancer cells (Halpern *et al.*, 1975).

Upon entering the cell, methotrexate is converted to polyglutamated methotrexate by polyglutamase synthase. This conversion makes it difficult to transport methotrexate across the cell membrane and therefore the half-life of the drug will be increased inside the cell (Genestier *et al.*, 2000). These polyglutamated conjugates not only inhibit DHFR but also other folate dependent enzymes such as thymidylate synthase. Lack of this polyglutamation in cancer cells is one of the key reasons of drug resistance to methotrexate (Rubino, 2001; Genestier *et al.*, 2000)

1.4.2.2 Purine antagonists

These drugs are similar to the biological purines, adenine or guanine. They include mercaptopurine (Figure 1.19) and azathioprine (Figure 1.20) which can enter the cell where they get converted to non-natural nucleoside monophosphates and then inhibit purine synthesis at several points. They can also insert into DNA and RNA which then leads to malfunctioning of DNA or RNA for example 6-mercaptopurine (Figure 1.19) is converted to thio-guanosine triphosphate (thio-GTP) (Figure 1.21) which will incorporate into DNA and hence cause apoptosis of the cell (LePage, 1977).

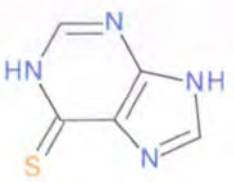

Figure 1.19 6-Mercaptopurine (6-MP)

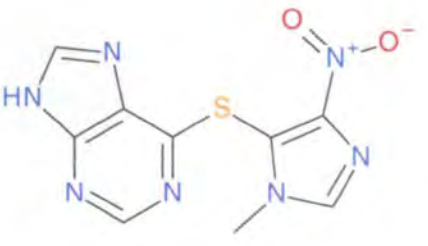

Figure 1.20 Azathioprine

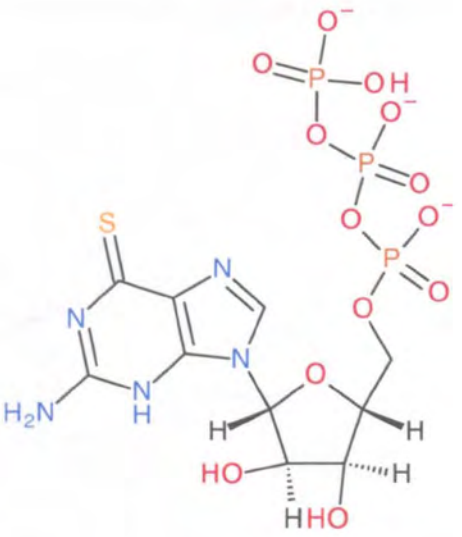

Figure 1.21 Thio-GTP

1.4.2.3 Thymidylate synthase inhibitors

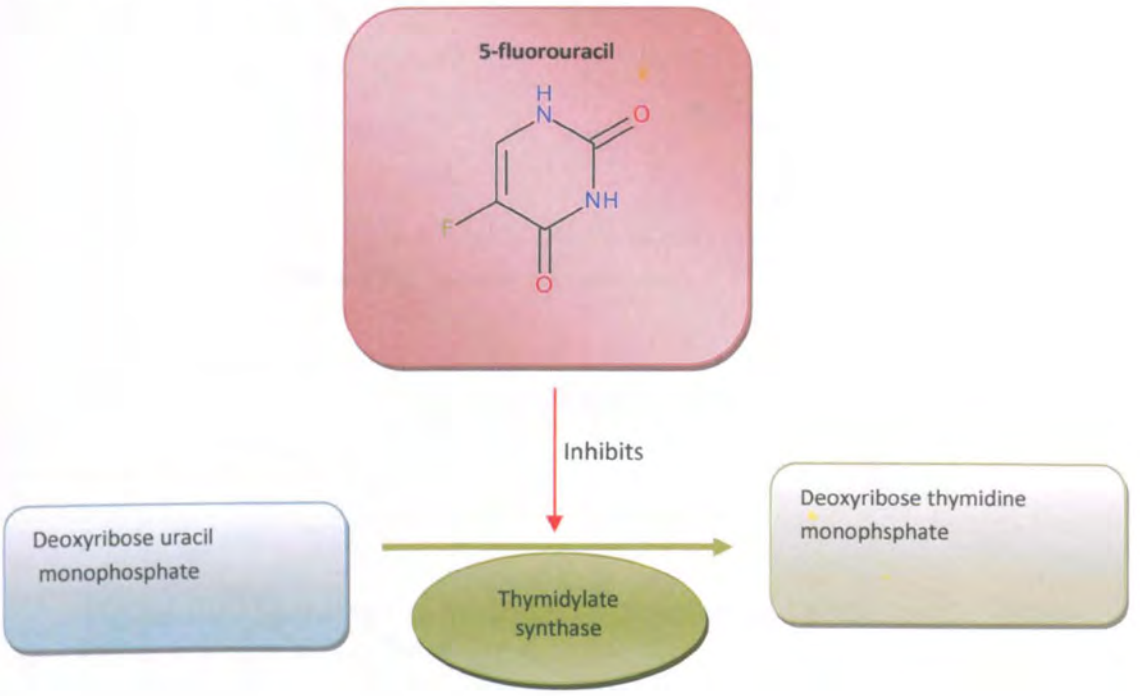

Figure 1.22 Showing mode of action of -5-Fluorouracil

5-Fluorouracil (Figure 1.22) halts the convertion of deoxyuridine monophosphate (dUMP) into deoxythymidine monophosphate (dTMP) (Figure 1.22) by

inhibiting the enzyme thymidylate synthase through formation of a suicide substrate (Figure 1.23)

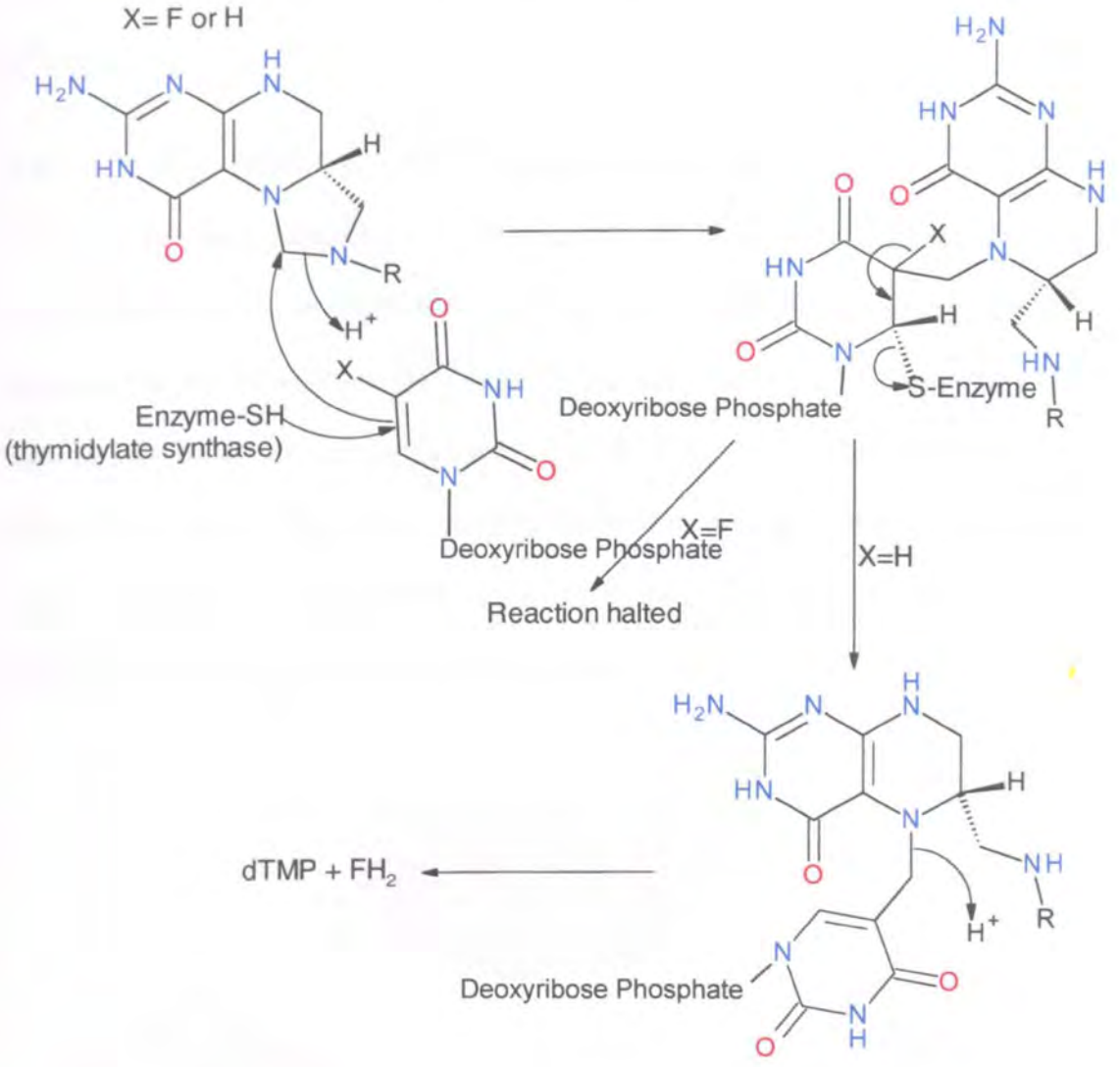

Figure 1.23 Showing the mechanism of action of 5-fluorouracil (Patrick, 2013; Longley *et al.*, 2003)

As shown in Figure 1.23 *in vivo*, the prodrug is activated by the addition of deoxyribose phosphate to give a nucleotide. In the next step the tetrahydrofolate reacts with the uracil moiety by forming a covalent bond.

In the case of uracil as a substrate, a proton is lost from the uracil moiety, whereas 5-fluorouracil has a fluorine atom instead. As this cannot form F^+ it

is bound to the enzyme irreversibly. This leads to the cessation of thymidine synthesis ultimately terminating the production of DNA and hence leading to cell death (Pinedo and Peters, 1988; Ghoshal and Jacob, 1997; Patrick, 2013).

1.4.2.4 Ribonucleotidereductase inhibitors

The enzyme ribonucleotidsereductase converts ribonucleotide phosphates to deoxyribonucleotide phosphates. Its inhibition by hydroxyurea stops this conversion (Figure 1.24) there by it inhibits the DNA synthesis which ultimately lead to cell death. Hydoxyurea can be taken orally in the therapy of cervical and neck cancers. The major disadvantage of this drug is that it can cause drug resistance as cells start to express greater amounts of the reductase (Elford *et al.*, 1979; Shao *et al.*, 2006; Sinclair, 1981).

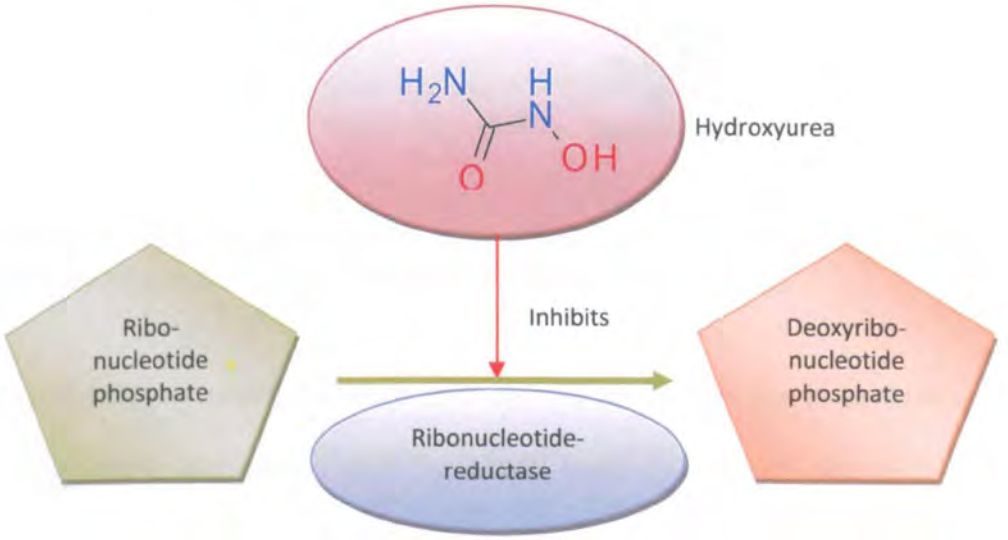

Figure 1.24 Mode of action of hydroxyurea

1.4.3 Vinca alkaloids

Microtubules are heterodimeric proteins made of alpha and beta tubulin which form protofilaments during mitosis, which then assemble to form tube like structures hence the name micro-tubules.

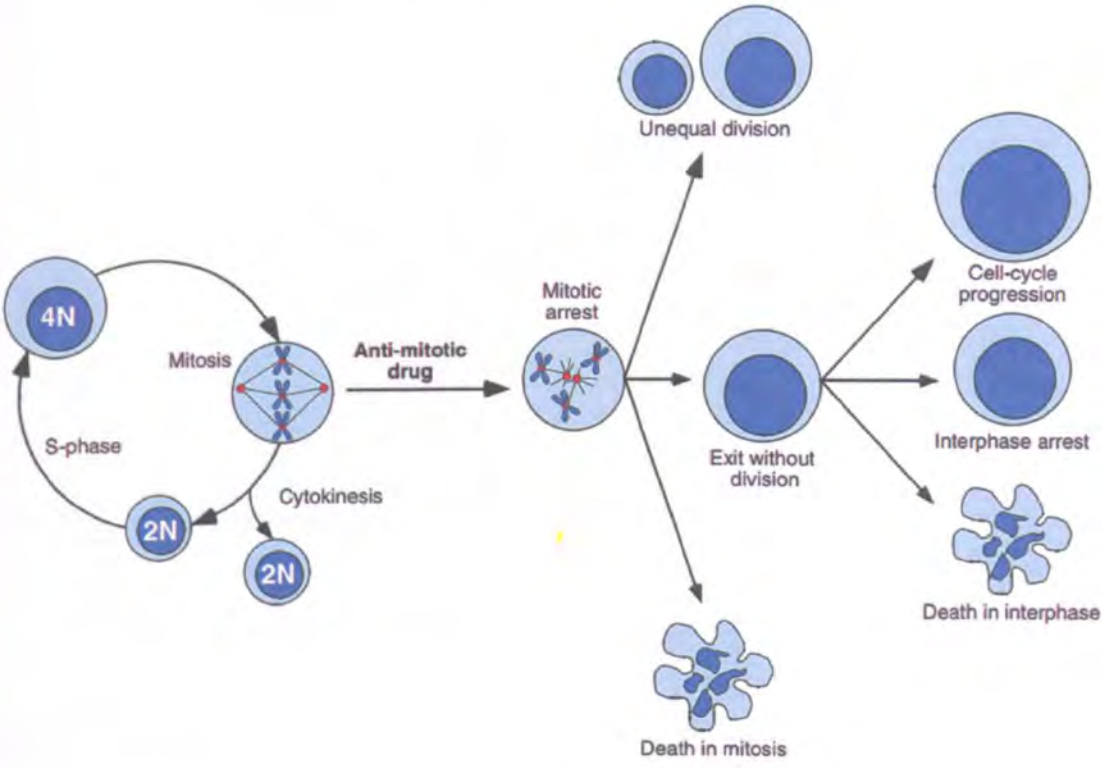

Figure 1.25 showing results of an antimitotic drug (vinca alkaloids and taxanes) action on cell (Gascoigne and Taylor, 2009)

The dynamics of polymerisation and depolymerisation are important to form and dissemble the mitotic spindle, which enables capture and alignment of the chromosomes to facilitate cell division (Jordan and Wilson, 2004; Tsukidate *et al.,* 1993; Rai and Wolff, 1997). Polymerisation involves hydrolysis of GTP bound to the tubulin, hence inhibition of this process results in improper division or apoptosis (Figure 1.24).

Vinca alkaloids (Figure 1.26) are phytochemicals isolated from the plant known as *catharanthus roseus,* also known as periwinkle (da Rocha *et al.,*

2001). Vincristine (Figure 1.26), vinblastine, vindesine and vinorelbine are typical vinca alkaloids. They inhibit tubulin polymerisation by directly binding to tubulin at a region adjacent to the GTP binding site in dividing cells.

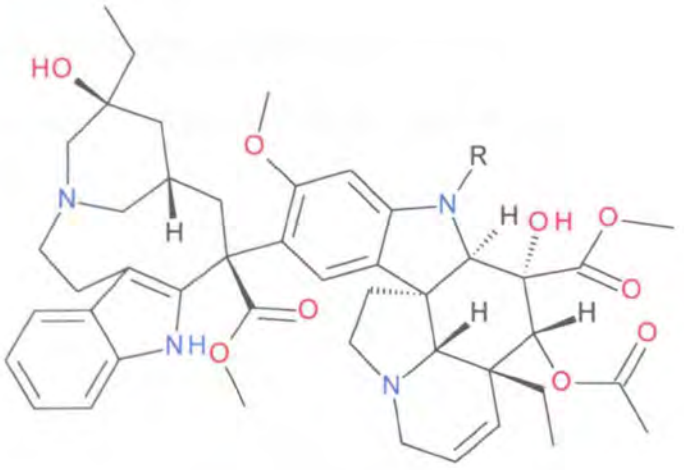

vincristine R = CHO, vinblastine R= CH_3

Figure 1.26 Vinca alkaloids

1.4.4 Taxanes

In contrast to vinka alkaloids, this class of anticancer agents act by inhibiting tubulin depolymerisation (McGrogan *et al.*, 2008; Maccari *et al.*, 2003). The main compounds of this class are placitaxel (Figure 1.27) and docitaxel. Paclitaxel shows very good anticancer activity and was first approved by the FDA in 1992 for breast and ovarian cancer therapy (Ojima *et al.*, 1994). The main problem with these drugs is that they cannot be taken by the oral route as they have poor bioavailability (Jibodh *et al.*, 2013). Currently research is being carried out to increase the bioavailability of these compounds by making pharmaceutical formulations including nanoparticles and polyester based micelles (Jung *et al.*, 2012; Gaucher *et al.*, 2010).

Another drawback of these drugs is that they can cause multidrug resistance via amplification of membrane phosphoglycoproteins which act as efflux pumps for the drug leading to cross drug resistance to bulky natural cytotoxic agents (Horwitz *et al.*, 1993). Formulations have been made in a view to reduce this resistance using polyethylated castor oil and tween 20 which showed a reduction in the restistance occurance(Webster *et al.*, 1993; Rischin *et al.*, 1996).

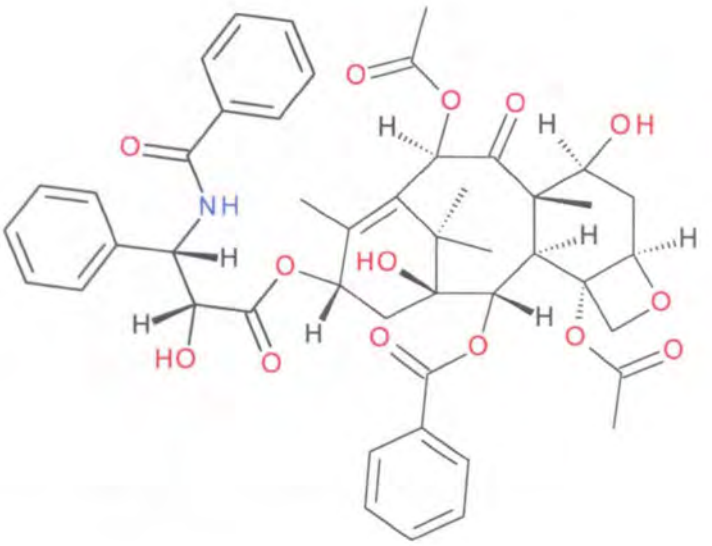

Figure 1.27 Paclitaxel

1.4.5 Camptothecin analogues

Camptothecin (Figure 1.28) is a phytochemical obtained from the Chinese bush, *camptotheaca acuminate* and its analogues are non-intercalating anti-cancer agents that inhibit the topoisomerase I enzyme (Rivory and Robert, 1995; Lu *et al.*, 2014).

Topotecan (Figure 1.28) and irinotecan are semisynthetic analogues of camptothecin which have greater aqueous solubility and less toxicity compared to the parent compound (Lv *et al.*, 2013).

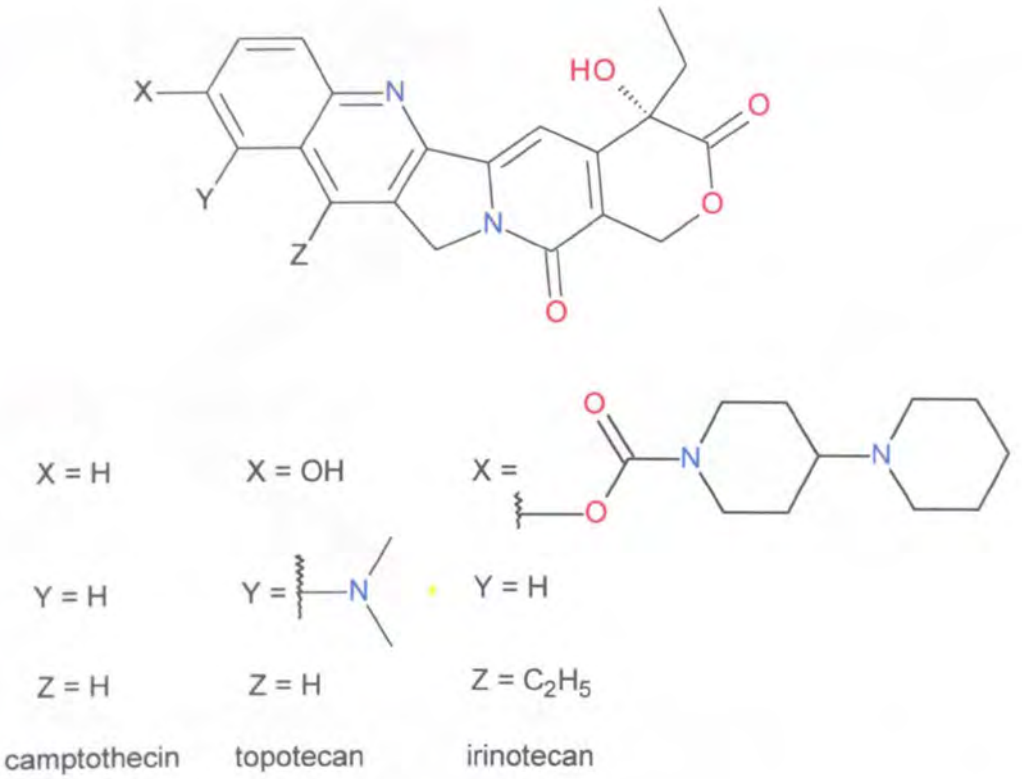

Figure 1.28 Showing camptothecin analogues

The topoisomerase I enzyme (topo I) catalyses the relaxation of superhelical twists in DNA (Wang, 1996). As shown in the Figure 1.28 topo I cleaves DNA then campotethicin binds to the cleaved topo I-DNA complex thereby preventing the relegation of the DNA leaving breaks in the DNA fork which is lethal to dividing cells (Hsiang *et al.*, 1989). Based on this mechanism, levels of topo I in cells may be a critical parameter in the drug potency. Topo I is expressed abundantly in both dividing and normal cells unlike the Topo II enzyme which is over expressed in proliferating cells, this might be the rea-

son behind the toxicity of camptothecin to the healthy cells. (Li *et al.*, 1972; Horwitz and Horwitz, 1973).

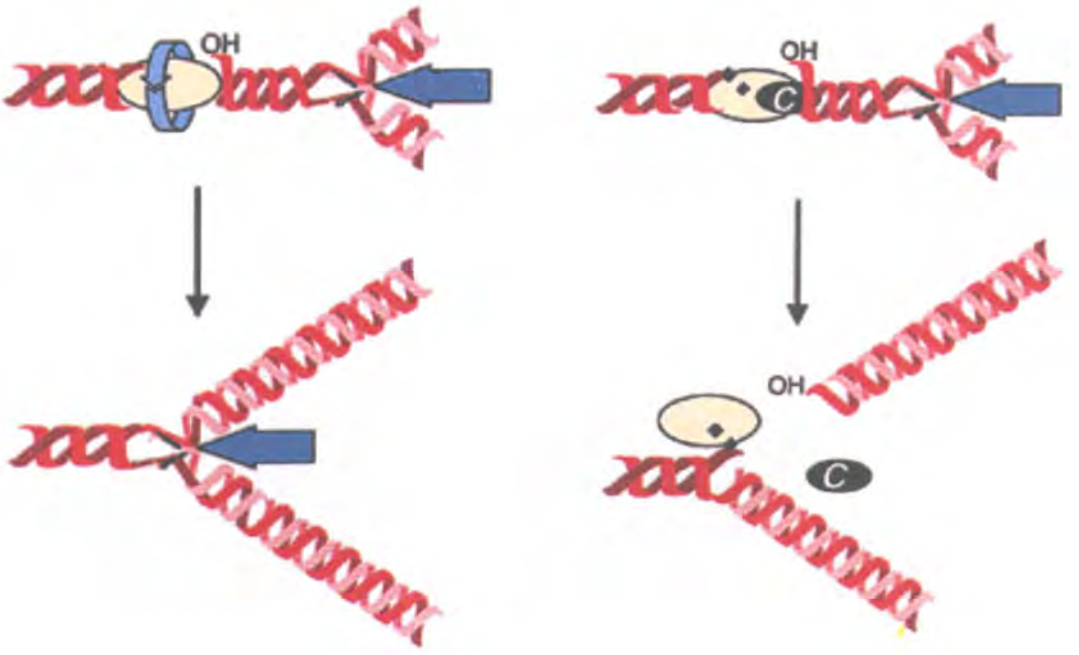

Figure 1.29 showing the mode of action of camptothecin, where C is camptothecin, and oval shape is enzyme topo I (Hsiang *et al.*, 1989) (Baran Group Meeting 9/ 26/ 2007), (C= camptothecin).

1.4.6 Drugs of other classes

1.4.6.1 L-Asparaginase

This drug is mainly used to treat leukaemia. Genetic mutations cause cells to produce non-functional enzymes therefore the essential cellular functions will be affected. In leukemic patients, leucocytes lose the capacity to synthesise the important amino acid asparagine so they have to get it from the blood supply. Asparaginase degrades the amino acid asparagine in the blood circulation making it less available for the cancer cells causing them to undergo apoptosis (AVRAMIS, 2012; Capizzi *et al.*, 1970). Side effects of this drug include pancreatitis, thrombosis, liver toxicity and allergy (Rytting, 2012).

Lyophilisate of the enzyme is delivered as an intramuscular or subcutaneous injection.

1.4.6.2 Drugs altering hormonal actions

Errors in DNA replication create gene mutations, in oncogenes (eg. BRCA1, BRCA2 in breast) these mutations lead to malignant cell types. Hormonal stimuli of these particular cells continue to support cell proliferation as the malignancy progresses (Figure 1.30) (Henderson and Feigelson, 2000).

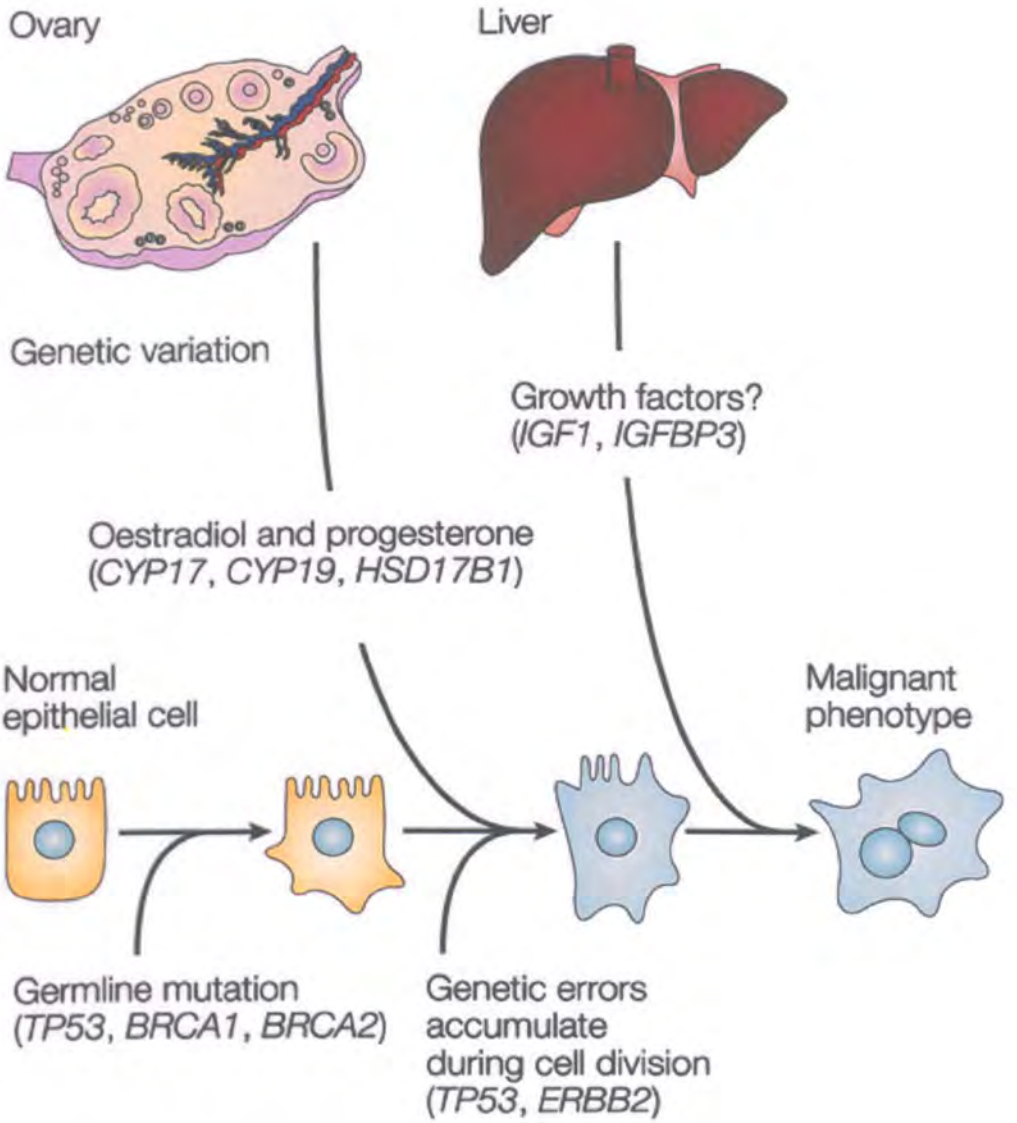

Figure 1.30 Showing cell proliferation control mechanism and involvement of different hormones and growth factors. ((Kolonel *et al.*, 2004)

Anti-hormonal drugs including tamoxifen (Figure 1.31) and fluvestrant (Figure 1.32) slow this process by binding to corresponding hormonal receptors and blocking the binding of hormones therefore they reduce the malignant cell proliferation. They are not cytotoxic but reduce growth of the tumour. The major types of cancers which respond to hormonal activity are; breast, prostate, testis, ovarian, thyroid endometrial and bone (Henderson and Feigelson, 2000).

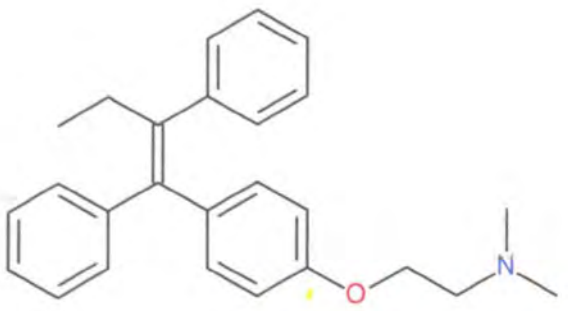

Figure 1.31 Tamoxifen

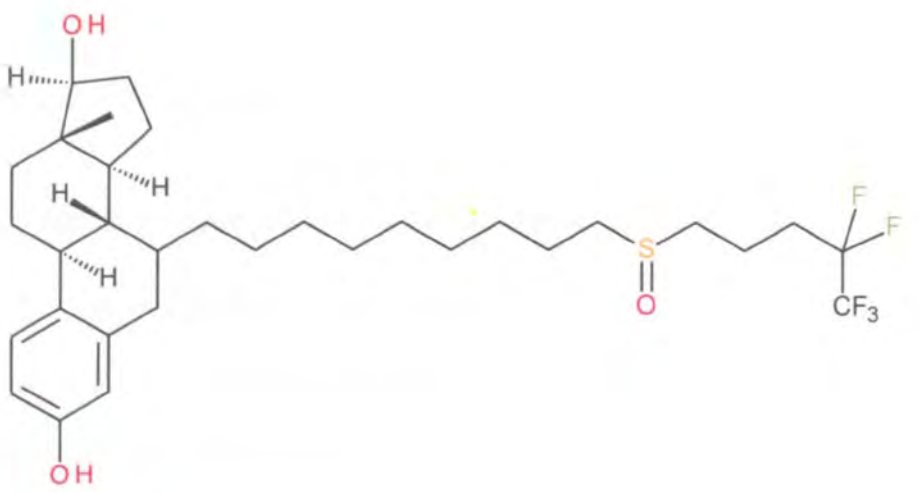

Figure 1.32 Fluvestrant

1.4.6.3 Aromatase inhibitors

The aromatase enzyme converts androgens into oestrogens in the body. It is required in the last stage of the biosynthesis of oestrogens from androgens. Aromatase inhibitors are mainly used in the treatment of anti-oestrogen resistant (caused by increased expression of oestrogen receptors) hormone-dependent breast cancer as a second line choice (Wood *et al.*, 2003; Goss and Strasser, 2001). Letrozole (Figure 1.33) and anastazole (Figure 1.334) are potent drugs in this class selectively inhibiting aromatase.

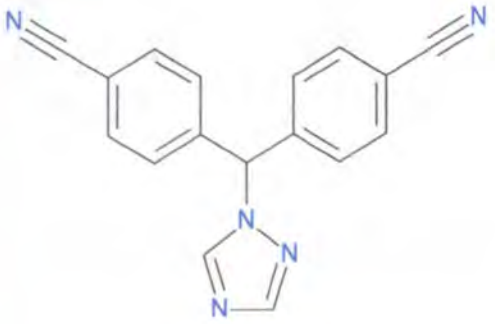

Figure 1.33 Letrozole

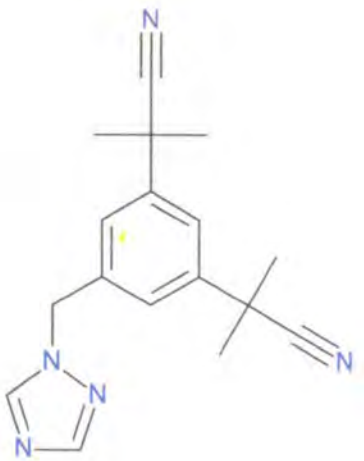

Figure 1.34 Anastrozole

1.4.7 Topoisomerase inhibitors and poisons

1.4.7.1 Introduction to topoisomerases

DNA replication is an important process on which cell proliferation is dependent. Replication of DNA is associated with the functions of many intracellular enzymes including the topoisomerases, which play a vital role in DNA replication and transcription by unwinding complex higher order structures (super-coiled or knotted) to allow DNA to be replicated (Figure 1.35). Broadly, there are two classes of topoisomerases: topoisomerase I and topoisome-

rase II. The latter is an enzyme that decatenates the intact double stranded DNA, whereas topo I relaxes DNA by cutting and re-joining a single strand (Champoux, 2001). Topoisomerase II is a major target for anticancer activity (Kellner *et al.*, 2002). In the last 10 years many papers have been published on this topic including production of libraries of topo II inhibitors based on QSAR studies (Salerno *et al.*, 2010; Pogorelcnik *et al.*, 2013; Rogojina *et al.*, 2012; Bailly, 2012).

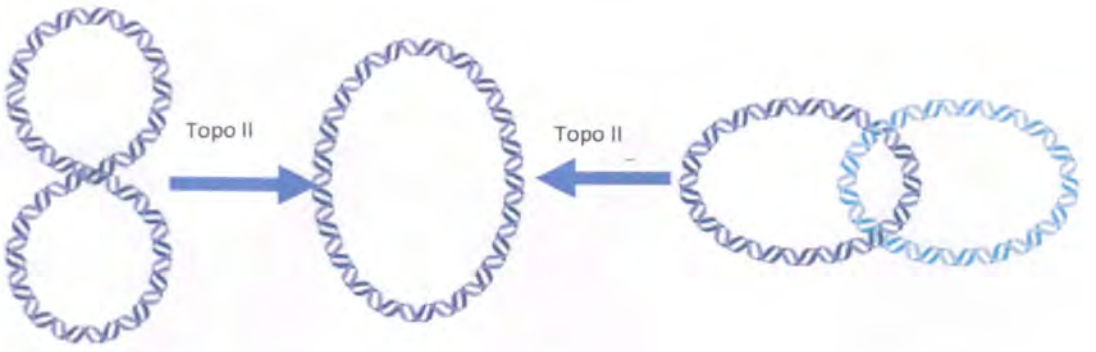

Figure 1.35 Showing relaxation of supercoiled and knotted DNA by topoisomerase II (Nitiss, 2009)

1.4.7.2 The topoisomerase catalytic cycle

As shown in Figure 1.36 the topoisomerase II dimer contains three functional parts; ATPase (yellow), cleavage (buff) and C-terminal (Blue) (Kellner *et al.*, 2002). Enzyme catalysis starts with the binding of topo II with its DNA substrate which does not require ATP. Unfortunately nucleic acid selectivity of topo II is still unknown (Burden and Osheroff, 1998). This interaction is mainly dependent on the sequence and topological structure of DNA (Burden and Osheroff, 1998). Then the enzyme cleaves a double stranded piece of DNA (the gate or G segment) (Kellner *et al.*, 2002). Then two molecules of ATP bind to the enzyme causing a conformational change in its structure which initiates the other section of double stranded DNA (transported segment or T

segment) to cross through the gap created in the gate DNA (Kellner *et al.*, 2002; Lindsley and Wang, 1991). Then the gap will be bridged to reform the original DNA (Kellner *et al.*, 2002; Stuchinskaya *et al.*, 2009; Berger *et al.*, 1996). In the final step topo II hydrolyses ATP causing the release of DNA products and the enzyme is recycled (Lindsley and Wang, 1991; Miller *et al.*, 1981). The Figure 1.36 also shows where different topo II inhibitors act on the enzyme catalytic cycle.

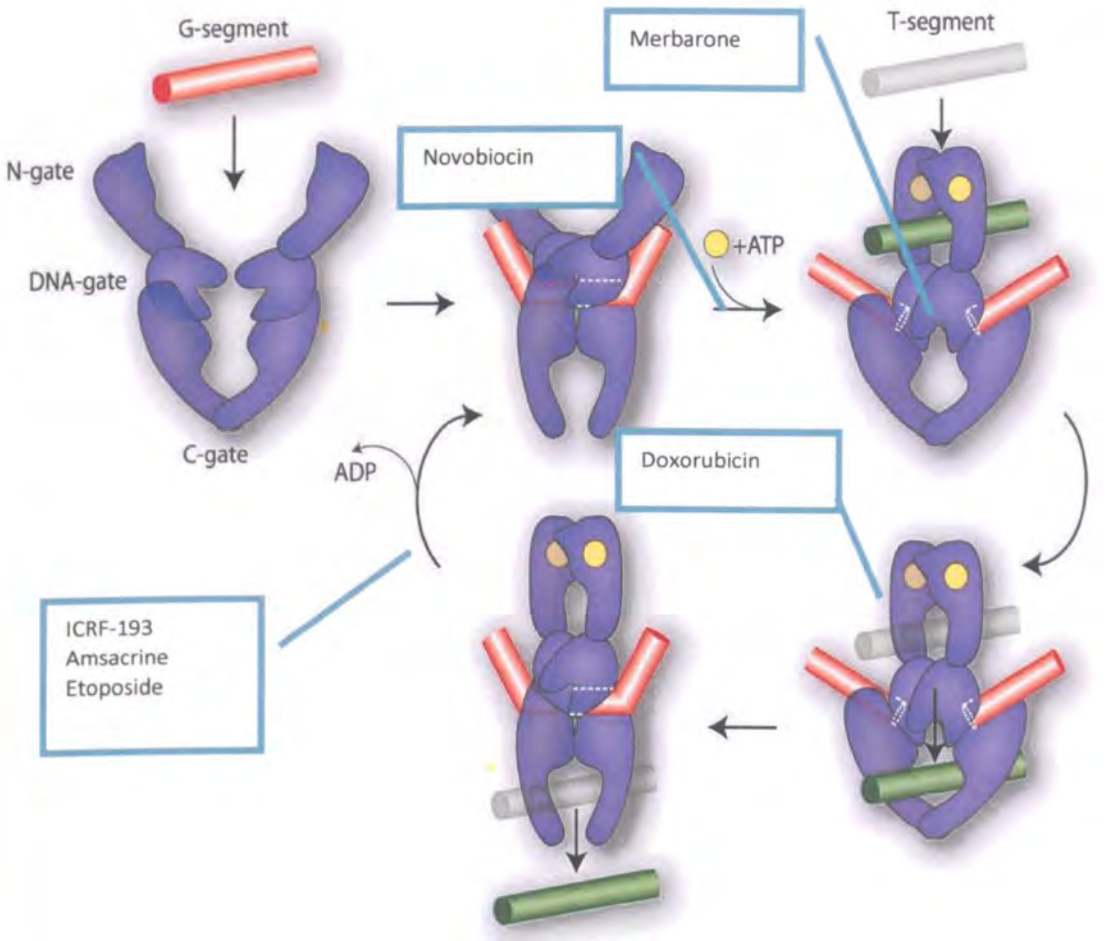

Figure 1.36 Mode of action of topoisomerase II and points of action of drug molecules (modified) (Berger *et al.*, 1996; Larsen *et al.*, 2003)

1.4.7.3 Topoisomerase II catalytic Inhibitors

Compounds including ICRF-193 (Figure 1.37), merbarone (Figure 1.38), novobiocin (Figure 1.39) and suramin (Figure 1.40) belong to this class. De-

pending on the structure, these inhibit different steps of the enzyme catalytic cycle and hence stop the enzyme from working.

ICRF-193 (Figure 1.37) is a bisdioxopiperazine derivative which is a topo II inhibitor but inert to topo I. According to Roca *et al.* (1994) it acts by converting the enzyme into a form which cannot bind to DNA. It also stabilises the ATP mediated non-covalent form of the enzyme-DNA complex (Roca *et al.*, 1994) which then inhibits the ATPase enzyme activity (Huang *et al.*, 2001).

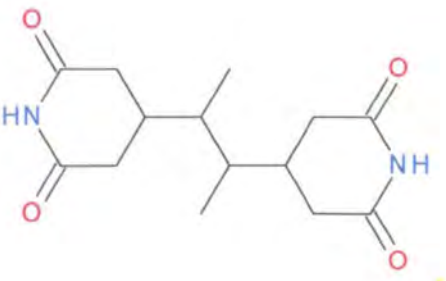

Figure 1.37 ICRF-193

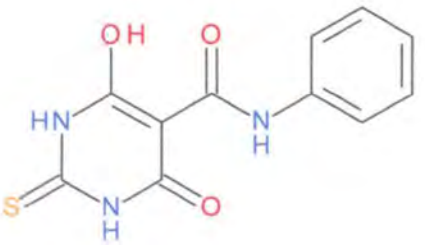

Figure 1.38 Merbarone

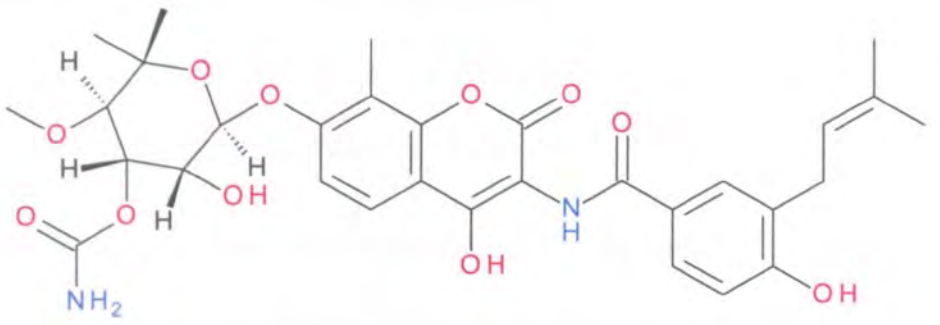

Figure 1.39 Novobiocin

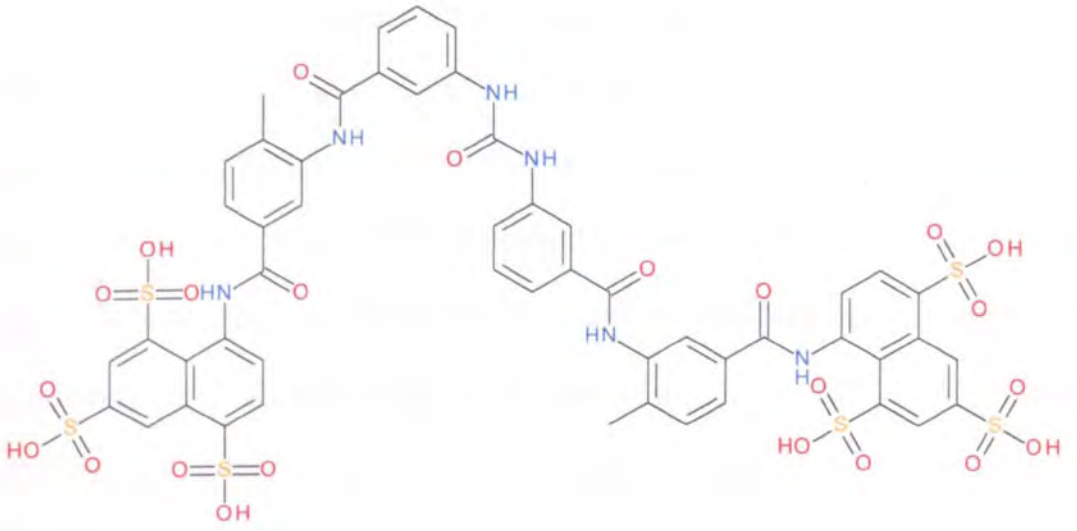

Figure 1.40 Suramin

Suramin (Figure 1.40) is an anionic compound which prevents the topo II enzyme from binding to DNA with an IC_{50} value of 5 μM (Bojanowski *et al.*, 1992). Studies show that suramin also inhibits the growth factors including fibroblast growth factor and IGF, responsible for tumour growth. Clinical use of suramin gives side effects including neuropathy and lymphopenia (Larsen *et al.*, 2003).

Chemically novobiocin (Figure 1.39) belongs to the family of coumarins. It acts as as topo II inhibitor by blocking the ATP binding site and hence halts the enzyme catalytic cycle (Gormley *et al.*, 1996).

Merbarone (Figure 1.38) is a thiobarbituric acid derivative. Though the site of action of the drug is not clear, it is suggested that the molecule interferes with the enzyme mediated DNA cleavage (Fortune and Osheroff, 1998).

1.4.7.4 Topoisomerase II Poisons

These molecules show cytotoxicity by stabilising the DNA-topoisomerase II covalent complex. Relegation of the cleaved DNA is prevented and hence making permanent double strand DNA breaks which ultimately leads to cell death. Etoposide (Figure 1.41) and mitoxantrone (Figure 1.42) are examples of this kind of topo II poisons. Etoposide is a semisynthetic analogue of the phytochemical epipodophyllotoxin (4′ -demethylepipodophyllin benzylidene glucoside), which is also an isomer of another natural phytochemical, phodo-phyllotoxin. Etoposide is used in the treatment of number of cancers such as lung and testicular.

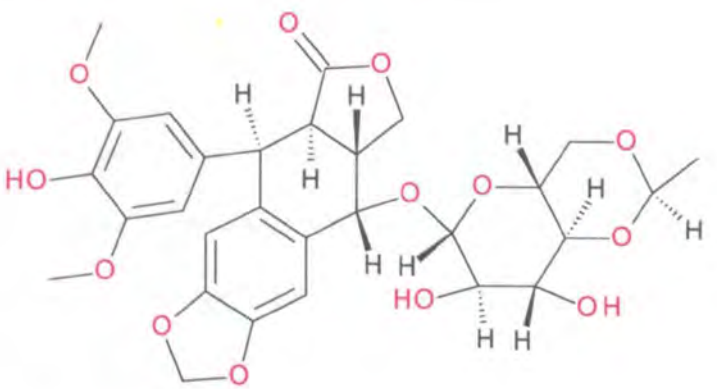

Figure 1.41 Etoposide

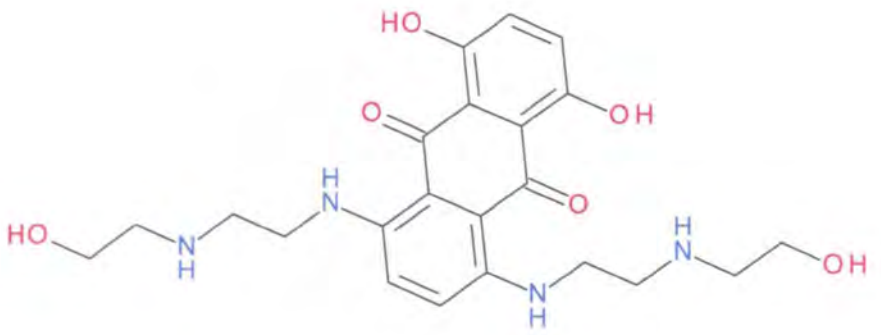

Figure 1.42 Mitoxantrone

It acts at the relegation step of topo II cycle preventing the rejoining of cleaved DNA strand. Etoposide is a poor water soluble drug and needs to be formulated with polysorbate 80 or polyethylene glycol to achieve the desired bioavailability (Hande, 1998).

Mitoxantrone causes the topo II poisoning effect by stabilising the DNA-topo II complex. It can also inhibit the RNA polymerase during transcription. The main difference between etoposide and mitoxantrone is that mitoxantrone is a DNA-intercalating topo II poison whereas etoposide is not (Avendaño and Menendez, 2008). Doxorubicin acts as a topo II poison by forming a stable drug-DNA-topo II compex. In addition doxorubicin is a minor groove binder of DNA.

The drawback of using topoisomerase poisons is that tumour cells can become resistant due to mutations occurring in the enzyme, which reduces the interaction between enzyme and drug. Amsacrine (Figure 1.43) and ellipticine (Figure 1.44) are two other molecules which also act as topoisomerase II poisons. Amsacrine is clinically used in leukaemia (Louie and Issell, 1985).

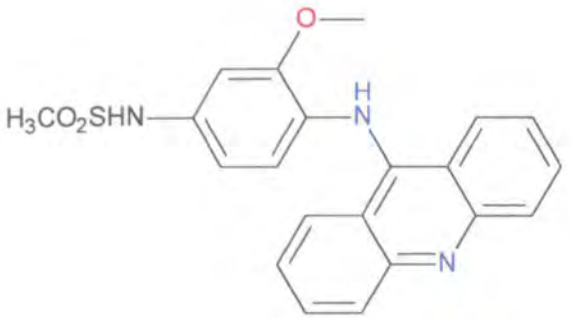

Figure 1.43 Amsacrine

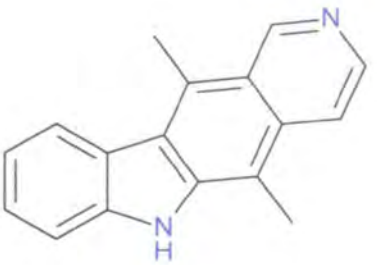

Figure 1.44 Ellipticine

1.4.8 Drugs which interact with DNA reversibly

There are two types of reversible drug-DNA interactions observed in relation to anticancer activity. These are groove binding and intercalation.

1.4.8.1 Groove binders

Based on their binding location, molecules which groove-bind to DNA are classified into two groups; major or minor groove binders. Generally big molecules like proteins hydrogen bond in the major groove (see section 1.3). The donor, acceptor moieties and the specific orientation of the DNA at the binding site makes it different from minor groove binding (Hamilton and Arya, 2012; Xiong and Sundaralingam, 2001)

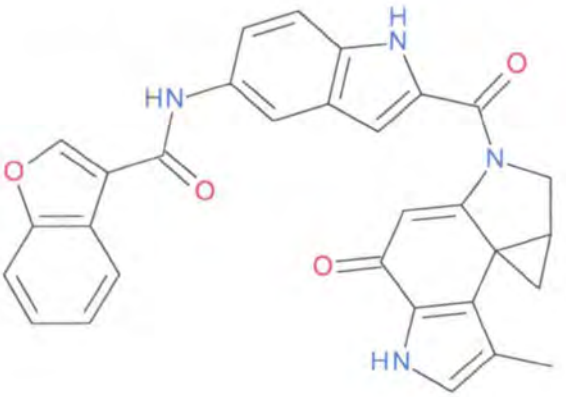

Figure 1.45 Adozelesin

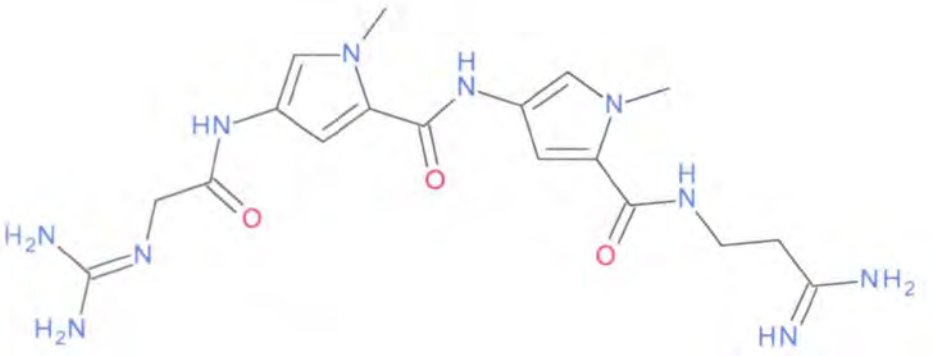

Figure 1.46 Netropsin

Most DNA minor groove binders have been shown to have good DNA-sequence specificity. These compounds are non-symmetrical and are mostly curved in shape having different types of aromatic rings fused together. These structural features of the molecules allow them to bind at minor groove with the best fit. It is suggested that electrostatic and hydrophobic interactions drive the binding. Further Van der Waals forces and hydrogen bonding between ligand and DNA helps the binding (Reddy *et al.*, 1999).

Minor groove binders are an important group of compounds in terms anticancer drug development as they serve as models of drug-DNA interactions. Though molecules including adozelesin (Figure 1.45) showed good *in vitro* anticancer activity, clinical use of that drug was hindered because of its marginal efficacy on metastatic breast cancer in phase II trials (Baraldi *et al.*, 2004).

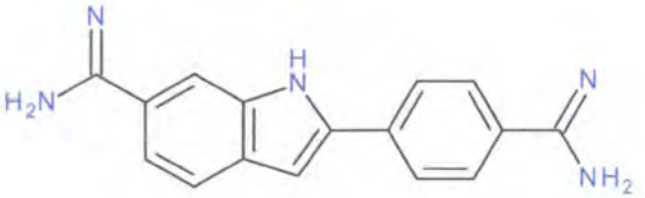

Figure 1.47 DAPI (4',6-diamino-2-phenylindole)

Distamycin, netropsin (Figure 1.46) and DAPI (4', 6-diamino-2-phenylindole) (Figure 1.47) are examples of minor groove-binders. In the last 20 years much progress has been made to increase the efficacy of these compounds, for example derivatives of distamycin have been investigated by attaching alkylamino sidechains and halogens in various positions in attempts to increase the anticancer activity and minimise side effects and toxicity to healthy tissues (Baraldi *et al.*, 2004).

Because of its fluorescent properties, DAPI is used as a nuclear specific cell-staining agent. It binds to DNA preferably to AT rich regions in the minor groove of the DNA (Tanious *et al.*, 1992; Eriksson *et al.*, 1993). It was used in the current project as nuclear stain (see section 3.9).

1.4.8.2 Intercalators

Intercalators are important reversible DNA binders, which are often studied for their anticancer activity. In 1961, Lerman investigated the interaction of acridine (Figure 1.48), acridine orange (Figure 1.49) and proflavine (Figure 1.50) with DNA and stated that planar polycyclic aromatic compounds could intercalate into DNA (Lerman, 1961). Later, in 1965, Waring studied and characterised the DNA-ethidium bromide complex using UV spectrophotometry (Waring, 1965).

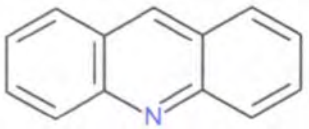

Figure 1.48 Acridine

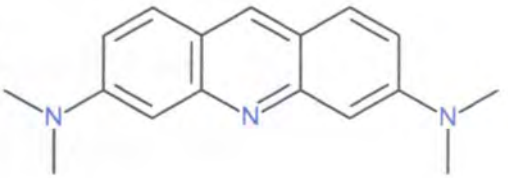

Figure 1.49 Acridine orange

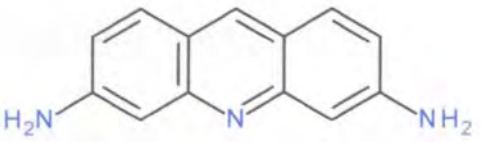

Figure 1.50 Proflavin

A few years later, in 1968 Muller investigated the physico-chemical properties involved in the DNA intercalation of actinomycin D (Figure 1.51) and suggested that the DNA sequence plays an important role in DNA-small molecule interactions (Müller and Crothers, 1968). All of these studies have driven further research on polycyclic aromatic compounds as potential DNA-intercalators.

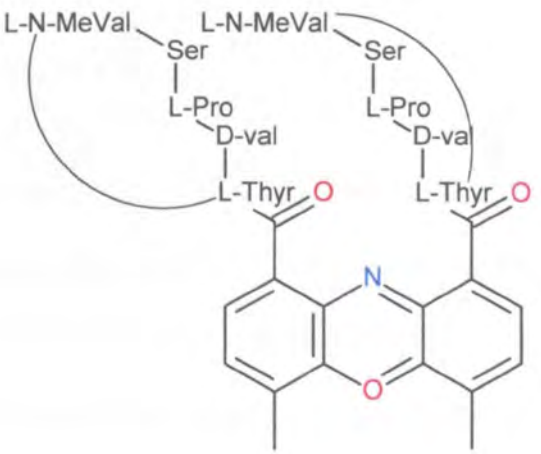

Figure 1.51 Actinomycin D

According to Graves and Velea (2000) to be able to classify a molecule as a DNA intercalator, it should have three basic features. One is the molecule should be planar in order to be able to slip between the DNA base pairs, the second is that it should possess a positive charge so that it can interact with the negatively charged phosphate backbone and the third requirement is that it should be poly-aromatic compound to give the best geometrical overlap with the base pairs (Graves and Velea, 2000).

Broadly, intercalators can be placed into two classes. One is parallel intercalators which do not have additional bulky groups along their long axis and their aromatic system is relatively parallel to the base pairs (Comba and Boeyens, 2010). Molecules including eithidium bromide (Figure 1.52) and proflavine belong to this class.

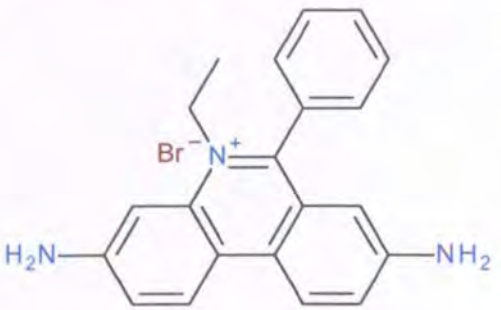

Figure 1.52 Ethidium bromide

Molecules of the second type are called perpendicular intercalators, which contain bulky functional groups on one or both sides of the molecule along the long axis (Figure 1.54). Long axis of these molecules will be perpendicular to the basepairs at the intercalation site. Compounds including doxorubicin (Figure 1.53) and daunomycin belong to this group (Comba and Boeyens, 2010).

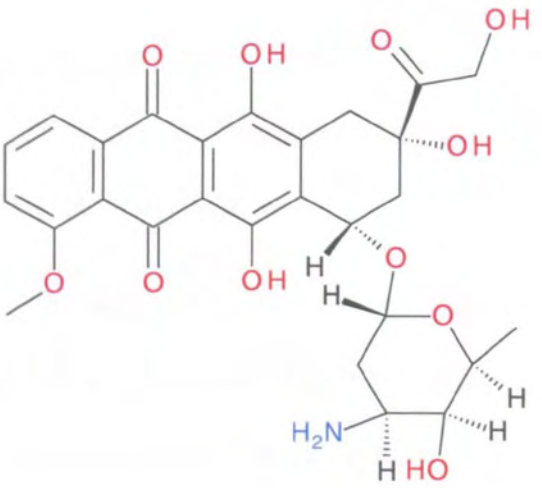

Figure 1.53 Doxorubicin

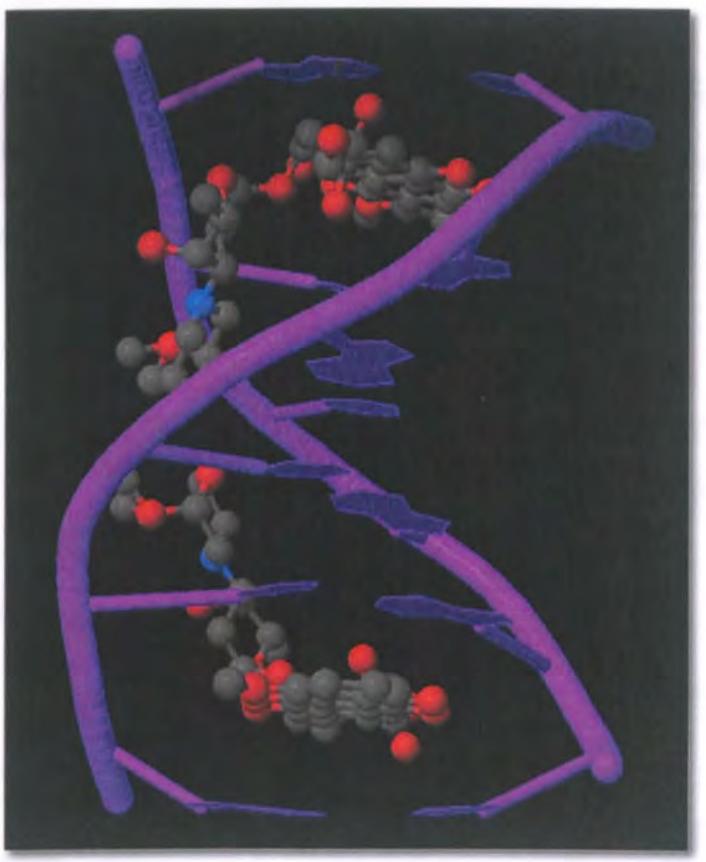

Figure 1.54 Figure showing perpendicular intercalation of doxorubicin in to DNA, where green=guanine, yellow=cytosine, red=adinine, blue=thiamine (Howerton *et al.*, 2003).

"The mechanism of DNA intercalation is similar to inclusion of a false coin into a roll of pennies" (Lerman, 1961). Planar molecules such as acridine slip between the base pairs by causing the extension of the DNA helical structure and shifting the bases from the binding site in the opposite direction along the long axis of DNA (Williams *et al.*, 1992).

When the insertion of the ligand occurs, the energy of the DNA-ligand complex is optimised through electrostatic and π-stacking interactions (Martinez and Chacon-Garcia, 2005; Mukherjee *et al.*, 2008).

In 1992 Loren and his team proposed that, in parallel intercalation, DNA is unwound at the site of intercalation, and the DNA helix is also slightly distorted in the surrounding area of the intercalation. Whereas as in perpendicular intercalation, unwinding of DNA talks place to a larger extent and the distortion of helical structure is also transmitted to longer distances from the site of intercalation along the helical axis of DNA (Figure 1.55).

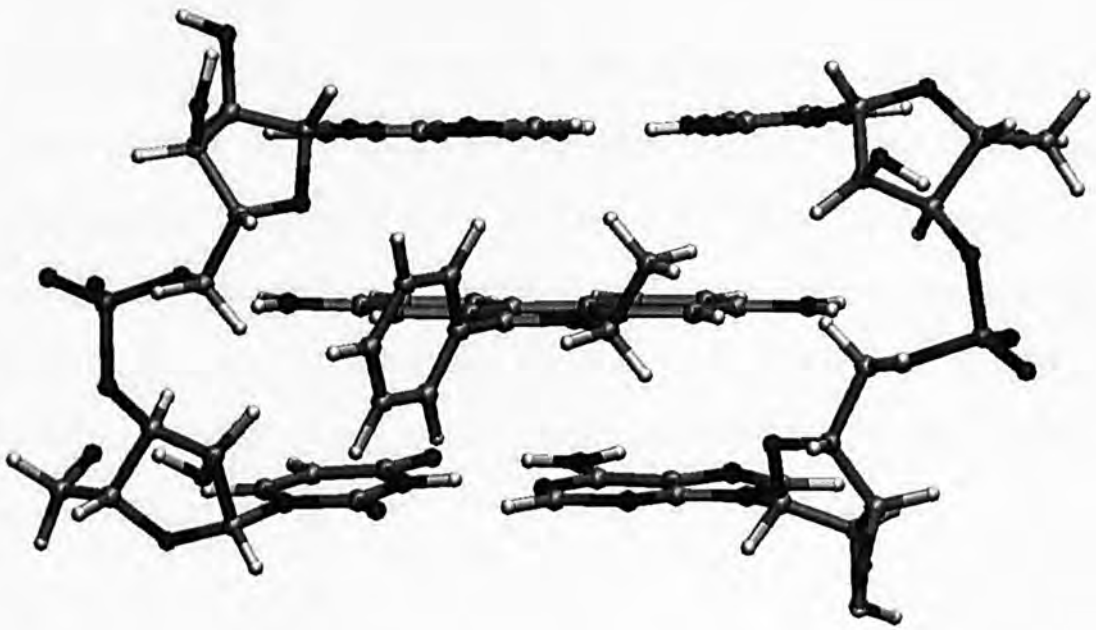

Figure 1.55 Figure showing parallel intercalation of ethidium bromide in to DNA (R˘eha *et al.*, 2002)

Once DNA intercalation takes place, physiological enzymes (including topoisomerases) which act on DNA, will not be able to function which can then induce apoptosis. Although normal healthy cells are also prone to cytotoxicity, on treatment with intercalators, fast dividing cells, which includes many cancer cells, are affected more than healthy cells (Martinez and Chacon-Garcia, 2005; Baguley, 1991).

Over the past decade, a lot of research has been carried out in this area modifying the structures of intercalating drugs including, doxorubicin and mitoxantrone (Gresh and Kahn, 1990; Mewes *et al.*, 1994; Nagy *et al.*, 1996). cryptolepines are an excellent example among intercalators, structural modification of these molecules showed promising results (R˘eha *et al.*, 2002; Wright *et al.*, 2001; Chhikara *et al.*, 2011; Seville *et al.*, 2007a).

1.4.8.3 Cryptolepine

Cryptolepine **(1)** (Figure 1.56) is an alkaloid found in the roots of the West African climbing shrubs known as *Cryptolepis triangularis and Cryptolepis sanguinolenta*. Its synthetic name is 5-methyl-10*H*-indolo [3, 2-b]quinolone. Although cryptolepine**(1)** was identified in an extract of *cryptolepis triangularis* by Clinquart in 1929 (Clinquart, 1929), it was first synthesised for its potential use as a dye by Fichter and Boehringer in 1906 (Fichter and Boehringer, 1906).

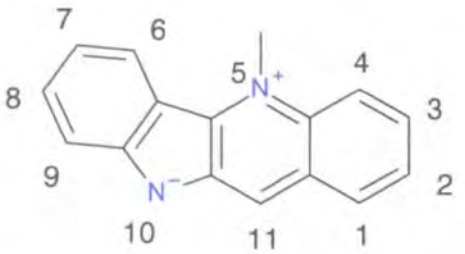

(1)

Figure 1.56 Cryptolepine

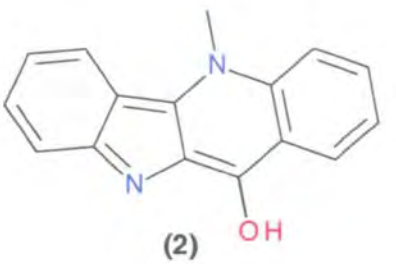

(2)

Figure 1.57 11-hydroxy cryptolepine

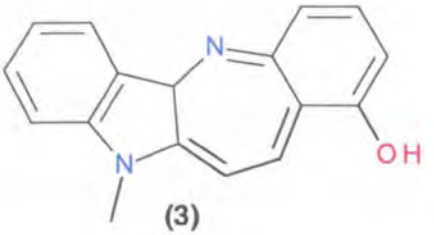

(3)

Figure 1.58 12-hydroxy cryptoheptine

Along with cryptolepine **(1)**, there are other natural analogues which have been isolated from plants including 11-hydroxycryptolepine **(2)** (Figure 1.57), 12-hydroxycryptoheptine (Figure 1.58), neocryptolepine**(4)** (Figure 1.59) and isocryptolpine (Figure 1.59) (Cimanga *et al.,* 1996; Cimanga *et al.,* 1997; Cimanga *et al.,* 1998).

Neocryptolepine **(4)** is an isomer of cryptolepine **(1)** also found in cryptolepis sanguinolenta (Cimanga *et al.,* 1997). In Africa, a crude extract of this plant was traditionally used for the treatment of multiple diseases including hypertension, diabetes, inflammation and bacterial infections (Wright, 2007; Oyekan, 1995; Fabry *et al.,* 1998; Kaou *et al.,* 2008; Boye, G. L., Ampofo, O., 1983).

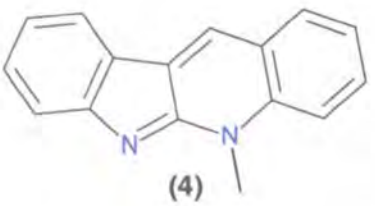

(4)

Figure 1.59 Neocryptolepine

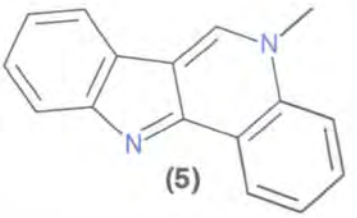

(5)

Figure 1.60 isocryptolepine

A commercial preparation containing ground roots of *C.sanguinolenta*, called Phyto-Laria is also available (Fabry *et al.,* 1998; Willcox *et al.*, 2004).

Although cryptolepine**(1)** showed a range of pharmacological activities, after discovery of its anticancer activity, research work has been done on this in order to increase its potency. Many analogues have been made by modifying different positions of the molecule and some of these are more potent than the original drug (Wright *et al.,* 2001; Onyeibor *et al.,* 2005; Lavrado *et al.,* 2008a).

1.4.8.3.1 Pharmacological activities of cryptolpeine and structural activity relations

1.4.8.3.1.1 Antihyperglycemic activity

Cryptolepine**(1)** not only has hypoglycaemic activity but also possess hypolipidemic activity (Ajayi *et al.,* 2012). This is due to its ability to reduce glucose absorption and enhance beta cell functioning (Ajayi *et al.,* 2012; Bierer *et al.,* 1998). Bierer tested cryptolepine **(1)** on murine 3T3-L1 preadipocytes and showed that it has caused a reduction in the glucose absorption (Bierer *et al.,* 1997; Bierer *et al.,* 1998). Upon cryptolepine treatment, improved beta cell functioning was observed in the histograph of rat pancreas as a result of cell hypertrophy, which probably will have an indirect effect on insulin produc-

tion (Ajayi *et al.*, 2012). At molecular level, the exact mechanism of its anti-diabetic activity is still unknown.

In 1997, Bierer and co-workers synthesised a series of cryptolepine analogues**(6)** (Figure 1.61) as potential anti-hyperglyemic agents. Based on QSAR studies, increasing the alkyl side chain length at the N5 position increased the activity dramatically.

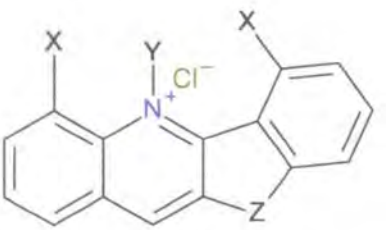

(6)

Z=NH, O, S, CH_2 X= H, OMe, F Z= Me, Et

Figure 1.61 Showing cryptolepinederivatives with antihyperglycemic activity

This may be due to increased lipophilicity of the molecule. Similarly, addition of a methoxy group at position 4 also increased the activity significantly. In contrast, addition of ethyl and butyl side chains at the N5 position made the derivatives more toxic. Cryptolepine and 11-methoxy cryptolepine showed the best anti-hyperglycemic activity with the lowest toxicity profiles (Dubenko *et al.*, 1997; Bierer, 1999; Bierer, 1997).

1.4.8.3.1.2 Antimalarial

In vitro, cryptolepine**(1)** showed the antimalarial activity with an IC_{50} value of 0.27 and 0.44 µM on chloroquin-sensitive and chloroquin resistant-strains of *P. Falciparum* respectively (Wright *et al.*, 2001).

In 2001, Wright and his co-workers synthesised a series of cryptolepine derivatives having halogens and nitro groups (Figure 1.62) on different positions of the molecule. When the compounds were tested against the *plasmodium falciparum* parasites *in vitro*, they found that the 2, 7-dibromo derivative (Figure 1.63) showed highest activity on chloroquine sensitive parasites. It also suppressed the *plasmodium berghei* parasites *in vivo* (mice) up to 89%. This group also demonstrated that antimalarial activity of the derivatives does not depend on their intercalation capacity (Wright *et al.*, 2001).

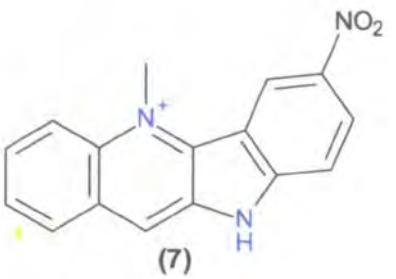

(7)

Figure 1.62 7-Nitrocryptolepine

In 2004, Van Miert investigated the antimalarial activity of neocryptolepine, and its derivatives *in vitro* on *Plasmodium falciparum* and found that 2-bromoderivatives**(8)** showed higher and more selective activity than the parent compound (Van Miert *et al.*, 2004).

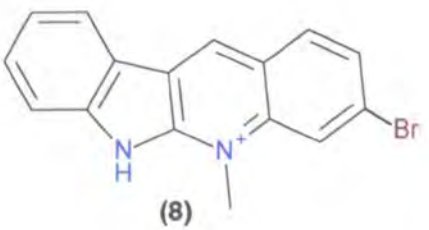

(8)

Figure 1.63 2-Bromocryptolepine

In 2010, Larvado synthesised library of cryptolepine derivatives having alkylamino side chains**(9)** (Figure 1.64) and halogen substituents and tested them against *Plasmodium falciparum* parasites *in vitro* and concluded that they showed significant increase in activity (Example: IC50 = 51 ±5 nM, Figure 1.64) compared to chloroquine (IC50 = 138 ±15 nM).

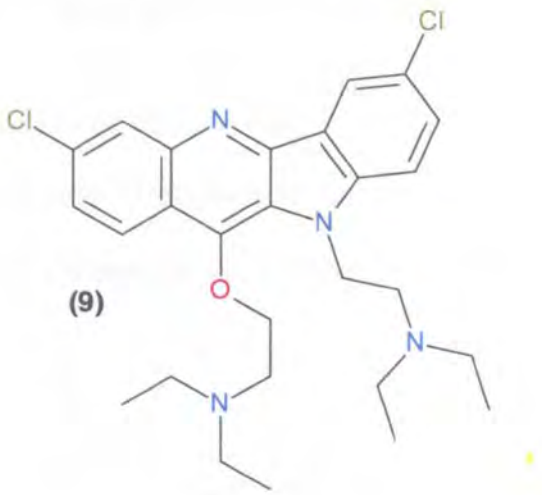

(9)

Figure 1.64 Showing a derivative having alkylamino side chains shown highest activity (IC_{50} = 51 ±5 nM)

1.4.8.3.1.3 Other parasites

In 2012 larvado *et al* demonstrated that adding alkylamino sidechains at 11- and 5 positions of cryptolpeine increased the anti-parasitic activity against *Trypanosoma brucei brucei*. More importantly, placing a piperazin-1-amine group at the 11-position**(10)** (Figure 1.65) increased the activity significantly (IC_{50} 10 nM) along with greater selectivity towards the same parasite.

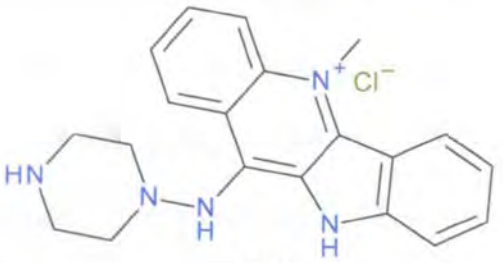

(10)

Figure 1.65 Showing derivative having alkylamino side chain

In 2012, Hazra *et al* showed that 2,7-dibromo cryptolepine**(11)** (Figure 1.66) has anti leishmanial activity. They tested the molecule on *Leishmania donovani* parasites and and recorded an IC_{50} value of 1.6 µM (Hazra *et al.*, 2012).

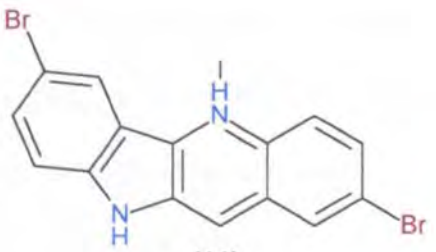

(11)

Figure 1.66 2,7-dibromocryptolepine

1.4.8.3.1.4 Anti-inflammatory

In 2009, Olajide, Wright and co-workers tested cryptolepine on rats for anti-inflammatory activity; they tested cryptolepine at a dose of 10-40mg/kg on rats, and reported that it showed a dose dependent reduction in carrageenan-induced rat paw oedema and pleurisy (Olajide *et al.*, 2009).

The same group also demonstrated that cryptolepine showed a dose dependent anti-inflammatory activity by reducing the micro-vascular permeability in mice. It also showed analgesic activity against acetic acid induced writhing in mice. In 2013, the same group showed that plant extract of cryptolepis san-

guinolenta and cryptolepine alone possess anti neuroinflammatory properties, they tested both plant extract and pure cryptolepine on neuroinflammtion induced IL-1B in neuroblastoma cells and concluded that inflammatory factors were inhibited in both cases significantly (Olajide *et al.*, 2013).

1.4.8.3.1.5 Anticancer activity

Cryptolepine showed anti-tumoural activity on different cancer cell lines. Among the different primary cultures of patient tumour samples, cryptolepine showed greater sensitivity on breast cancer cells. It showed greater activity on haematological tumors when compared to solid tumors. The average IC_{50} value on solid tumours was 2.8 µM whereas on haematological malignancies it gave an IC_{50} value of 1 µM (Laryea *et al.*, 2009). This group also showed that along with topo II activity, the cytotoxicity of cryptolepine also depends on P53, a tumor suppressor protein which regulates the cell cycle. IC_{50} values of 1.4 µM and 12.7 µM were observed on HCT116-P53+/+ and HCT 116-P53-/- cells respectively (Laryea *et al.*, 2009). In these tested cell lines the anti-tumour activity of cryptolepine was not affected by any resistance mechanism found so far (Laryea *et al.*, 2009). This was shown using Pearson's correlation coefficients, which compares the resistant-gene correlation between cells treated by cryptolepine and a series of other anticancer drugs. See Table 1.1 for cytotoxicity of cryptolepine against a range of cell lines.

Cell type	IC_{50} values of cryptolepine in µM	Reference
VERO	3.2	(Zhu *et al.*, 2007)
B16 melanoma cells	1.3	(Bonjean *et al.*, 1998)
Mouth epidermoid carcinoma (KB) cells	1.3	(Bailly *et al.*, 2000)
Human leukaemia (HL-60) cells,	3.2	(Dassonneville *et al.*, 2000)

Promyclocytic leukaemia (HL-60/MX2) and	7.4	(Dassonneville *et al.*, 2000)
Murine leukaemia (P388) cells	0.94	(Dassonneville *et al.*, 2000)
Human osteosarcoma (MG63) cells	>0.5	(Matsui *et al.*, 2007)
MAC15A cells	67.2 ± 26.3	(Wright *et al.*, 2001)
Human bladder carcinoma Epithelial (RT112)	0.80	(Seville *et al.*, 2007b)
Human pleural effusion Adenocarcinoma (H460)	1.45	(Seville *et al.*, 2007b)
Biliary epithelial (BE) cells	1.28	(Seville *et al.*, 2007b)
human umbilical vein endothelial cells (HUVEC)	1180 ± 1	(Lavrado *et al.*, 2008a)
murine myoblast-derived (L6) cells	1.5()	(Arzel *et al.*, 2001)
Chinese hamster lung cells (V79)	2.1	(Ansah *et al.*, 2005)

Table 1.1 Showing cytotoxic activity of cryptolepine against various cancer cell lines.

Upon exposing MAC15a cell lines for 1 hour and 96 hours separately to cryptolepine, it showed considerable activities with IC_{50} values of 67.2 ± 26.3 μM and 9.65 ± 1.37 μM respectively (Wright *et al.*, 2001). Cryptolepine has shown lower toxicity against non-tumour HUVEC cells with an IC_{50} value of 1180 ± 1 μM which may indicates that cryptolepine is more active towards cancer cells than the normal cells.

Cell cycle changes upon treatment with cryptolepine were studied and it came under light that cryptolepine induces apoptosis in HL-leukaemia cells. Based on the experimental results the same group also suggested that cryptolepine must have produced cell death signals other than topo-II associated DNA breakage (Dassonneville *et al.*, 2000).

Cryptolepine shows cytotoxcicity by interacting with DNA (Wright *et al.*, 2001; Gokcek *et al.*, 2000) and it is 4-5 times potent than ellipticine on mouse me-

lanoma cells. Based on all of the studies above it has been suggested that cryptolepine derivatives are suitable leads for the development of anti-cancer agents (Bonjean *et al.,* 1998). It has been found that addition of electron donating or with drawing groups at different positions (Figure 1.67) on the molecule lead to changes in the anticancer activity, for example addition of a N-[4-(methanesulfonoamido)-2-methoxyphenyl] amino group at the 11-position showed greater activity on haematological tumour cells compared to the original molecule (Chang *et al.,* 1992; Takeuchi *et al.,* 1992).

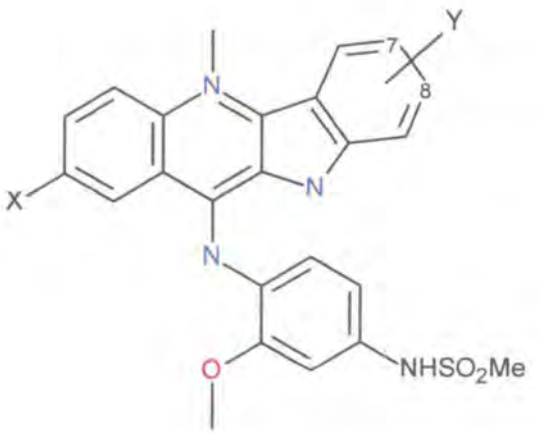

X = H, NH-galactopyranosyl

Y = 7-NO_2, 7-NH_2, 7-NHCOMe,
7-NH-glucopyranosyl,
8-NH-galactopyranosyl

Figure 1.67 showing various modifications of cryptolepine

Addition of electron withdrawing group, amino group at the 7-posiion also showed increased cytotoxicity than the parent compound, however addition of nitro group at the same position led to reduction in the activity significantly (Takeuchi *et al.,* 1992). Introduction of a glalctopyranosylamino group at the C-2 and C-8 positions reduced the activity however, introduction of glucopy-ranosyl group has shown greater activity than cryptolepine (Takeuchi *et al.,* 1992). Further studies were carried out by Wright and his team by the intro-duction of halogens at different positions of the ring on the cryptolepine (Wright *et al.,* 2001). It was found that the 9, 11-dichlorocryptolepine**(12)**

(Figure 1.68) is five times more cytotoxic than the parent molecule (Wright *et al.*, 2001).

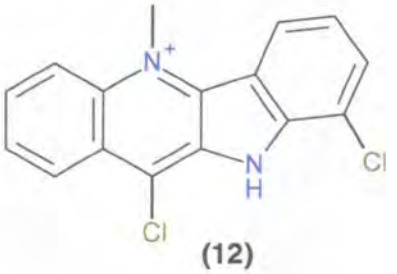

(12)

Figure 1.68 9, 11-dichlorocryptolepine

1.4.8.3.1.6 Mode of action of cryptolepine as an anticancer agent

Cryptolepine acts as an anticancer agent not only by interclating into DNA but also by inhibiting the topo II (Lisgarten *et al.*, 2002b). Lisgarten conducted a Ren and Chaires competition dialysis experiment to see which of the DNA sequences cryptolpepine is interacting with. In this assay, a range of nucleic acid sequences is dialysed against a test ligand solution. After equilibrium is established, the amount of ligand bound to each sequence is determined by spectrophotometry (Ragazzon *et al.*, 2007; Chaires, 2005).

They used both alternating and non-alternating CG, and alternating and non-alternating AT sequences of DNA. The results showed that the molecule preferably intercalates into DNA at GC rich sequences having non-alternating CC sites over AT rich sequences (Lisgarten *et al.*, 2002b).

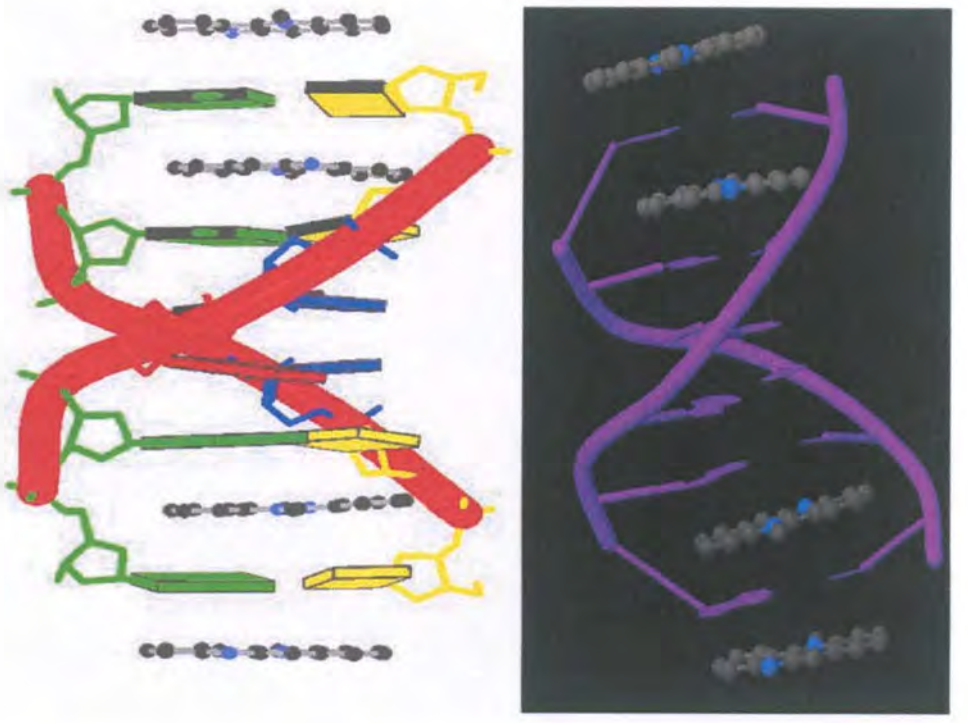

Figure 1.69 Figure showing cryptolepine intercalating in to DNA, where green=guanine, yellow=cytosine, red=adinine, blue=thiamine (Lisgarten *et al.*, 2002b)

When there are two guanine bases on one DNA strand binding to two cytosines on the other, this particular site gives good stacking for the cryptolepine structure. Cryptolepine is an asymmetric molecule so the asymmetric space provided between the Cytosine-Cytosine sites favours the interaction (Figure 1.69). These interactions between cryptolepine and bases are not identified as hydrogen bonding, suggesting that the π-stacking forces between the ligand and DNA bases cause these interactions (Figure 1.70) (Lisgarten*et al.*, 2002); (Guittat *et al.*, 2003a).

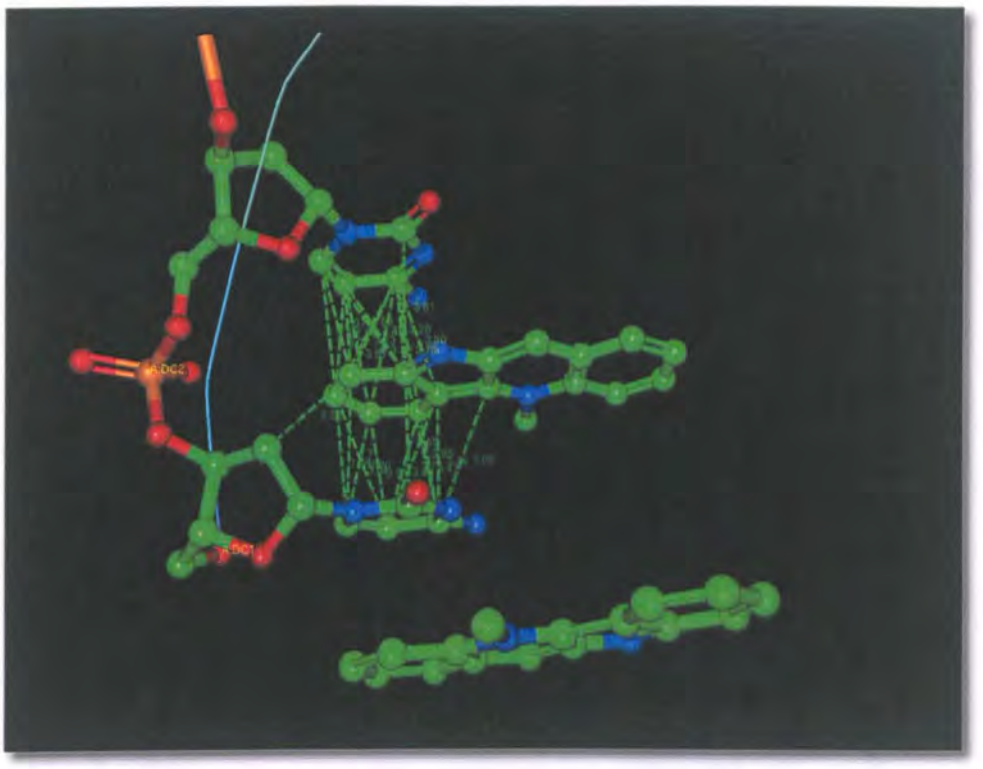

Figure 1.70 Figure showing interaction between crptolepine and DNA bases, molecular interaction redrawn from (Lisgarten *et al.*, 2002b)

These stacking interactions confirm that alkaloid is aligned parallel to the Watson crick base pair hydrogen bonds. While all this happening, positively charged cryptolepine penetrates deeply in to the helical stack forming strong hydrophobic interactions with DNA base pairs and aligning itself to the centre of the helix where the negative electrostatic potential is maximum (Lisgarten *et al.*, 2002b). In terms of DNA-binding affinity, cryptolepine showed similar strength to established intercalators such as actininomycin D, daunomycinand chromomycin (Lisgarten *et al.*, 2002a).

1.4.8.3.2 G-quadruplex DNA binding of cryptolepines

Telomeres are the terminal DNA-protein complexes which possess distinct structural and functional features compared to other DNA sequences (Blackburn, 1991). The word telomere is derived from two greek words; telos

means end and meros means part. Teleomere sequences are rich in guanine and are made by ribonucleoprotein telomerase. The repetition of these guanine rich telomeres form quadruplex DNA structures also called as G-quadruplexes (Parkinson *et al.,* 2002) (Figure 1.71).

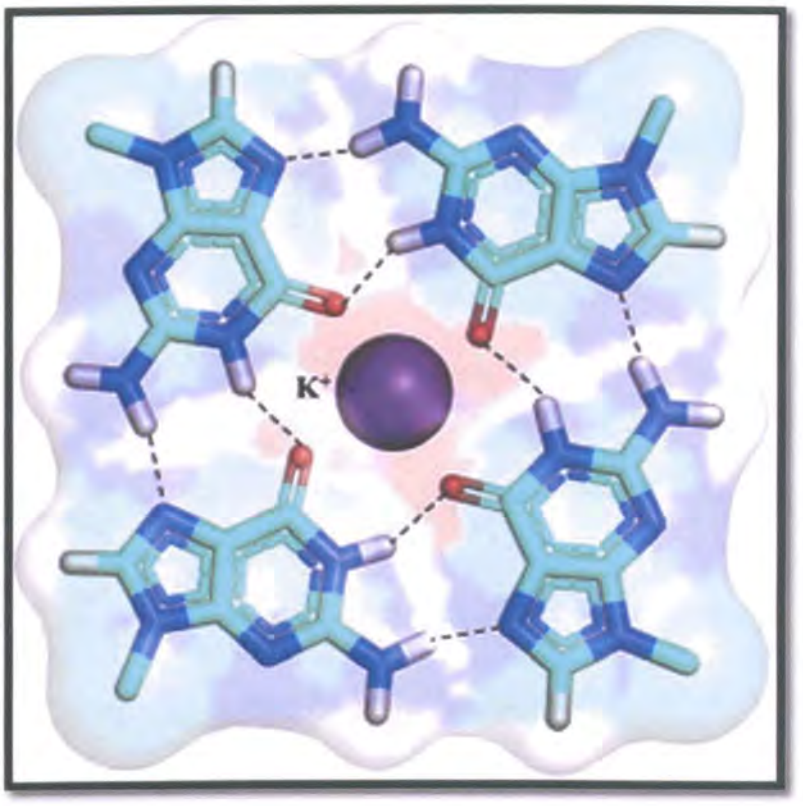

Figure 1.71 showing a G-quadruplex

The 3' end terminal region of telomerase has guanine rich single strand of DNA which folds itself in to a G-quadruplex (Figure 1.72), which has been shown to stop the elongation of teleomeres (Sen and Gilbert, 1988; Sen and Gilbert, 1991).

Teleomers are important in protecting the ends while the chromosomal DNA undergoes full replication. Mostly telomersase (Figure 1.73) is expressed in cancer cells, stabilisation of these G-quadruplexes can lead to complications in telomerase elongation and prevent proliferation of cancer cells.

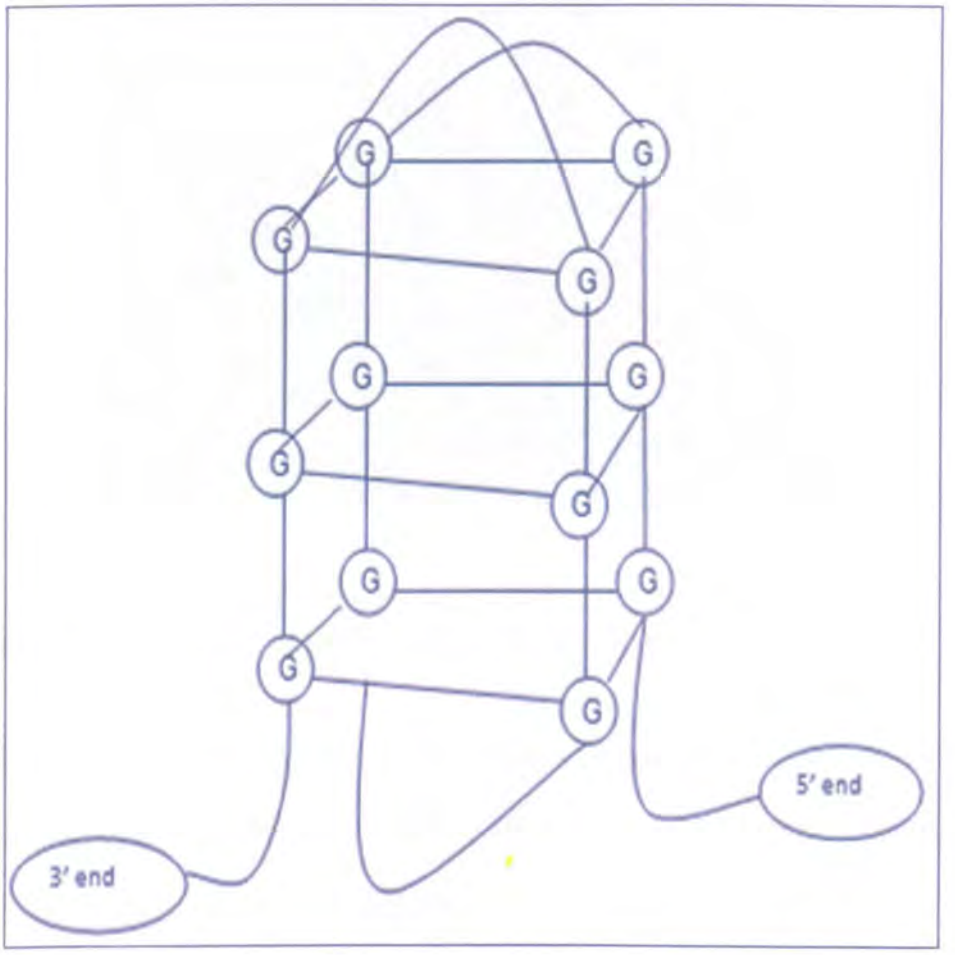

Figure 1.72 G-quadruplex structural arrangement

In the past 10 years G-quadruplexes have been of great interest as targets in oncology, attempts have been made to target these structures with some naturally occurring cryptolepines and their analogues. (Neidle and Parkinson, 2002; Mergny *et al.*, 2002; Lavrado *et al.*, 2010a; Xu *et al.*, 2011). Besides duplex DNA, cryptolepine has been shown to bind to other DNA structures including triplexes and G-quadruplexes, however its affinity towards duplex DNA is higher than for G-quadruplxes (Guittat *et al.*, 2003b).

Figure 1.73 Showing presence of telomerase at chromosomal tips via immunofluorescence (Jaskelioff *et al.*, 2010)

Although both cryptolepine and neocryptolepine are weak G-quadruplex stabilisers, comparatively neocryptolepine showed slightly higher binding affinity towards the AG22 (G-quadruplex) sequence than cryptolepine (Guittat *et al.*, 2003b). This could be due to the changes in the shape or symmetry of the molecule.

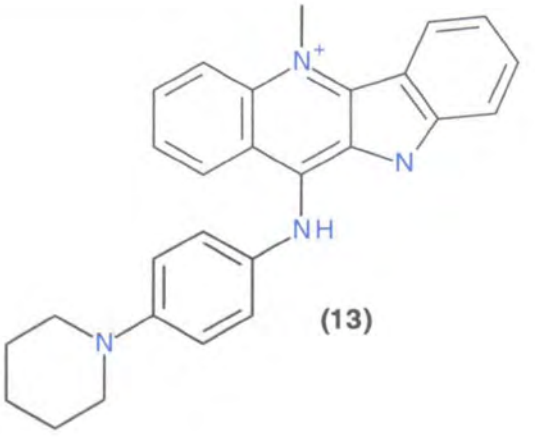

(13)

Figure 1.74 NSC748394

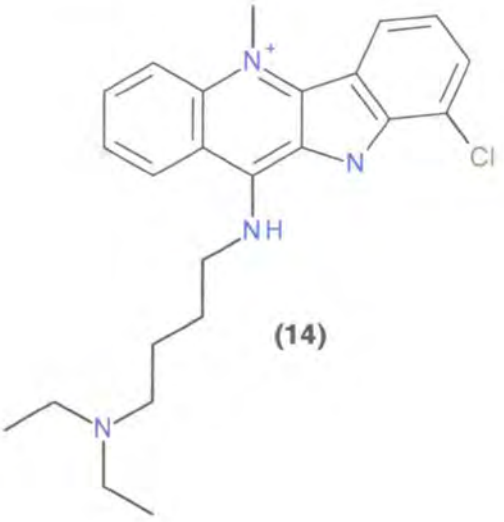

(14)

Figure 1.75 NSC748393

In 2010 Lavrado and his team made a series of cryptolepine derivatives attaching diaminoalkyl sidechains (

Figure 1.74 and 1.75) and showed that these derivatives possess good G-quadruplex stabilising capacity. In this study they have shown that attaching cycloalkyl or aromatic chain at the 11-position**(13)** (Figure 1.74) significantly reduced the G-quadruplex DNA stabilising effect (change in DNA melting temperature, ΔT_m = 4.2 °C). Whereas having linear alkylamino sidechain **(14)** (Figure 1.75) increased the G-quadruplex DNA stabilisation (ΔT_m = 20.9 °C).

1.5 Synthesis of cryptolepine

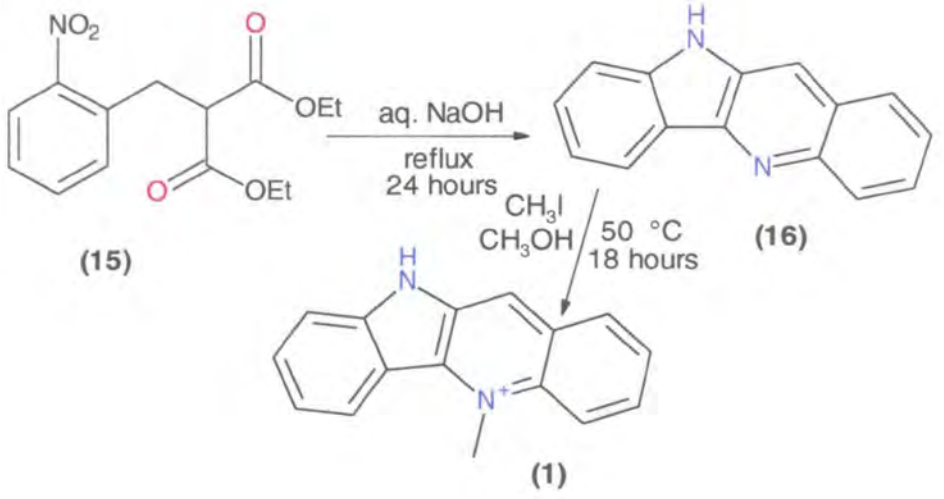

Figure 1.76 Synthesis of cryptolepine by Fichter and Boehringer

Cryptolpeine was first synthesised by Fichter and Boehringer in 1906. O-nitrobenzyl malonic ester**(15)** was heated to reflux in the presence of aqueous sodium hydroxide to give quindoline**(16)** which was then methylated using methyl iodide in the presence of methanol to give cryptolpine**(1)** as a yellow dye with an overall yield of 3% (Figure 1.76) (Fichter and Boehringer, 1906).

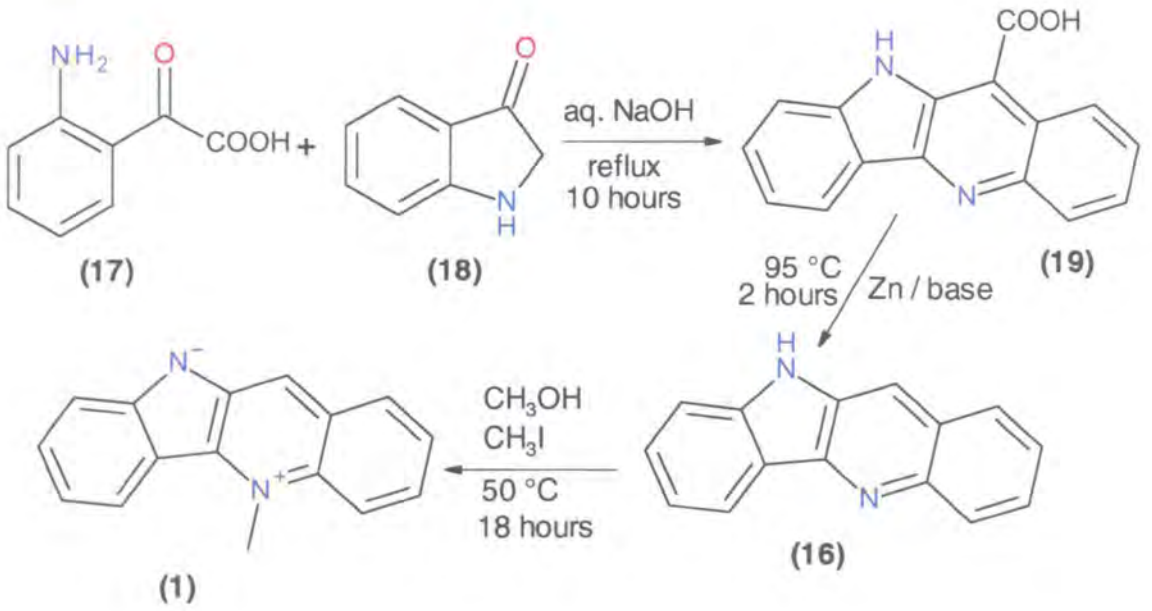

Figure 1.77 Scheme Synthesis of cryptolepine by Fichter and Rohner

Later Fichter and Rohner worked further on the synthesis to improve the yield by using isatinic acid**(17)** and indoxyl**(18)** as starting materials to produce quindoline-11-carboxylic acid as an intermediate. Decorboxylation of this gave quindoline**(16)** and then methylation gave cryptolpeine**(1)** with an overall yield of 8% (Figure 1.77) (Fichter and Rohner, 1910).

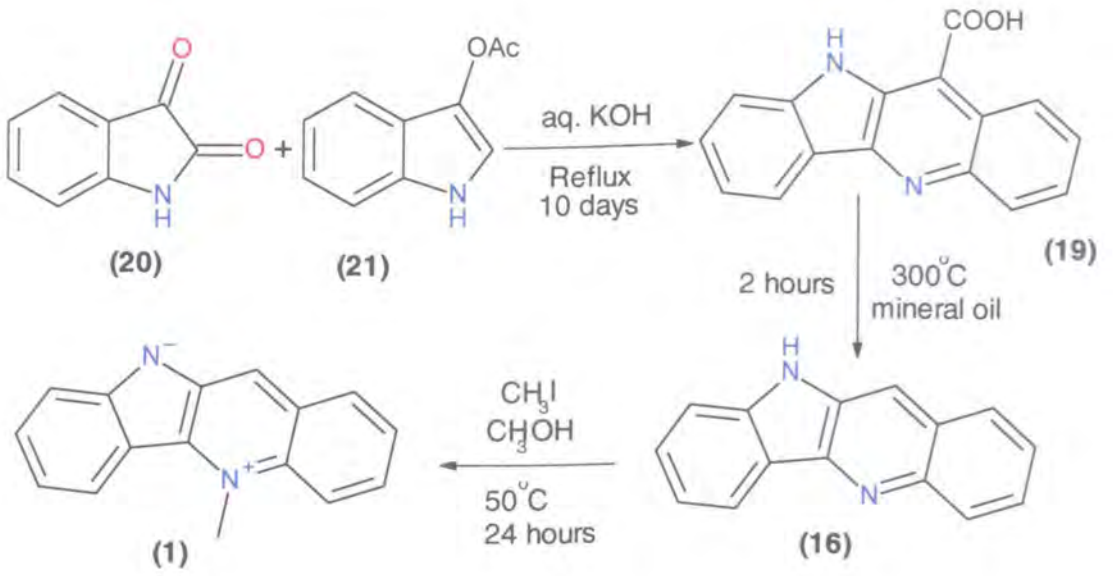

Figure 1.78 Scheme Synthesis of cryptolepine by Holt and Petrow

In 1947 two chemists; Holt and Petrow modified the Fichter and Rohner's synthetic route by condensing indoxyl acetate and isatin in the presence of aqueous sodium hydroxide for 10 days to produce quindoline 11-carboxylic acid. Decorboxylation by heating quindoline -11-carb7oxylic acid at 300 °C gave quindoline which then methylated to give cryptolepine. Despite of their efforts overall yield of the synthesis was not greatly improved but was limited only to 9-10% (Figure 1.78) (Holt and Petrow, 1947).

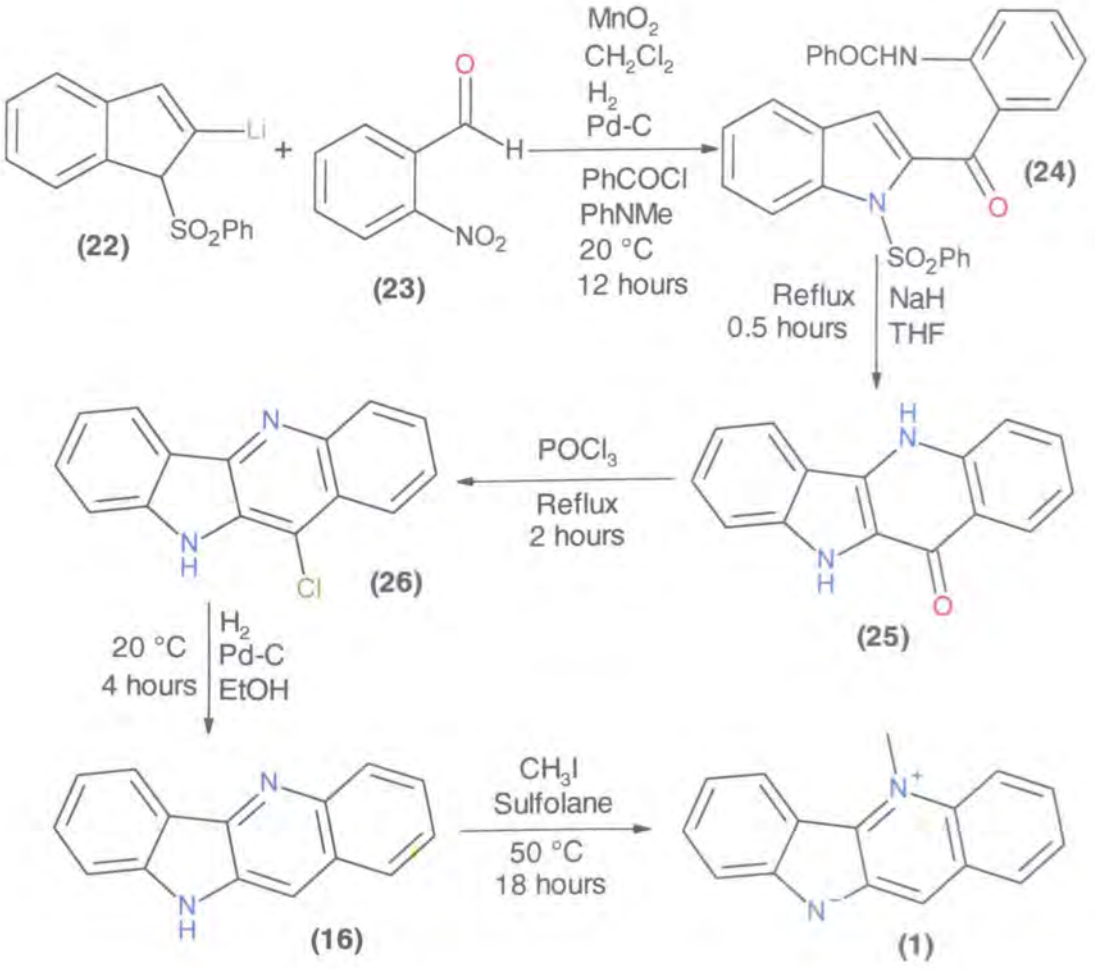

Figure 1.79 Scheme Synthesis of cryptolepine by Cooper

In 1996, another synthetic route was followed by Copper and his team to synthesise cryptolepine. 1-(Phenylsulfonyl)indole was treated with 2-nitrobenzaldehyde in the presence of manganese dioxide and reduction of the nitro group followed by Z-benzoylation gave a ketone intermediate. N-Deprotonation with NaH in THF resulted in cyclisation to produce quindolone followed by chlorination using $POCl_3$ giving 11-chloroquindoline. Then hydrogenolysis using a Pd-C catalyst in ethanol at room temperature gave quindoline which, upon methylation gave cryptolpeine with an overall yield of 12% (Figure 1.79) (Cooper *et al.*, 1996c).

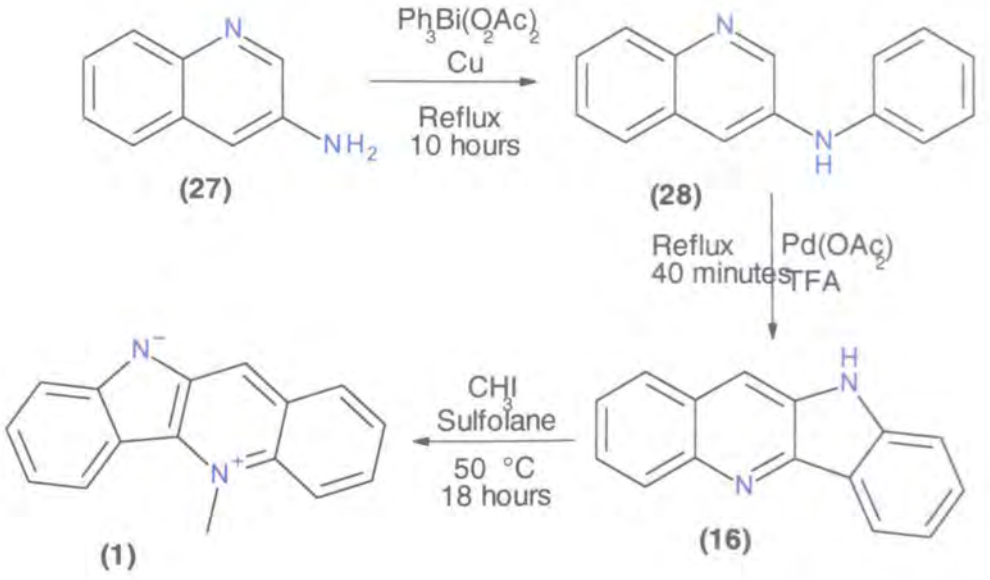

Figure 1.80 Scheme Synthesis of cryptolepine by Fan and Ablordeppey

In 1997 Fan and Ablordeppey reported another method for synthesis of cryptolepine with an improved overall yield of 22%. 3-aminoquinoline was treated with triphenyl bismuth diacetate and copper to give 3-anilinoquinoline followed by cyclisation using palladium acetate and trifluoroacetic acid to produce quindoline which was then methylated using methyliodide in the presence of sulfolane to give crypolepine (Figure 1.80) (Fan and Ablordeppey, 1997).

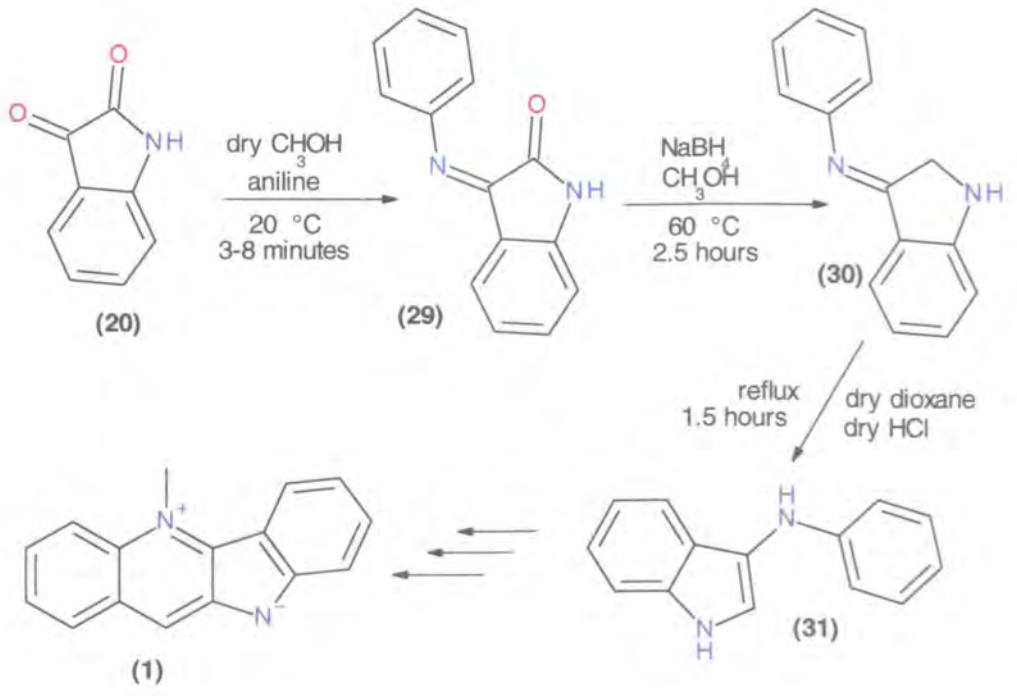

Figure 1.81 Scheme Synthesis of cryptolepine by (Banerji *et al.*, 2005).

More recently in 2005, Benerji and colleagues reported another route for cryptolepine synthesis. Isatin**(20)** was treated with aniline to give an intermediate imesatin**(29)** which was then treated with sodium borohydride in the presence of methanol to produce 3-N-phenylmino indolenine**(30)** ,this was then heated to reflux for 1.5 hours with dioxane and hydrochloric acid to give nor-seco-cryptolepine**(31)**, which was then cyclised to produce cryptolpeine**(1)** with an overall yield of 17% (Figure 1.81)

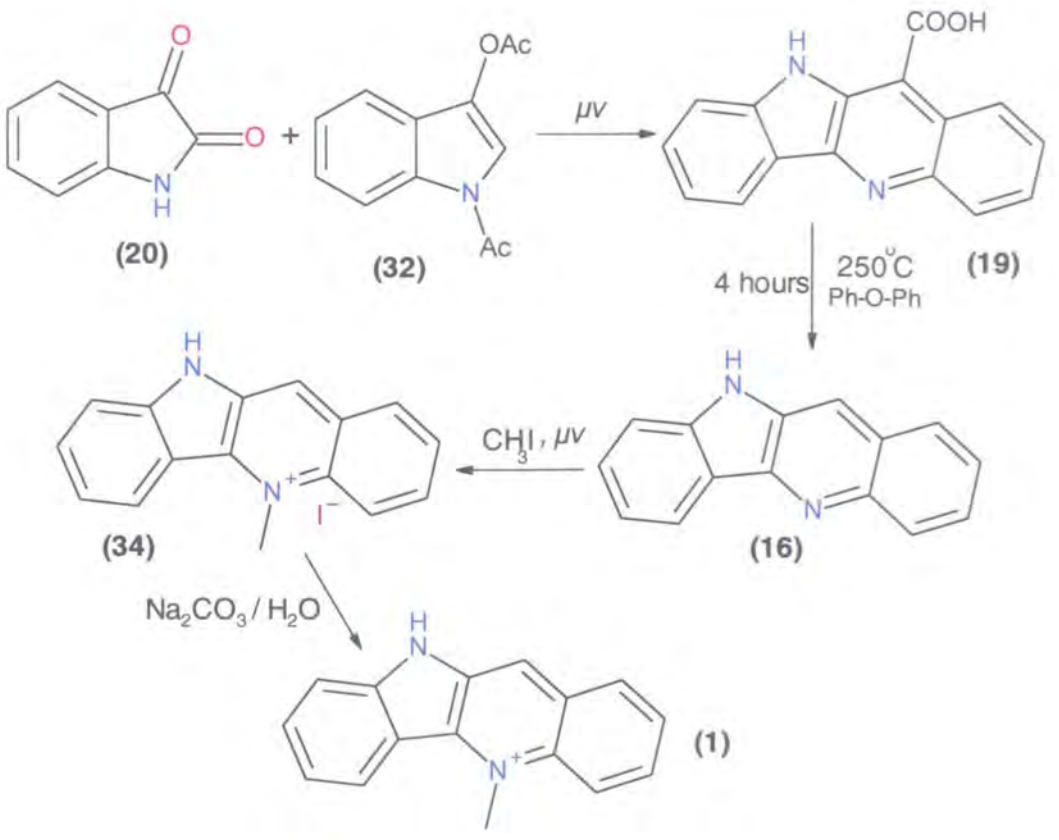

Figure 1.82 Scheme Synthesis of cryptolepine by (Lai *et al.*, 2008a).

More recently Lai and colleagues developed another modern synthetic route using microwave energy to synthesise cryptolepine. N-Acetyl-3-acetoxyindole**(32)** and isatin**(20)** were microwaved in 6N KOH to afford quindoline-11-carboxylic acid**(19)** which then decorboxylated by heating in the presence of biphenyl ether at 250 °C to give quindoline**(16)**. Methyliodide was used to methylate the N- position of quindoline which produced cryptolepine iodide salt which then converted to the free basic form of cryptolepine**(1)** using aqueous sodium carbonate. The overall yield of the synthesis was 29% which is higher than any other method previously reported (Figure 1.82) (Lai *et al.*, 2008b).

1.6 Design of the target molecules

Since cryptolepine was first discovered to be a DNA intercalator, researchers have investigated its potential as an anticancer agent (Ansah *et al.*, 2005; Guittat *et al.*, 2003a; Lisgarten *et al.*, 2002a). Many analogues have been synthesised and tested for cytotoxicity.

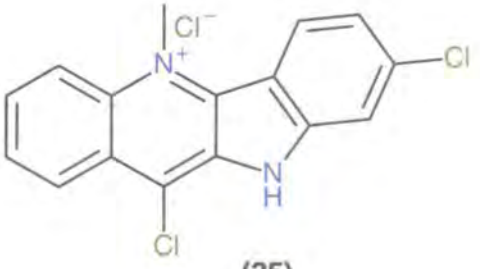

(35)

Figure 1.83 7, 11 Dichlorocryptolepine hydrochloride

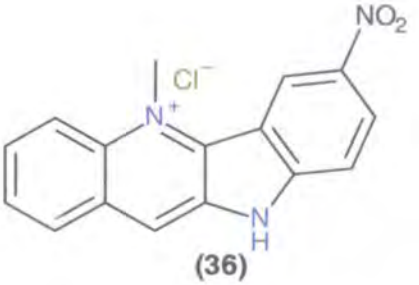

(36)

Figure 1.84 7-Nitrocryptolepine hydrochloride

Amongst these, derivatives have been made incorporating nitro groups**(36)** (Wright *et al.*, 2001; Onyeibor *et al.*, 2005), linkers to make dimers (Mardenborough *et al.*, 2005) and halogens at various ring positions**(35)** (Wright *et al.*, 2001; Seville *et al.*, 2003). Of particular interest are the 11-halogenated cryptolepines (Wright *et al.*, 2001; Jerrum *et al.*, 2007).

Wright and co-workers made a series of derivatives attaching halogens at the 11 position, amongst those 7,11 dichlorocryptolepine (Figure 1.83) showed the highest cytotoxic activity against MAC15a (colon adenocarcinoma) cells with an IC50 value of 14.4 ± 2.8 μM (after 1 hour exposure) (Gouni *et al.*, 2006; Jerrum *et al.*, 2006). Work by Gouni and then Jerrum investigated the synthesis and the activity of cryptolepines with chloro, bromo and iodo atoms at the 11 position. 11-bromo and iodocryptolepines showed an improved cytotoxicity profile, whereas the 11-chlorinated compound showed a reduction in the activity compared to the parent compound in the tested cell lines. From the literature it is observed that the cytotoxicity of cryptolepine is linked to its ability to inhibit the topo II enzyme (Bonjean *et al.*, 1998; Jerrum *et al.*, 2007; Dassonneville *et al.*, 1999; Luniewski *et al.*, 2012) so it was expected that bromo and iodo compounds would show greater topo II inhibition.

Cryptolepine Analogue	**Topo II inhibition (μM)**	**MCF-7 cells (μM) (mean ± SD)**	**DLD-1 cells (μM) (mean ± SD)**	**5637 cells (μM) (mean ± SD)**	**A-549 cells (μM) (mean ± SD)**
Cryptolepine	5.0	5.39± 0.33	**1.65 ± 0.33**	6.28 ± 1.53	**0.67 ± 0.02**
11-chloro	**0.02**	55.75± 1.42	73.87 ± 0.39	44.58 ± 4.46	48.71 ± 1.06
11-bromo	1.0	**0.55 ± 0.15**	2.55 ± 1.72	5.15 ± 0.66	4.32 ± 1.97
11-iodo	**0.5**	**0.07 ± 0.01**	**0.26 ± 0.04**	3.28 ± 1.42	**0.37 ± 0.05**

Table 1.2 Showing the activity of 11-halogenated cryptolepine analogues (shaded cells show high activity) (Jerrum *et al.*, 2009).

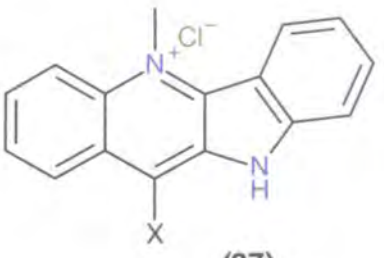

(37)

X=Cl, Br, I **(37, 38, 39)**

Figure 1.85 11-Halogenated cryptolepines

Looking at the topo II assay results of these 11-halogenated compounds (Table 1.2) all of them showed greater inhibition compared to the parent molecule but surprisingly the 11-chloro derivative**(37)** (Figure 1.85) showed the highest topo II inhibition despite its lower *in vitro* cytotoxicity. It was thought that this could be due to the changes in drug-DNA interactions or drug uptake based on the structure and size of the molecule (Grasby *et al,* 2006). In the current project, with a view to investigate the irregularities in these past results, these halogenated cryptolepines were synthesised and assayed *in vitro* including experiments to establish the extent of cellular uptake and localisation. It was hoped that these assays, which had not been attempted before with these compounds, would help to clarify structure activity relationships.

1.7 Synthesis of 11-halogenated cryptolepines

There are a number of procedures to synthesise 11-halogenated derivatives **(37, 38, 39)** of cryptolepine. Most of these use quindolone as an intermediate followed by halogenation at the 11-position and then methylation at N5. The key step in synthesising quindolone is closing the final ring to make the te-

tracyclic skeleton because this is a low yielding step which required dry conditions.

Although various synthetic procedures successfully give quindolone**(25)**, the best cyclisation yields were obtained by three methods. Masatoshi and coworkers achieved a good cyclisation yield of 70% by treating 2-[(N-phenylamino)acetamido] benzoic acid**(42)** with polyphosphoric acid (Figure 1.86) (Yamato *et al.*, 1990).

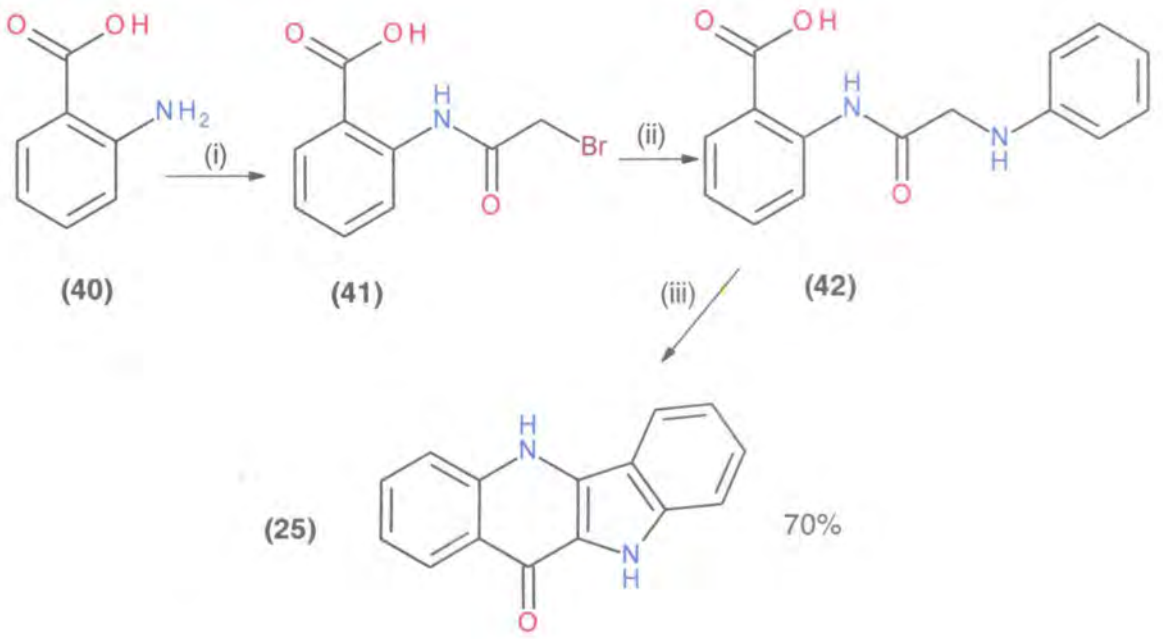

Reagents: (i) bromoacetyl bromide, 24 hrs, 96%; (ii) aniline, reflux, 30 hrs, 72%; (iii) polyphosphoric acid, 130 °C, 2 hrs, 11%

Figure 1.86 Showing the synthesis of quindolone by polyphosphoric acid mediated ring closing (Yamato *et al.*, 1990).

A method with a fewer number of steps was developed by Cooper et al with a maximum yield of 82% for the ring closure (Figure 1.87) (Cooper *et al.*, 1996b).

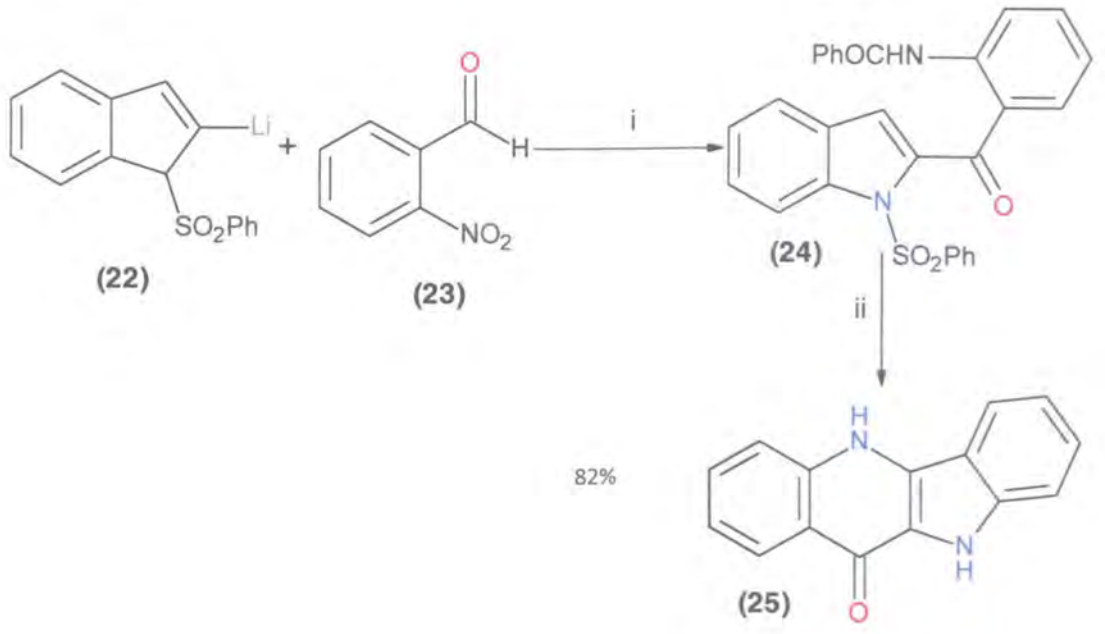

Reagents: (i) MnO_2, CH_2Cl_2, H_2, Pd-C, PhCOCl, $PhNMe_2$, 12 hrs; (ii) NaH, reflux, 0.5 hrs.

Figure 1.87 Showing the synthesis of quindolone (Cooper *et al.*, 1996a)

A yield of 90% was observed from Radl *et al.* by treating 3-amino-*N*-2-(7-nitrobenzoyl) indoline-1-carboxylate**(45)** with sodium hydride in THF (Figure 1.88) (Radl *et al.*, 2001). In the current project, based on the highest percentage yields reported in the literature, Radl's method was used to synthesise the 11-halogenated cryptolepines.

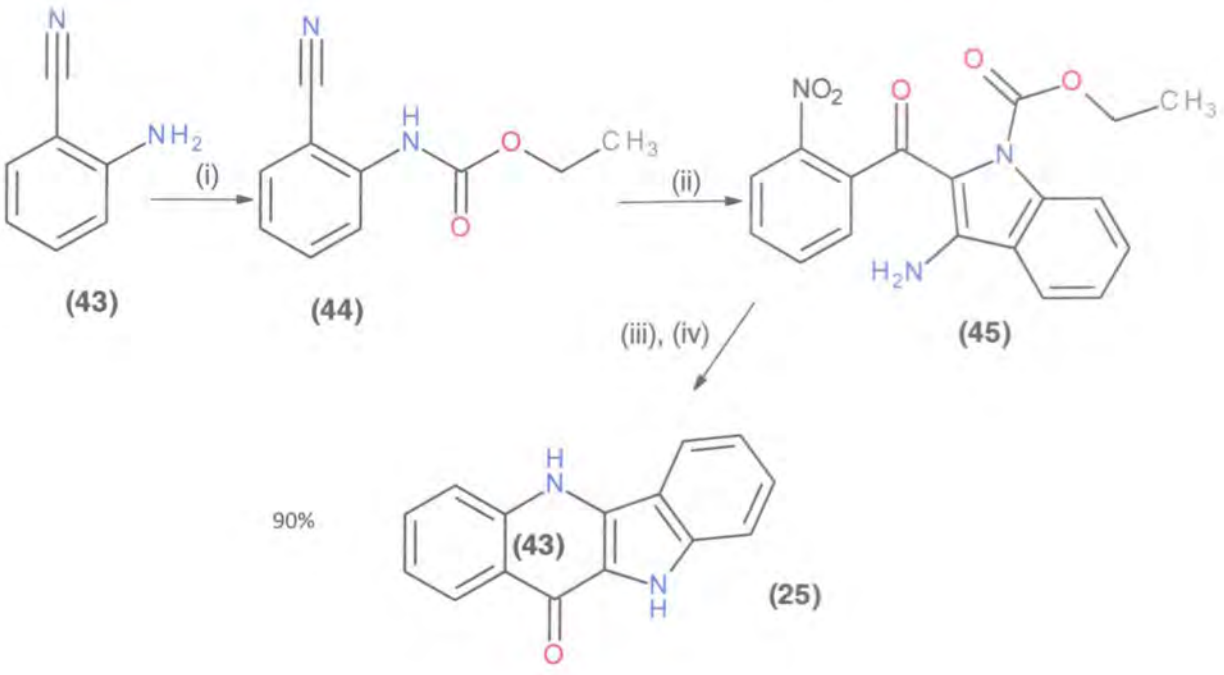

Reagents: (i) ethyl chloroformate, reflux, 6 hrs; (ii) 2-bromo-2'-nitroacetophenone, K_2CO_3, DMF, room temperature, 2.5 hrs,; (iii) NaH, THF, room temperature, 1 hr, (iv) acetic acid, ethanol, NaOH, 0.5 hrs, over 2 steps

Figure 1.88 Showing the synthesis of quindolone (Radl *et al.*, 2001).

Chapter 2 Chemistry Discussion

In Radl's method (Figure 1.88) starting material 2-amino benzonitrile**(43)** acts as a nucleophile which, on treatment with ethyl chloroformate gave a carbamate**(44)** (Figure 2.1). TLC showed two spots of which one was faint and matching to the Rf value of the starting material and the other was product.

Figure 2.1 Showing the formation of ethyl (2-cyanophenyl carbamate)

After recrystallisation there was only one spot on the TLC indicating that the remaining starting material had been removed. The ^{1}H NMR spectrum of the product showed a quartet at 4.27 ppm and a triplet at 1.35 ppm, arising from CH_2 and CH_3 groups (Figure 2.2).

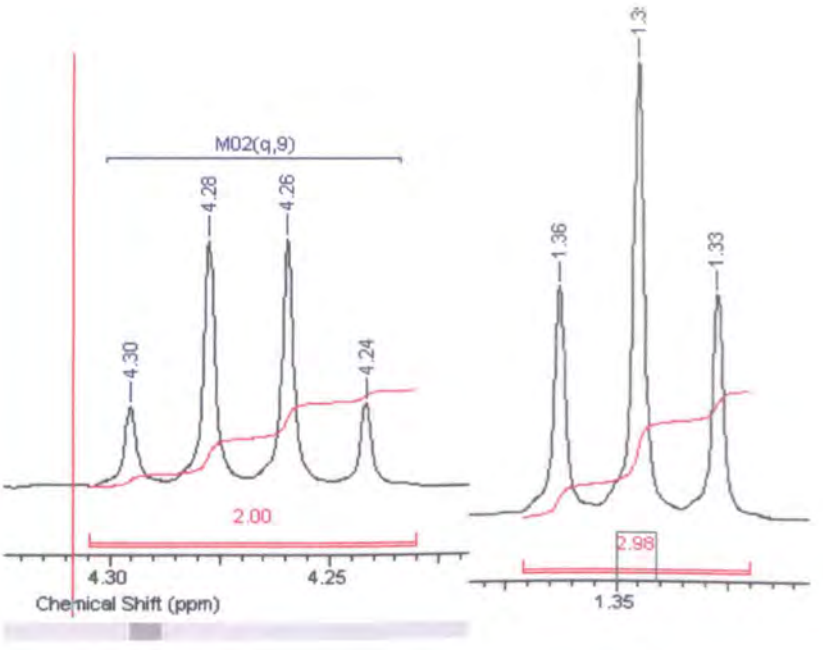

Figure 2.2 Showing the proton signal arising from ethyl ester

As they have the same coupling constant of 7.1 Hz this indicates that these two groups are joined together, which is a typical of an ethyl ester. These peaks were not present in the spectrum of the starting material indicating that the product has formed. ^{13}C NMR gave 10 peaks arising from 10 carbon atoms present on the product including a carbonyl peak at 152.9 ppm and a nitrile peak at 134.2 ppm (Figure 2.3).

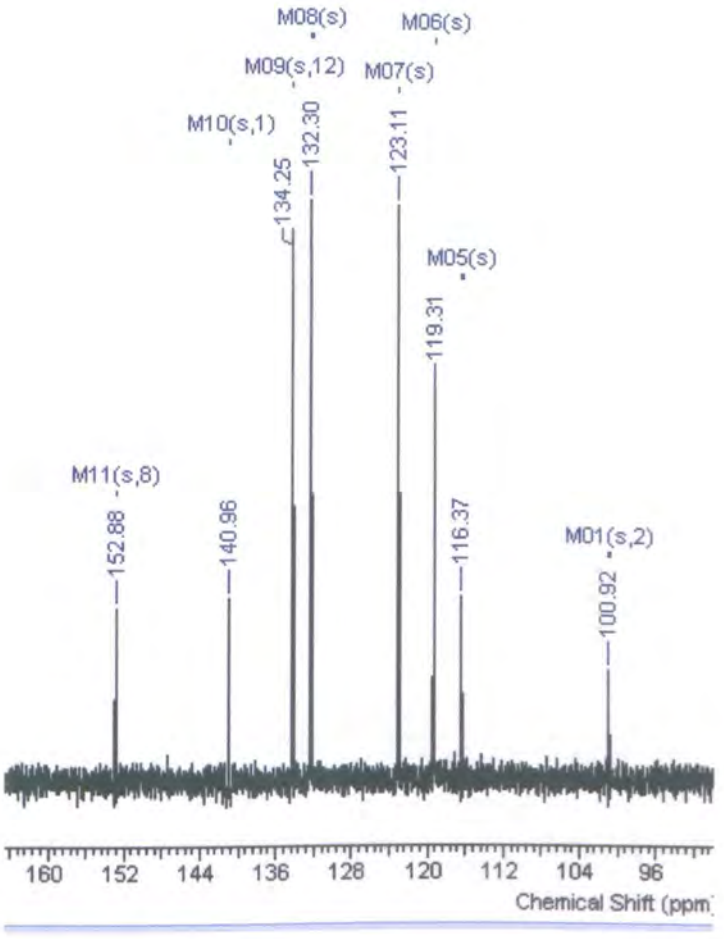

Figure 2.3 Showing carbon peaks arising from carbonyl and nitrile groups.

The IR spectrum clearly shows peaks at 3300, 2221, 1705 cm^{-1} which indicate the presence of amido (NH from amide), cyano and carbonyl groups respectively. From the GC-MS, a molecular ion peak at M/z 190, indicating that the product had been formed. This carbamate was then treated with 2-bromo 2-nitroacetophenone to synthesise a carboxylate intermediate (Figure 2.4)

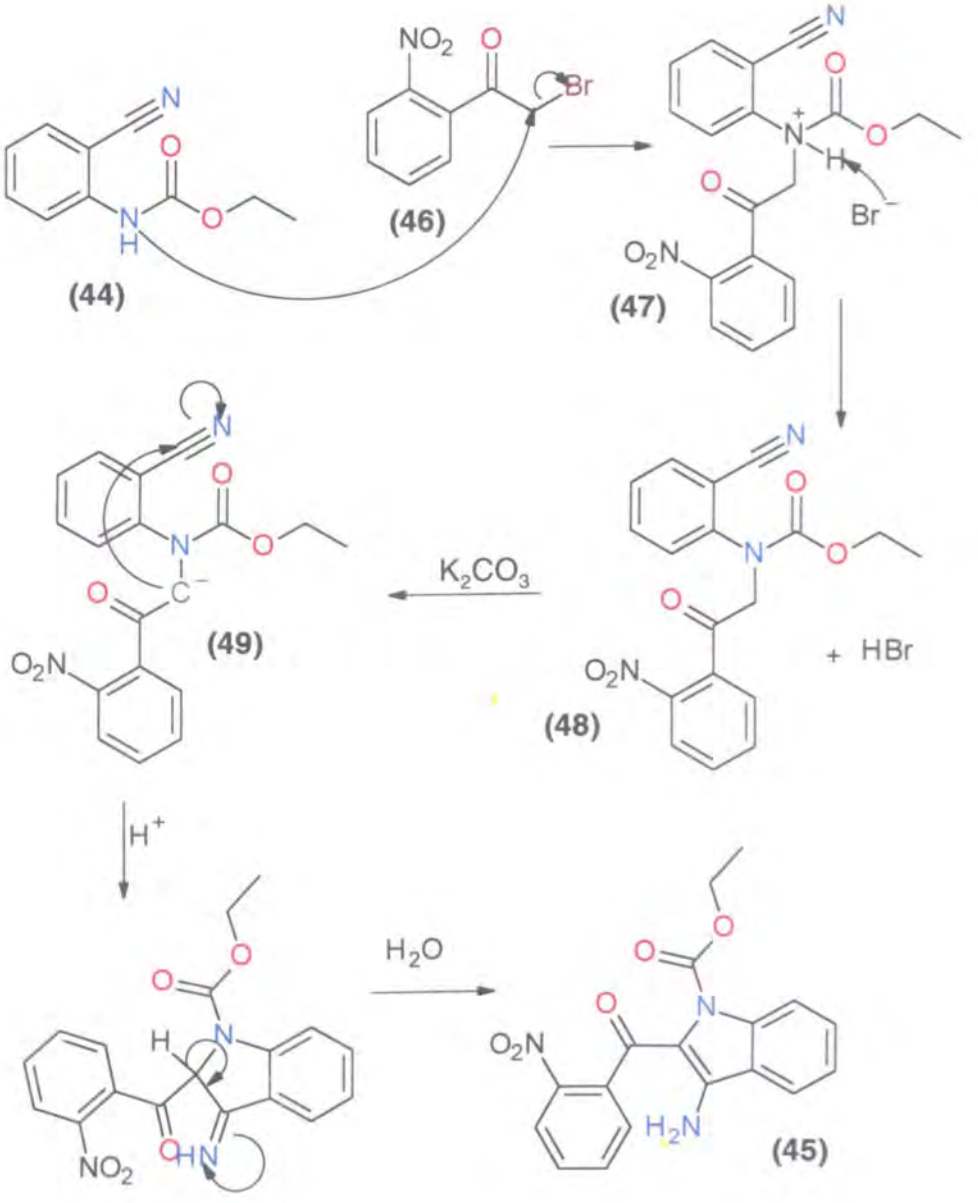

Figure 2.4 Showing the formation of 3-amino-*N*-2-(7-nitrobenzoyl) indoline-1-carboxylate

The reaction is a nucleophilic substitution reaction between the amino nitrogen in the carbamate**(44)** and the α-carbon of 2-bromo 2'-nitroacetophenone**(46)** giving an intermediate**(48)** by losing bromide **(**Figure 2.4**)**. By reacting with a base, (K_2CO_3) the acidic proton present in the CH_2 of

the intermediate produces a carbanion**(49)**, which attacks the nitrile group to form the product**(45)**.

TLC of the crude product showed two spots one of which had the same Rf value as the starting material. Two recrystallisations from methylated spirits were needed to purify the product to give a maximum of 50% yield. In the proton NMR eight protons were observed in the aromatic region, only four were present in the starting material, which indicates that cyclisation was successful. A broad peak at 6.32 ppm integrating for two protons indicates the presence of a primary amine group (Figure 2.5).

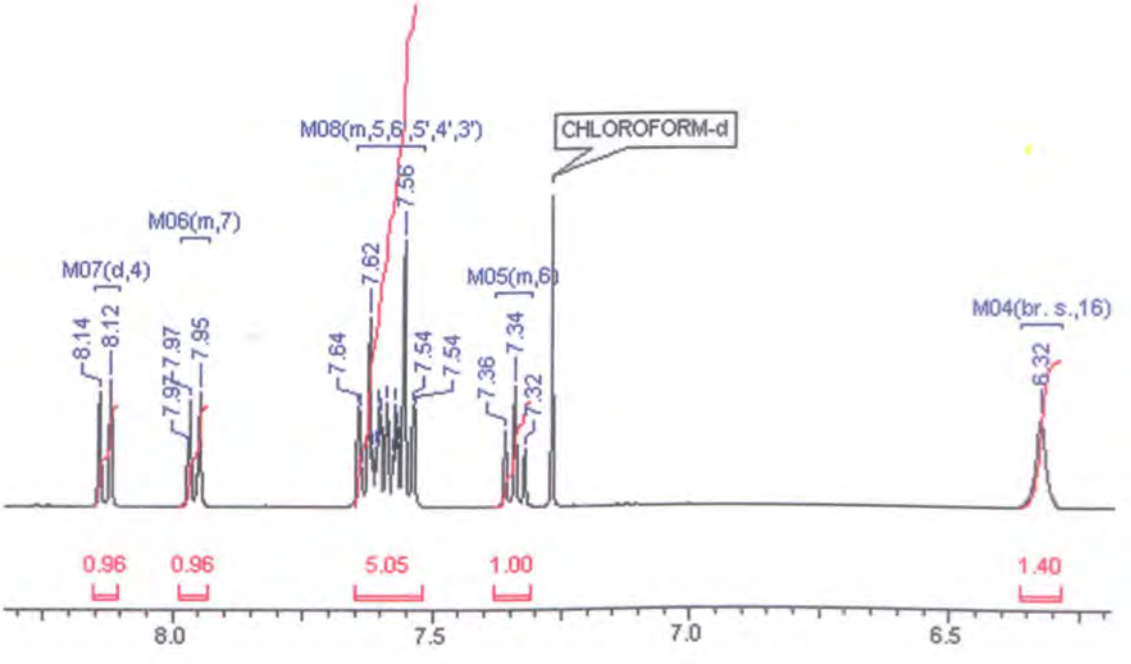

Figure 2.5 Showing ^{1}H NMR spectrum of 3-amino-*N*-2-(7-nitrobenzoyl) indoline-1-carboxylate

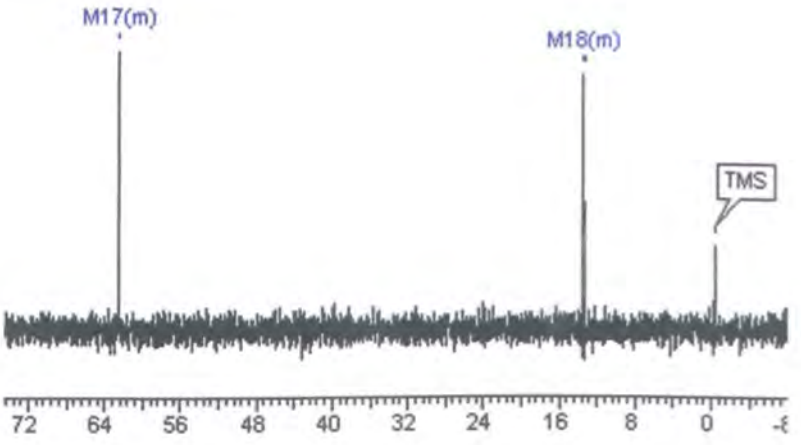

Figure 2.6 Showing ^{13}C NMR spectrum of 3-amino-*N*-2-(7-nitrobenzoyl) indoline-1-carboxylate

^{13}C NMR clearly showed 18 peaks including a peak at 182.1 ppm from the carbonyl group. Peaks at 62.6 ppm and 13.44 ppm are due to the presence of the ethyl ester (Figure 2.6). Moreover, the absence of a nitrile carbon is also clearly seen.

Aromatic systems having nitro groups can undergo cyclisation as shown in a model reaction in Figure 2.7 (Radl, 1993).

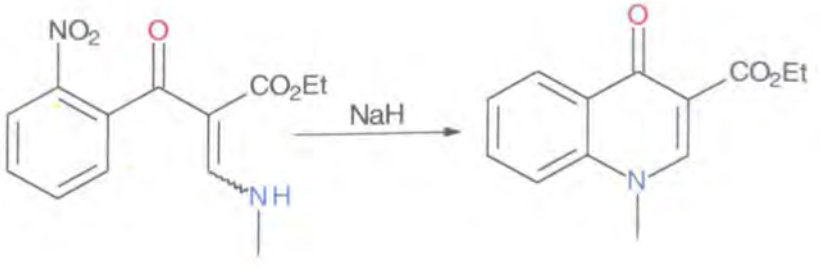

Figure 2.7 Showing the formation of quindolone

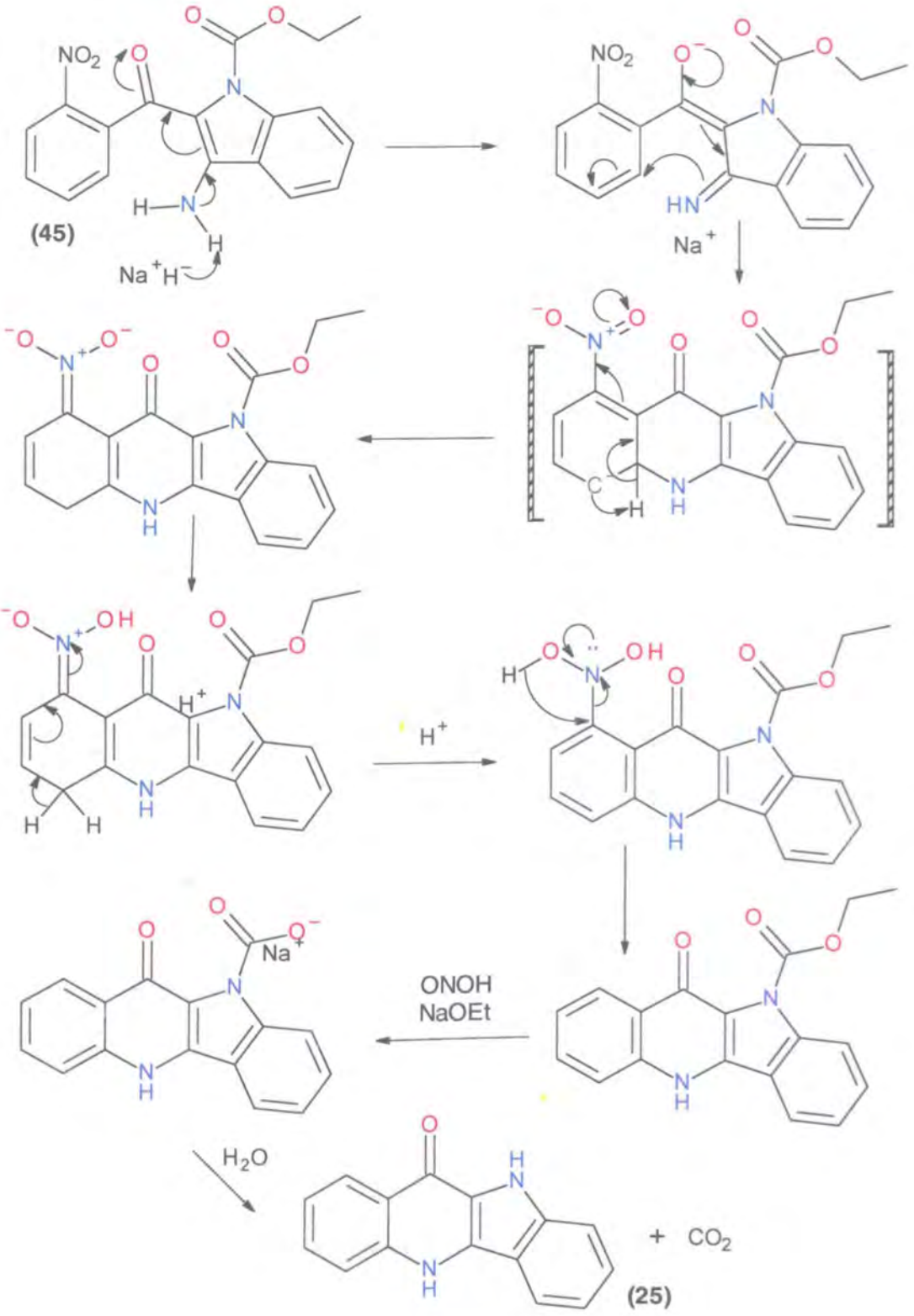

Figure 2.8 Showing the formation of quindolone

As the nitro group in the carboxylate intermediate**(45)** is electron withdrawing, it can pull the electrons from the aromatic ring system making it liable to nucleophilic attack. This reaction involves deprotonation of the amine using sodium hydride, which increases its nucleophilicity leading to the cyclisation reaction (Figure 2.8).

Using this method, quindolone**(25)** was successfully synthesised with a yield of 69%. TLC showed two spots when the crude product was analysed and it required two recrystliisations to purify. ^{1}H NMR showed two broad peaks at 12.4 ppm and 11.6 ppm representing two hydrogens attached to the two aromatic nitrogen atoms. In addition, the integration at 7.16-8.39 ppm gave eight aromatic hydrogens present on the molecule (Figure 2.9). ^{13}C NMR also gave 15 peaks for the same total number of carbon atoms present in the structure including a carbonyl peak at 167.2 ppm. A molecular weight of 234 from ESI-MS confirmed that quindolone had been successfully made.

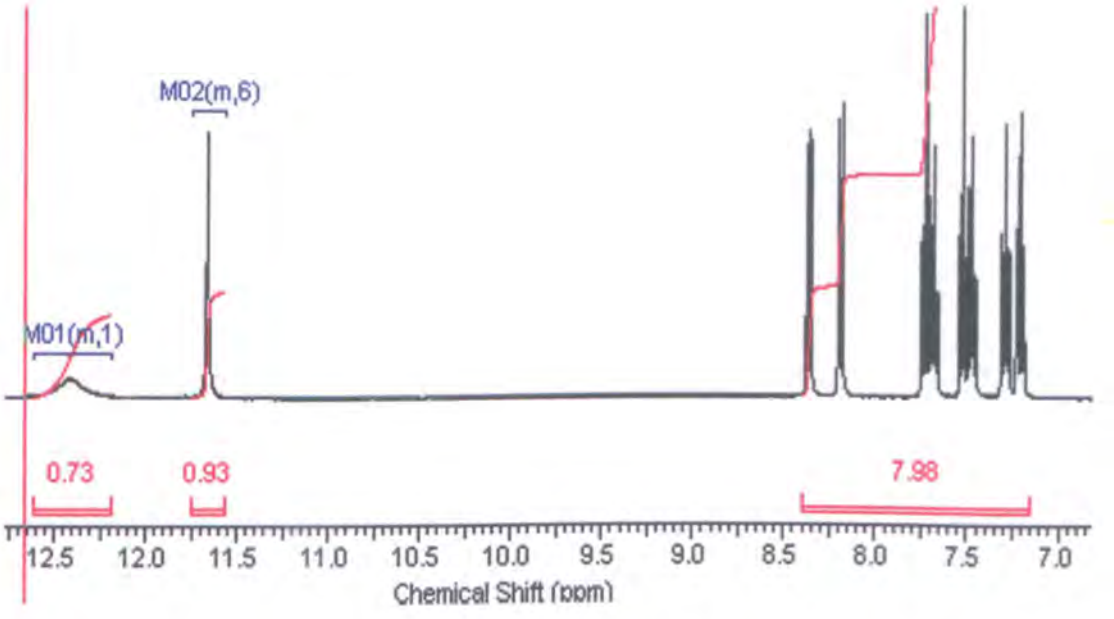

Figure 2.9 Showing ^{1}H NMR spectrum of quindolone

Once quindolone was synthesised, it was halogenated at the 11-position. The carbonyl group present on the ring at the γ position to the aromatic nitrogen, makes molecule prone to electrophilic substitution reactions (Radl, 2000). On treatment with phosphoryl oxyhalide ($POCl_3$ or $POBr_3$), transfer of oxygen on the ring to the corresponding phosphoryl halide occurs by substitution of one halogen present on the phosphorous oxybromide or chloride (Figure 2.11).

When quindolone was treated with phosphorus oxybromide for 16 hours, TLC of the reaction mixture showed two spots arising from starting material and product. In a view to recovering the starting material and to save the loss of product during recrystallisation, column chromatography was needed to separate the unreacted starting material to give pure product**(50)** in a 36% yield.

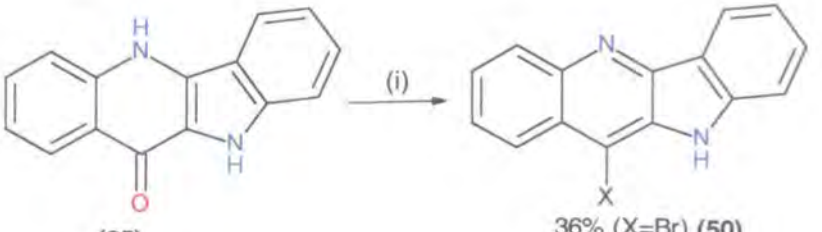

(25)

36% (X=Br) **(50)**
54% (X=Cl) **(51)**

(i) PBr_3, $POBr_3$ or $POCl_3$, PCl_5 150 °C, 10 hrs, reflux for 3 hrs, 36%

Figure 2.10 Showing the synthesis of 11-halogenated quindolines from quindolone.

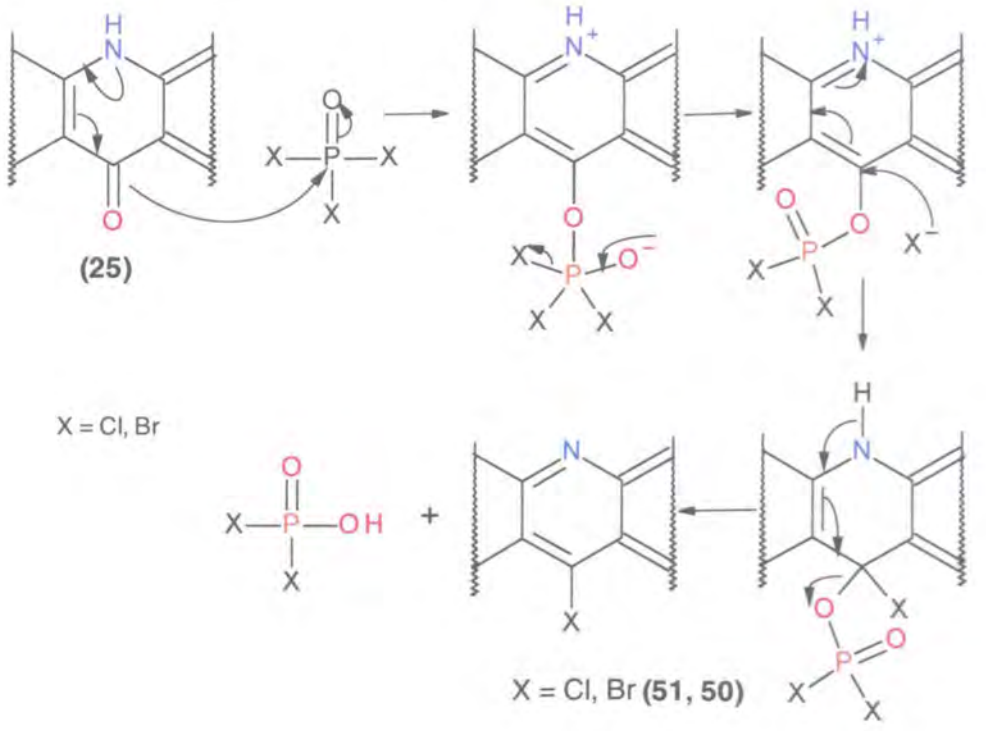

Figure 2.11 Showing the formation of 11-bromo quindoline**(50)**

^{13}C NMR clearly the confirmed the presence of fifteen carbon atoms in the molecule**(50)**. It was observed was that a peak at 124.7 ppm was not present in the starting material**(25)**, which arose because of the brominated carbon. The carbonyl peak present in the starting material**(25)** at 167.2 ppm was absent, indicating that carbonyl group was successfully replaced by a bromine atom. In contrast to the ^{1}H NMR of the starting material the product**(50)** gave only one broad peak at 11.66 ppm arising from the single proton present on the nitrogen (Figure 2.12). The remaining proton peaks integrate to the eight aromatic protons present on the rest of the molecule.

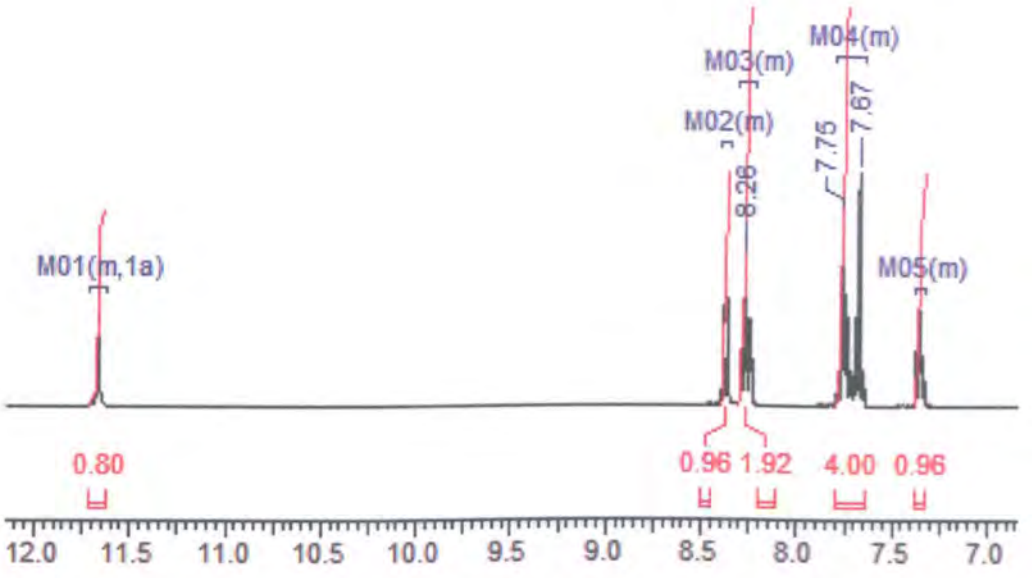

Figure 2.12 Showing the 1H NMR spectrum of 11-bromoquindoline

From the mass spectrum, the molecular ion peaks at M/z 295 297 indicate that bromination has been successful, moreover these isotope peaks are due to the presence of a bromine atom in the molecule. The peak heights are equal, which is an indication of brominated compounds as bromine naturally exists as mixture of two isotopes ^{79}Br and ^{81}Br in 1:1 ratio.

In the case of synthesising 11-chloroquindoline**(51)**, it took only 4 hours of reflux to complete the reaction whereas bromination required 16 hours. The chlorinated product was also purified using column chromatography to give a yield of 54% meaning that a higher yield was observed for chlorination than for bromination, this was may be because of high electronegativity of chlorine than bromine.

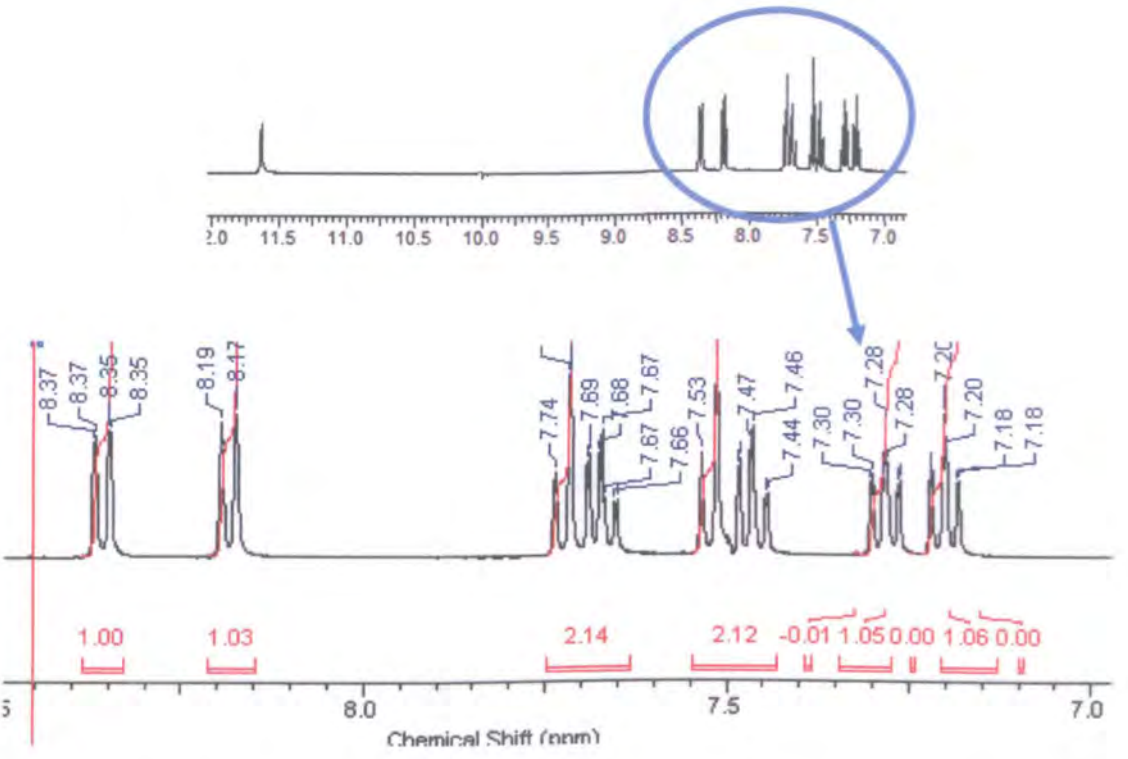

Figure 2.13 Proton NMR of 11-chloroquindoline showing aromatic protons

Supporting the ^{1}H NMR and ^{13}C NMR data (Figure 2.13), the mass spectrum of the chloroquindoline gave two peaks from the molecular in 3:1 ratio with a difference of 2 m/z units arising from chlorine isotopes, which confirmed that the synthesis was successful.

Syntheisis of iodoquindoline was not required to make 11-iodocryptolepine, instead a procedure was adapted from Jerrum *et al.* In this method 11-bromoquindoline was treated with methyl iodide to allow the halogen exchange to takes place between bromine and iodine at the 11 followed by methylation at the N5 position (Figure 2.14). the product was then converted to its hydrochloride salt using HCl in methanol.

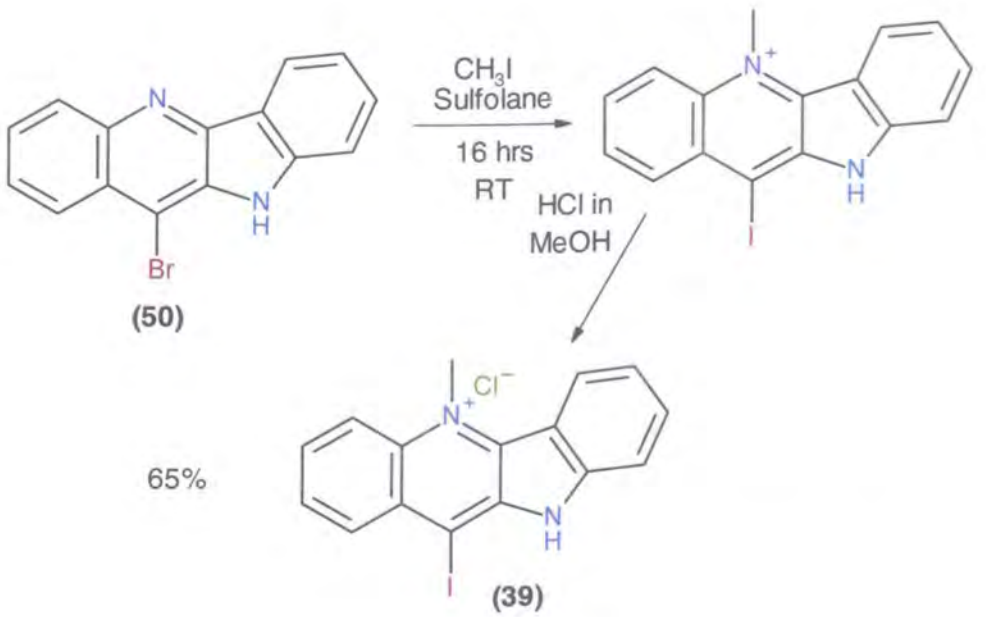

Figure 2.14 Showing the synthesis of 11-iodocryptolpeine

In the final step in the synthesis of halogenated cryptolepines, methytriflate in toluene (a non-polar solvent) was used as the methylating agent (Gouni *et al.,* 2006) to methylate the 11-chloro**(51)** and bromo**(50)** quindolines at the N5 position. As the compound obtained was in its triflate salt form, it was then converted to its free base by treating with ammonia and was then subjected to column chromatography on silica gel. Finally the free base was acidified by using HCl in methanol (0.1 M) to form the hydrochloride salt of 11-halogenated cryptolepine.

^{1}H NMR of 11-bromocryptolepine**(50)** showed a single peak at 5.13 ppm integrating to 3 protons arising due to the methyl group present on the N5. In contrast to the product that peak was absent in the starting material which indicates that methylation had been successful. A single peak at 9.16 ppm indicating the presence of hydrogen attached to the nitrogen (N5).

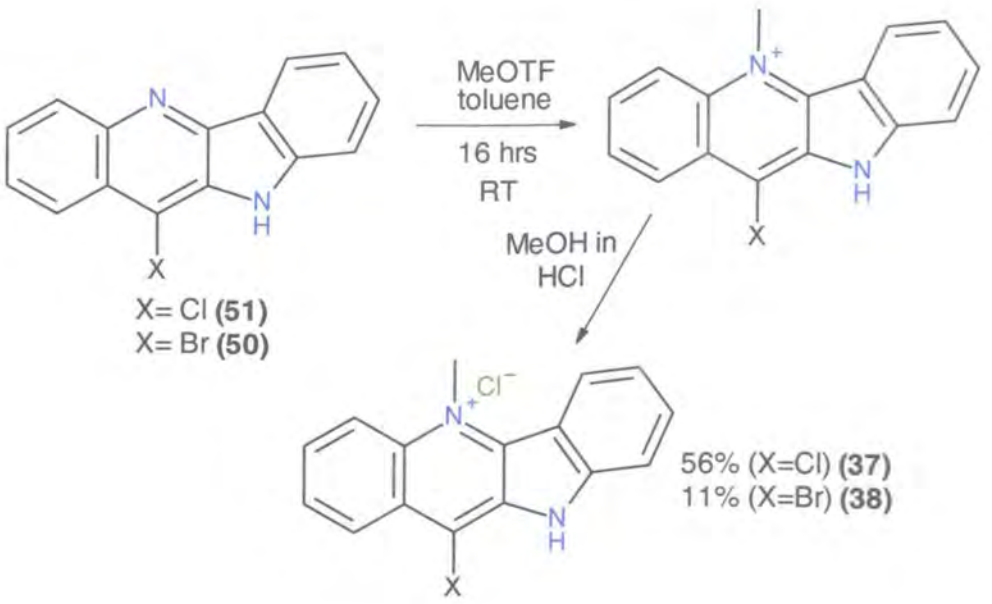

Figure 2.15 Showing formation of cryptolepine hydrochloride

^{13}C NMR of 11-bromocryptolepine**(38)** also revealed the presence of an extra carbon atom from the methyl group at 29.73 ppm. From the mass spectrum, molecular ion peaks at m/z 312 and 310 were present in equal ratio(bromine isotopes), which confirmed that the compound had been made.

Similarly synthesis of 11-chlorocryptolepine**(37)** was confirmed from the ^{1}H NMR and ^{13}C NMR data. Additionally from mass spectrum, chlorine isotope peaks in 3:1 ratio were also observed (Figure 2.16).

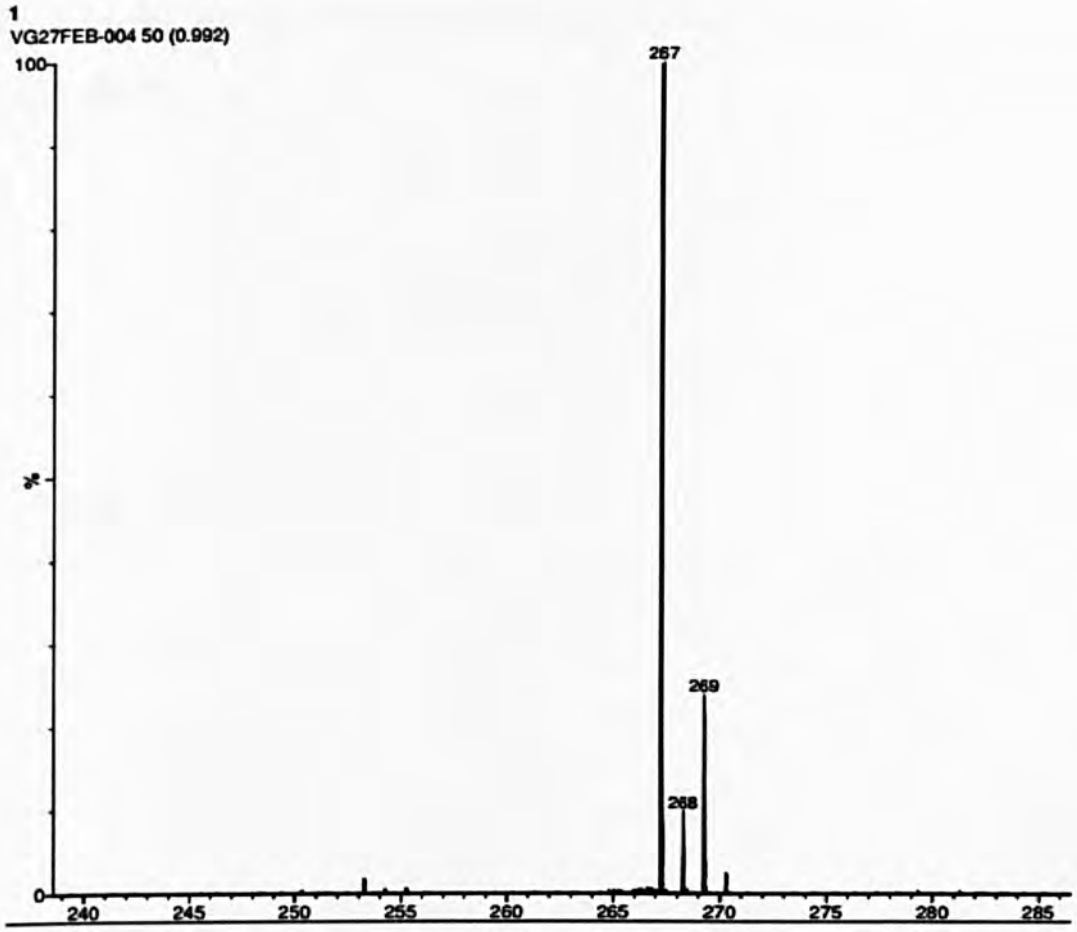

Figure 2.16 Mass spectrum of 11-chlorocryptolepine showing isotopes in 1:3 ratio (269, 267)

Along with the NMR data, the mass spectrum of the 11-iodo cryptolepine showed the absence of bromine isotopes present in the starting material and gave a single molecular ion peak at 259 indicating that the iodination was successful.

The halogenated cryptolepines synthesised so far contain 3 of the 4 smallest halogens, with fluorine notably being missing. Halogenated organic compounds have been of pharmaceutical importance and several of them being used in treatment of diseases. Chloroquine, a chlorine-containing compound has been used in the treatment of malaria, brompheniramine is used as an antihistamine drug (Barth *et al.,* 1973) and it was also shown to inhibit sero-

tonin reuptake giving antidepressant property (Stahl and Felker, 2008; Silins *et al.*, 2007)

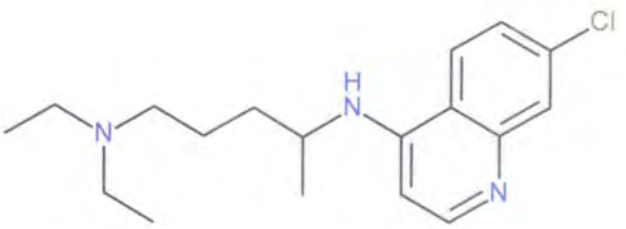

Figure 2.17 Chloroquine

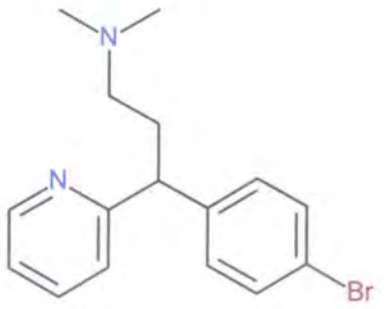

Figure 2.18 Brompheniramine

Amiodarone (Figure 2.19) is an iodine containing drug used as an antiarrhythmic agent, it stabilises the heartbeat by modulating the potassium channel functioning in the cardiac cells (Bardy *et al.*, 2005).

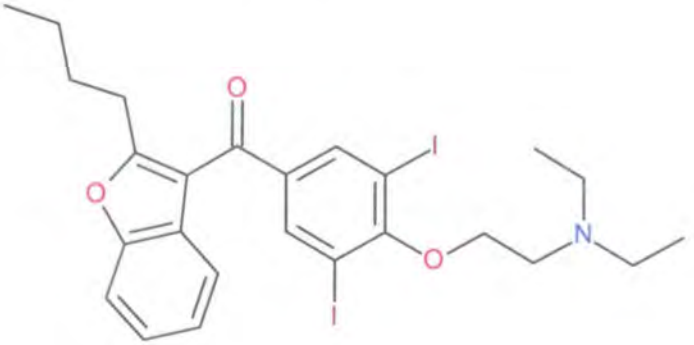

Figure 2.19 Amiodarone

When a halogen atom is attached to an organic compound, it can affect its drug-receptor interactions. Halogenated compounds are considered as lewis bases and hydrophobic moieties from the medicinal chemistry point of view (Erdelyi, 2012; Wermuth, 2011). With reference to the structure of biological cell membranes, liphophilicity or hydrophobicity is one of the key parameters which determine the drug uptake in animal cells.

It is often important to optimise molecules with a specific halogen to achieve optimal drug interaction with the target. When looked as a series, physico-chemical properties such as atomic size (I < Br < Cl < F) and electronegativity change from chlorine to iodine which affects their reactivity.

Halogen	**Electronegativity**
Fluorine	4.0
Chlorine	3.0
Bromine	2.8
Iodine	2.5
Astatine	2.2

Table 2.1 Showing electronegativity of halogens

Although all halogens are used in drug development, recently molecules being produced having fluorine atom (O'Hagan, 2010) are on the rise. A number of organic fluorine compounds have been already approved for the treatment of diseases. For example, aprepitant (Figure 2.20), a fluorine containing drug is used in the treatment of chemotherapy-induced nausea and vomiting and another molecule in the current pharmaceutical industry is atorvastatin (Figure 2.208), which is a HMG-CoA reductase inhibitor, used in the treatment of hypercholesterolemia and atherosclerosis (O'Hagan, 2010). Ac-

cording to Hagmann in last the 60 years about 15-20% of all approved new chemical entities for the clinical market contain fluorine (Hagmann, 2008).

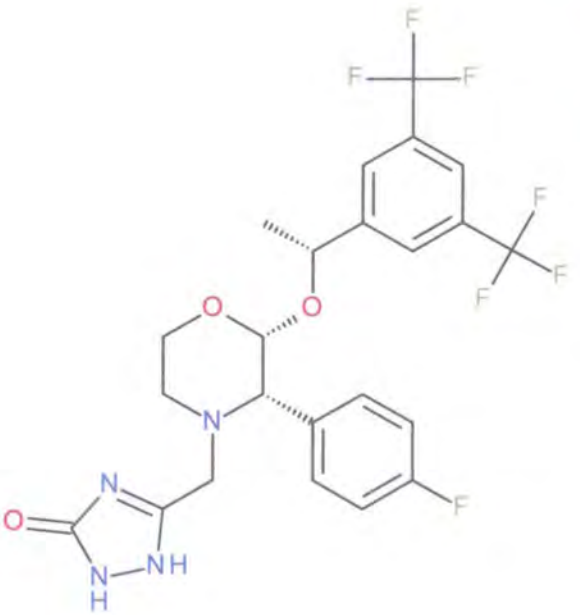

Figure 2.20 Aprepitant

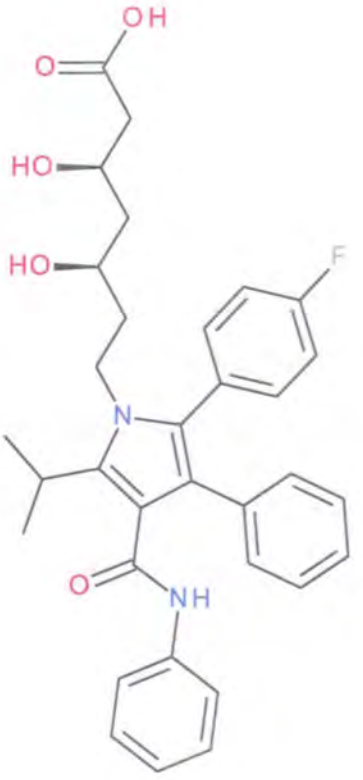

Figure 2.21 Atorvastatin

Genarally during the lead optimisation stage of the drug development process fluorine is introduced either to increase the liphophilicity or to block metabolic pathways. In some cases introduction of a fluorine atom dramatically changes potency of the drug, for example the addition of a fluorine atom to cortisol improved its anti-inflammatory activity intensely because having 9-alpha fluorine (Figure 2.22) means hydroxylase enzymes will not be able to metabolise the product leading to prolonged activity (O'Hagan, 2010).

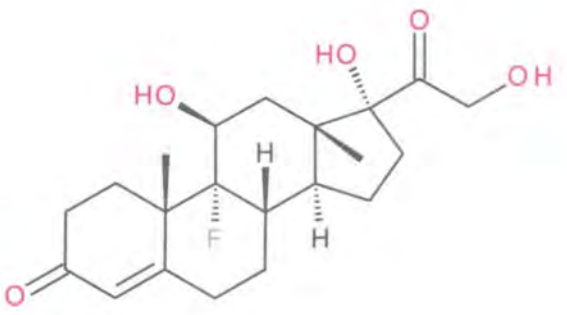

Figure 2.22 Fludrocortisone

11-Fluorocryptolepine cannot be made using the chemistry used for the other halogenated derivatives and there were no reported synthetic routes observed in the literature. This could be because of the high electronegativity and electronic properties of fluorine. The closest analogues were 4-fluoropyridines. A number of synthetic methods were investigated with a view to find a way of making 11-fluorocryptolepine.

Balz-Schiemann Reaction: In this method aniline is treated with fluoroboric acid in the presen ce of sodium nitrite. In the first step aniline is converted in to a diazonium salt and then subsequent thermal decomposition gives a fluoroarene (Figure 2.23), releasing nitrogen gas as by-product. Yoneda and Fukuhara reported the synthesis of 4-fluorobenzene using this method with an overall yield of 14% (Yoneda and Fukuhara, 1996).

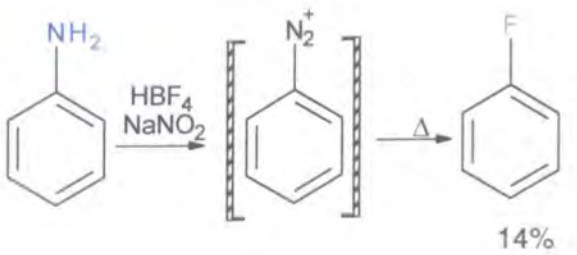

Figure 2.23 synthesis of fluorobenzene

When Roe and Hawkins used the same reaction to prepare fluoro pyridines, they were able to synthesise 2- and 3-fluoropyridines but failed to synthesise 4-fluoropyridine. Later Wibaut and Holmes-Kamminga reported the synthesis of 4-fluoropyridines from 4-amino pyridine in poor and impure yield and it was mentioned in that article that 4-fluoropyridine was quickly polymerised making it an unstable compound (Desai, 1973).

By using the same reaction Desai and Prabhakar successfully synthesised 4-fluoropyridine in pure form with a yield of 22% (Figure 2.24). They prevented the polymerisation of 4-fluoropyridine by using dry apparatus and alkali (KOH pellets) after a thermal decomposition step (Desai, 1973).

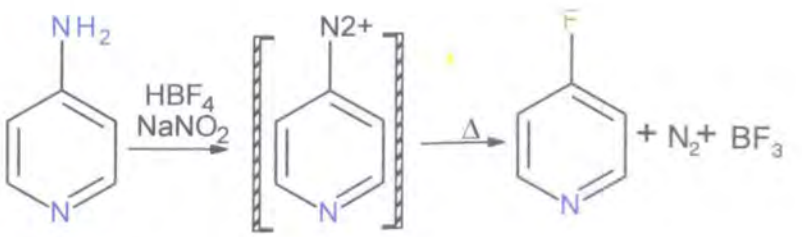

Figure 2.24 synthesis of 4-fluoropyridine

This method was chosen to make 11-fluorocryptolepine**(53)** based on the reported yield. As a first step an amination reaction was carried out to synthesise 11-aminoquindoline from the 11-carboxylicacid**(19)**. Using the Curtius method (Figure 2.26), quindoline carboxyl chloride hydrochloride acid was treated with sodiumazide to form acyl azide. Then it was heated to form nitrene. Nitrenes are unstable, substituent R migrates from carbon to electron deficient nitrogen of nitrene to from an isocyanate. Up on hydrolysis it gives a carbamic acid, which further decomposes to give an amine. A molecular weight of 233 was observed from the ESI-mass spectrometry.

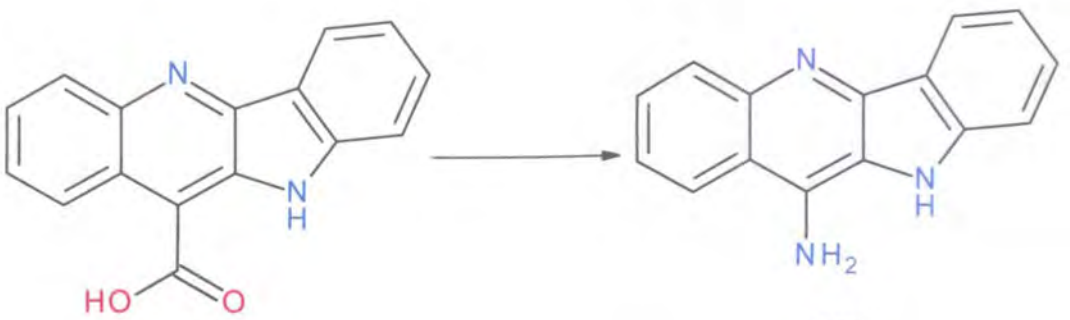

Figure 2.25 showing the synthesis of 11-aminoquindoline

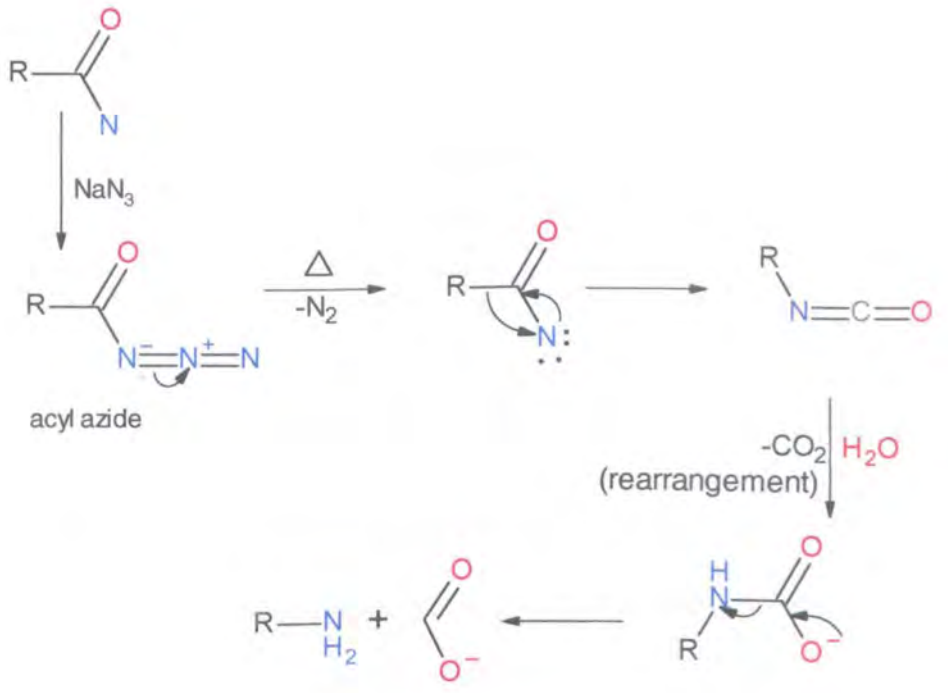

Figure 2.26 Curtius re-arrangement

Once the 11-aminoquindoline**(52)** was synthesised, the Balz-Schiemann Reaction was applied using fluoroboric acid and sodium nitrite (Figure 2.27). Unfortunately this reaction did not work showing no signs of fluorination from ^{19}F NMR. So the reaction conditions were modified increasing the reaction

temperature to 70 °C but still there were no signs of fluorination and the reaction mixture gave multiple spots on TLC. The mixture was separated using column chromatography and it was found that two of the components present are quindoline and quindolone so a further literature search was carried out to see if there are any other methods described.

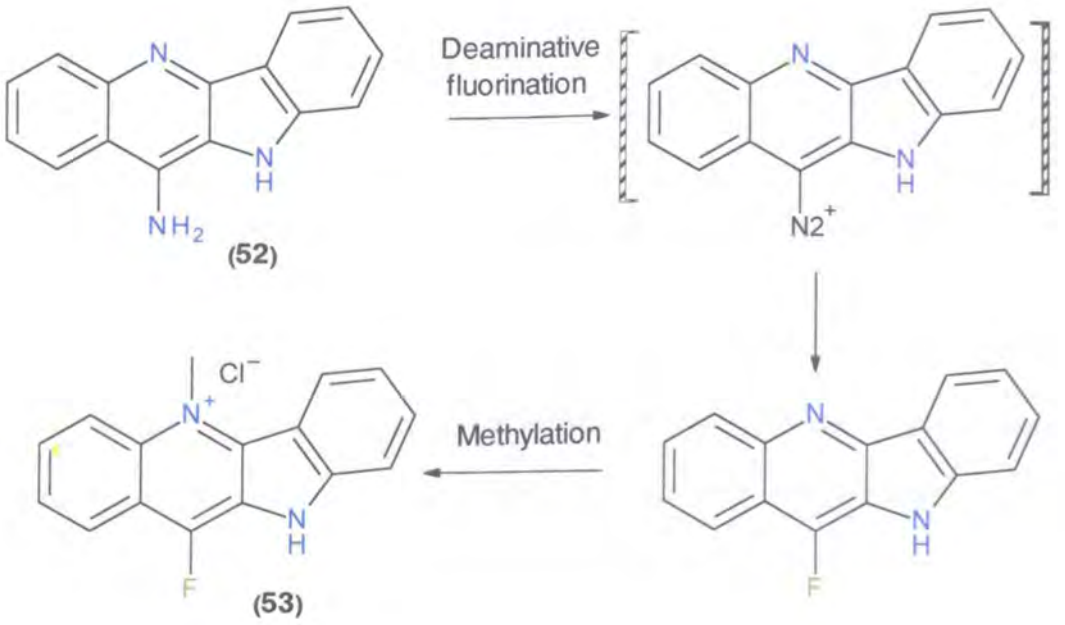

Figure 2.27 Showing deaminative fluorination

Fang and co-workers reported an electrochemical synthetic route to make 4-fluoropyridines in 2004. They carried out selective anodic fluorination of pyridine using triethylamine trihydrofluoride (Et3N.3HF) to give 4-fluoropyridine (Figure 2.28). This procedure gave a yield of 20% (Fang Bin *et al.*, 2011).

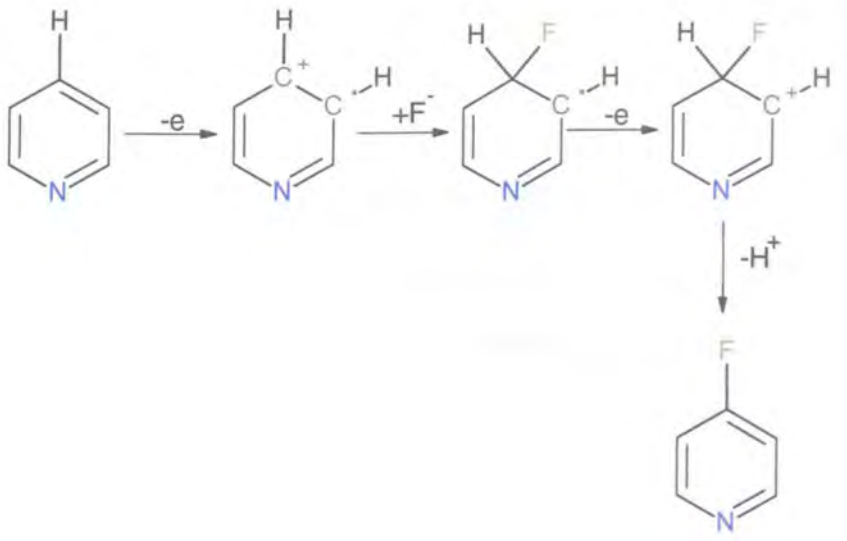

Figure 2.28 Showing the synthesis of 11-fluoropyridine by Fang

Another method was considered from from Patrik and Johri who successfully replaced a carboxylic functioinal group with fluorine atom using, fluorodecarboxylation. In this process carboxylicacid was treated with xenon fluoride to perform fluorination in the presence of methylene chloride at room temperature (Figure 2.29). The carboxylic acid is first converted to its fluoroxenon ester then the ester reacts by nucleophilic displacement by fluoride (Patrick *et al.*, 1986).

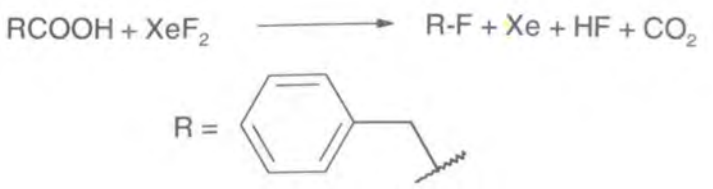

Figure 2.29 showing the synthesis of 11-fluorocryptolepine from carboxylic acids

Unfortunately this method did not work and there was no sign of fluorination from the fluorine NMR. There was not enough time for further investigation of

this fluorination reaction so it was paused to carry out synthesis of rest of the targets.

2.1 Derivatives with alkylamino side-chains

Three types of derivatives were designed by attaching various alkylamino and amido side chains at two different positions; at N5 and C11 of cryptolepine

Figure 2.30 Showing the target derivatives with alkylamino side-chains at 11 positions

Butylamino, *iso* propylamino and 2-hydroxy ethylaminoethylamine side-chains were attached at the C11 position via two different linkages; amino

and amido. A third set of compounds were designed by attaching ethyl and ethylamino sidechains at the N5 position (Figure 2.30).

Alkylamino side chains were attached for their lipophilicity so the overall drug uptake can be increased. For the same reason alkylamino side chains with different lengths were selected to see if there is any correlation between side chain length and the drug uptake in the cell lines *in vitro*. 11-Chlorocryptolepine served as the key intermediate to make the derivatives with amino linkages at 11-position via nucleophilic substitution.

In the derivatives with amino linkages, it is doubted that the secondary amine present on the side chain can be protonated at physiological pH but there is chance that the positive charge arising from N5 is in conjugation with the aromatic system (Figure 2.31). These positively charged derivatives can potentially interact with the negatively charged phosphate backbone of DNA which ultimately leads to increased strength of interaction.

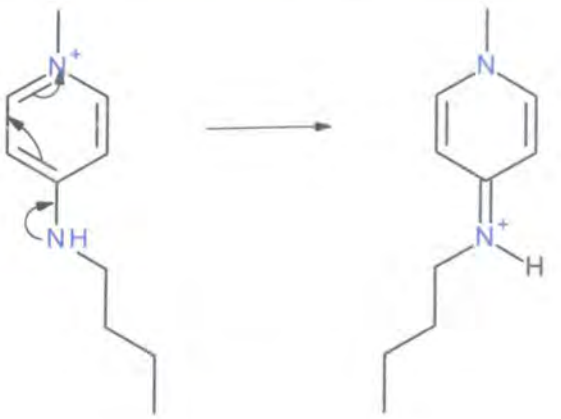

Figure 2.31 Showing the electron distribution in cryptolepines with 11-amino linkages

The 2-hydroxyethylaminoethylamine side chain was taken from the established drug, mitoxantrone. It was reported that attaching 2-hydroxy ethylami-

noethylamine group to an anthracenedione moiety enhanced the anticancer activity significantly (Murdock *et al.*, 1979).

Alkylamino sidechains were attached to the cryptolepine at the 11 position by heating to reflux 11-chlorocryptolepine**(37)** with the desired alkylamine side-chain overnight via nucleophilic substituition reaction (Figure 2.32). The precipitated derivative**(54, 55, 56)** was then purified using column chromatography (20-60% yield).

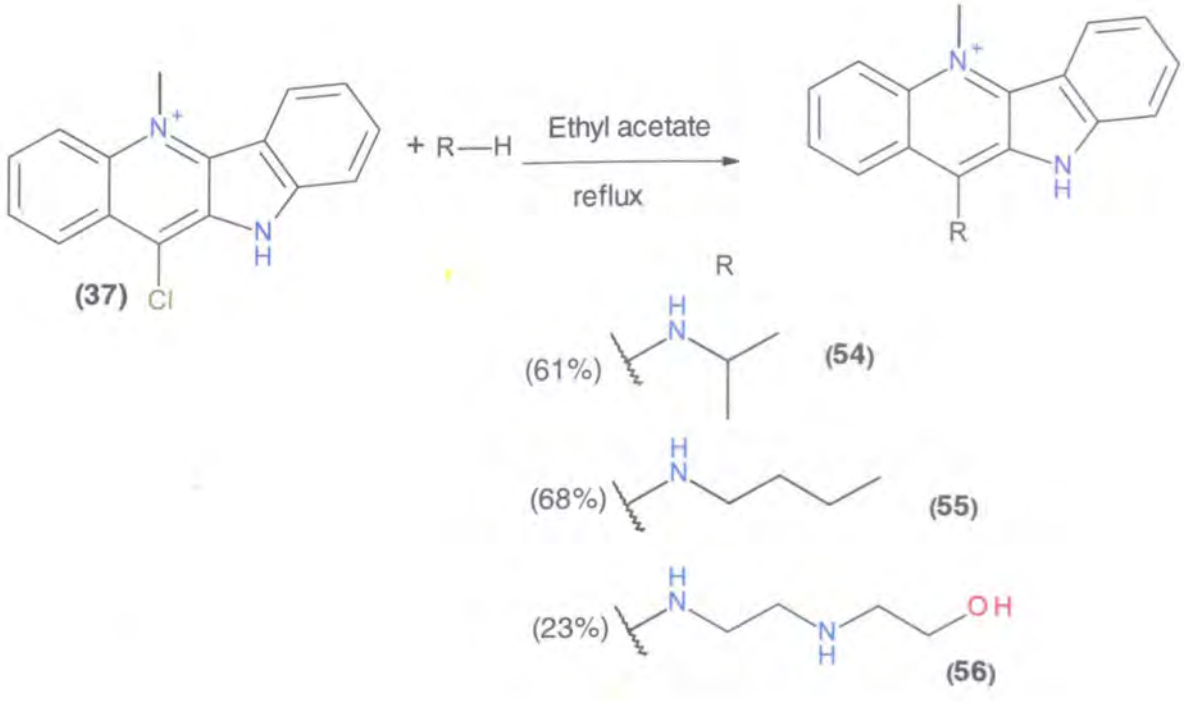

Figure 2.32 Showing the synthesis of cryptolepine derivatives with alkylamino sidechains at 11 position

Compared to alkylamido derivatives, making alkylamino derivatives is rather less complex. After refluxing 11-chlorocryptolepine with the desired alkylamino sidechain, resulting product is precipitated in the reaction mixture so it was easier to purify. Incase of isopropylamino derivative, simple washing

with ethanol and diethyl ether gave pure crystals. Whereas rest of the amino derivatives needed recrystallization.

Pyridines can be able to be attacked by nucleophiles at the 4 position. Attack at 3 or 5 positions of pyridine is not a favourable pathway because of the negative charge on the intermediate cannot be delocalised onto the electronegative nitrogen atom. This aromatic nucleophilic substitution is more favourable when good leaving groups like halogen are present instead of hydrogen (Figure 2.33).

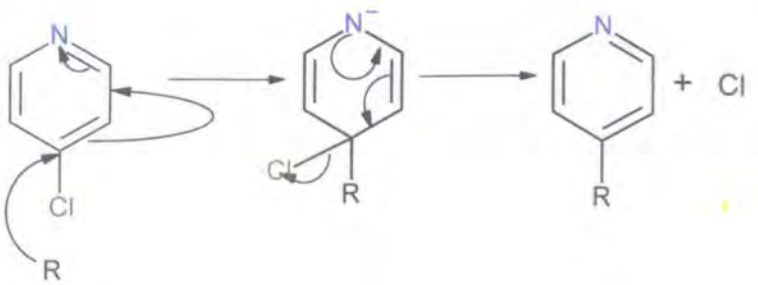

Figure 2.33 Showing aromatic nucleophilic substitution in pyridine and chloropyridine

^{1}HNMR of each alkylamino derivative showed additional aliphatic protons arising from the side chains for example, ^{1}H NMR of the isopropylamino derivative gave a peak at 1.57 ppm integrating to 6 protons arising from the two methyl groups. Further analysis through high resolution mass spectrometry confirmed that these compounds have been successfully made. For example Hi resolution mass for isopropylamino derivative gave an accurate mass of 290.1643 [M - Cl] (calculated = 290.1657).

In order to understand the more detailed structure activity relationships, the methyl group on N5 was replaced with a bulkier ethyl group. It was thought

that it would give more information about effect of length of the alkyl chain at N5 position on cytotoxicity.

Two compounds were made having an ethyl group on the N5 position, 11-chloro-5-ethyl-10H-indolo[3,2-b]quinolin-5-ium chloride**(57)** was made by treating 11-chloroquindoline**(51)** with ethyltriflate in the presence of toluene.

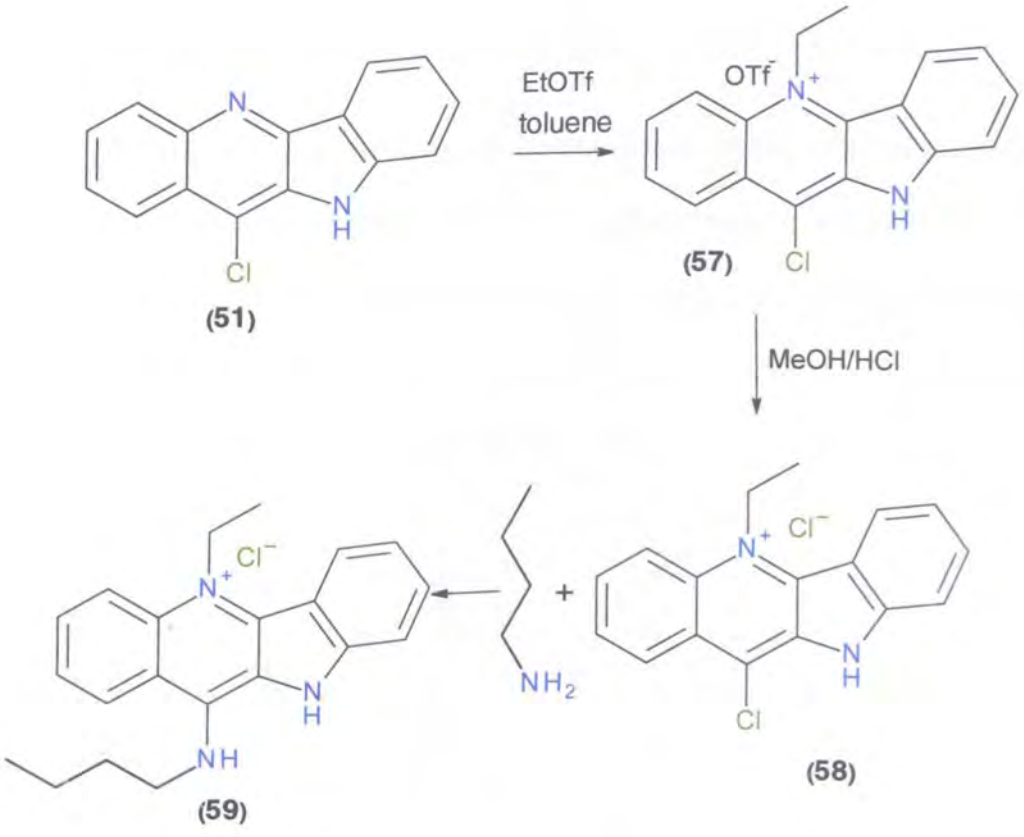

Figure 2.34 Showing the synthesis of N-butyl-5-ethyl-10H-indolo[3,2-b]quinolin-5-ium-11-amine chloride

A molecular mass of 281.0842 (required 281.0846) was obtained from high resolution mass spectrometry indicating that product had been fromed. Additionally extra carbon aridsing from N-5 position was seen in the carbon NMR

at 47.8 ppm (N5-CH_2) and 13.8 ppm (N5-CH_3). Also addition aliphatic protons were seen in the proton NMR at 1.8 ppm arising from the N5-CH_2.

Another compound was made treating product with butylamine giving N-butyl-5-chloro-5-ethyl-10H-indolo[3,2-b]quinolin-11-amine**(59)** (Figure 2.34). An accurate mass of 318.1961 (required m/z 318.1970) was obtained from the high resolution mass spectrometry and additional aliphatic protons arising from the butysidechain were seen in the proton NMR.

Unlike derivatives with amino linkages, in the derivatives with amido linkages, the positive charge will not be able to move to the aromatic ring (Figure 2.35). So these compounds were made to see how having an amide bond between side chains and the aromatic system of cryptolepine will affects the cytotoxicity and the drug uptake in the *invitro* cancer cells.

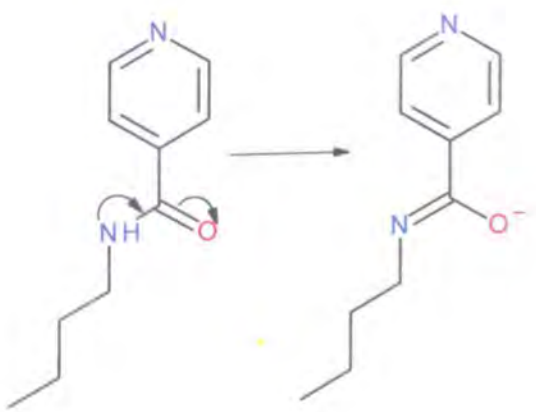

Figure 2.35 Showing the electron distribution in cryptolepines with 11-amido linkages

Isatin and *N*-acetyl indoxyl were condensed in a strongly alkaline solution to form quindoline-11-carboxylic acid (72% yield). The alkylamine side chain was then coupled with this carboxylic acid in the presence of (1-cyano-2-ethoxy-2-oxoethylidenaminooxy) dimethylamino-morpholino-carbenium hexa-

fluoro-phosphate (COMU) to make the amide linkage (50-80%). After purification, these were methylated at the N5 position using methyl triflate to give the cryptolepine derivatives (20-30%).

Using Holt and Petrow's method, indoxyl acetate and isating were condensed in the presenc e of a base for 10 days. Nucleophilic attack by indoxylacetate**(21)** at C2 position of isatin**(20)** opens the indole-ring and then followed by the intramolecular exo-trig cylisation gave the product (Figure2.36).

As the quindoline 11-carboxylic acid**(19)** was obtained as a hydrochloride salt it did not elute on TLC plate but it was observed that only one spot was present on the baseline. The compound was recrystallised and dried for analysis without any further purification.

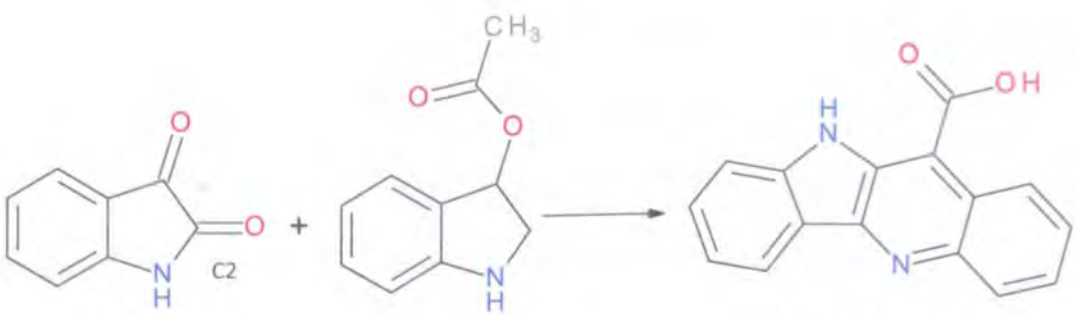

Figure2.36 Showing the synthesis of quindoline-11-carboxylicacid

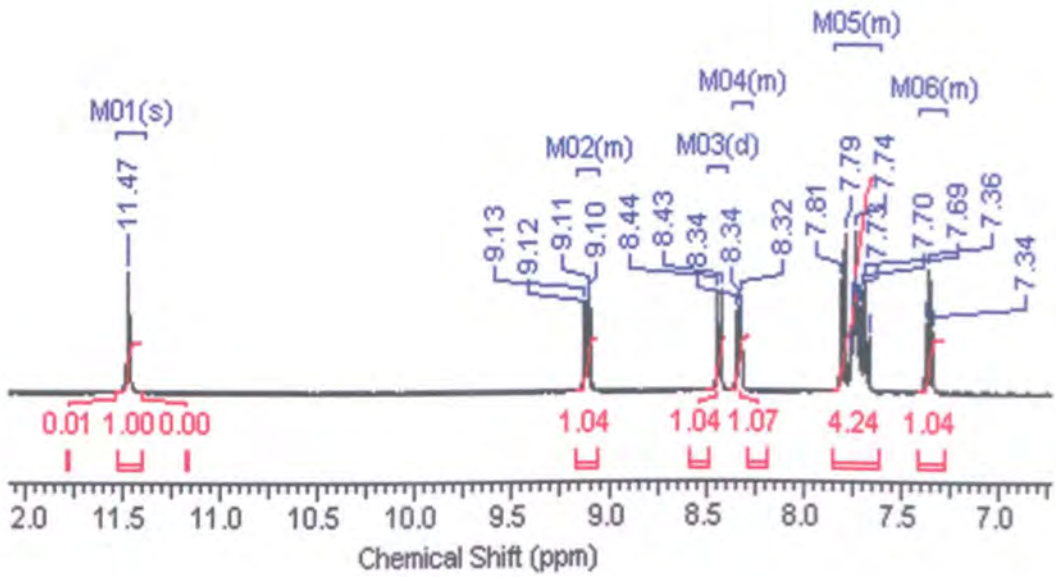

Figure 2.37 Showing ^{1}H NMR spectrum of Quindoline 11- carboxylic acid

^{1}H NMR gave a broad peak at 11.46ppm integrating to one proton which confirms the presence of NH in the aromatic ring (Figure 2.37). In addition to that total number of aromatic protons was integrating to the required number of 8 which shows that cyclisation was successful. The total number of 16 carbons were identified including one 168.14 ppm from carboxylic acid.

The aim of the next reaction was to attach alkylamino sidechains at the C11 position of the aromatic ring by making an amide linkage to the carboxylic acid. To synthesise the quindoline amides firstly the carboxylic acid was treated with thionylchloride and the resulting acyl chloride**(60)** was then treated with an amine to form the corresponding amide**(61)** (Figure 2.38). Unfortunately the final yield of the product was very low as 2% and the amount of product was not enough to carry further steps of the synthesis (Figure 2.39).

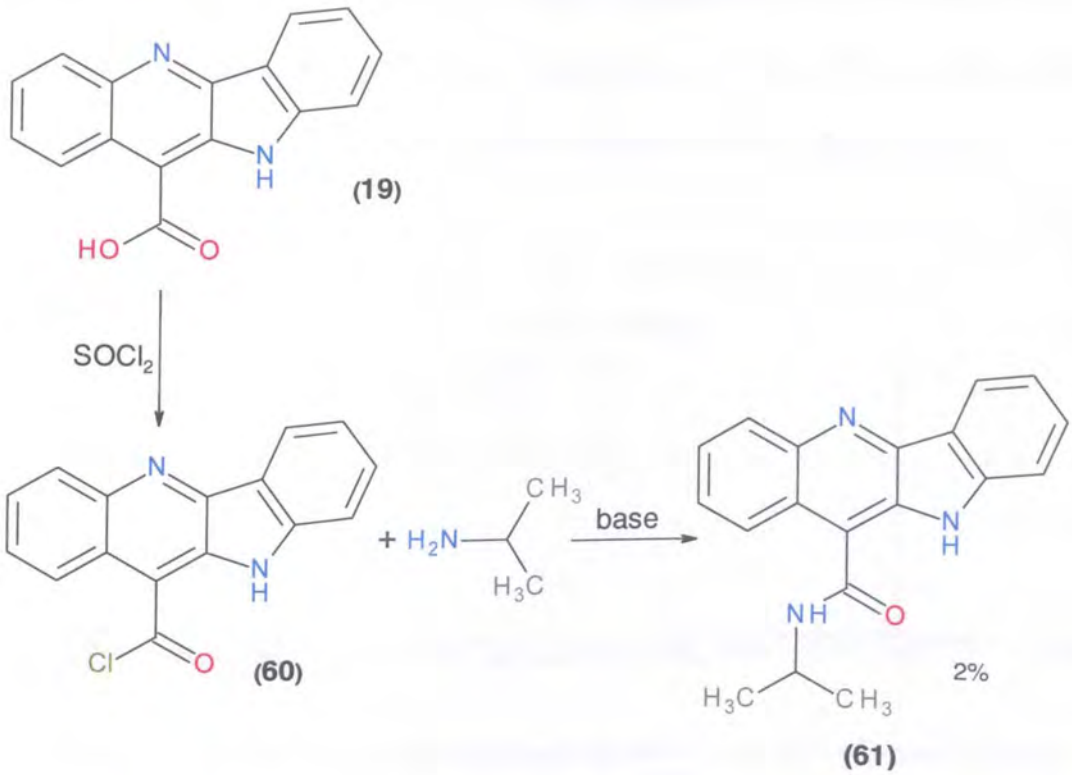

Figure 2.38 Showing the synthesis of quindoline amides

Figure 2.39 Showing a gas chromatrogram of reaction mixture containing the isopropylamido quindoline (using thionyl chloride)

Instead a coupling agent, COMU ((1-Cyano-2-ethoxy-2-oxoethylidenaminooxy)dimethylamino-morpholino-carbenium hexafluoro-

phosphate) was used to make the amides. Compared to the previous method using COMU yields were improved greatly up to 90% (Figure 2.40). This method was followed to introduce all of the side chains (Figure 2.42).

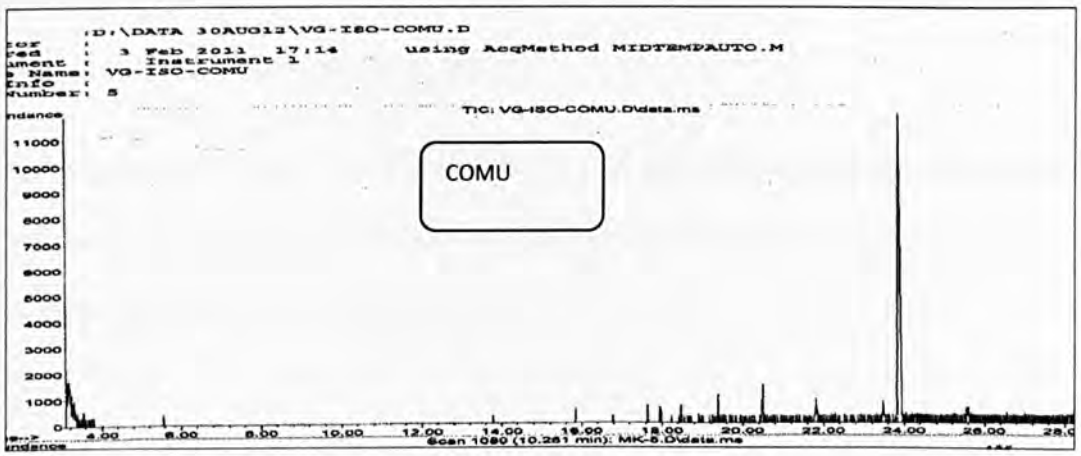

Figure 2.40 Showing a gas chromatrogram of reaction mixture containing the isopropylamido quindoline (using COMU)

The synthesis of derivatives with amido linkages is a difficult process mainly due to the purification procedures. After attaching the side chains using COMU (Figure 2.41) the reaction mixture was acid washed to remove any further unreacted amine left and the residue was subjected to column chromatography. After running the first column it was found that the amine was still present in most fractions so the mixture was subjected to another column however still the amine was present. It was found that the amide was decomposing on the silica giving free amine in a small amount which was contaminating all of the fractions. Few washes with aqueous copper sulfate solution gave pure compound. Whereas making derivatives with amine linkages was relatively easy.

^{1}HNMR of Isopropylamido quindoline gave a singlet at 3.77 integrating for one proton and another peak at 1.04 integrating for 6 protons confirms the

presence of an Isopropyl group and a broad peak at 11.76 integrating to one proton indicating the presence of NH from the aromatic ring. The presence of a carbonyl group was confirmed from ^{13}C NMR with a peak at 166.7 ppm. In addition to that IR spectrometry gave a peak 1646 cm^{-1} which indicates the presence of an amide carbonyl group.

Supporting the above analytical data mass spectrometry gave a molecular ion peak at 303, equal to the molecular weight of the compound indicating that the compound had been made.

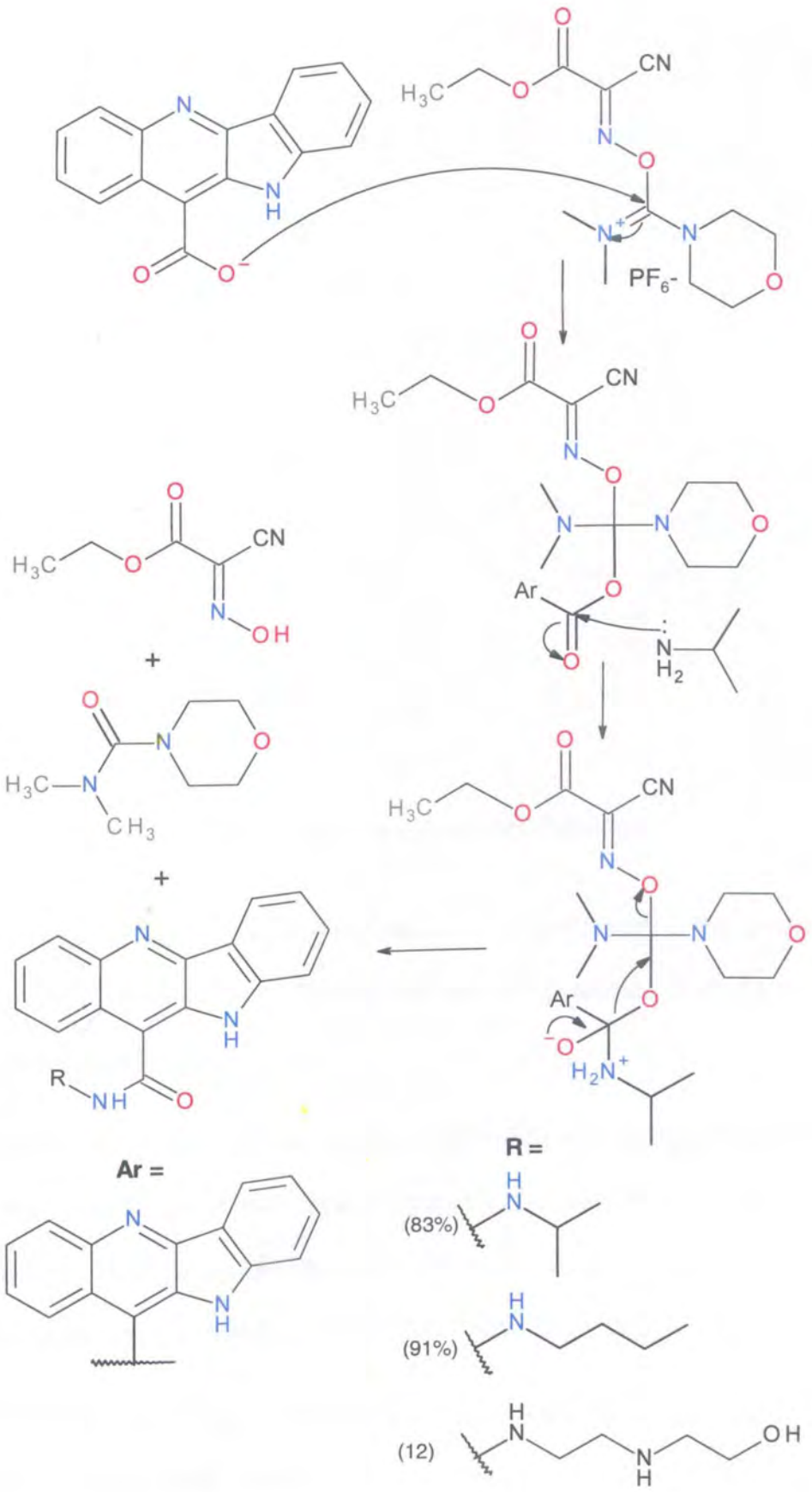

Figure 2.41 Showing the formation of of isopropylamido quindoline**(61)**

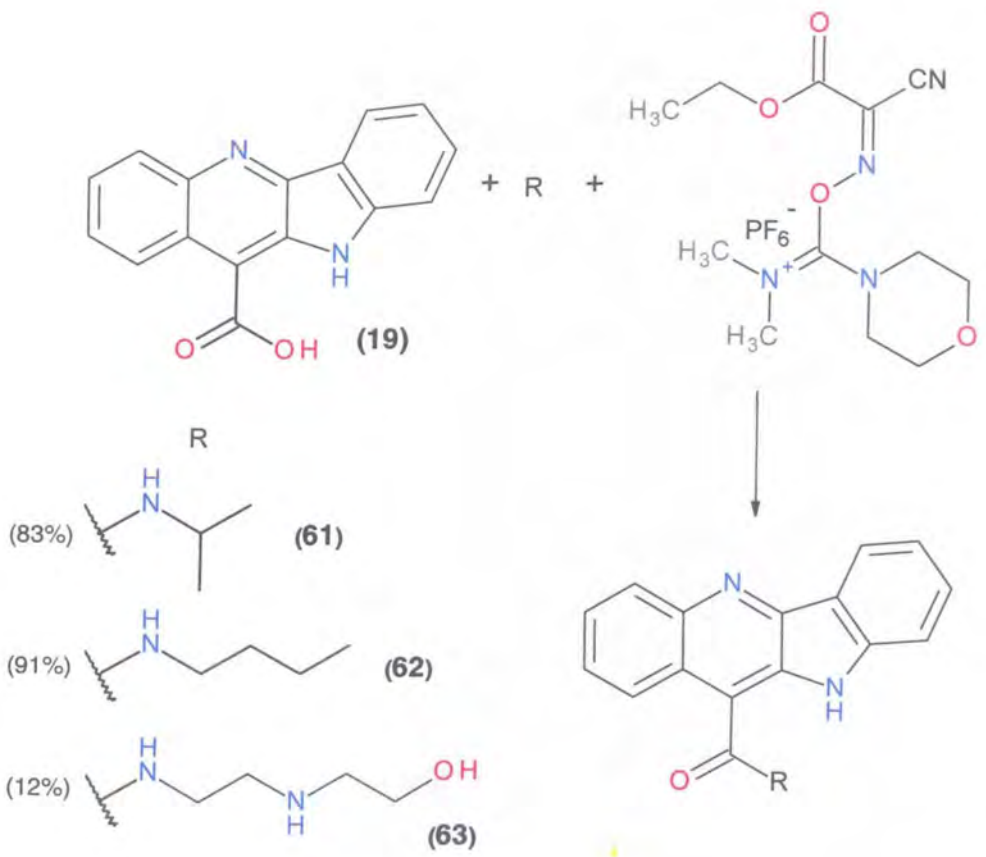

Figure 2.42 Showing target alkylamidoquindolines

Formation of the butylamide derivative was confirmed by the presence of 9 aliphatic protons in the ^{1}H NMR along with the presence of a carbonyl carbon at 165.4 ppm.

Attaching 2-hydroxy ethylaminoethylamine **(63)** was rather difficult compared to the other to alkylamino side chains. it could be because of the other secondary amine group present on the side chain. So less yield was obtained when compared to butyl and isopropylamido derivatives.

Quindolines were then methylated at the N5 position using the methylating agent, methyl triflate (Figure 2.43)

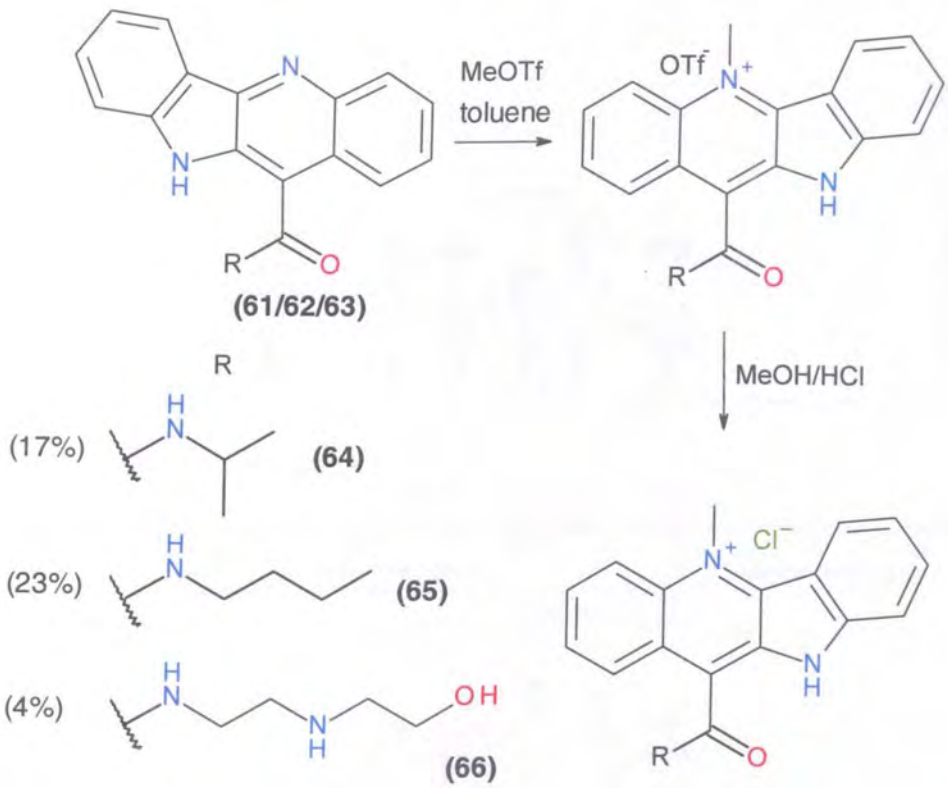

Figure 2.43 Showing methylation of alkylamido quindolines

The cryptolepine triflate salts were converted to their free bases using a sodium carbonate solution and were converted to their hydrochloride salt forms using methanolic hydrochloric acid solution.

NMR spectra of 11-isopropylamido cryptolepine**(64)** showed the presence of the aliphatic protons from the sidechain along with the aromatic protons (Figure 2.44).

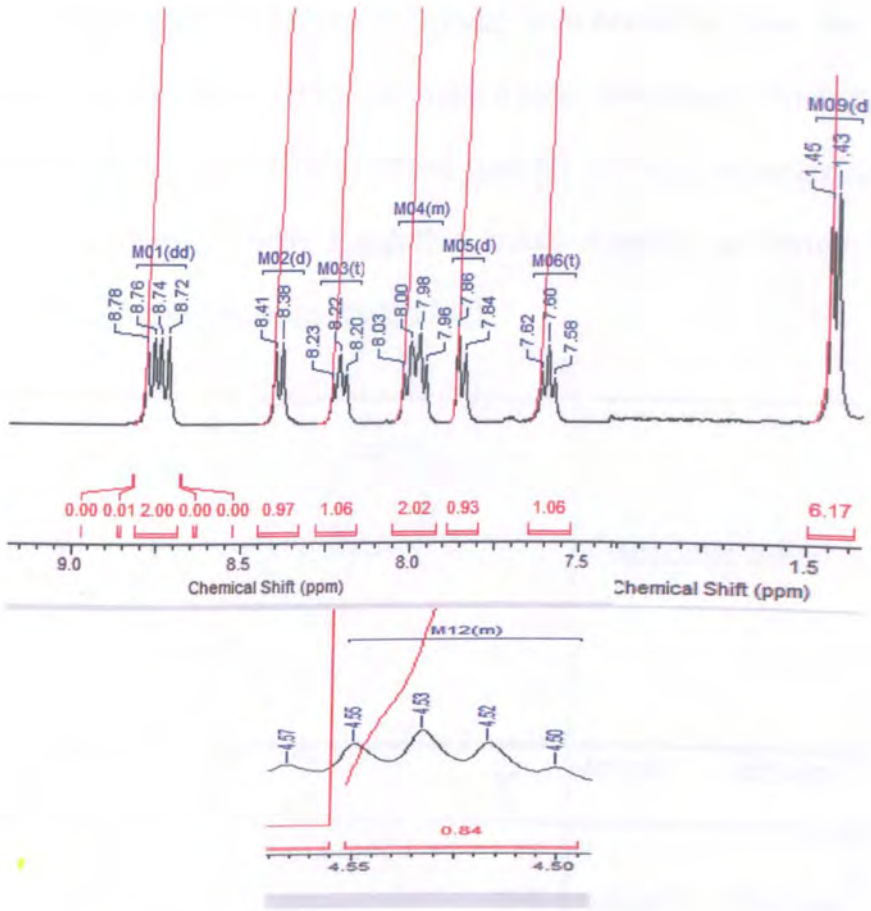

Figure 2.44 CNMR spectra of 11-isopropylamido cryptolepine showing the presence of protons from aliphatic protons present on the side chain

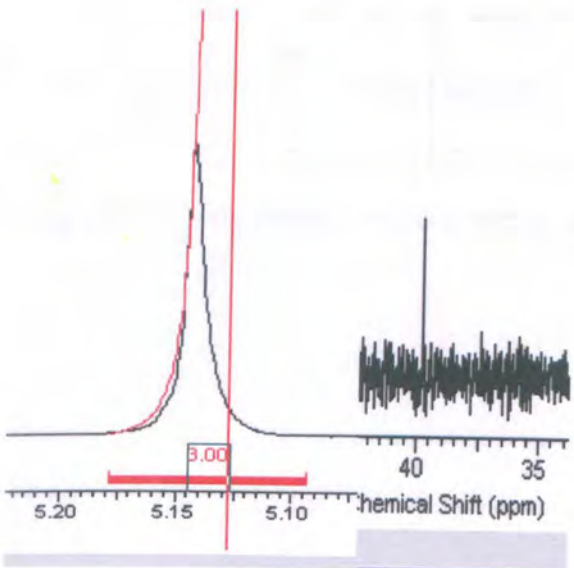

Figure 2.45 Showing the presence of methyl group using 1H NMR and 13C NMR spectra of 11-isopropylamido cryptolepine

Presence of the additional N-methyl group was observed from the ^{1}H NMR, which gave a peak at 5 ppm for all three amido derivatives. An ddditional carbon was seen in the ^{13}C NMR at 39-40 ppm for all three cryptolepine amides (Figure 2.45). Further, high resolution mass spectra confirmed the molceluarweight of the compound (Table 2.2).

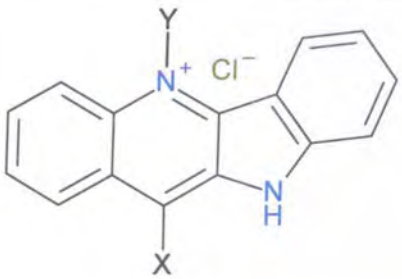

X	Y	Accurate mass found	Accurate mass required
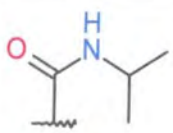	CH_3	318.1615	318.1606
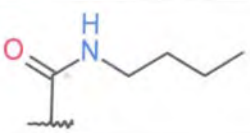	CH_3	332.1769	332.1763
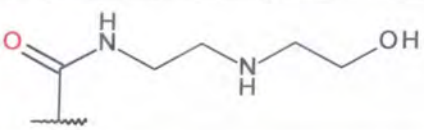	CH_3	363.1828	363.1821

Table 2.2 showing the high resolution mass spectral results of cryptolepine amides

Chapter 3 Invitro and Bio-physical Studies

3.1 In vitro cytotoxicity measurements

Testing of *in vitro* cytotoxicity of compounds is a useful tool in the discovery of novel anti-cancer compounds. There are various types of assays available to assess the cytotoxicity of potential drug candidates at the preclinical level. The selection of suitable assay is often dependent on research aim and sensitivity of the assay. The main things to consider while choosing a cytotoxicity assay are: quality of data, ease of experimental set up, stability of reagents being used and the cost of the assay (Niles *et al.,* 2008). At large research institutes these assays are carried out on a big scale using automated systems, this process is called high-throughput screening (HTS). Sensitivity and scalability of are the two main parameters based on which a cytotoxicity assay is selected in HTS.

Broadly there are two cytotoxicity assay methodologies: one is colonogenic and the other is non colonogenic. The former is based on measuring the number of colonies formed after incubating the cells in the presence of potential drug candidates and alone as a control group (Hoffman, 1991). This type of assay was popular in the 1970s (Weisenthal and Lippman, 1985). More recent use of this assay has been limited due the quality of results in terms of their precision and reproducibility (Weisenthal and Lippman, 1985). Noncolonogenic assays rely on the changes in concentration of bi-

omarkers during cell apoptosis and necrosis. As shown in, Table 3.1, necrotising cells die more quickly than cells which go through apoptosis. Mitochondrial dehydrogenase and ATP are two key biomarkers which give ideas about cell viability.

Time	zero	0.5 to 4 h	4 to 48 h	>48 h
Apoptosis				
Lactate dehydrogenase activity	++++	+++	+	0
Metabolism dehydrogenase activity	++++	+++	+	0
ATP activity	++++	+++	+	0
Necrosis				
Lactate dehydrogenase Activity	++++	0	0	0
Metabolism dehydrogenase activity	++++	0	0	0
ATP activity	++++	0	0	0

Table 3.1Showing the cellular changes during apoptosis and necrosis (Niles *et al.*, 2008).

In apoptotic cells these cease to be produced after 4-48 hours whereas in necrotising cells production is ceased within 30 minutes (Table 3.1). Another important bio- marker is LDH (lactate dehydrogenase), which leaks from

dying cells into the culture medium. The activity of these biomarkers is essential for the cell survival and inactivity of the same lead the cells to undergo either apoptosis or necrosis. By measuring the activity of these biomarkers, cell viability can be determined. Based on this principle three major non-colonogenic assays were developed.

- By measuring the activity of the LDH enzyme released into the culture medium using a redox dye.
- By measuring the mitochondrial reductase activity using MTT
- By measuring the ATP activity via a bioluminescence assay (luciferase-ATP assay) (Niles *et al.*, 2008).

3.1.1 Cytotoxicity assay based on enzyme release

This method measures the activity of a specific enzyme which is released from dying cells. The concentration of that particular enzyme is directly proportional to the number of dead cells (Korzeniewski and Callewaert, 1983; Decker and Lohmann-Matthes, 1988). Lactate dehydrogenase is widely accepted as a key biomarker which leaks from the cells which are undergoing apoptosis or necrosis (Niles *et al.*, 2008; Korzeniewski and Callewaert, 1983). A tetrazolium salt, (2-[4-iodophenyl]-3-[4-nitrophenyl]-5-phenyltetrazolium chloride), interferes with LDH activity of oxidation of lactate to pyruvate, and shows a colour change by forming a formazan (Figure 3.1). This can be measured using spectrophotometry.

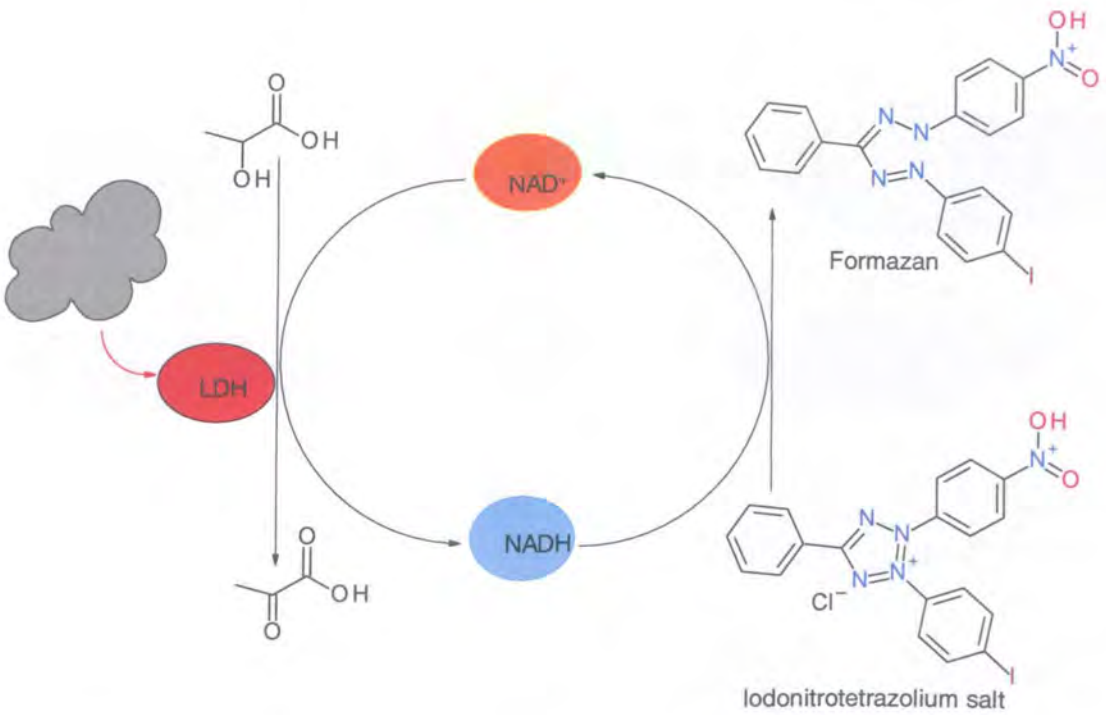

Figure 3.1 Showing the principle of the LDH colorimetric assay

Using this inexpensive assay, researchers have produced consistent and precise results. However, only cell death marked by LDH can be measured, for example cytotoxicity caused by respiratory chain inhibition cannot be estimated (Weyermann *et al.,* 2005) because this assay only measures the LDH associated cell death but not mitochondrial reductase.

3.1.2 ATP assay to measure cell viability

The presence of ATP *in vitro* in cells has been accepted as a marker of their viability. ATP produces bioluminescence in the presence of luciferase (a peptide prepared from the abdomen of the firefly *Photinus pyralis*) (Figure 3.2)

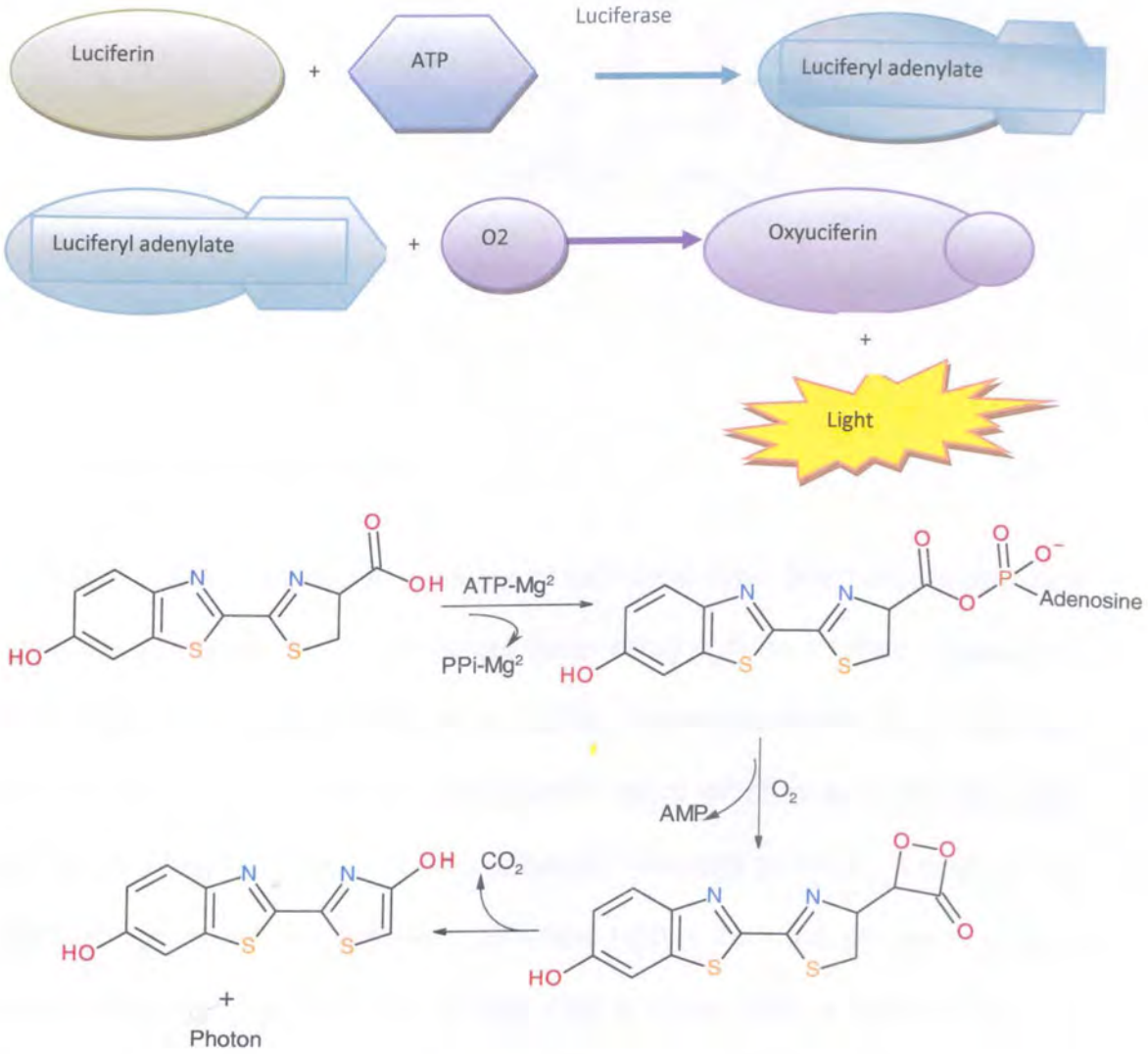

Figure 3.2 Showing production of bioluminescence (Fraga *et al.*, 2006).

The amount of bioluminescence is directly proportional to the number of viable cells (Niles *et al.*, 2008; Weyermann *et al.*, 2005; Riss *et al.*, 2005). The main drawback of this method is that the bioluminescence produced is short lived lasting for a few seconds only, as the cells are quickly depleted of their stock of ATP (Fraga *et al.*, 2006).

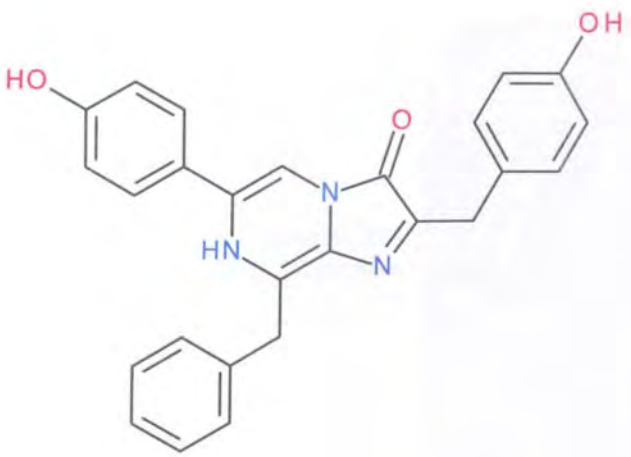

Figure 3.3 Colenterazine

In recent years more stable versions of luciferase have been prepared which improves the reliability of this assay by emitting a more intense bioluminescence (Niles *et al.,* 2008; Riss *et al.,* 2005). Gaussia luciferase is a novel enzyme secreted by expression of a synthetic gene which is a modification of a luciferase obtained from a marine copepod, *Gaussia princeps.* It produces a flash of light which has intensity 10 times higher than the bioluminescence produced by natural firefly luciferase. This enzyme uses a different type of luciferin molecule called colenterazine (Figure 3.3) (Zhao *et al.,* 2004; Maguire *et al.,* 2009; Wurdinger *et al.,* 2008; Ray and Gambhir, 2007).

3.1.3 MTT assay

This assay is based on the fact that the mitochondrial dehydrogenase enzyme present in viable cells can cleave the tetrazolium ring in 3-(4,5-dimethylthiazolyl)-2,5-diphenyltetrazolium bromide (MTT) to give purple coloured formazan crystals (Figure 3.4) (Mosmann, 1983).

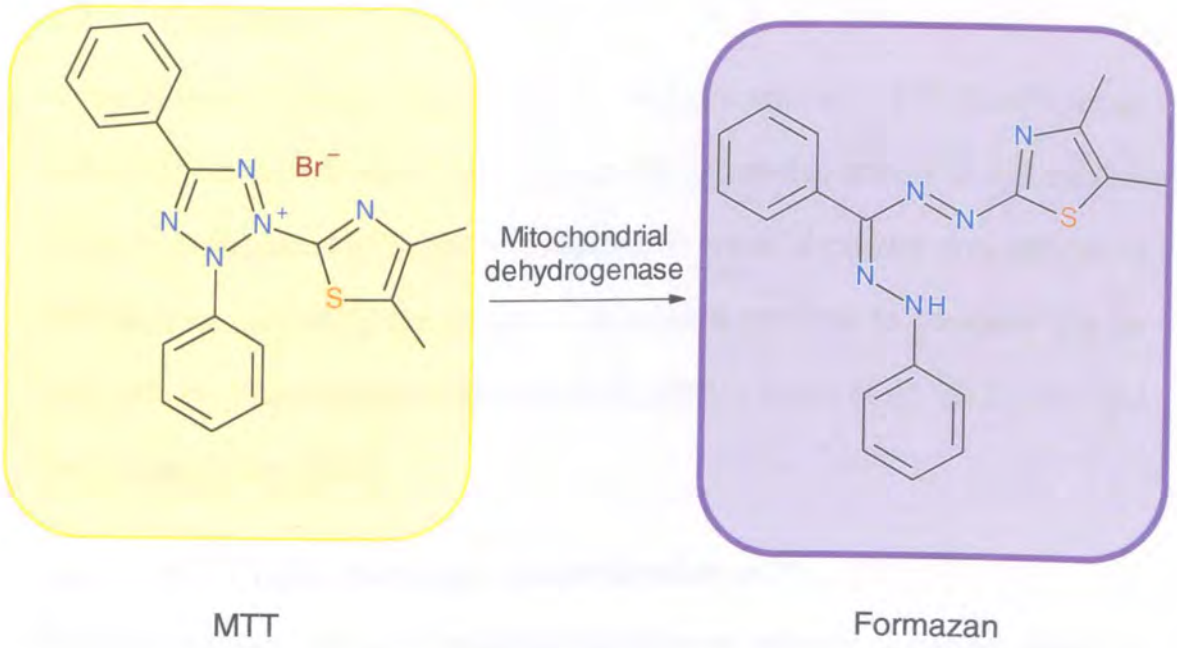

Figure 3.4 Showing the formation of formazan crystals

Using dimethyl sulfoxide (DMSO) these crystals are dissolved and their absorbance is measured at 590nm (their λ_{max}) allowing the cell viability to be quantified. The absorbance obtained from the formazan solution is directly proportional to the number of viable cells in the culture (Mosmann, 1983). This assay is rapid, robust, less time consuming and precise in terms of data quality compared to colonogenic assays. In the current project, the MTT assay was chosen because it is inexpensive, easy to setup, rapid and many researchers have produced precise results using it. Another important reason for its selection was most of the similar cryptolepine work conducted elsewhere was done using this assay for easy comparison of the results (Onyeibor *et al.*, 2005; Gokcek *et al.*, 2000; Jerrum *et al.*, 2006).

3.2 Cell lines

Three different cancer cell lines: MCF-7 (breast cancer) A549 (lung cancer) DLD-1 (colon cancer) were used to test the anticancer activity of the synthesised cryptolepine analogues. In addition to ease of culture and laboratory maintenance, choosing these cell lines make it possible to compare the results with previous literature (Wright *et al.,* 2001; Laryea *et al.,* 2009; Zhu and Gooderham, May 2006).

3.2.1 MCF-7 cells (Michigan Cancer Foundation-7)

This cell line was originally obtained from pleural effusion of patient suffering from metastatic breast cancer.

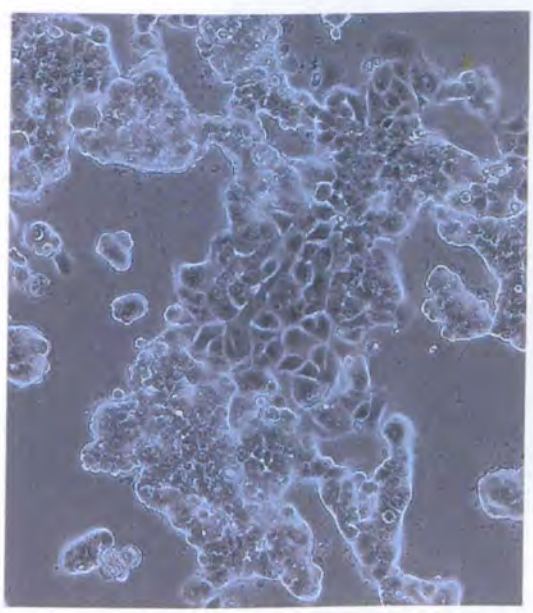

Figure 3.5 MCF-7 cells after 24 hours from seeding time (magnification: 20x, bright field)

The cell line is easy to grow in the laboratory with a population doubling time of 29 hours (Horwitz *et al.,* 1975; Soule *et al.,* 1973; Levenson and Jordan, 1997). MCF-7 cells contain estrogen receptors which indicate that the growth of these cells could be influenced by estrogen (Horwitz *et al.,* 1975; Saceda

et al., 1988). It was mainly selected because of its reported sensitivity to cryptolepine (Laryea *et al.,* 2009). These cells are sensitive to intercalators including doxorubicin and anti-estrogens including tamoxifen.

3.2.2 A549 cells (lung carcinoma)

This cell line was first cultured from a lung carcinomatous tissue from a 58 year old male patient by Giard (Giard *et al.,* 1973).This cell line can be easily cultured and maintained in the labs. It has a population doubling time of 22 hours. This cell line previously showed sensitivity to cryptolepine (MIC 10 µM) (Zhu and Gooderham, May 2006).

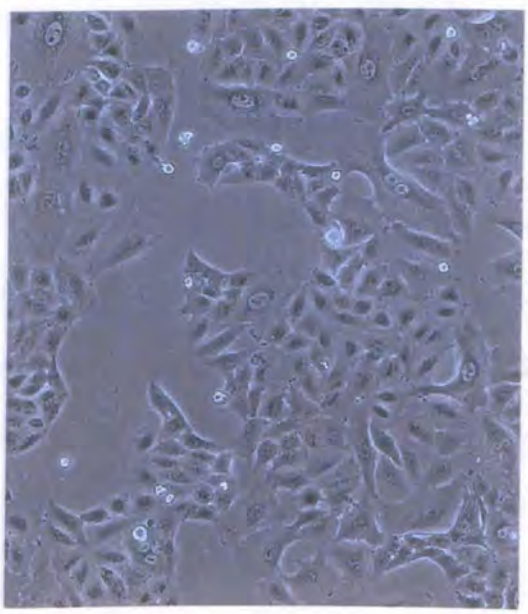

Figure 3.6 A549 cells after 24 hours from seeding time (magnification: 20x, bright field)

3.2.3 DLD-1 cells (lung cancer):

These were derived from a human colorectal adenocarcinoma by Dexter (Dexter *et al.,* 1979). Cryptolepine was active against these cells as an anti-cancer agent with an IC_{50} value of 1.44 µM (Wright *et al.,* 2001; Laryea *et al.,* 2009).

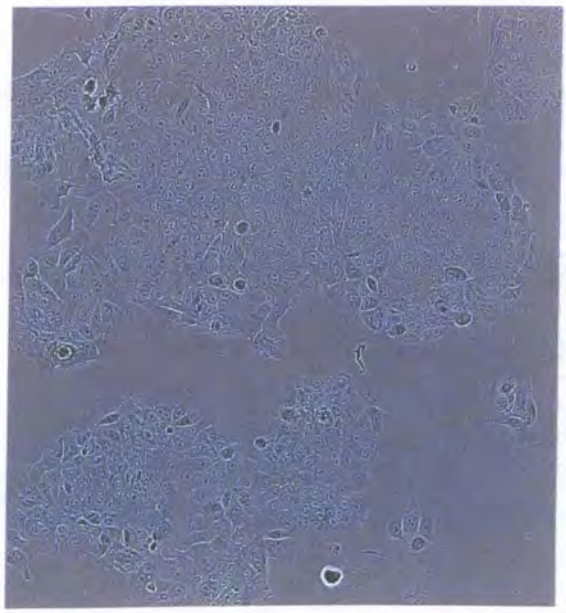

Figure 3.7 DLD-1 cells after 24 hours from seeding time (magnification: 20x, bright field)

3.3 Growth media

The main aim of cell culture media is to provide the physiological conditions for the growing cells in the culture plates. It ideally contains essential nutrients (carbohydrates, amino acids and vitamins), growth factors, hormones, salts and trace elements. The common carbohydrate used in media preparation is glucose. This could be replaced with galactose which metabolises at a slower rate and produces smaller amounts of the undesirable lactic acid. L-Glutamine is an important essential amino acid required for cell growth and functioning. It is used by cells both as an energy source and also to synthesise proteins. Where metabolism is not effective due to low levels of glucose, cells use L-glutamine as an energy source.

Foetal bovine serum is another important constituent of complete growth medium which provides growth factors, hormones, binding proteins and minerals. When the cells are dividing and growing in the culture media, metabolic

waste will build-up which can change the pH of the media. To prevent this, a suitable buffer system is used as part of the complete growth media. Bicarbonate or phosphate buffers are most commonly used.

The pH indicator phenol red is widely used to detect the change in pH due to cellular metabolic reactions. It shows red colour in neutral conditions and it turns in to yellow colour in acidic conditions (ATTCC® animal cell culture guide – www.atcc.org).

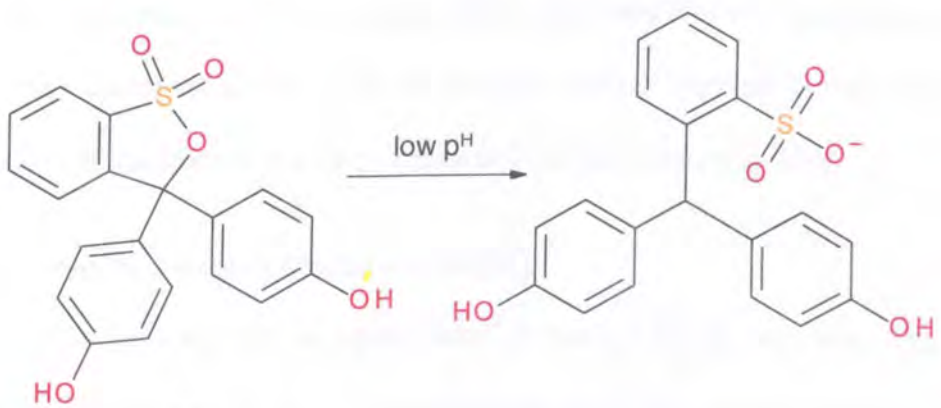

Figure 3.8 Showing the molecular changes in phenol red causing colour change

Phenol red is a weak estrogen agonist, it binds to estrogen receptor with a low affinity, so it should be kept in mind that it could affect the cell growth (Berthois *et al.,* 1986).

Depending upon the culture requirements, a wide range of salt solutions are available to go with culture media. Hank's balanced salt solution, Earle's balanced salt solution and phosphate buffered saline and balanced salt solutions are commonly used. The main roles of salts in the culture media are to

maintain osmolality, to maintain constant pH by the buffer effect and to maintain the permeability and integrity of cell membrane.

There are a number of cell culture growth media which are commercially available. It is necessary to identify what kind of media is suitable to grow a particular type of animal cell line. Commonly used complete growth media are:

3.3.1 Eagle's Minimum Essential Medium (EMEM)

This was first made by Harry Eagle which contains Earle's balanced salt solution, non-essential amino acids and a low level of sodium bicarbonate concentration. It contains 1 g/L of glucose (ATCC cell culture guide).

3.3.2 Modified Eagle's Medium (DMEM)

This contains double the concentration of amino acids, vitamins and ferric nitrate compared to EMEM. It also contains 1000mg/L of glucose. According to ATCC and PHE (Public Health England), this medium is suitable for culturing MCF-7 and A549 cells (ATCC).

3.3.3 Roswell Park Memorial Institute (RPMI-1640)

This was first formulated at Roswell Park Memorial Institute in the USA. It is supplied with a higher concentration of glucose then DMEM (4,500 mg/L). It is also provided with a reduced level of sodium bicarbonate to allow use under 5% CO_2 during incubation. According to ATCC and PHE this medium is suitable to grow the DLD-1 (colon cancer) cell line (PHE).

3.4 The standard cell proliferation assay

Different types of cancer cells grow at different rates under the same conditions. Before performing the cytotoxicity assay on a cancer cell line, it is

necessary to determine optimal seeding cell count. This was done by plotting the absorbance obtained from MTT treated cells which were seeded on a serial dilution basis against cell number. It not only established the linear relationship between absorbance and cell count but also gave an idea about growth characteristics of specific cell lines which helped in designing the cytotoxicity assay.

According to the ATCC-LGC (American Type Culture Collection) standards, the optimal seeding count for an MTT assay should give an absorbance which lies between 0.75 and 1.25 (Figure 3.10, Figure 3.11, Figure 3.12). Using that standard absorbance value, the optimal seeding cell count was obtained from the standard curve of each cell line.

Figure 3.9 Picture showing different concentrations of Formazan formed from cells grown at serial dilutions.

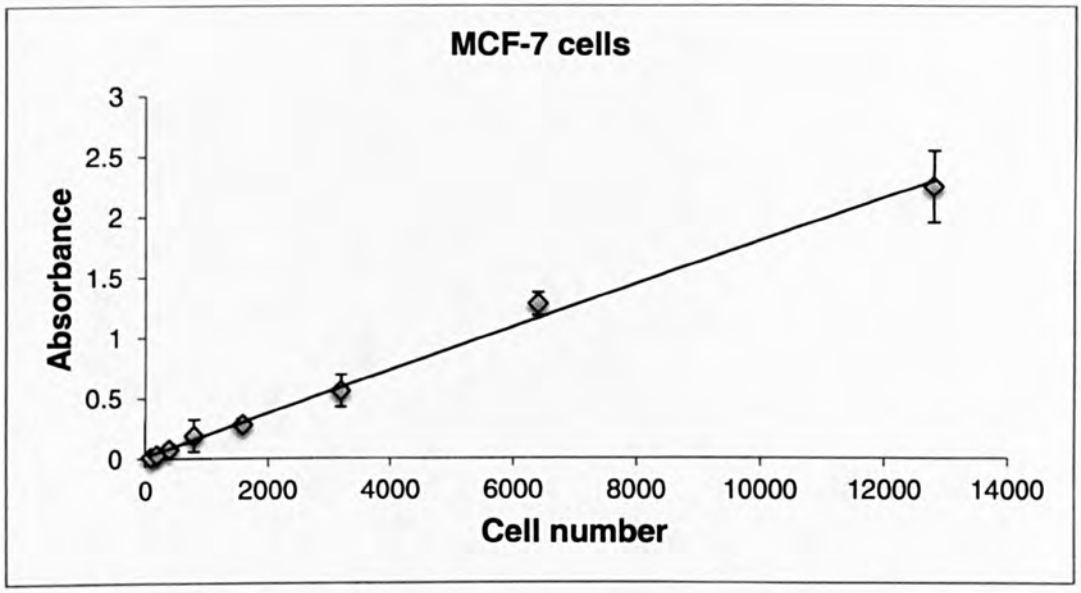

Figure 3.10 Standard cell proliferation of MCF-7 cells using MTT assay n=3

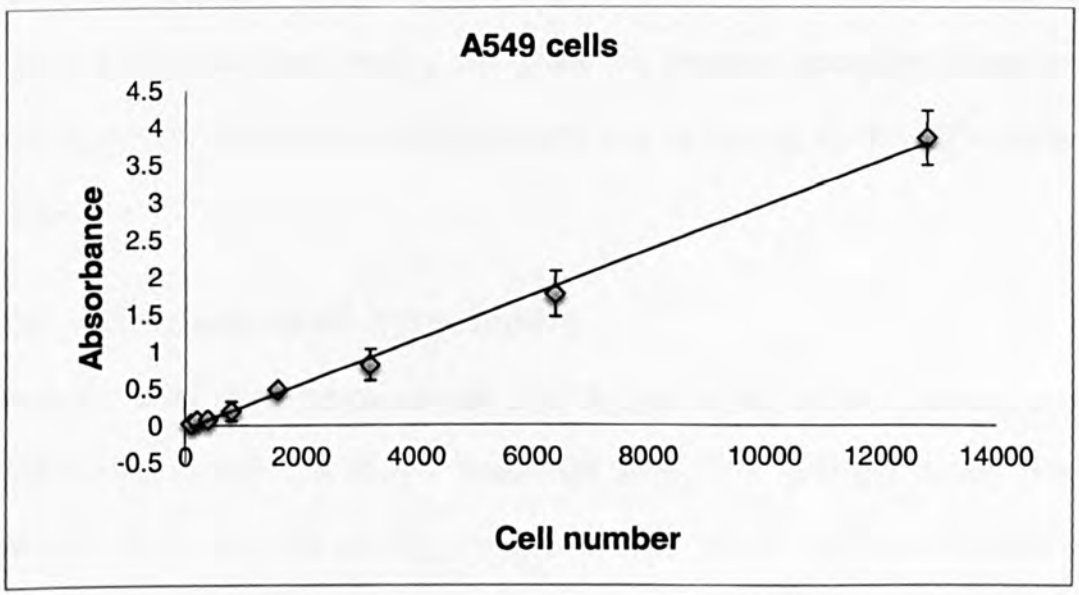

Figure 3.11 Standard curve of A549 cells using MTT assay n=3

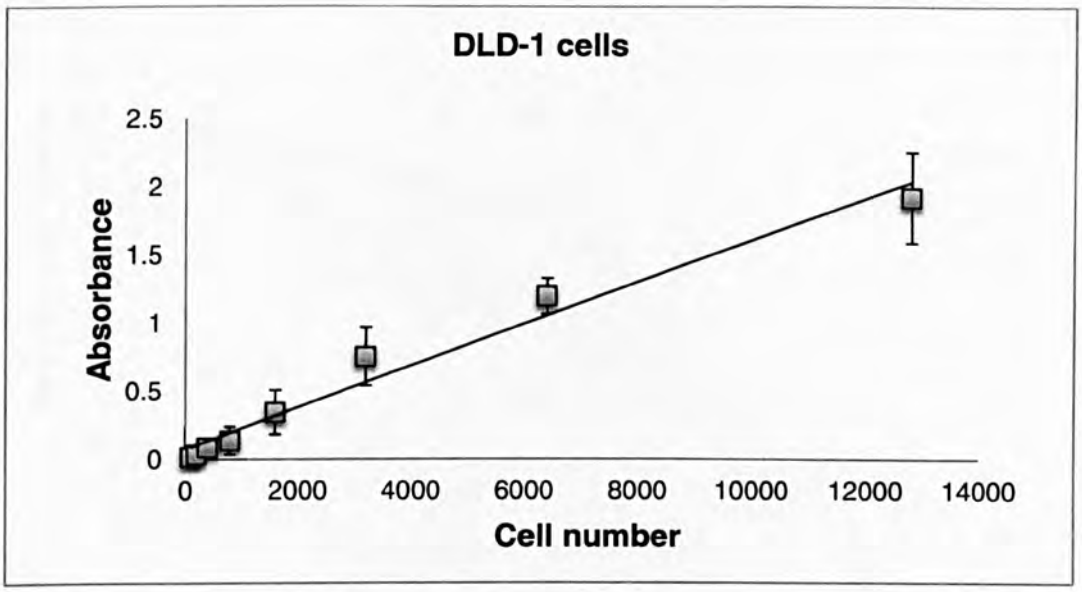

Figure 3.12 Standard curve of DLD-1 cells using MTT assay, n=3

Upon observing the standard curves of all three cell lines, it became apparent that a cell seeding density of 5, 000 gives the required absorbance between 0.75 and 1.25. The same seeding density was applied to all the MTT assays carried out.

3.5 Cytotoxicity of cryptolepine

When the cells were incubated with cryptolepine for 96 hours, it showed anti-proliferative activity on all the three cell lines. The greatest activity was against A459 cells with an IC_{50} value of 0.47±0.12 μM compared to MCF-7 and DLD-1 cells on which it gave IC_{50} values of 5.9±0.69 μM and 1.25±0.77 μM respectively (Table 3.2).

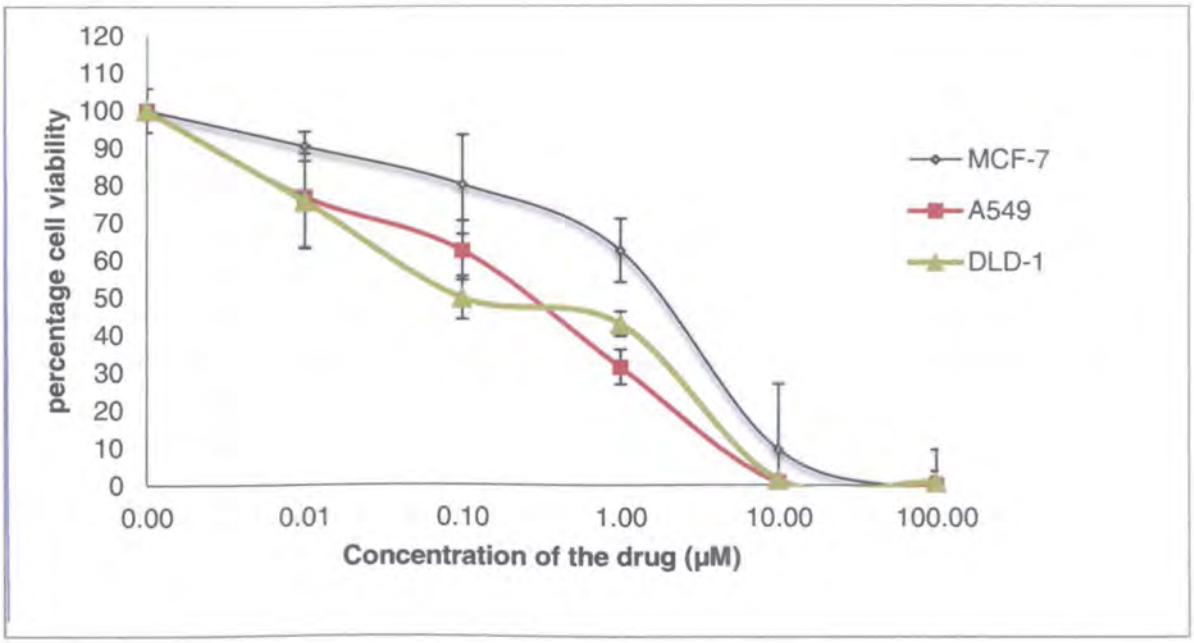

Figure 3.13 Dose response curve for cryptolepine using MTT assay

In 2002 Gokcek carried out the same experiments on A-549 and DLD-1 cells and reported IC_{50} values of 0.55 ± 0.05 μM and 1.44 ± 0.002 μM (Gokcek *et al.*, 2000).

From the dose response curve it is observed that no significant activity was seen until a 0.10 μM concentration of cryptolepine was applied. After that there is a gradual downward trend until 1.00 μM. Once the concentration reached 10 μM the percentage cell survival was essentially zero.

After exposing cells to 1 μM or higher It was observed under the microscope that cells started to change their morphology. As the concentration increased more cells were lysed and more cell debris was observed.

3.6 Cytotoxicity of cryptolepine derivatives

The 11-butylamino and 11-pentylamino compounds showed a higher level of activity compared to the isopropyl amino linked compounds suggesting that having an alkylamino sidechain is structurally significant

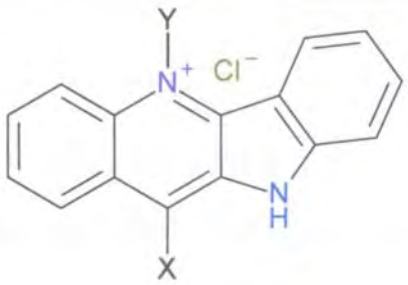		A549 cells IC_{50} val-ues in µM	MCF -7 cells IC_{50} val-ues in µM	DLD-1 cells IC_{50} val-ues in µM
X	Y			
H	CH_3	0.47±0.12	5.90±0.69	1.25±0.77
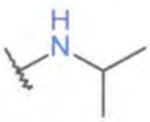	CH_3	20.38±2.01	17.92±2.31	37.05±2.36
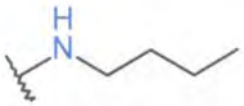	CH_3	1.05±0.15	0.63±0.51	2.85±0.87
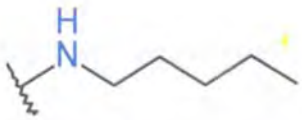	CH_3	0.83 ±0.28	4.253 ± 1.88	2.4±0.96
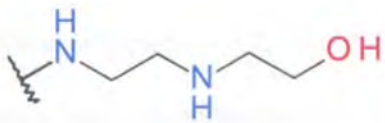	CH_3	10.41±0.75	6.77±2.03	12.23±1.20
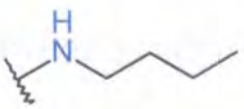	C_2H_5	12.58 ± 2.12	43.59±4.72	26.73±3.92

Table 3.2 Cytotoxicity results of cryptolepine derivatives with 11-alkylamino side chains

Particularly on MCF-7 cells, these two compounds showed greater activity than the parent compound with the butyl amino compound being 10 times more potent with an IC_{50} value of 0.63±0.51 µM. The 11-pentylamino derivative showed a greater activity than the 11-butylamino compound on A549 and DLD-1 cells with IC_{50} values of 0.83±0.28 µM and 2.4±0.96 respectively.

From these results it is identified that the activity of the derivatives not only depends on the structure of the compound but also the type of cell lines being used for the testing. It is also observed that the length of the side chain also played a role in the activity of the amino linked derivatives.

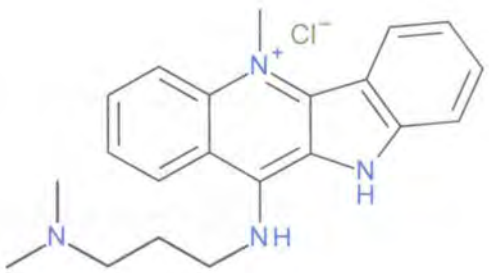

Figure 3.14 Cryptolepine derivative with alkylamino side chains as synthesised by (Lavrado *et al.*, 2008b)

The high activity of 11-butylamino cryptolepine might be due to the delocalized positive charge. (Lavrado *et al.*, 2008b) (see section 2.3)

Similar types of compounds (Figure 3.14) with alkylamino side chains were previously synthesised by Larvado and co-workers which showed cytotoxicity 8 times higher than cryptolepine on Human umbilical vein endothelial cells (HUVEC) cells (Lavrado *et al.*, 2008b). Another important factor to consider here is that alkylamino side chains can potentially increase the lipophilicity of the molecule increasing the drug uptake into cells.

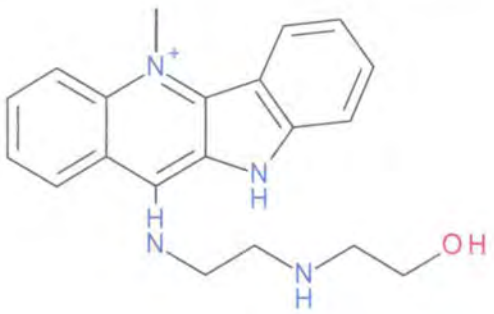

Figure 3.15 Derivative with an aminoalcohol side chain at 11 position

The design of this compound (Figure 3.15) was taken from mitoxantrone (Figure 3.16), an amino alcohol side chain containing acridine. Alkyl amino side chains may be particularly important because they could form electrostatic interactions with negatively charged DNA backbone (Avendaño and Menendez, 2008; Alberts *et al.*, 1985).

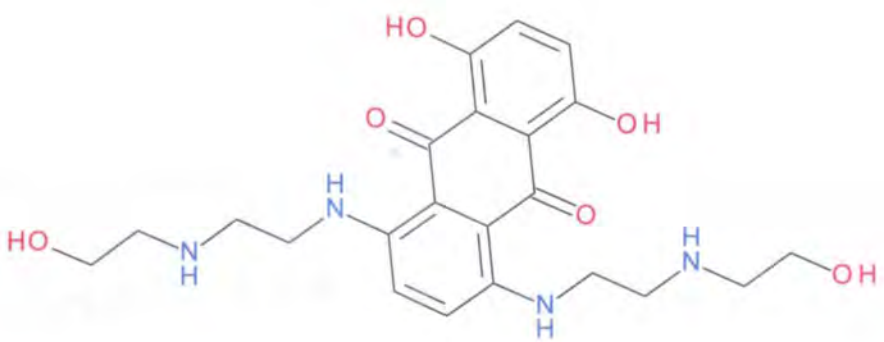

Figure 3.16 Mitoxantrone

When it comes to the derivative with the amino alcohol side chain, though the activity of this compound was less than butyl and pentylamino derivatives, it showed considerably higher activity compared to the isopropyl amino derivative. It compound showed greater activity on the breast cancer cells with an IC_{50} value of 6.77±2.03 μM this was also observed when Von Hoff and his team tested mitoxantrone on 20 different tumour cell lines it showed great

activity against breast cancer (MCF-&) cells compared to DLD-1 cells (Von Hoff *et al.*, 1981).

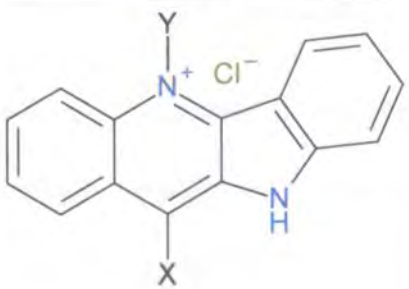		A549 cells IC_{50} values in µM	MC-7 cells IC_{50} values in µM	DLD-1 cells IC_{50} values in µM
X	Y			
H	CH_3	0.47±0.12	5.90±0.69	1.25±0.77
Br	CH_3	5.16±1.25	2.15±0.41	3.35±1.62
I	CH_3	0.28 ± 0.1	0.1±0.02	0.34±0.05
Cl	CH_3	42.83± 3.74	62.87±2.71	81.58 ±2.61
Cl	C_2H_5	15.24± 2.2	21±3.62	31.84±3.86

Table 3.3 Cytotoxicity results of 11-halogenated cryptolepine derivatives

When 11- halogenated derivatives are compared to the other sets of molecules, the activity shown by the 11-iodo compound was most potent. 11-Bromo cryptolepine showed second highest activity among all the halogenated compounds tested. And 11-Chlorocryptolepine showed the lowest activity.

In summary 11-halognated analogues followed a downward trend of activity from 11-iodo to the 11-chloro derivative. But when these halogenated derivatives are compared with the parent compound, 11-chlorocryptolepine showed a decreased activity whereas 11-bromo and 11-iodo derivatives showed in-

creased. These changes can be explained by considering the following properties:

Size of the halogen attached

The size of constituent atom can plays a role in the drug receptor interaction. To achieve an optimum drug-receptor interaction size of the atom should be optimum based on the available spatial orientation at the site of interaction.

Polarisation

Halogens exhibit the capacity of causing distortions in chemical bonds which can gives raise to polarising power which can affect the overall charge on the molecule which can affect the pharmacokinetics of cryptolepine

Eg. Calicheamicin as a case study

The calicheamicin is an enediyne antibiotic derived from the bacterium *Micromonospora echinospora*. It binds to DNA with role played by the iodine atom present on the thiazoate ring assisting in forming a good DNA-ligand complex. Hawley and his team demonstrated that there is an intermolecular contact between the polarisable iodine atom present on the thiazoate ring with the exposed amino proton outside the ring from the 5' guanine base of the DNA (Hawley *et al.*, 1989).

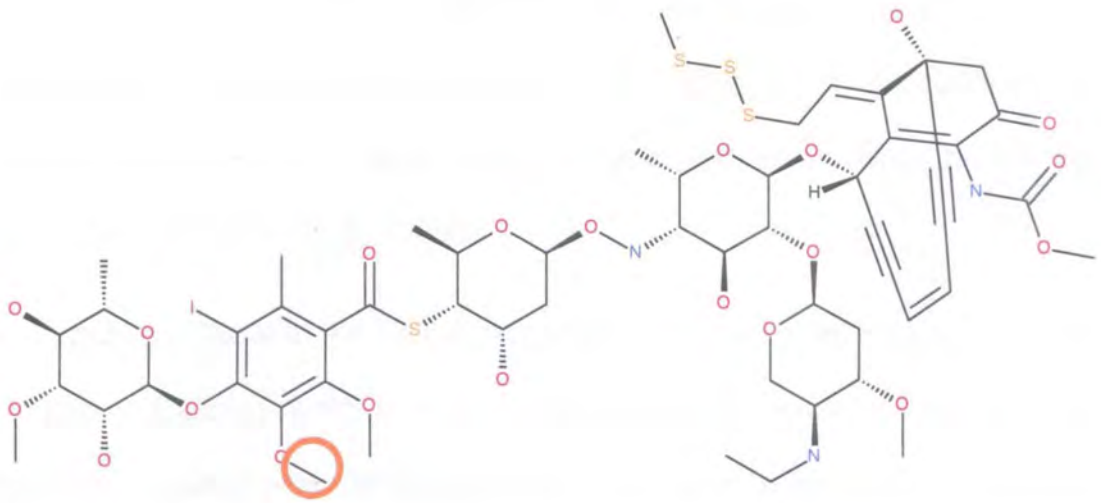

Figure 3.17 Showing the structure of Calicheamicin

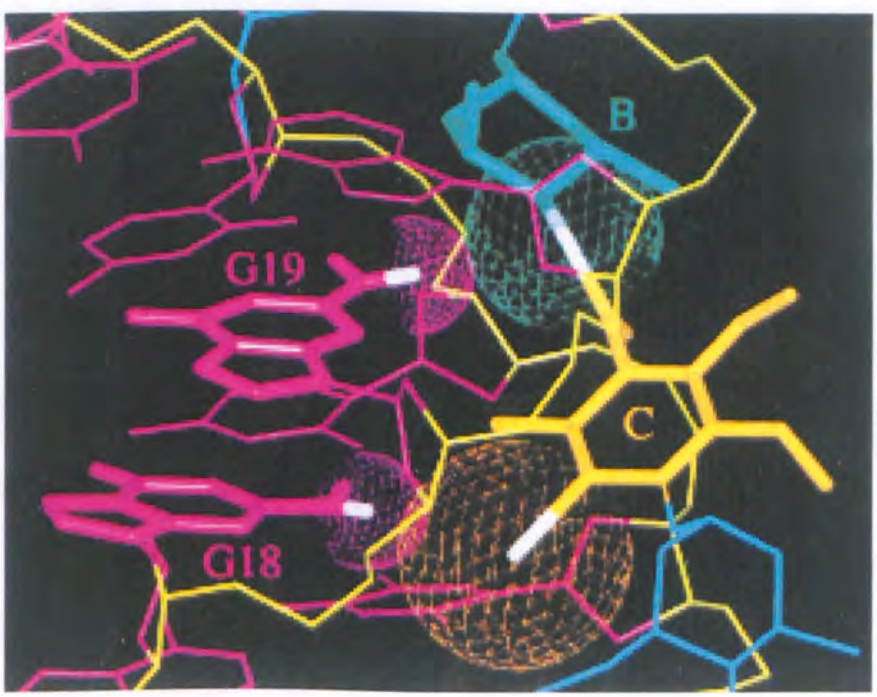

Figure 3.18 Showing intermolecular contact between polarisable iodine atoms present on the thiazoate ring with the amino proton outside the ring from the 5' guanine bases (yellow mesh; Iodine, pink mesh: amino hydrogen from guanine, green mesh: sulphur).

This Van der Waals interaction between iodine and amino hydrogens is important (3.43 ± 0.33 A^{o}) for optimal binding and selectivity of drug towards that particular DNA sequence (Hawley *et al.,* 1989), which was confirmed by making and testing the other halogenated analogues choloro, bromo and fluoro derivatives (Li *et al.,* 1994).

A gradual decrease in the DNA-binding was observed from iodo to fluoro analogues of Calicheamicin (Li *et al.,* 1994). Similar results were seen from halogenated cryptolepine derivatives; the anticancer activity was decreased from iodo to chloro gradually.

This could mean that the presence of Iodine atom at 11- position may have been involved in similar molecular interactions which were contributing for the DNA binding efficiency of 11-iodocryptolepine. DNA binding results of these compounds were discussed in section 3.11.

When it comes to derivatives with 11-amido linkages, these compounds showed comparitavely less activity than other sets of compounds. Amongst the amido-derives, 11-butyamido compound showed highest activity whereas the 11-isopropylamido derivative showed lowest activity (Table 3.4). Also the electron movement from nitrogen creating a negative charge on the on the oxygen (Figure 2.35).

Regardless of whether it is an amino derivative and an amido derivative, having an isopropyl group reduced the activity significantly. This could be due to the steric effects arising due to bulky isopropyl functional group.

X	Y	A549 cells IC_{50} values in µM	MCF-7 cells IC_{50} values in µM	DLD-1 cells IC_{50} values in µM
	CH_3	42.64± 3.17	31.72±2.56	75.01±2.92
	CH_3	21.41±1.76	7.26±1.24	4.14±0.891
	CH_3	12.38±2.16	9.15±1.56	15.21±3.23

Table 3.4 Cytotoxicity results of cryptolepine derivatives containing 11-alkylamino sidechains with amidolinkages

Amongst all the molecules synthesised, derivatives with 11-alkylamino linkages and 11-halogenated compounds showed comparatively greater activity than compounds having 11-amido side chains.

3.7 Topoisomerase II inhibition studies

DNA topoisomerases unknot the higher order structures of DNA to simple double stranded versions; this was discussed in section 1.4.8. This process involves breakage and relegation of the double stranded DNA. Essential cellular functions including DNA replication, transcription, and chromosomal segregation require topoisomerase II activity (topo II). Topo II poisons may cause DNA breaks along with enzyme inhibitory action which ultimately affects the cell cycle (Clifford *et al.,* 2003).Testing cryptolepine derivatives for

topo II activity not only gives information about the capacity of a particular compound to inhibit the enzyme but, upon comparing the results with DNA binding studies (see section 3.12), it gives insights into the mode of action by which cytotoxicity may be exhibited. Two widely used procedures to assess the topo II poisoning effect of a compound are; one using supercoiled plasmid DNA and the other using catenated kDNA (Marini *et al.*, 1980).

In the super coiled plasmid based DNA method, after treatment with topo II DNA becomes relaxed and the products formed can be identified by running gel electrophoresis (Cheng *et al.*, 2012; Gong *et al.*, 2006) (Topogen, 2005). If a drug has topo II catalytic inhibitory action it does not allow the supercoiled DNA to be relaxed which will be seen on the gel as a band remaining at the baseline the same as the negative control.

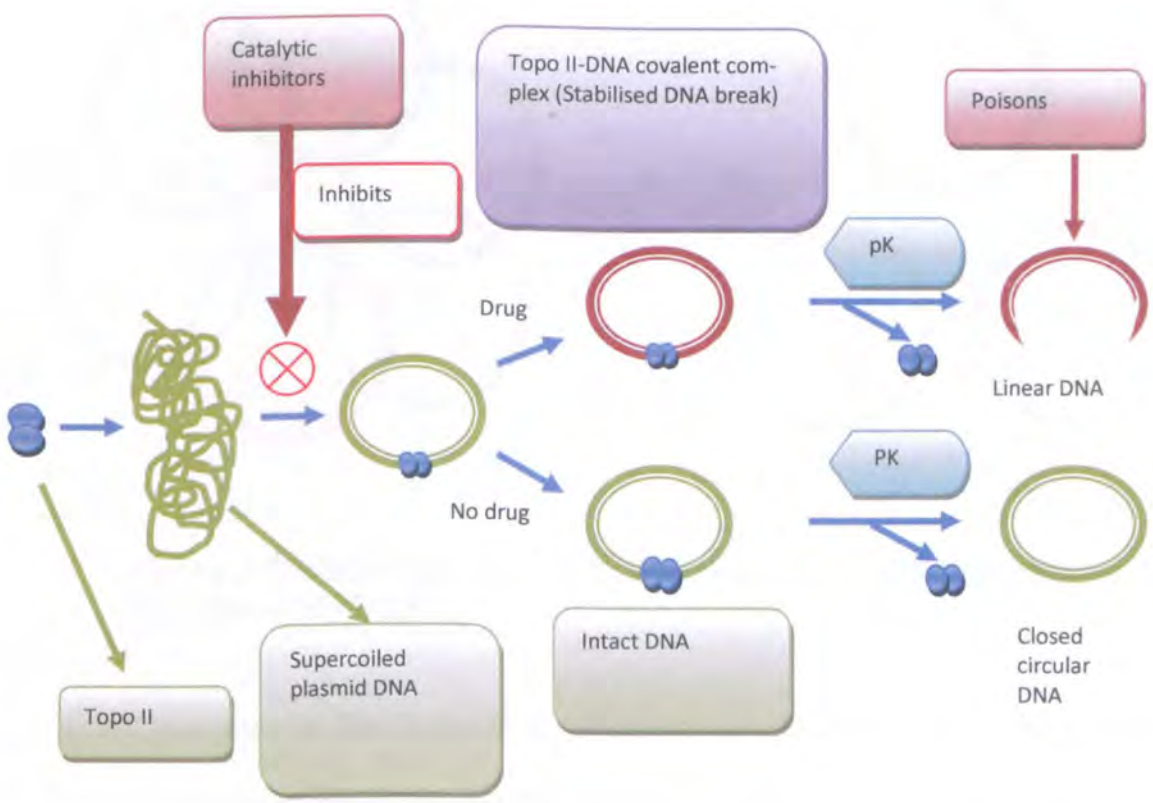

Figure 3.19 Schematic representation of topo II activity experiment using supercoiled plasmid DNA

If a drug has a topo II poisoning effect it will produce strand breaks in the DNA by stabilising the DNA-Topo II complex which produces linearised DNA after removal of topo II by using protein kinases (PK) (Figure 3.19) (Topogen, 2005). These DNA products will show a different band pattern compared to either the initial supercoiled or the intact closed circular DNA.

The other method for measuring topo II inhibition or poisoning uses **catenated kDNA** as a substrate which becomes decatenated upon treatment with topo II (Bonjean *et al.*, 1998; Marini *et al.*, 1980; Gong *et al.*, 2006). In the current project this method was employed because band recognition is simple.

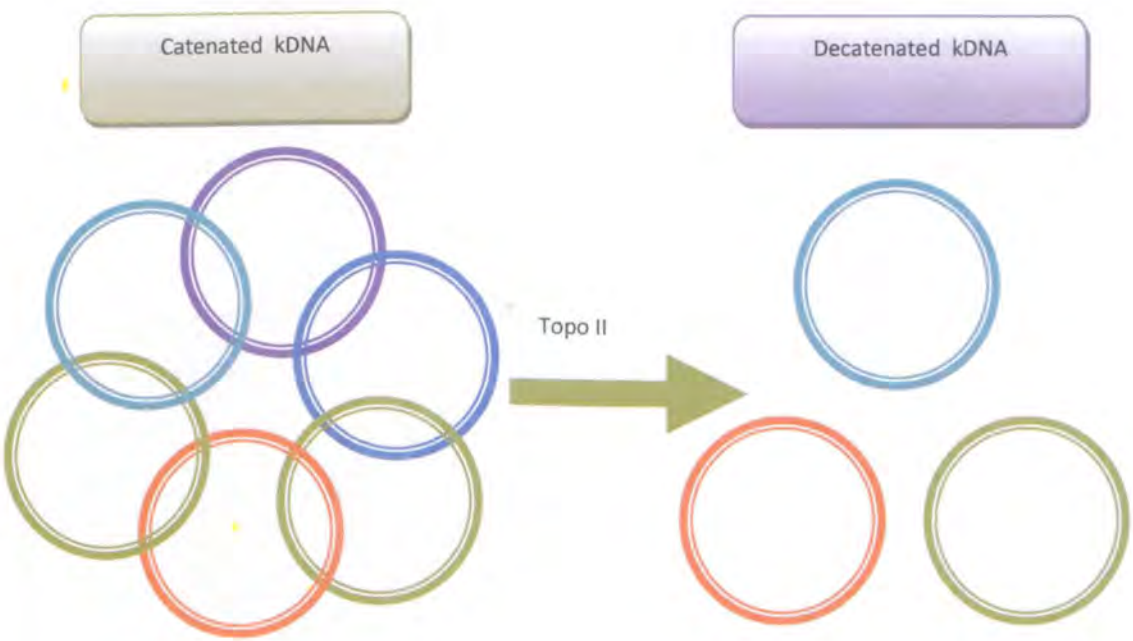

Figure 3.20 Schematic representation of topo II activity experiment using catenated kDNA

In the presence of the drug the decatenation processes do not occur so the heavier catenated DNA stays at the baseline of gel electrophoretograph.

3.8 Topo II activity of cryptolepine derivatives

Table 3.5 shows the results for the current study. Cryptolepine has been tested for topo II activity in the past using both of the methods outlines above and it has been proposed that cryptolepine acts as a topo II poison (Bonjean *et al.*, 1998; Bailly *et al.*, 2000; Dassonneville *et al.*, 2000).

		Topo II activity expressed as minimum inhibitory concentration (MIC) in μM
X	Y	
H	CH_3	0.5
Cl	CH_3	0.25
	CH_3	>100
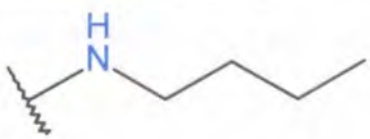	CH_3	0.25

Table 3.5 Showing activity of cryptlepine and its analogues on topo II expressed in MIC values.

When cryptolepine was tested for its topo II activity it gave a minimum inhibitory concentration value (MIC) of 0.5 μM. The same result was reported by

Bonjean and his team on supercoiled plasmid DNA obtained from *Esterichia coli* (Bonjean *et al.*, 1998).

This group also demonstrated that the topo II activity of cryptolepine is linked to the anti-proliferative or anti-tumoral capacity of the drug.

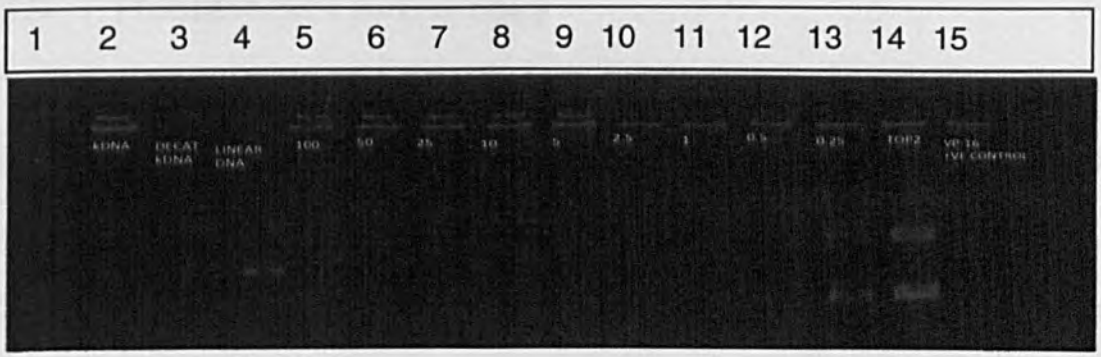

Figure 3.21 Showing the Topo II activity of cryptolepine

Where, Lane1 = Blank, Lane 2 = kDNA, Lane 3 = Decat kDNA, Lane 4 = Linear kDNA, Lane 5-13 = cryptolepine (100-0.25 µM), Lane 14= Top2 only and Lane 15 = Vp-36(positive control)

11-Butylamino cryptolepine showed the highest topo II inhibition of the compounds tested (Table 3.5) and also the highest cytotoxicity (Table 3.2). This continues to support the link between the two. The analogue with the 11-isopropylamido group gave much lower topo II activity than parent compound and this reflected the low cytotoxcicity of cryptolepine derivatives having isopropyl group.

However the 11-chloro derivative failed to confirm this relation and gave a low cytotoxicity despite having high topo II activity. The topo II activities obtained from both compounds are significantly higher than that of the parent compound.

It was thought that these irregularities between cytotoxicity and topo II activity results could be due to the differences in the pharmacokinetics of the compounds in so it was considered that drug uptake was an important factor to investigate.

3.9 Fluorescence microscopy

To investigate whether the drug is reaching the nucleus by crossing the cellular barriers fluorescence microscopy can be used. For this experiment A549 cells were selected by observing the morphology under a microscope. Though the cultured cells are in monolayers, MCF-7 and DLD-1 cells tend to form clusters in the culture plate whereas A549 cells are evenly spread.

Cells were first treated with drug for one hour and then the nuclei were stained with DAPI (staining due to DNA minor grove binding) and observed under a fluorescence microscope. DAPI exhibits a blue colour fluorescence (Figure 3.23) when it binds to DNA, and cryptolepine analogues were analysed for their fluorescence activity for their usability as fluorescent ligands so fluorescence spectra were recorded (Chhikara *et al.,* 2012; Jansen *et al.,* 2004).

First the maximum absorbance was recorded using a UV-VIS spectrophotometer and then that wavelength (Figure 3.24) was used as the excitation wavelength to obtain fluorescence spectra (Figure 3.25 and 3.26) of the derivatives. Out of the compounds scanned, the 11-halogenated analogues and the derivative with the 11-butylaminosidechain emitted high enough fluorescence intensity to enable fluorescence microscopy. For this reason 11-chlorocryptolepine and 11-butylaminocryptolepine were picked. 11-chlorocryptolepine was included in a view to figure out the reasons behind its low cytotoxicity despite its high topo II activity.

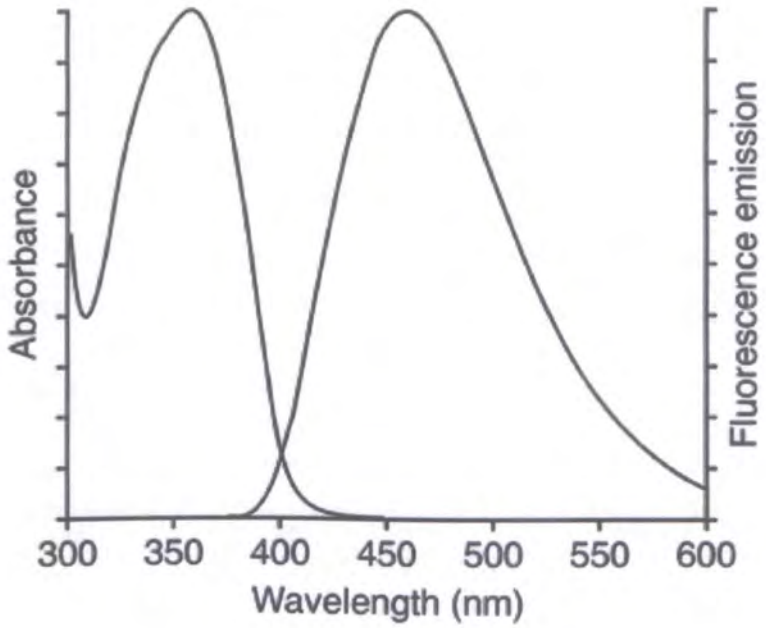

Figure 3.22 Showing the fluorescence spectrum of DAPI

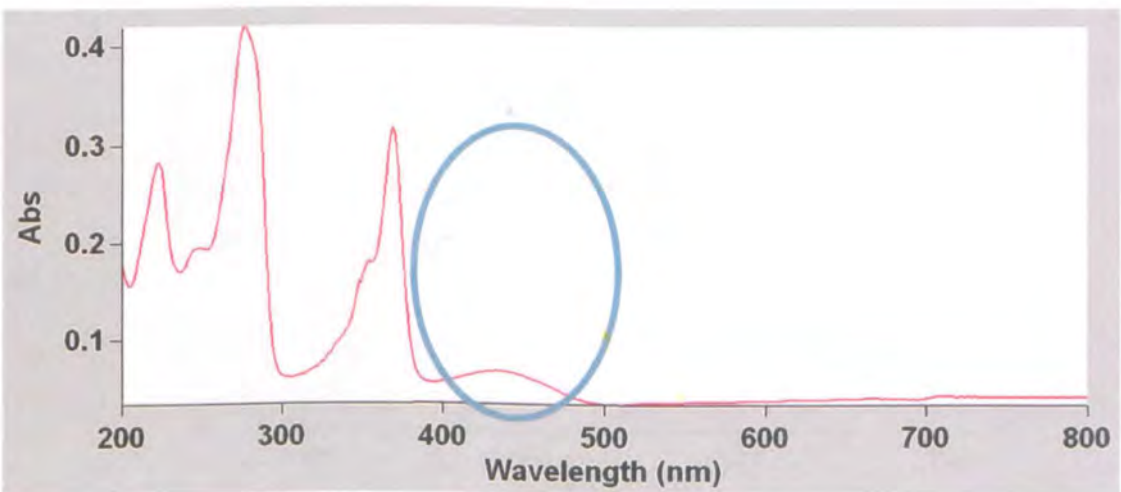

Figure 3.23 UV spectrum of 11-chlorocryptolepine

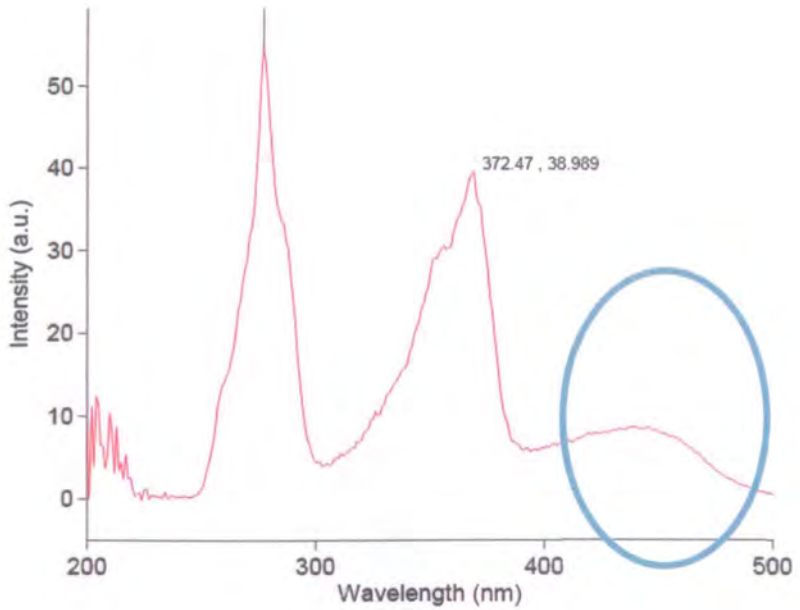

Figure 3.24 Excitation spectrum of 11-chlorocryptolepine

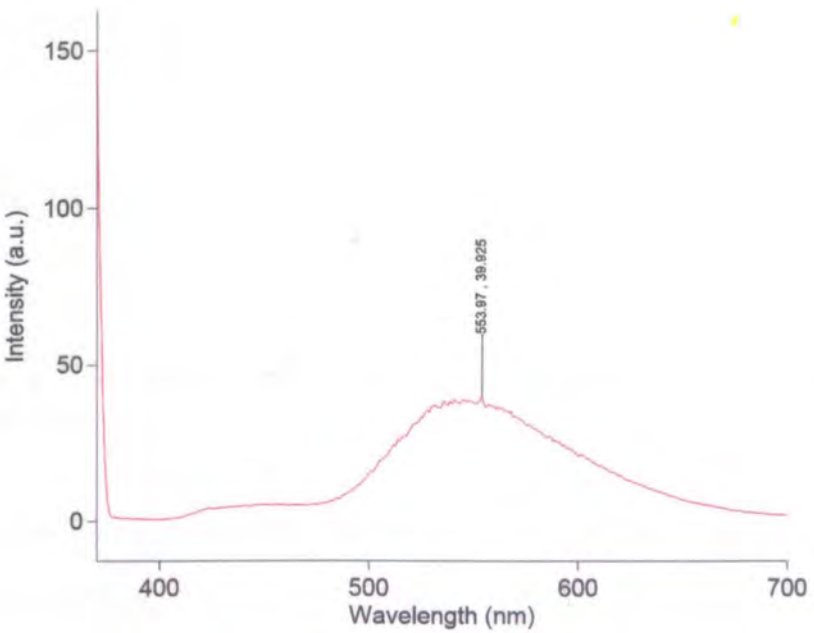

Figure 3.25 Emission spectrum of 11-chlorocryptolepine

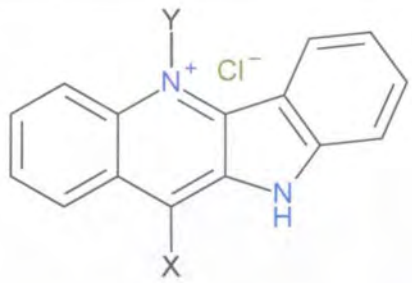		Excitation wavelength	Emission wavelength
X	Y		
H	CH_3	431	540
Cl	CH_3	440	554
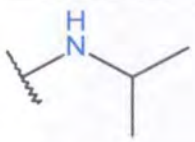	CH_3	422	477
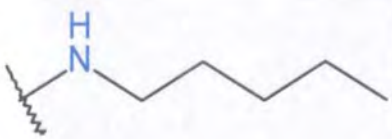	CH_3	424	463

Table 3.6 Showing excitation and emission spectra of cryptolepine derivatives

Fluorescence microscopic pictures were taken for both DAPI and drug by exciting them at their respective excitation wavelengths and then overlaying them to look for co-localisation (Molenaar *et al.,* 2000; Burger *et al.,* 1999). These microscopic pictures (Figure 3.26Figure 3.26 Showing colocalisation of DAPI and drug in the nucleus of A549 cells. Magnification: 40x, green: 11-butylamino cryptolepine (C), blue: DAPI nuclear dye (B), Overlay of both drug and DAPI (D)) revealed that 11-butylamino cryptolepine has successfully

reached to nucleus. Though the drug (11-butylaminocryptolepine) was spread all over the cell, high concentration is

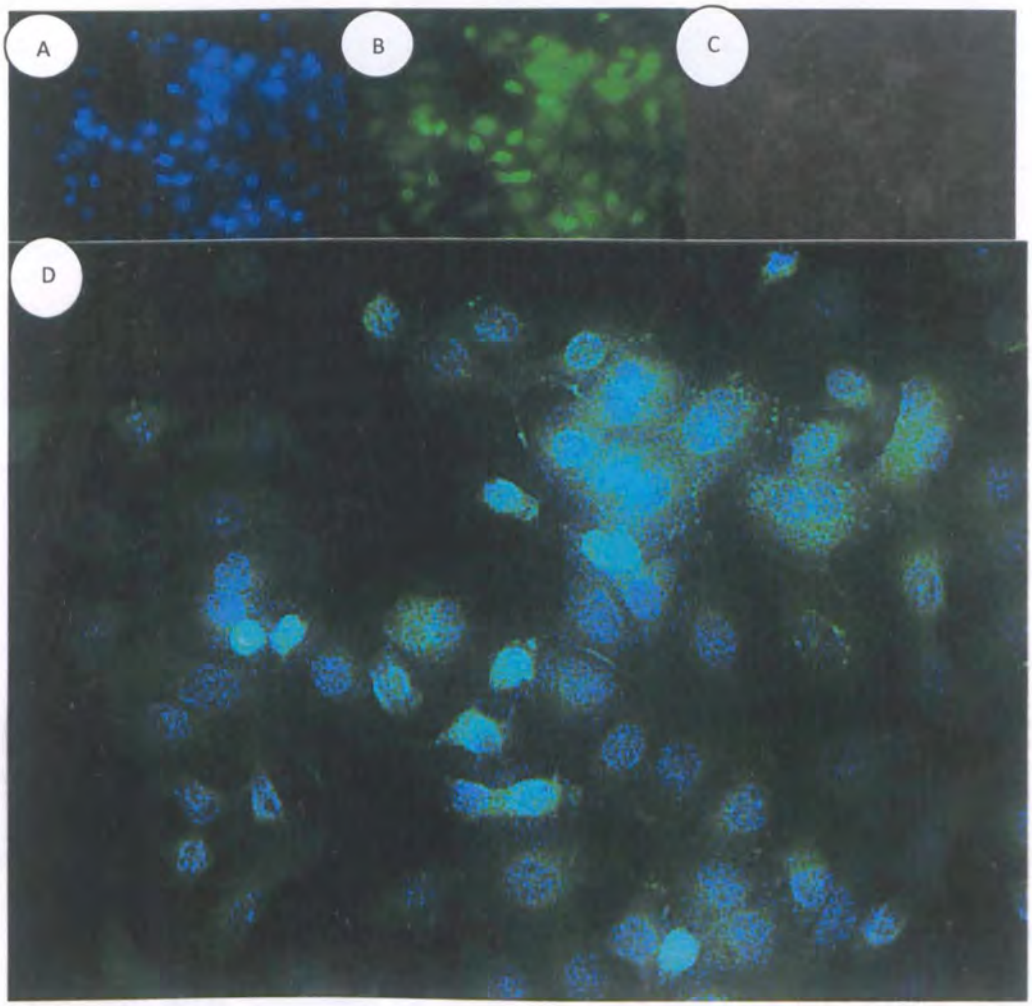

Figure 3.26 Showing colocalisation of DAPI and drug in the nucleus of A549 cells. Magnification: 40x, green: 11-butylamino cryptolepine (C), blue: DAPI nuclear dye (B), Overlay of both drug and DAPI (D)

localised at nucleus, which was clearly seen in the pictures as more bright fluorescence was arising from the nucleus of the cell which is co localised with DAPI. The same was observed with 11-chlorocryptolepine but the fluorescence intensity seemed to be lower than 11-butylaminocryptolepine. Similar experiments were conducted by Carl and his team to see the cellular loca-

lisation of fluorescent zinc complexes using DAPI as a counterstain (Redshaw *et al.*, 2012).

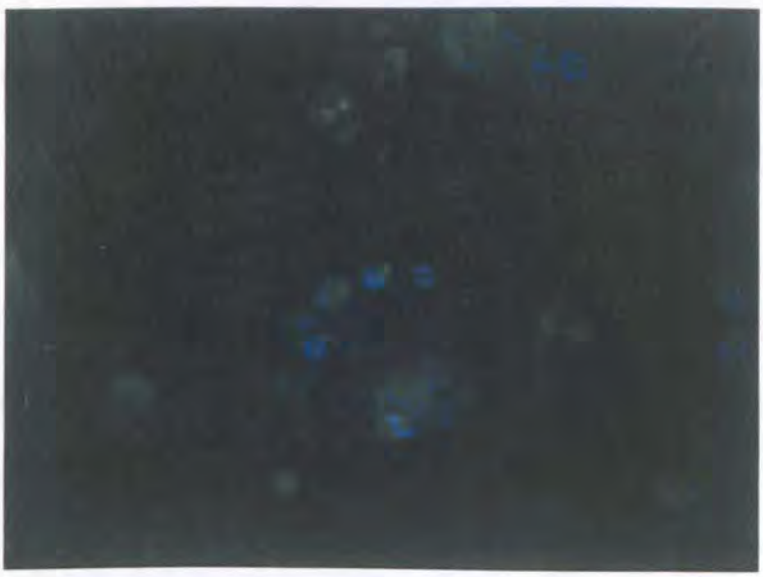

Figure 3.27 Showing Colocalisation DAPI and drug in the nucleus of A549 cells. Magnification: 40x, green: 11-chloro cryptolepine, blue: DAPI nuclear dye, Overlay of both drug and DAPI

These drug localisation experiments only gave information about whether the drug is present in the nucleus or not. By measuring the amount of drug taken up by the cells after treatment for particular time will give quantitative information about the rate of drug uptake in the cells.

3.10 In vitro drug-uptake studies

In the literature there are only a few reports on the pharmacokinetics of cryptolepine (Noamesi *et al.*, 1991) and no studies were found on quantitative *in vitro* drug uptake studies. One study by Bonjean showed that cryptolepine was easily taken up by B16 melanoma cells by crossing the cell membrane. They have also showed that the drug predominantly localised in the nuclear region than cytoplasm (Bonjean *et al.*, 1998).

One *in vivo* study shows that upon IV injection, cryptolepine was rapidly distributed and localised in most tissues of the mouse body but high localization was observed in the liver, adrenal medulla and melanin containing eye tissues. It was also reported that it did not reach the central nervous system (CNS) (Noamesi *et al.*, 1991).

In another study it has been demonstrated that cryptolepine reaches blood circulation within the first half hour after an oral dose of 10mg/kg in rats. From these studies it was understood that cryptolepine was rapidly absorbed by the *in vivo* systems (McCurrie *et al.*, 2009).

Being unable to find a suitable methodology to carry out invitro drug uptake studies on cryptolepine from the previous literature, a search was continued for similar work on other molecules.

Kunwar and his co-workers studied quantitative drug uptake, localisation and cytotoxicity of curcumin in cancer cells using fluorescence spectroscopy and fluorescence microscopy (Kunwar *et al.*, 2008). They treated cells with drug for four hours and then the cells were separated from the culture medium and the drug taken up by the cells as extracted using methanol from the cell lysate. Then the amount of drug taken up was quantified using UV spectroscopy with the help of curcumin's extinction coefficient value of 48000 $M^{-1}cm^{-1}$.

In the same study they also carried out sub-cellular fractionation using centrifugation on the cell lysate to separate the drug contained nuclear and cell membrane portions so the drug localisation could be quantified. They used DAPI as a nuclear stain to show the co-localisation of the curcumin at nu-

cleus by overlaying the fluorescence images of curcumin and DAPI (Kunwar *et al.*, 2008).

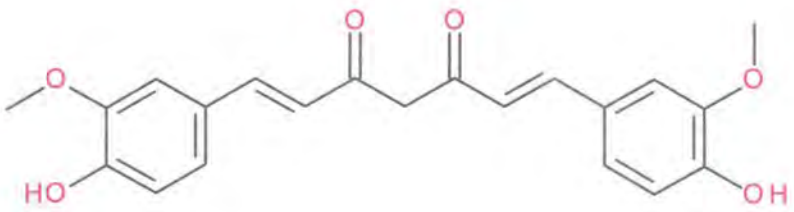

Figure 3.28 Curcumin

In another study Anand and co-workers also used fluorescence microscopy to estmate the cellular uptake of a curcumin-loaded nano particle formulation (Anand *et al.*, 2010). They also measured fluorescence intensity after drug treatments.

Jain and Jain used fluorescence microscopy to evaluate the cellular uptake of calcein (a green fluorescent dye) loaded hyaluronic acid coupled chitosan nanoparticles containing 5-fluorouracil.

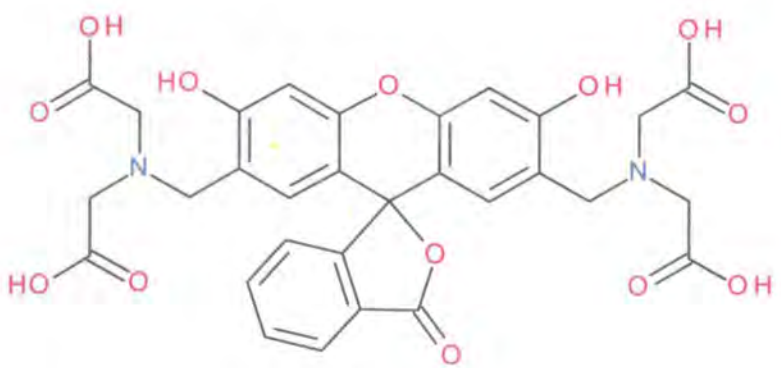

Figure 3.29 Calcein

This qualitative work was done by incubating the cells with drug for four hours and then washing using PBS, lysing and then fluorescence intensity was measured (Jain and Jain, 2008).

One other important study to determine the amount of doxorubicin uptake in MCF-7 cell lines was done by Mariko and co-workers. They took advantage of the fluorescent properties of doxorubicin and used fluorescence assisted flow-cytometry to measure the drug uptake. In this method the flow-cytometer measure the fluorescence intensities arising from each doxorubicin contained cell and integrates to give a total fluorescence intensity which can be used to measure quantitative drug uptake.

This team also used HPLC to quantify the amount of drug taken up by the cells on a 6 hourly basis for 24 hours (Bontenbal *et al.,* 1998). The majority of the literature methods used fluorescence spectroscopy and fluorescence microscopy to determine the drug uptake in the cells. For this purpose drugs are generally tagged with fluorescent ligands unless the drugs themselves are fluorescent like doxorubicin.

Cryptolepine is a fluorescent compound and so it can be observed using a fluorescent microscope allowing a quantitative drug uptake method to be designed.

Though cryptolepine is fluorescent, making derivatives can alter the fluorescence properties of the analogues, so all the compounds were first scanned using a fluorescence spectrophotometer. It was observed that the amido compounds showed less fluorescence than the derivatives with amino lin-

kages, whereas the 11-halogenated compounds emitted the highest fluorescence. However all the tested compounds emitted fluorescence.

To carry out the drug uptake studies A549 cells were selected because, after drug treatment, they make evenly spread monolayers. MCF-7 and DLD-1 cells tend to form clusters in the culture plates this was observed under microscope while performing cytotoxicity assays.

Based on the above mentioned literature, a method was designed based on fluorescence spectroscopy. This method mainly follows the methodology used by Kunwar and his co-workers. A549 cells were cultured for 24 hours and then incubated in the drug solution to be tested. Drug uptake was measured every 30 min for 3 hours by washing cells with PBS and then cells were lysing using Tritonx-100 (a non-ionic surfactant which increases the cell permeation) and extracting the drug using methanol. Fluorescence intensity was measured and compared using a positive control of the same drug solution and result was expressed as percentage drug uptake.

The amount of fluorescence exhibited by each drug can be different, so the same drug was taken as positive control (without any cells being present-100%) percentage drug uptake was calculated. This percentage drug uptake was directly proportional to the amount of drug present in the cells.

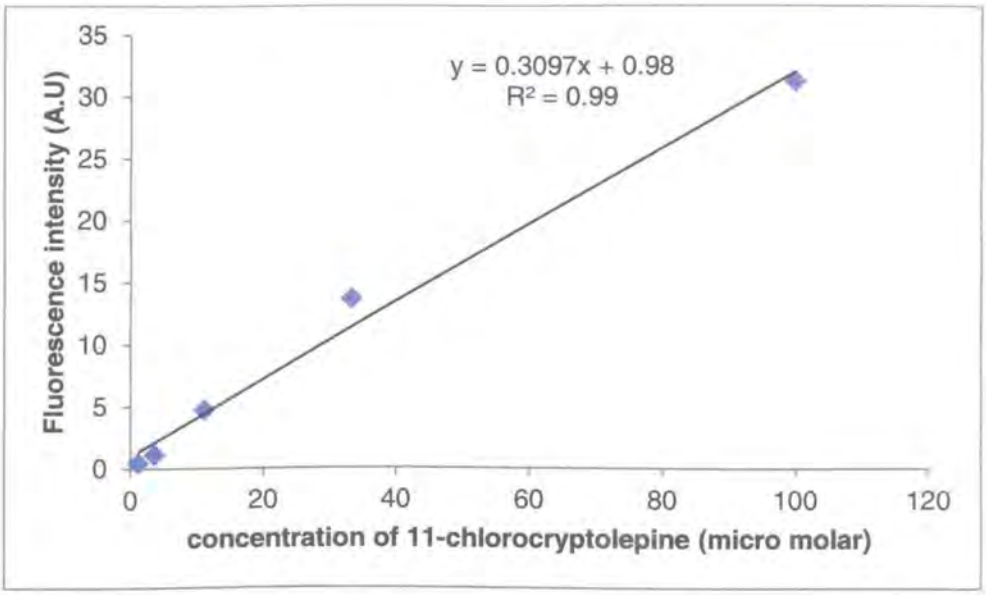

Figure 3.30 Calibration graph of 11-chlorocryptolpeine

Looking at the in vitro drug uptake results, 11-butylamino cryptolepine was taken up into the cells more quickly than any other compounds tested reaching 40% within first 30 min after drug treatment, then it continued to rise up to 60% in 1.5 hours. After 1.5 hours percentage drug uptake started to decrease reaching to a 20% at 3 hours this could be due the oozing of cellular contents along with drug from ruptured cell membranes of dying cells. This high rapid percentage drug uptake in to the cells may be the reason for high activity of 11-butylamino cryptolepine.

When it comes to 11-chlorocryptolepine, the percentage drug uptake was comparatively lower than 11-butylamino derivative. It only reached 25% in the first 30 minutes and then raising to a 40% at two hours then it started to decline and reached about 30% at three hours. This lower rate might be the reason behind the lower cytotoxcicity of 11-chlorocryptolepine.

Another important issue in the drug uptake profile of this compound was that the intracellular concentration of 11-chloro derivative did not fall as quickly as

11-butylaminocryptolepine. This may be due to lower cytotoxicity of the 11-chlorocryptolepine.

When the drug uptake of 11-chlorocryptolepine was compared with its parent compound, cryptolepine was loaded in to the cells quicker and reached a higher maximum concentration than 11-chlorocryptlepine.

11-Isopropylaminocryptolepine gave a poor drug uptake profile with a percentage drug uptake of 8% in the first thirty minutes which is 6 times lower compared to 11-butlamino cryptolepine and approximately 4 times lower than the parent compound. The maximum drug uptake of 18% was seen at 2.5 hours which is 3 times lower than 11-butlamino cryptolepine.

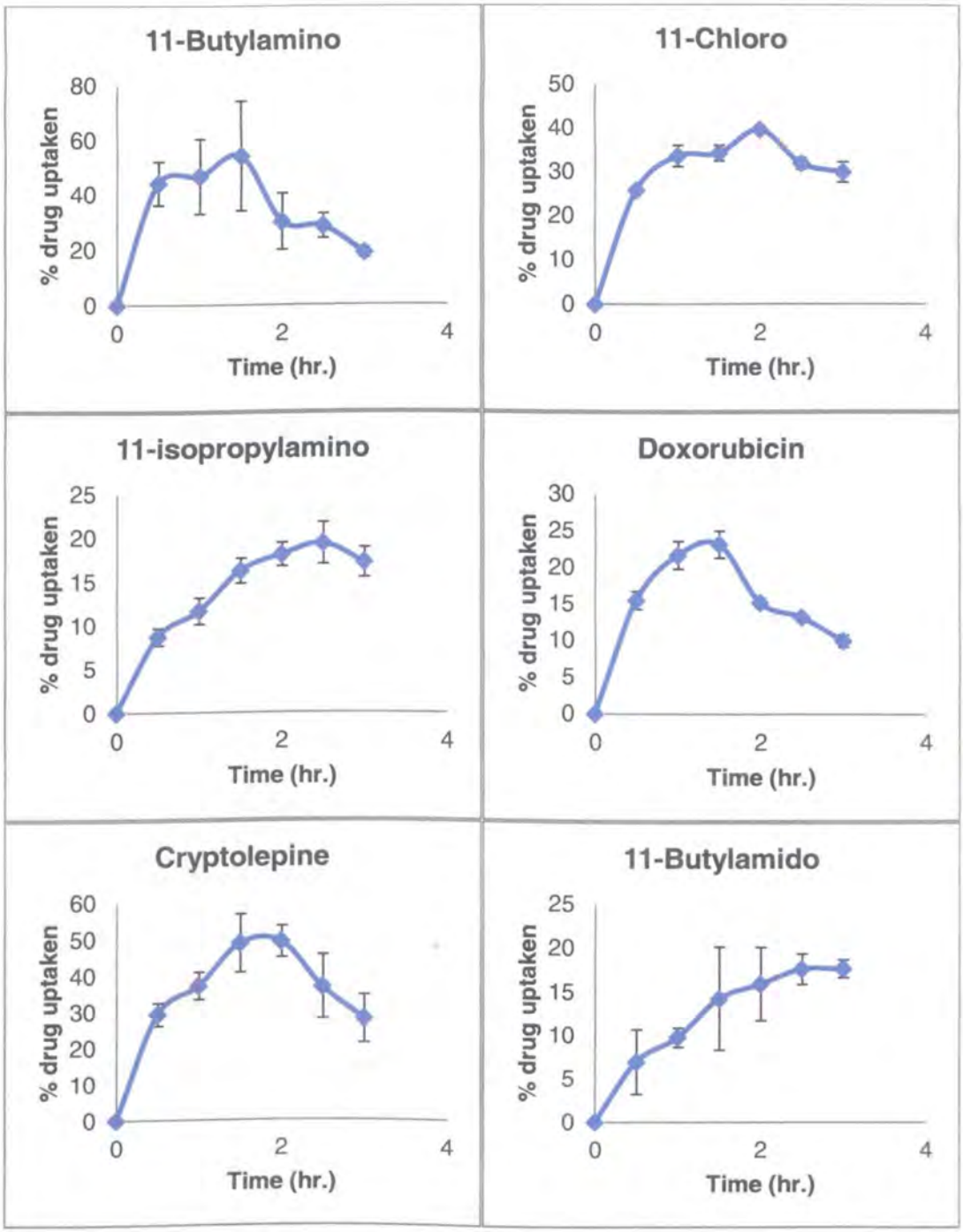

Figure 3.31 Showing the rate of drug uptake of tested Ligands in A549 cells

3.11 Drug-DNA binding assay

Cryptolepine has potential to act as an anticancer agent by intercalating into DNA (Lisgarten *et al.*, 2002a). DNA binding efficiency should be determined to see whether synthesized derivatives have increased this DNA binding efficiency or not. It also gives clarity on the mode of action by which a particular derivative is showing cytotoxicity. For example despite its high topo II activity the 11-chloro derivative showed less cytotoxicity.

In the literature there are number of ways to assess the DNA binding of a ligand. These are dependent on the type of DNA is being used in the experiment (Pei and Stojanovic, 2008; Monchaud *et al.*, 2008).

3.11.1 Calorimetric techniques

Isothermal titration calorimetry and differential scanning calorimetry depends on the changes in the confirmation of the polymorphism of DNA during binding. This conformational change process involves either absorption or release of heat from the system. By measuring this it allows the quantification of binding strength (Hopkins Jr, 1997; Palchaudhuri and Hergenrother, 2007b).

3.11.2 ESI-MS (electro spray ionization – mass spectrometry)

In this method quadruplex DNA is mixed with different molar ratios of ligand and the products are compared by analysing the mass spectrum of the products. Disappearance of the DNA peak in the spectrum or appearance of the DNA-ligand complex indicates binding. The ratio of aboundances of the Drug-DNA complex to DNA gives the binding affinity (Monchaud *et al.*, 2008; Zhou and Yuan, 2007).

3.11.3 Circular Dichroism

This technique uses a plane polarised light rotated along its own axis to form a helical waveform. When a circular polarized light beam passes through a solution containing an optically active species, the speed and wavelengths of left and right polarisations would be absorbed to different extents. This difference is characteristic for optically active compounds and is concentration dependent. This is normally expressed in molar ellipticity which is the tangent of the ratio of the minor to major elliptical axes. When a ligand binds to DNA this molar ellipticity will be changed and the spectrum shows this (Zhou and Yuan, 2007; Kobayashi, Muranaka and Mack, 2012).

3.11.4 Fluorescence resonance energy transfer melting assay (FRET melting assay)

In this method two fluorescent probes are attached to a specific DNA sequence. Fluorescent probes are selected in such a way that the excitation spectrum of one is matched to other's emission spectrum, meaning when the one probe is excited the released energy is absorbed by the other giving no emission for the first excited probe. For this to happen the DNA sequence should be approximately 10 - 80 ^{0}A long.

Figure 3.32 Showing fluorescence resonance energy transfer FRET system

When this distance increases by any means, the system is altered so that the emission of the first excited probe will show up on the fluorescence spectrum

as the energy is not transferred to the other probe attached to the other side of the sequence. DNA binding of a ligand can be measured by increasing the temperature of the system gradually by causing the DNA to melt meaning the distance between the donor and the acceptor probes will increase(De Cian *et al.*, 2007).

The temperature data is collected based on melting results and this is significantly different if the ligand is able to bind to the given sequence. When ligand stabilizes the nucleotide, the denaturation temperature of the ligand bound oligonucleotide will increase. This assay is particularly useful in assessing the binding ability of G-qudruplex DNA ligands (De Cian *et al.*, 2007; Juskowiak, 2006; Mergny and Maurizot, 2001).

Larvado and co-workers tested cryptolepine anlogues using this method which were shown to stabilise G-quadruplex DNA (Lavrado *et al.*, 2010b).

The main advantages of this method are it is quick and can be applied to high-throughput screening (HTS). Disadvantages are potential quenching of the probe by the ligand and chemical modification of the nucleotide is required.

3.11.5 Fluorescent Intercalator Displacement assay (FID)

Thiazole orange produces fluorescence only when it binds to DNA. Adecrease in the fluorescence will occur when it unbound or displaced from DNA. When thiazole orange is bound to DNA in solution, if another ligand with a higher DNA affinity displaces thiazoleorange from DNA then a fall in the fluorescence will be seen. Based on this principle ligands have been tested for their DNA binding efficiency for duplex and quadruplex DNA se-

quences (Pei and Stojanovic, 2008; Monchaud *et al.*, 2008; Monchaud *et al.*, 2006)

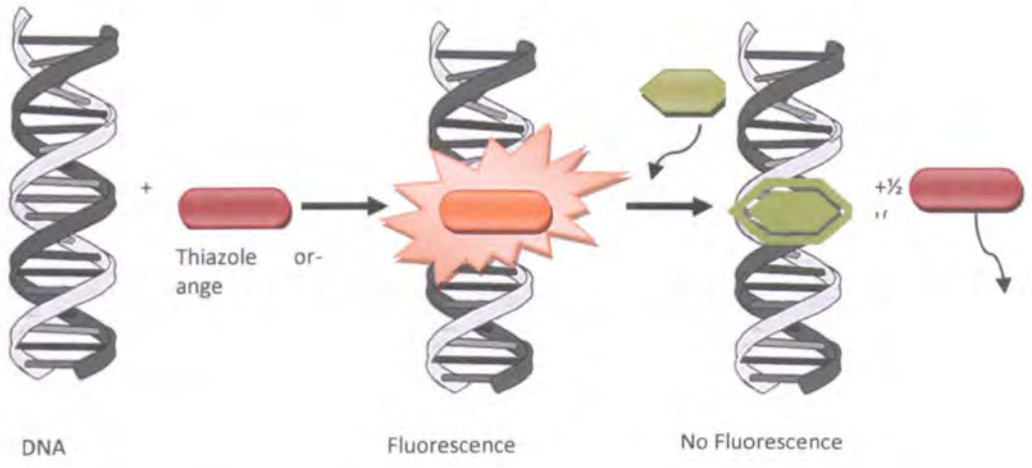

Figure 3.33 Scheme showing thiazole orange displacement by ligand in a duplex

The amount of thiazoleorange displaced by the tested ligand can be calculated using the following equation:

% Thiazole orange displacement displacement = 100- [(FA/FA$_0$)*100]

Where FA0 is the fluorescence area of thiazole orange in the absence of external ligand, FA is the fluorescence area of thiazole orange in the presence of cryptolepine derivatives (Monchaud *et al.*, 2008). The fluorescence area is the integral of the total area under the fluorescence curve.

Advantages

- A variety of nucleotides and ligands can be tested without any modification required

- Ease of experimental setup
- Easy to simulate physiological conditions including maintenance of temperature and pH most of the modern fluorimeters offers this facility
- HTS applicability

Disadvantages

- Competition between ligand and the thiazole orange can give minor false results.
- There should not be any overlap between absorption spectrum of ligand and emission spectra of thiazole orange.

Upon on studying all the methods FID was selected as method of choice for the current project for its robustness and the fact that we can use different types of DNA sequences (duplex, quadruplex) to test various ligands.

Using this fluorimetric titration assay, cryptolepine derivatives were tested for their selectivity and efficiency of DNA binding. This assay was done using two types of DNA sequences; one was a duplex DNA (DS26) and the other was quadruplex DNA (22AG)

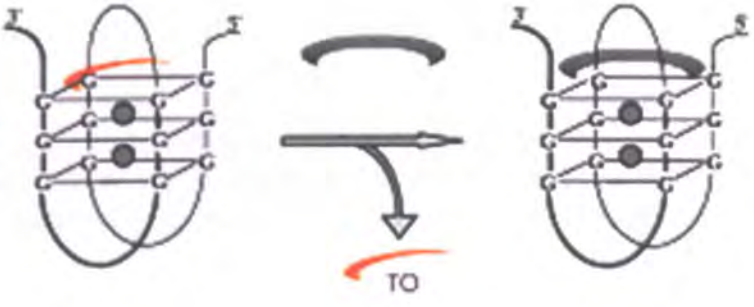

Figure 3.34 Scheme showing thiazole orange displacement by ligand in a quadruplex DNA.

22AG is an oligonucleotide which is similar to the human telomeric sequence. It is a repeat of the [5'-$AG_3(T_2AG_3)_3$-3'] which forms G quadruplex DNA. DS26 is a self-complementary DNA sequence 5'-$CA_2TCG_2ATCGA_2T_2CGATC_2GAT_2G$-3'] which form a duplex DNA (Monchaud *et al.*, 2008). Figure 3.35 and Figure 3.36 shows the gradual decrease in the fluorescence arising from displacement of thiazoleorange from quadruplex (Figure 3.35) and duplex DNA (Figure 3.36) up on gradual increase of the ligand concentration.

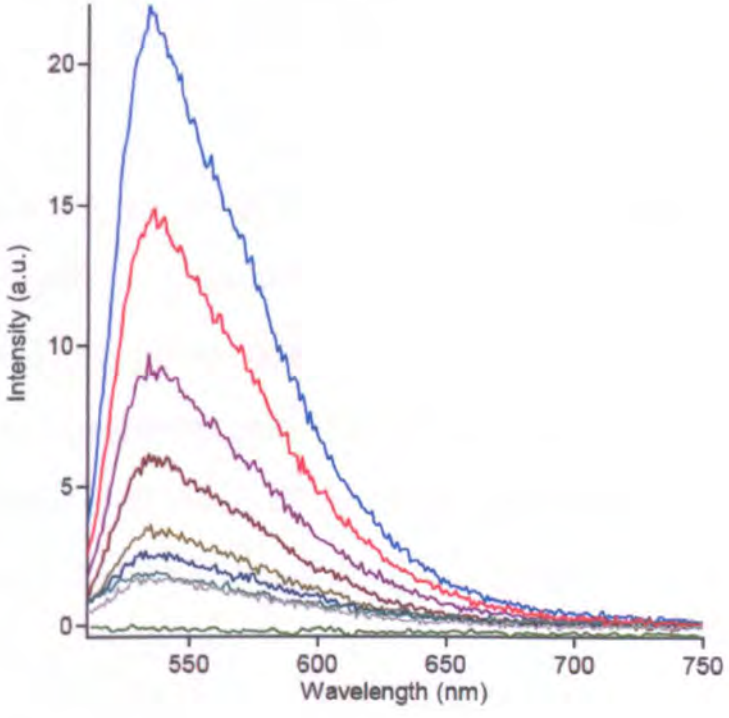

Figure 3.35 Showing displacement of thiazole orange by 11-Chlorocryptolepine in 22AG (G-quadruplex DNA) using increased ligand concentrations (7.5, 4.5, 3, 1.5, 0.75, 0.375 μM), cell volume = 3ml.

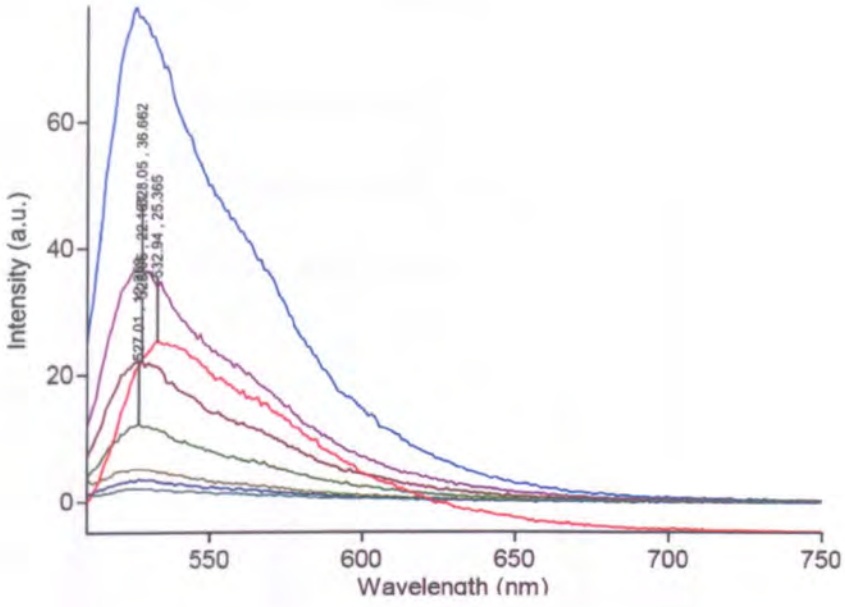

Figure 3.36 Showing displacement of thiazole orange by 11-Chlorocryptolepine in DS26 (duplex DNA) using increased ligand concentrations (7.5, 4.5, 3, 1.5, 0.75, 0.375 μM), cell volume = 3ml.

From the Table 3.7, the 11-halogented derivatives showed the highest DNA binding with slightly more selectivity towards duplex DNA over G-quadruplex DNA. Particularly the 11-iodo compound showed the highest DNA binding in both duplex and quadruplex sequences. This reinforces the cytotoxicity data as high cytotoxicity was shown by the 11-iodo compound. The 11-chloro derivative showed better DNA binding efficiency than parent molecule.

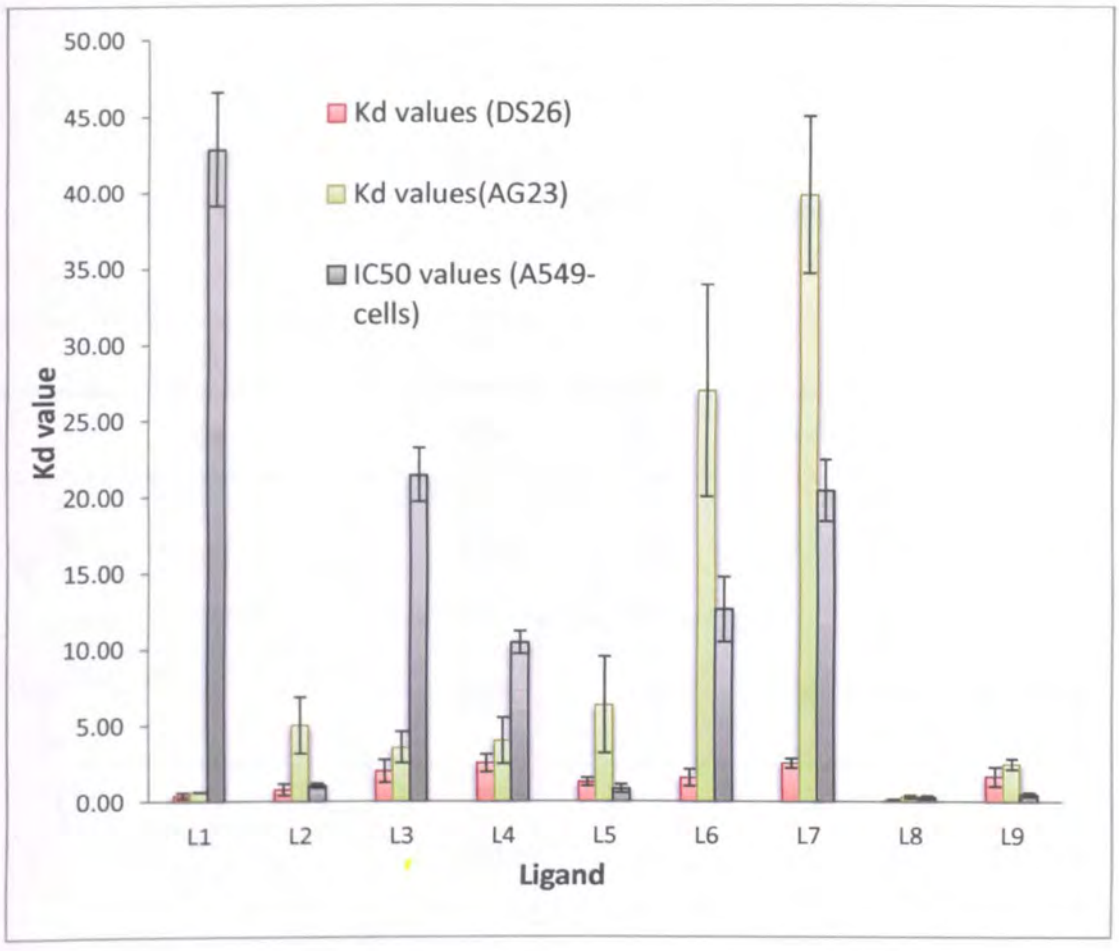

Figure 3.37 Showing a comparison between DNA binding and cytotoxicity profiles (A549 cells) of tested derivatives (see table 3.7 for details of L1-L9))

11-alkylamino derivatives showed greater DNA binding than the original compound, especially the molecules with the 11-butylamino and pentylamino sidechains.

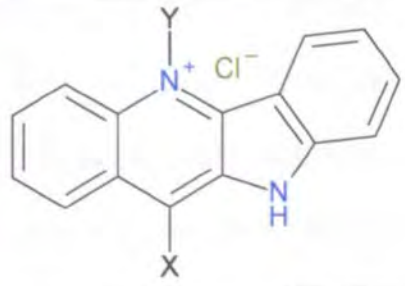		Ligand	Kd values (DS26 – duplex DNA) ± (SD)	Kd values (AG22- quadruplex DNA) ± (SD)
X	Y			
Cl	CH_3	L1	0.40 ± 0.20	0.63 ± 0.002
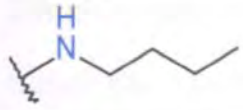	CH_3	L2	0.79 ± 0.37	5.01 ± 1.85
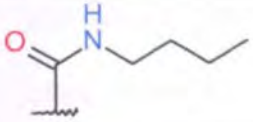	CH_3	L3	2.00 ± 0.74	3.55 ± 1.04
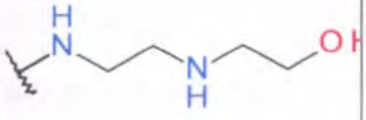	CH_3	L4	2.51 ± 0.58	3.98 ± 1.53
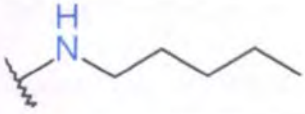	CH_3	L5	1.26 ± 0.26	6.31 ± 3.15
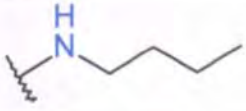	C_2H_5	L6	1.55 ± 0.55	26.92 ± 6.96
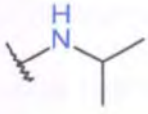	CH_3	L7	2.51 ± 0.33	39.81 ± 5.17
I	CH_3	L8	0.10 ± 0.06	0.32 ± 0.10
H	CH_3	L9	1.62 ± 0.62	2.45 ± 0.36

Table 3.7 Shows DNA binding efficiency of tested cryptolepine analogues in Kd values.

The same pattern was observed as in the cytotoxicity data. Isopropylamino containing molecules did not show better activity than butylamino containing compound (see section 3.7). Of a particular note, the isopropylamino com-

pound showed binding efficiency to G-quadruplex which is 16 times lower than its duplex DNA affinity. When compared to the original compound, 11-butyl and pentylamino derivatives showed higher binding efficiency to duplex DNA, whereas the same compounds showed low binding efficiency towards G-quadruplex sequences inferring that the compounds with 11-alkylamino sidechains prefer duplex DNA over quadruplex DNA.

Even though the derivative with the aminoalcohol sidechain did not show higher DNA binding to duplex DNA, its quadruplex binding efficiency is considerably higher than derivatives with 11-alkylamino sidechains. More importantly there is not much difference between its binding capacities towards both types of DNAs. Whereas derivatives with 11-alkylaminosidechains displayed a high selectivity towards duplex DNA.

When it comes to derivatives with alkylamido sidechains, only the 11-butylamido compound was tested as it showed higher cytotoxicity compared to the other amido derivatives. It showed less binding efficiency towards both duplex and quadruplex DNAs when compared to original compound but its quadruplex binding capacity is higher than 11-alkylamino derivatives implying that it prefers G-quadruplex structures than duplexes. Overall cryptolepine preferred duplex DNA over G-quadruplex DNA, this may be because of its selectivity towards GC rich sequences present in the duplex DNA.

Chapter 4 Chemistry Experimental

4.1 General details

All the chemicals used in the synthesis were purchased from Sigma Aldrich, UK.

4.1.1 Column chromatography

Columns were prepared using silica gel with a pore diameter of 0.035 - 0.070 mm and a mesh size of 220-440.

4.1.2 Nuclear Magnetic Resonance(NMR)

NMR spectra were recorded on Brüker Avance III 400 two-channel FT-NMR spectrometer (AV400). It is equipped with a 5 mm BBFO+ probe (broadband multinuclear, auto-tune, with Z-gradients), a 60-position sample changer and a variable temperature control unit (VT range of the probe -150°C to 150°C) that may be used in conjunction with a 26 L liquid nitrogen Dewar for sub-zero experiments. Spectra were recorded using TopSpin 3.0 pl4, © 2010 Brüker BioSpin, control and processing software and IconNMR 4.5.1 Build 51 for TopSpin 3.0 automation software.

Spectra were processed and analysed using ACD NMR processing software, version12.

4.1.3 Mass spectra (MS)

Mass spectra of compounds were obtained using Waters LCT-TOF- MS instrument using ESI selective mass detector and Agilent 5973 GC-MS.

4.1.4 High-resolution mass spectra (HI-RES MS)

High resolution mass spectra of compounds were obtained from Medac labs, UK (BS EN ISO9001:2008) using Waters LCT Premier (ES-ToF)/Acquity i-Class mass spectrometer

Ionisation: Electrospray (ES). High resolution data was recorded via singly charged ions up to 1500 Da.

4.1.5 Infrared (IR)

Infrared spectra were recorded on Thermo Scientific™ Nicolet™ iS™5 FT-IR Spectrometer.

4.1.6 Melting point

Melting points were measured using Gallenkamp digital Melting-point apparatus 5A 6797. Up to 350 °C (Divison: 0.1 °C. 220 V)

4.2 Ethyl N-(2-cyanophenyl)carbamate

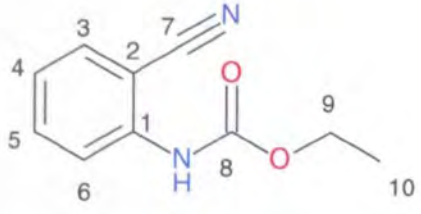

(44)

Figure 4.1 Ethyl N-(2-cyanophenyl)carbamate

2-Aminobenzonitrile (6.28 g, 53 mmol) and ethyl chloroformate (26 ml, 273 mmol) were mixed and heated to reflux for 6 hours. Excess solvent was evaporated *in vacuo* then 16 ml of toluene were added and then the reaction mixture was cooled to approximately 80 °C and then 38 ml of cyclohexane were added to induce crystallisation. The product was recrystallised from cyclohexane and dried under vacuum to obtain the product **(44)** (Figure 4.1) as pale yellowish crystals (7.26 g, 38.1 mmol, 95%).

Melting point 104-105 °C (Lit. 103-104 °C) (Gelotte *et al.*, 1990).

^{1}H NMR (400MHz, chloroform-d_3) δ ppm 8.24 (d, J = 8.4 Hz, 1H, H-6), 7.53 - 7.61 (m, 2H, Ar-H), 7.15 (br, s, 1H, NH), 7.09 - 7.14 (m, 1H, Ar-H), 4.27 (q, J = 7.1 Hz, 2H, CH_2), 1.35 (t, J = 7.1 Hz, 3H, CH_3).

^{13}C NMR (101 MHz, chloroform-d_3) δ ppm 152.9 (C=O), 141.0(C-1), 134.2 (C≡N), 132.3 (C-Ar), 123.1(C-Ar), 119.3 (C-Ar), 116.4 (C-Ar), 100.9 (C-Ar), 62.0 (CH_2), 14.4 (CH_3).

GC-MS m/z (relative intensity, %) 190 (20) (M^+), 144 (100)

IR ν cm^{-1} 3300 (NH stretch), 2221 (CN stretch), 1705 (C=O stretch).

4.3 3-Amino-N-2-(7-nitrobenzoyl) indoline-1-carboxylate

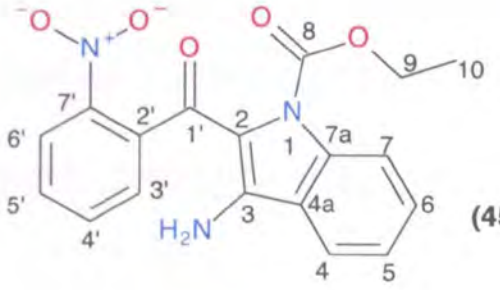

(45)

Figure 4.2 3-Amino-N-2-(7-nitrobenzoyl) indoline-1-carboxylate

Ethyl (2-cyanophenyl) carbamate **(44)** (Figure 4.1) (2.01 g, 13.8 mmol) was added to a solution of potassium carbonate (4.21 g, 30.46 mmol) in dimethyl-formamide (21 ml). The solution was stirred at room temperature for 45 minutes. A solution of 2-bromo-2' nitro acetophenone (3.05 g, 12.40 mmol) in DMF (10 ml) was added drop wise (over 5 min) to the reaction mixture and stirring was continued for 2.5 hours. Then the reaction mixture was slowly poured into 200 ml of distilled water and a yellow precipitate formed which was allowed to settle for 18 hours, which was then collected by filtration and dried *in vacuo*. Recrystallisation was carried out twice from methylated spirits and shiny yellow crystals of **(42)** (Figure 4.2) were obtained (2.18 g, 50%).

Melting point 204-205 °C

^{1}H NMR (400MHz, chloroform-d3) δ ppm 8.13 (dd, *J* = 0.7 Hz, *J*= 7.7Hz, 1H), 7.93 - 7.99 (m, 1H), 7.52 - 7.65 (m, 5H, Ar-H), 7.31 - 7.38 (m, 1H, H-6), 6.32 (br. s, 2H, NH_2), 3.90 (q, *J* = 7.1 Hz, 2H, CH_2), 1.00 (t, *J* = 7.1 Hz, 3H, CH_3).

^{13}C NMR (101MHz, chloroform-d3) δ ppm 182.1 (C-1'), 151.4 (C-8), 147.4 (C-7'), 146.5 (C-Ar), 138.6 (C-7a), 136.5 (C-4a), 132.1 (C-3), 130.5 (C-7'), 129.8 (C-Ar), 128.0 (C- Ar), 124.0 (C- Ar), 123.1 (C- Ar), 121.3 (C- Ar), 119.6 (C- Ar), 116.3 (C- Ar), 114.6 (C- Ar), 62.6 (C-9), 13.4 (C-10).

ESI-MS M/z (relative intensity %) 354 (12) (M^+), 376 (100) (M+Na)

IR ν cm^{-1} 3461 (NH stretch), 3333 (CN stretch), 1732 (C=O stretch).

4.4 5,10-dihydroindolo[3,2-b]quinolin-11-one

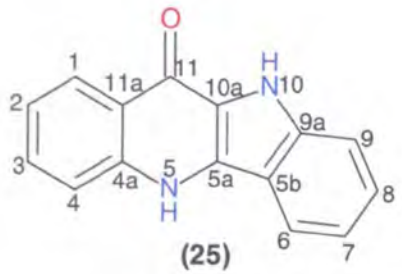

(25)

Figure 4.3 5,10-dihydroindolo[3,2-b]quinolin-11-one

To a solution of 3-amino-*N*-2-(7-nitrobenzoyl) indoline-1-carboxylate **(45)** (Figure 4.2) (0.77 g, 2.18 mmol) in THF (10ml), sodium hydride (0.20 g, 8.30 mmol) (60% w/v NaH in mineral oil) was added under dry conditions and the mixture was stirred for 1.75 hours. The reaction mixture was poured into 75 ml of distilled water then acidified by dropwise addition of concentrated acetic acid. A yellow-brown colour precipitate was collected by filtration which was then washed twice with water and dried *in vacuo*.

To the solid, 10 ml of ethanol were added with stirring to form a solution. Then aqueous sodium hydroxide solution (1.5 g in 10 ml) was added and the mixture was heated to reflux for 30 minutes. The reaction mixture was evaporated and the remaining residue was gently triturated with distilled water (25 ml). The solid was dried and recrystallised twice from ethanol to form yellow-brown crystals of 5,10-dihydroindolo[3,2-b]quinolin-11-one **(25)** (Figure 4.3) (230 mg, 69%).

Melting point > 300 °C.

^{1}H NMR (400 MHz, DMSO- d_6) δ ppm 12.18 - 12.61 (s , 1 H), 11.57 - 11.75 (m, 1 H), 8.36 (dd, *J*=8.13, 1.14 Hz, 1 H), 8.19 (d, *J*=7.92 Hz, 1 H), 7.62 -

7.78 (m, 1 H), 7.42 - 7.55 (m, 1 H), 7.29 (ddd, *J*=8.06, 6.78, 1.14 Hz, 1 H,), 7.15 - 7.24 (m ,1 H)

^{13}C NMR (101MHz, DMSO-d_6) δ ppm 167.2 (C=O), 138.8 (C-4a), 138.4(C-9a), 130.5(C-5a), 128.7 (C-Ar), 127.2 (C-Ar), 125.0 (C-Ar), 122.9 (C-Ar), 122.7 (C-Ar), 120.6 (C-Ar), 120.2 (C-Ar), 118.7 (C-Ar), 117.6 (C-Ar), 115.7 (C-Ar), 112.4 (C-Ar).

ESI-MS m/z (relative intensity, %) 234 (13) (M^+) 233 (100).

IR ν cm^{-1} 3158 (NH stretch), 2953 (NH stretch), 1632 (C=O stretch), 1547.

4.5 11-Bromo-10H-indolo[3,2-b]quinoline

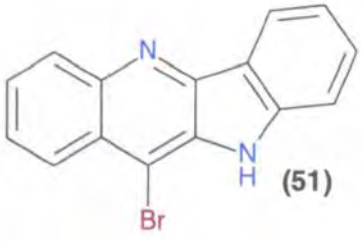

(51)

Figure 4.4 11-Bromo-10H-indolo[3,2-b]quinoline

To 5,10-dihydroindolo[3,2-b]quinolin-11-one **(25)** (Figure 4.3) (0.20 g, 0.85 mmol), phosphorous oxybromide (0.2 g, 0.69 mmol) and phosphorous tribromide (2.5 ml, 26.32 mmol) were added. The mixture was heated to reflux for 16 hours. The reaction mixture was basified by using potassium hydrogen carbonate (10% aqueous solution) and extracted with chloroform (4 X 100 ml) and the organic phases were collected, combined and dried with magnesium sulfate. The solvent was evaporated *in vacuo* to give a yellow solid (180

mg) was obtained which was purified by using column chromatography on silica gel (eluent 1:4 diethyl ether in hexane) to give a bright yellow coloured solid **(51)** (Figure 4.4) (92 mg, 36%).

Melting point 117-118 °C

^{1}H NMR (400 MHz, DMSO- d_6) δ ppm 11.66 (br.s, 1H, NH), 8.37 (m 1, H), 8.26 (m, 2H), 7.64 - 7.79 (m, 4H, Ar-H), 7.33 - 7.38 (m, 1H).

^{13}C NMR (101 MHz, DMSO- d_6) δ ppm 145.7 (C-5a), 144.1 (C-9a), 143.9 (C-4a), 132.5 (C-10a), 130.5 (C-Ar), 129.4 (C-Ar), 127.0 (C-Ar), 126.7 (C-Ar), 125.1 (C-Ar), 124.7 (C-Ar), 121.9 (C-Ar), 121.4 (C-5b), 120.4(C-Ar), 112.3 (C-Ar), 109.6(C-Ar).

ESI-MS m/z (relative intensity, %) 295(100) (M^{-1}) 297 (99) (M^{+}) (bromine isotopes).

4.6 11-Bromo-5-methyl-10H-indolo[3,2-b]quinolin-5-ium chloride

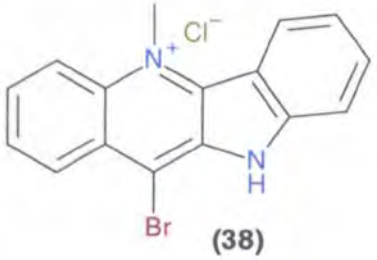

(38)

Figure 4.5 11-Bromo-5-methyl-10H-indolo[3,2-b]quinolin-5-ium chloride

Under dry conditions, 11-Bromo-10H-indolo[3,2-b]quinoline **(51)** (Figure 4.4) (0.40 g, 1.35 mmol) and methyltriflate (0.26 ml, 2.38 mmol) were stirred in 12 ml of toluene for 24 hours at room temperature. The reaction mixture was

poured into diethyl ether (150 ml) and the yellow precipitate was collected by filtration and dried *in vacuo*. Aqueous ammonia solution (3.3% v/v, 10 ml) was added to the solid which was stirred to convert the product to its free base form and then the mixture was extracted using chloroform (4 x 75ml). The collected organic layers were combined and were evaporated *in vacuo* to give the crude product which was then purified by column chromatography on silica gel by using DCM: methanol: NH_4OH (5:1:0.1) as the eluent. Finally the free base was converted to its hydrochloride salt by neutralising with 0.1 M methanolic hydrochloric acid (5 ml) and the solution was evaporated *in vacuo* to give 11-Bromo-5-methyl-10H-indolo[3,2-b]quinolin-5-ium chloride, a bright yellow coloured solid **(38)** (Figure 4.5) (45 mg, 11%).

Melting point 120-122 °C

^{1}H NMR (400 MHz, methanol -d_4) δ ppm 9.14 - 9.17 (s, 1 H, NH), 8.75 - 8.80 (m, 1 H), 8.65 - 8.71 (m, 1 H), 8.47 - 8.53 (m, 1 H), 8.16 - 8.23 (m, 1 H), 7.92 - 8.00 (m, 1 H), 7.82 - 7.87 (m, 1 H), 7.54 - 7.61 (m, 1 H), 5.13 (s, 3 H, CH_3)

^{13}C NMR (101 MHz, methanol-d_4) δ ppm 147.31 (C-9a), 145.2 (C-10a), 143.31 (C-5a), 130.40 (C-4a), 130.29 (C-Ar), 129.32 (C-Ar), 127.81 (C-Ar), 126.03 (C-11) (C-Ar), 124.10 (C-11a), 122.64 (C-Ar), 122.54 (C-Ar), 120.96 (C-Ar), 119.54 (C-Ar), 111.10 (C-5b), 111.24 (C-Ar), 29.73.12 (N-CH_3)

ESI-MS m/z (relative intensity, %) 312 (3) [M+2], 310 (3) [M+], (bromine isotopes), 232 (100).

IR ν cm^{-1} 3556 (NH stretch), 1684 (C=N conjugated system).

4.7 10H-indolo[3,2-b]quinoline-11-carboxylic acid

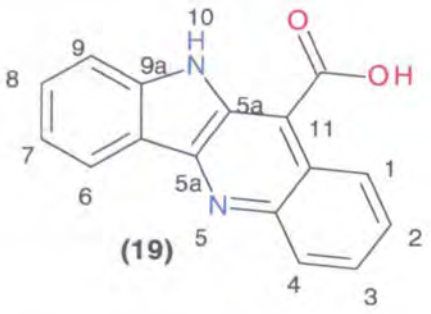

(19)

Figure 4.6 10H-indolo[3,2-b]quinoline-11-carboxylic acid

Isatin (4.25 g, 28.89 mmol) in aqueous sodium hydroxide solution (25.75 g in 115 ml of water) was added to indoxyl acetate (5.00 g, 28.54 mmol) and the mixture was stirred for 10 days under nitrogen. Water (50 ml) was added to the mixture and air was passed through the solution slowly to allow excess indoxyl acetate to oxidise, then the solution was heated to boiling and filtered to collect the hot filtrate. Concentrated hydrochloric acid (36% v/v aqueous) was added drop wise to the filtrate with vigorous stirring until a slight permanent precipitate was formed then 0.5 g of activated charcoal was added and then the mixture was filtered.The filtrate was added to the same volume of ethanol with stirring then the solution was acidified using concentrated hydrochloric acid, to form a precipitate which was collected by filtration and dried *in vacuo* to give quindoline-11-carboxylic acid (Figure 4.6) a bright yellow coloured solid **(19)** (5.38 g, 72%).

^{1}H NMR (400 MHz, DMSO- d_6) δ ppm 11.46 (br. s, NH), 9.03 - 9.17 (m, 1 H, H-1), 8.43 (d, 1 H, J=7.79 Hz, H-4), 8.25 - 8.37 (m, 1 H, H-9), 7.61 - 7.85 (m, 4 H), 7.27 - 7.41 (t, 1 H, J =8).

^{13}C NMR (101 MHz, DMSO- d_6) δ ppm 168.14 (C=O), 147.2 (C-9a), 145.3 (C-4a), 143.1 (C-Ar), 138.6 (C-Ar), 132.9 (C-Ar), 131.2 (C-Ar), 129.3 (C-Ar), 127.4 (C-Ar), 126.8 (C-Ar), 125.6 (C-Ar), 124.2 (C-Ar), 122.2(C-Ar), 120.9(C-Ar), 120.5 (C-Ar), 113.2 (C-Ar), 112.5(C-Ar).

IR ν cm^{-1} 1705 (C=O stretch), 3343 (amine NH stretch)

ESI-MS m/z (relative intensity, %) 262(100) (M^+)

4.8 11-chloro-10H-indolo[3,2-b]quinoline

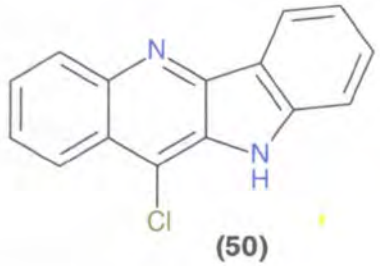

(50)

Figure 4.7 11-chloro-10H-indolo[3,2-b]quinoline

To 5,10-dihydroindolo[3,2-b]quinolin-11-one **(25)** (Figure 4.3) (0.50 g, 2.13 mmol), phosphorous oxychloride (0.50 g, 3.26 mmol) and phosphorous pentachloride (0.5 g, 2.13 mmol) were added then the mixture was heated to reflux for 4 hours. Then the reaction mixture was basified using aqueous sodium hydroxide solution (10% w/v, cooled to 0 °C) and extracted with ethyl acetate (4 X 100 ml). The organic phases were dried with magnesium sulfate then the solvent was evaporated *in vacuo*. A yellow coloured solid (180 mg) was obtained which was purified by using column chromatography on silica gel (eluent 1:5 diethyl ether in hexane) to give a pale-brown coloured solid **(50)** (Figure 4.7) (0.29 g, 53.8%).

^{1}H NMR (400 MHz, DMSO- d_6) δ ppm 11.89 (1H, NH), 8.37 (d, *J*=7.7 Hz, 1H), 8.30 (m, 2H), 7.76 (m, 2H), 7.68 (dd, *J* = 6.9, 8Hz, 1H,), 7.64 (d, *J* = 8.1 Hz, 1H), 7.35 (dd, *J* = 7.3, 7.7 Hz, 1H).

^{13}C NMR (101 MHz, DMSO- d_6) δ ppm 146.34 (C-4a), 145.31 (C-5a), 143.28 (C-9a), 130.87, 130.15 (C-11), 129.34 (C-9), 127.00 (C-Ar), 125.26 (C-Ar), 123.18 (C-Ar), 121.41 (C-Ar), 121.27 (C-Ar), 121.13 (C-Ar), 120.71 (C-Ar), 118.43 (C-Ar), 112.51 (C-Ar)

ESI-MS M/z (relative intensity, %) 253 (20) [M+], 255 (100) [M+2] (chlorine isotopes)

IR ν cm^{-1} 3164 (N-H stretch), 2851 (C-H aromatic stretch)

4.9 General procedure A

Under dry conditions, 10H-indolo[3,2-b]quinoline(**16**) and methyl triflate were stirred in anhydrous toluene for 24 hours at room temperature. The reaction mixture was poured in diethyl ether and the resulting yellow precipitate was collected by filtration. Aqueous ammonia solution (3.3% v/v) was added to the precipitate and the mixture was stirred to convert the product to its free base form. Then the mixture was extracted using chloroform (4 x 75ml). The collected organic layers were combined and evaporated *in vacuo* to give the crude product which was then purified by column chromatography on silica gel by using DCM: methanol: NH_4OH (5:1:0.1) as the eluent. Finally the free base was converted to its hydrochloride salt by neutralising with 0.1 M methanolic hydrochloric acid (5ml) and then solution was evaporated *in vacuo* to give the desired cryptolepine derivative, as a yellow coloured solid.

4.10 General procedure B

Methyl iodide was added drop wise to a solution of sulfolane and desired quindoline (Figure 4.9) and stirred under nitrogen for 16 hours at 50 °C. The reaction mixture was cooled to room temperature then ether (25 ml) and methanol (5 ml) were added to induce precipitation. Diethyl ether (25 ml) was added and then the mixture was filtered and the solid was dried *in vacuo*.

The solid was mixed with aqueous sodium carbonate solution (10% w/v, 30 ml) followed by extraction with chloroform (4x30 ml). The organic layers were combined and dried using magnesium sulfate and filtered. The solvent was removed *in vacuo* to concentrate the solution which was then treated with a solution of methanolic hydrochloric acid (0.1% v/v) drop wise to give hydrochloride salt of cryptolepine as a bright yellow coloured solid.

4.11 11-Chloro-5-methyl-10H-indolo[3,2-b]quinolin-5-ium chloride

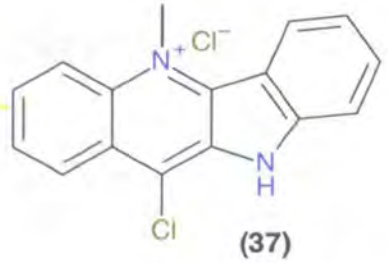

(37)

Figure 4.8 11-Chloro-5-methyl-10H-indolo[3,2-b]quinolin-5-ium chloride

According to general procedure B, 4.8 11-chloro-10H-indolo[3,2-b]quinoline **(50)** (Figure 4.7) (0.09 g, 0.4 mmol) and methyl iodide (0.057 g, 0.4 mmol)

were used to give 11-Chloro-5-methyl-10H-indolo[3,2-b]quinolin-5-ium chloride (Figure 4.8) as a yellow coloured solid (0.068 g, 56.1 %)

Melting point 270-273 °C

^{1}H NMR (400 MHz, DMSO- d_6) δ ppm 13.4 (s, NH), 8.84 (m, 2 H), 8.66 (d, *J*=8.28 Hz, 1 H), 8.26 (dd, *J* = 9.4, 7.7 Hz, 1H), 8.05 - 8.14 (m, 1 H), 7.93 - 8.01 (m, 1 H), 7.85 - 7.92 (m, 1 H), 7.55 (dd, *J*=8.9, 7.7 Hz, 1 H), 5.03 (s, 3 H, CH_3).

^{13}C NMR (101 MHz, DMSO-d_6) δ 146.4(C9a), 139.2 (C-5a), 136.2(C-4a), 135.0 (C-Ar), 133.3 (C-11), 132.2 (C-10a), 129.4 (C-11), 128.9 (C-Ar), 127.1 (C-Ar), 125.1 (C-Ar), 123.8 (C-Ar), 122.5 (C-Ar), 119.2 (C-Ar), 114.9 (C-Ar), 113.0 (C-9), 39.9 (N-CH_3)

ESI-MS M/z (relative intensity, %) 269 (32.4) [M+2], 267 (100.0) [M+] (chlorine isotopes)

IR ν cm^{-1} 3360 (N-H stretch), 1624(Conjugated cyclic C=N bend).

4.12 10H-indolo[3,2-b]quinoline

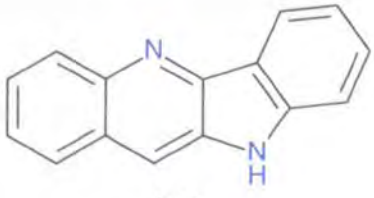

(16)

Figure 4.9 10H-indolo[3,2-b]quinoline

To 10H-indolo[3,2-b]quinoline-11-carboxylic acid **(19)** (Figure 4.6) (1.80 g, 6.83 mmol) diphenyl ether (20 ml) was added and the mixture was heated to

reflux for 6 hours. It was then cooled and petroleum ether (35ml) was added with stirring then the resulting crystals were collected by filtration and washed with excess petroleum ether and dried *in vacuo* to give pale green crystals of 10H-indolo[3,2-b]quinoline **(16)** (Figure 4.9)(1.28 g, 85%)

Melting point 249-251 °C

^{1}H NMR (400 MHz, DMSO- d_6) δ ppm 11.4 (s, 1H, NH), 8.37 (d, J = 8.0, 1H), 8.29 (m, 1H), 8.20 (d, J=8.01, 1H), 8.11 (d, J=7.36 1H), 7.66 (m, 1H), 7.64 (m, 1H), 7.58 (d, J=7.26, 1H), 7.56 (m, 1H), 7.28 (m, 1H)

^{13}C NMR (101 MHz, DMSO-d_6) δ 146.2 (C-5a), 144.5 (C-9a), 143.9 (C-4a), 133.0 (C-10a), 130.2 (C-Ar), 129.2 (C-Ar) 128.0 (C-Ar), 127.2 (C-Ar), 126.5 (C-Ar), 125.3 (C-Ar), 121.8 (C-Ar), 121.5 (C-Ar), 119.8 (C-Ar), 113.5 (C-11), 112.0 (C-9),

ESI-MS M/z (relative intensity, %) 217 (100) [M^+]

IR ν cm^{-1} 3329 (NH stretch) and absence of carbonyl group

4.13 5-Methyl-10H-indolo[3,2-b]quinolin-5-ium chloride

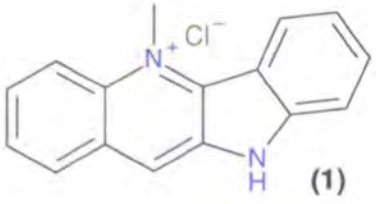

(1)

Figure 4.10 5-Methyl-10H-indolo[3,2-b]quinolin-5-ium chloride

According to the general procedure B, methyl iodide (1.28 g, 9.01 mmol) and 10H-indolo[3,2-b]quinoline **(16)** (1.20 g, 5.864 mmol) were used to give cryptolepine (Figure 4.10) as a yellow coloured solid **(1)** (104 mg, 8%).

Melting point 280 - 282 °C

^{1}H NMR (400 MHz, DMSO- d_6) δ ppm 12.78 (s, NH), 9.28 (s, 1H), 8.81(d, 1H, J=8.5 Hz), 8.76 (d, 1H, J=9.1 Hz), 8.59 (dd, 1H, J=7.4, 1.0 Hz),), 8.17 (ddd, 1H, J=8.0, 8.0, 1.4 Hz), 7.95 (dd, 1H, J=8.1, 8.1 Hz), 7.92 (dd, 1H, J=7.2, 7.2 Hz), 7.85 (d, 1H,J=8.3 Hz), 7.51 (ddd, 1H, J=7.7, 7.7, 1.0 Hz), 5.04 (s, 3H, N-CH_3).

^{13}C NMR (101 MHz, DMSO- d_6) δ ppm 145.4 (C-9a) 139.7 (C-5a), 137 (C-4a) 135,2 (C-8), 133.7 (C-3), 132.5 (C-1), 130.6 (C-2), 127.6 (C-11a), 127.2 (C-10a), 126.9 (C-6), 125.1 (C-11), 121.8 (C-7), 117.9 (C-4), 114.8 (C-5b), 39.9 (CH3-N)

IR ν cm^{-1} (KBr): 3432 (NH stretch) 1626 (C-H Aromatic stretch)

ESI-MS M/z (relative intensity, %) 233 (100, M-Cl) 139 (11)

4.14 11-Iodo-5-methyl-10H-indolo[3,2-b]quinolin-5-ium chloride

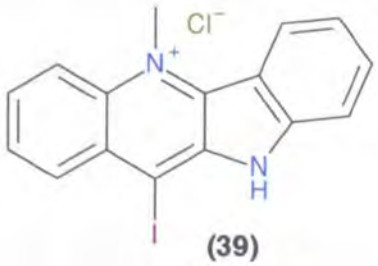

(39)

Figure 4.11 11-Iodo-5-methyl-10H-indolo[3,2-b]quinolin-5-ium chloride

According to the general procedure B, Methyl iodide (0.2 ml, 5.25 mmol) and 11-bromo-10H-indolo[3,2-b]quinoline **(51)** (Figure 4.4) (0.0265 g, 0.09 mmol) were used to give hydrochloride salt of 4.14 11-Iodo-5-methyl-10H-indolo[3,2-b]quinolin-5-ium chloride **(39)** (Figure 4.11) as a bright yellow coloured solid (0.015 g, 43%)

^{1}H NMR (400 MHz, methanol-d_4) δ ppm 8.71 - 8.79 (m, 1 H), 8.64 (s, 2 H), 8.17 - 8.26 (m, 1 H), 7.94 - 8.04 (m, 2 H), 7.91 (s, 1 H), 7.53 - 7.63 (m, 1 H), 4.86 (s, 3 H, N-CH_3)

^{13}C NMR (101 MHz, methanol-d_4) δ ppm = 143.32 (C-9a), 140.37 (C-5a), 135.7 (C-10a), 134.3 (C-4a), 134.1(C-3), 129.9 (C-Ar), 128.4 (C-Ar), 127.7 (C-Ar), 127.2 (C-Ar), 124.4 (C-Ar), 123.6 (C-7), 119.7 (C-Ar), 119.1 (C-Ar), 114.6 (C-Ar), 110.7 (C-Ar), 28.73 (N-CH_3)

MS M/z (relative intensity, %) 359 (100, M - Cl), 360 (29)

IR ν cm^{-1} 3322 (N-H stretch), 1613 (Conjugated cyclic C=N bend).

4.15 General procedure C (alkylamidoquindolines)

To finely ground quindoline-11-carboxylic acid (Figure 4.6), dichloromethane and DMF were added and the mixture was stirred for 15 min. TEA was added drop wise under continuous stirring before adding COMU to the solution, which was then stirred for 10 min. The desired amine was added drop wise and the reaction mixture was stirred for 16 hours at room temperature.

The reaction mixture was added to ethyl acetate (100 ml) and extracted with aqueous 1N HCl solution (2x30 ml) and aqueous 1N sodium bicarbonate so-

lution (2x30 ml). Then the organic layers were collected and dried using magnesium sulphate and evaporated *in vacuo* to give the crude quindoline amide, which was purified by column chromatography over silica gel using ethyacetate:hexane (1:1) and dried *in vacuo* to give desired alkylamidoquindoline

4.16 General procedure D (N5-ethyl quindoline derivatives)

Under dry conditions, quindoline and ethyl triflate were stirred in anhydrous toluene for 24hours at room temperature. The reaction mixture was poured in diethyl ether and the yellow precipitate was collected by filtration. Ammonia solution (3.3% v/v) was added to the precipitate and the mixture was stirred for 0.5 hours to convert the product to its free base form. Then the mixture was extracted using chloroform (4 x 75ml). The collected organic layers were combined and evaporated *in vacuo* to give the crude product which was then purified by column chromatography on silica gel by using DCM: methanol: NH_4OH (5:1:0.1) as the eluent. Finally the free base was converted to its hydrochloride salt by neutralising with 0.1 M methanolic hydrochloric acid and then solution was dried *in vacuo* to give desired N5-ethyl quindoline derivative as a yellow coloured solid

4.17 General procedure E (alkylaminocryptolepine)

To a solution of 11-Chloro-5-methyl-10H-indolo[3,2-b]quinolin-5-ium chlorideIn ethyl acetate, the desired amine was added and the contents of the flask were heated to reflux for 16 hours. The reaction mixture was cooled down to temperature and precipitate which formed was collected by filtration and washed with diethyl ether and dried *in vacuo to* give yellow colour crystals. Recrystallization was performed where necessary.

4.18 N-isopropyl-10H-indolo[3,2-b]quinoline-11-carboxamide

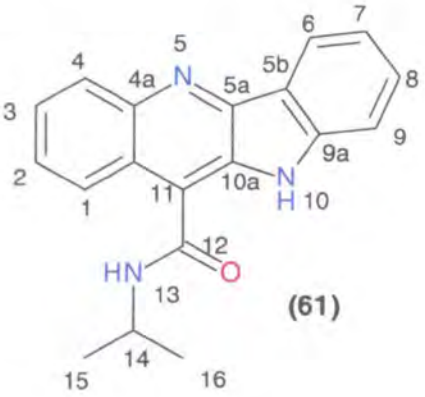

(61)

Figure 4.12 N-isopropyl-10H-indolo[3,2-b]quinoline-11-carboxamide

Using 10H-indolo[3,2-b]quinoline-11-carboxylic acid **(19)** (Figure 4.6) (0.5 g, 1.9 mmol) and and isopropylamine (0.14ml, 1.9 mmol), general procedure C was followed to give N-isopropyl-10H-indolo[3,2-b]quinoline-11-carboxamide (Figure 4.12) as a yellow colour solid **(61)** (0.77 g, 83.4%)

Melting point 263-265 °C

^{1}H NMR (400 MHz, methanol-d_4) δ ppm 11.76 (s, N H), 7.63 (s, H) 7.42 (m, 1H), 7.81 (m, 1H), 7.91 (m, 2H), 8.2 (m, 1H), 8.3 (m, 2H) 8.6 (m, 1H) 3.77 (m, 1H) 1.04 (d, 6H)

^{13}C NMR (101 MHz, methanol-d_4) δ 166.7 (C-12), 148.34 (C-5a), 145.2 (C-9a) 143.42 (C-4a), 137.4 (C-10a), 134.0 (C-11), 129.2 (C-Ar), 128.6 (C-Ar), 127.7 (C-Ar), 127.1 (C-Ar), 125.0 (C-Ar), 123.4 (C-Ar), 123.0 (C-Ar), 118.9 (C-Ar), 117.2 (C-Ar), 114.5 (C-9), 41.1 (C-14), 22.5 (C -15, C-16)

ESI-MS: M/z (relative intensity, %) 303 (100, M^+) 244 (80) 216 (85)

IR ν cm^{-1} 1646 (amide C=O stretch) 3169 (NH stretch)

4.19 N-butyl-10H-indolo[3,2-b]quinoline-11-carboxamide

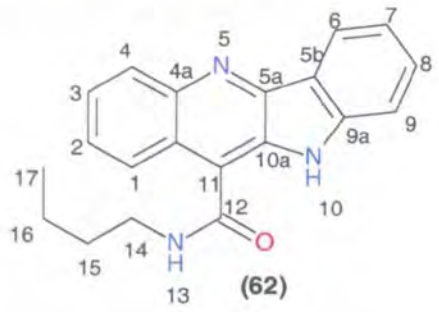

Figure 4.13 N-butyl-10H-indolo[3,2-b]quinoline-11-carboxamide

Using 10H-indolo[3,2-b]quinoline-11-carboxylic acid **(19)** (Figure 4.6) (0.5 g, 1.9 mmol) and andbutylamine (0.18ml, 1.9 mmol), general procedure C was followed to give N-butyl-10H-indolo[3,2-b]quinoline-11-carboxamide (Figure 4.13) as a yellow colour solid **(62)** (0.514 g, 91%)

Melting point 270-272 °C

^{1}H NMR (400 MHz, DMSO- d_6) δ ppm 11.42 (s, 1 H), 8.97 (t, *J*=5.40 Hz, 1 H), 8.41 (d, *J*=7.78 Hz, 1 H), 8.30 (d, *J*=7.78 Hz, 1 H), 8.09 - 8.18 (m, 1 H), 7.60 - 7.80 (m, 4 H), 7.30 - 7.40 (m, 1 H), 3.49 - 3.61 (m, 2 H), 1.71 (m, *J*=7.34 Hz, 2 H), 1.50 (m, *J*=14.81, 7.36 Hz, 2 H), 1.03 (t, *J*=7.40 Hz, 3 H)

^{13}C NMR (400 MHz, DMSO-d_6) δ ppm 165.4 (C-12), 146.7 (C-5a), 144.9 (C-9a), 143.7 (C- 4a), 130.5 (C-11), 129.6 (C-10a), 129.2 (C-Ar), 126.6 (C-Ar), 126.1 (C-Ar), 124.8 (C-Ar), 123.2 (C-Ar), 121.8 (C-Ar), 121.5 (C-Ar), 121.2 (C-Ar), 120.2 (C-Ar), 112.3 (C-9), 41.6 (C-14), 29.5 (C-15), 20.3 (C-16), 14.2 (C-17).

IR IR ν cm-1 1646 (amide C=O stretch)

ESI-MS: M/z (relative intensity, %) 317 (100, M) 244 (85), 216(79) 190 (50)

4.20 N-[2-(2-hydroxyethylamino)ethyl]-10H-indolo[3,2-b]quinoline-11-carboxamide

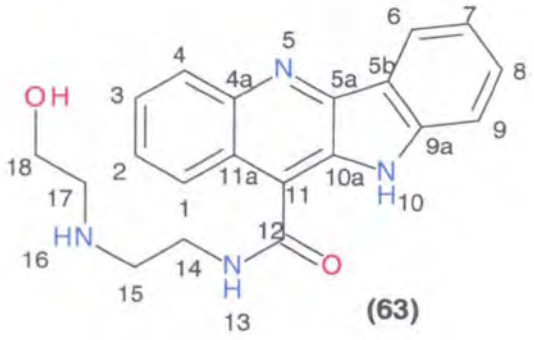

(63)

Figure 4.14 N-[2-(2-hydroxyethylamino)ethyl]-10H-indolo[3,2-b]quinoline-11-carboxamide

Using 10H-indolo[3,2-b]quinoline-11-carboxylic acid **(19)** (Figure 4.6) (0.5 g, 1.9 mmol) and and 2-(2 aminoethylamino)ethanol (0.14ml, 1.9 mmol), general procedure C was followed to give N-[2-(2-hydroxyethylamino)ethyl]-10H-indolo[3,2-b]quinoline-11-carboxamide (Figure 4.14) as a brownish yellow colour solid **(63)** (0.078 g, 12%)

^{1}H NMR (400 MHz, methanol-d_4) δ ppm 8.36 (d, *J*=7.78 Hz, 1 H), 8.10 (dd, *J*=8.16, 4.39 Hz, 2 H), 7.43 - 7.64 (m, 4 H), 7.25 (t, *J*=7.40 Hz, 1 H), 3.69 - 3.84 (m, 4 H), 3.54 - 3.63 (m, 2 H), 3.35 (s, 2 H), 1.23 (br. s., 1 H)

^{13}C NMR (101 MHz, methanol-d_4) δ 166.3 (C-12), 147.6 (C-5a), 145.9 (C-9a), 144.1 (C-4a), 131.6 (C-11), 130.8 (C-Ar), 129.0 (C-Ar), 127.7 (C-Ar), 127.1 (C-Ar), 125.3 (C-Ar), 124.0 (C-Ar), 122.7 (C-Ar), 121.5 (C-Ar), 121.4 (C-Ar), 121.2 (C-7) (C-1), 112.7 (C-9), 60.9 (C-18), 51.6 (C-17), 40.07 (C-15), 38.6 (C-14)

ESI-MS: M/z (relative intensity, %) 347 (100, M^+), 313 (49)

4.21 N-isopropyl-5-methyl-10H-indolo[3,2-b]quinolin-5-ium-11-carboxamide hydrochloride

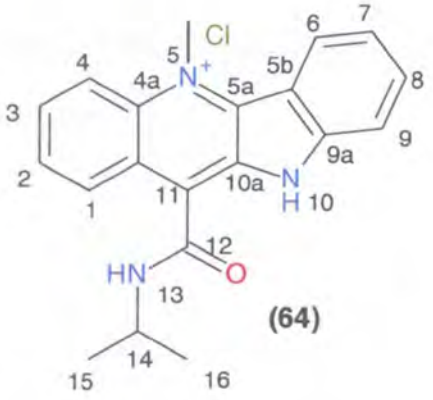

(64)

Figure 4.15 N-isopropyl-5-methyl-10H-indolo[3,2-b]quinolin-5-ium-11-carboxamide hydrochloride

According to the general procedure A N-isopropyl-10H-indolo[3,2-b]quinoline-11-carboxamide **(61)** (0.2 g, 0.7 mmol) (Figure 4.12) and methyltriflate were used to give N-isopropyl-5-methyl-10H-indolo[3,2-b]quinolin-5-ium-11-carboxamide hydrochloride (Figure 4.15) as yellow solid **(64)** (0.037 g, 17%)

^{1}H NMR (400 MHz, methanol-d_4) δ ppm 8.75 (dd, *J*=16.44, 8.91 Hz, 2 H), 8.40 (d, *J*=8.53 Hz, 1 H), 8.22 (t, *J*=7.78 Hz, 1 H), 7.91 - 8.09 (m, 2 H), 7.85 (d, *J*=8.28 Hz, 1 H), 7.60 (t, *J*=7.78 Hz, 1 H), 5.14 (s, 3 H), 4.46 - 4.57 (m, 1 H), 1.44 (d, *J*=6.53 Hz, 6 H)

^{13}C NMR (101 MHz, methanol-d_4) δ 168.4 (C-12), 147.6 (C-9a) 139.14 (C-5a) 136.3 (C-Ar) 134.6 (C-Ar), 132.5 (C-Ar), 127.9 (C-Ar), 126.2 (C-Ar), 125.6 (C-Ar), 124.6 (C-Ar), 122.0 (C-Ar), 121.5 (C-Ar), 117.5 (C-Ar), 115.9 (C-Ar), 114.1 (C-Ar), 113.0 (C-9), 44.2 (C-14), 41.2 (N5-CH3), 22.92 (C-15, 16)

ESI-MS: M/z (relative intensity, %) 318 (100, M), 319 (20, M+1)

HIRES-MS (ESI): calculated for [M - Cl] ($C_{20}H_{20}N_3OCl$) required m/z 318.1606, found 318.1615

4.22 N-butyl-5-methyl-10H-indolo[3,2-b]quinolin-5-ium-11-carboxamide chloride

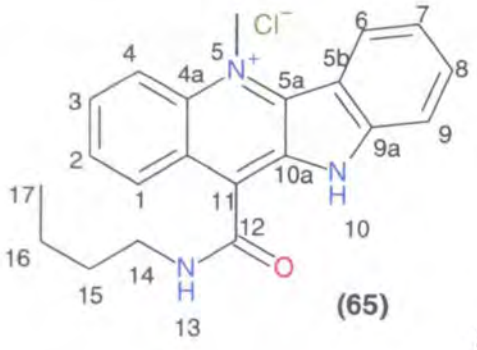

(65) 21

Figure 4.16 N-butyl-5-methyl-10H-indolo[3,2-b]quinolin-5-ium-11-carboxamide chloride

According to the general procedure A, N-butyl-10H-indolo[3,2-b]quinoline-11-carboxamide **(62)** (Figure 4.13) (0.2 g, 0.6 mmol) and methyltriflate were used to give N-butyl-5-methyl-10H-indolo[3,2-b]quinolin-5-ium-11-carboxamide chloride **(65)** (Figure 4.16) as yellow solid (0.048 g, 23%)

^{1}H NMR (400 MHz, methanol-d_4) δ ppm 12.66 (s, NH), 8.74 (dd, *J*=15.43, 8.78 Hz, 2 H), 8.39 (dd, *J*=8.47, 1.07 Hz, 1 H), 8.20 (d, *J*=1.38 Hz, 1 H), 7.91 - 8.03 (m, 2 H), 7.82 (d, *J*=8.41 Hz, 1 H), 7.58 (s, 1 H), 5.13 (s, 3 H), 3.70 (t, *J*=7.28 Hz, 2 H), 1.78 (t, *J*=7.34 Hz, 2 H), 1.48 - 1.61 (m, 2 H), 1.05 (t, *J*=7.34 Hz, 3 H)

^{13}C NMR (101 MHz, methanol-d_4) δ 163.4 (C-12), 146.8 (C-9a), 139.7 (C-5a), 136.0(C-Ar), 134.6(C-Ar), 132.5 (C-Ar), 130.8(C-Ar), 130.3(C-Ar), 127.8(C-Ar), 126.3(C-Ar), 125.6(C-Ar), 123.0(C-Ar), 122.0(C-Ar), 117.4(C-Ar), 114.1 (C-Ar), 113.0(C-9), 39.7(N5-CH_3), 30.9 (C-15), 20.0 (C-16), 12.4 (C-17)

ESI-MS: M/z (relative intensity, %): 332 (100, M^+), 333 (20, M+1)

HIRES-MS (ESI): calculated for [M - Cl]- ($C_{21}H_{22}N_3OCl$) required m/z 332.1763, found 332.1769

4.23 N-[2-(2-hydroxyethylamino)ethyl]-5-methyl-10H-indolo[3,2-b]quinolin-5-ium-11-carboxamide chloride

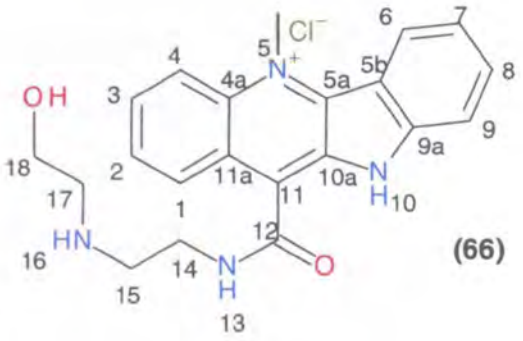

Figure 4.17 N-[2-(2-hydroxyethylamino)ethyl]-5-methyl-10H-indolo[3,2-b]quinolin-5-ium-11-carboxamide chloride

According to the general procedure A, N-[2-(2-hydroxyethylamino)ethyl]-10H-indolo[3,2-b]quinoline-11-carboxamide **(63)** (Figure 4.14) (0.2 g, 0.6 mmol)and methyltriflate were used to give N-[2-(2-hydroxyethylamino)ethyl]-5-methyl-10H-indolo[3,2-b]quinolin-5-ium-11-carboxamide chloride (Figure 4.17) as orange-yellow solid **(66)** (0.01 g, 4.39%)

^{1}H NMR (400 MHz, methanol-d_4) δ ppm 8.65 - 8.80 (m, 2 H), 8.41 - 8.53 (m, 1 H), 8.12 - 8.24 (m, 1 H), 7.89 - 8.01 (m, 2 H), 7.80 - 7.89 (m, 1 H), 7.50 - 7.61 (m, 1 H), 5.12 (s, 3 H), 4.00 - 4.09 (m, 2 H), 3.87 - 3.98 (m, 2 H), 3.55 (m, 2 H)3.35(m,2H)

^{13}C NMR (101 MHz, methanol-d_4) δ ppm 166.3 (C-12), 147.6 (C-9a), 145.9 (C-5a), 144.1(C-4a), 131.6 (C-Ar), 130.8 (C-Ar), 129.0 (C-Ar), 127.7 (C-Ar), 127.1 (C-Ar), 125.3 (C-Ar), 124.0(C-Ar), 122.7 (C-Ar), 121.5 (C-Ar), 121.4 (C-

Ar), 121.2 (C-Ar), 112.7 (C-Ar), 57.6 (C-18), 51.6 (C-17), 48.4 (C-15), 39.7(N-CH_3), 37.5 (C-14)

ESI-MS M/z (relative intensity, %): 363 (100, M-Cl), 364 (60, M+1)

HIRES-MS (ESI): calculated for [M - Cl]- ($C_{21}H_{23}N_4O_2Cl$) required m/z 363.1821, found 363.1828

4.24 N-isopropyl-5-methyl-10H-indolo[3,2-b]quinolin-5-ium-11-amine hydrochloride

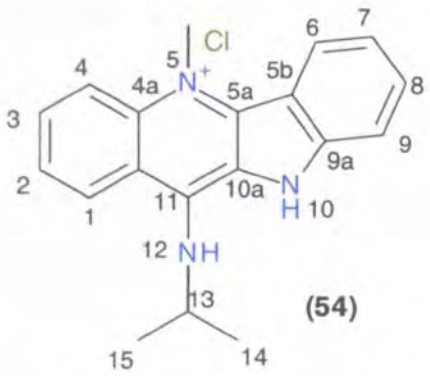

(54)

Figure 4.18 N-isopropyl-5-methyl-10H-indolo[3,2-b]quinolin-5-ium-11-amine hydrochloride

Using 11-Chloro-5-methyl-10H-indolo[3,2-b]quinolin-5-ium chloride **(37)** (Figure 4.8) (0.1 g, 0.3 mmol) and isopropylamine (0.05 ml, 0.6 mmol), general procedure E was followed to give N-isopropyl-5-methyl-10H-indolo[3,2-b]quinolin-5-ium-11-amine hydrochloride (Figure 4.18) as yellow colour crystals **(54)** (0.12 g, 61%)

Melting point 283-285 °C

^{1}H NMR (400 MHz, methanol-d_4) δ ppm 8.64 (d, *J*=8.53 Hz, 1 H), 8.54 (d, *J*=8.53 Hz, 1 H), 8.28 (d, *J*=8.78 Hz, 1 H), 7.98 - 8.09 (m, 1 H), 7.84 (d,

J=8.28 Hz, 1 H), 7.67 - 7.79 (m, 2 H), 7.38 - 7.48 (m, 1 H), 4.68 (s, 3 H), 4.23 (m, 1H),1.57 (d, *J*=6.27 Hz, 6 H)

^{13}C NMR (101 MHz, DMSO) δ ppm 144.6 (C-Ar), 143.7(C-9a), 137.5(C-4a), 135.8 (C-5a), 131.9(C-Ar), 127.8 (C-Ar), 127.6 (C-Ar), 125.9 (C-Ar), 124.5 (C-Ar), 123.1 (C-Ar), 121.44 (C-Ar), 119.8 (C-Ar), 116.5 (C-Ar), 112 (C-9), 53.94(C-13), 39.65 (N-CH_3), 22.9 (C-14, 15)

ESI-MS M/z (relative intensity, %) 290 (100, M^+)

HIRES-MS (ESI): Calculated for [M - Cl] ($C_{18}H_{18}N_3Cl$) required m/z 290.1657, found 290.1643

4.25 N-butyl-5-methyl-10H-indolo[3,2-b]quinolin-5-ium-11-amine hydrochloride

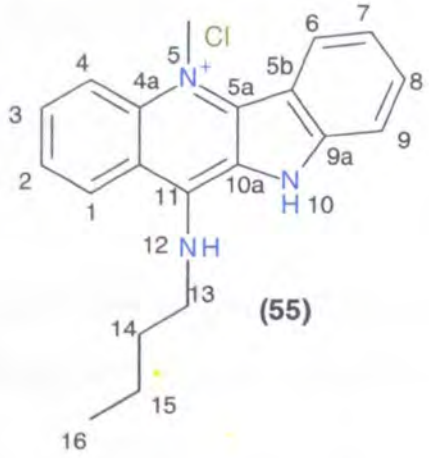

(55)

Figure 4.19 N-butyl-5-methyl-10H-indolo[3,2-b]quinolin-5-ium-11-amine hydrochloride

According to the general procedure E, 11-Chloro-5-methyl-10H-indolo[3,2-b]quinolin-5-ium chloride **(37)** (Figure 4.8) (0.1 g, 0.3 mmol) and butylamine (0.06 ml, 0.6 mmol) were used to give N-butyl-5-methyl-10H-indolo[3,2-

b]quinolin-5-ium-11-amine hydrochloride (Figure 4.19) as yellow crystals **(55)** (0.07 g, 68%)

Melting point >300 °C

^{1}H NMR (400 MHz, methanol-d_4) δ ppm 8.47 - 8.65 (m, 2 H), 8.27 (d, *J*=8.78 Hz, 1 H), 8.02 (t, *J*=7.78 Hz, 1 H), 7.78 - 7.86 (m, 1 H), 7.72 (dt, *J*=14.43, 7.34 Hz, 2 H), 7.42 (t, *J*=7.65 Hz, 1 H), 4.67 (s, 3 H), 4.10 - 4.22 (m, 2 H), 1.84 - 1.96 (m, 2 H), 1.43 (d, *J*=7.53 Hz, 2 H), 0.88 (s, 3 H)

^{13}C NMR (101 MHz, methanol-d_4) δ ppm 144.2 (C-11), 142.1 (C-Ar), 137.5 (C-Ar), 133.83 (C-Ar),131.95 (C-Ar), 127.84 (C-Ar), 127.65 (C-Ar), 125.93 (C-Ar), 124 (C-Ar), 123 (C-Ar), 121.44 (C-Ar), 119.8 (C-Ar), 116.5 (C-Ar), 112 (C-9), 56.41 (C-13), 38.65 (N5-CH_3), 33.2 (C-14), 21.07 (C-15), 13.76 (C-16).

ESI-MS M/z (relative intensity, %)304 (100, M^+)

HIRES-MS (ESI): calculated for $[M - Cl]^+$ ($C_{20}H_{22}N_3Cl$) required m/z 304.1814, found 304.1810

4.26 2-[2-[(5-methyl-10H-indolo[3,2-b]quinolin-5-ium-11-yl)amino]ethylamino]ethanol chloride

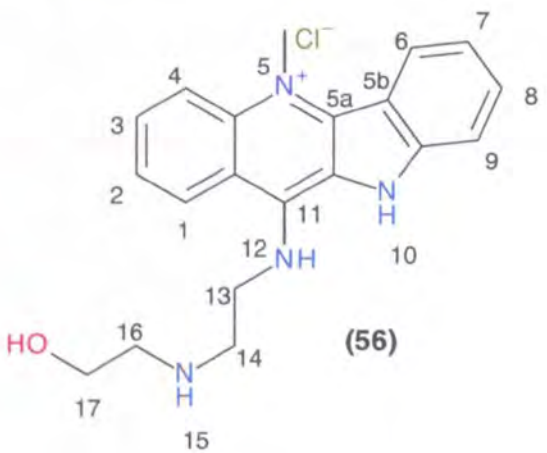

(56)

Figure 4.20 2-[2-[(5-methyl-10H-indolo[3,2-b]quinolin-5-ium-11-yl)amino]ethylamino]ethanol chloride

According to the general procedure E, 11-Chloro-5-methyl-10H-indolo[3,2-b]quinolin-5-ium chloride**(64)** (Figure 4.8) (0.5 g, 1.6 mmol) and 2-(2-aminoethylamino)ethanol (0.162 ml, 1.6 mmol) were used to give 2-[2-[(5-methyl-10H-indolo[3,2-b]quinolin-5-ium-11-yl)amino]ethylamino]ethanol chloride as yellow crystals **(56)** (0.1364 g, 23%).

Melting point >300 °C

^{1}H NMR (400 MHz, DMSO- d_6) δ ppm 11.58 (s,1H, NH), 8.85 - 8.91 (m, 1H), 8.54 - 8.61 (m, 1H), 8.35 - 8.41 (m, 1H), 7.96 - 8.06 (m, 2H), 7.67 - 7.76 (m, 2H), 7.33 - 7.42 (m, 1H), 4.65 (s, 3H), 3.57 - 3.70 (m, 2H), 2.83 - 2.92 (m, 2H), 2.66 - 2.71 (m, 2H), 2.56 - 2.65 (m, 2H)

^{13}C NMR (101 MHz, DMSO- d_6) δ ppm 145.9 (C-11), 139.3 (C-9a), 137.4 (C-4a), 133.43 (C-Ar), 131.95 (C-Ar), 127.84 (C-Ar), 127.65 (C-Ar), 125.93 (C-Ar), 124 (C-Ar), 123 (C-Ar), 121.4 (C-Ar), 119.8 (C-Ar), 116.5 (C-Ar), 114.6 (C-Ar), 112.7 (C-9), 57.51 (C-17), 57.03 (C-13), 52.4 (C-16), 49.6 (C-14) , 38.4 (N5-CH_3)

ESI-MS M/z (relative intensity, %) 335 (100, M) 336 (35, M+1)

HIRES-MS (ESI): calculated for $[M - Cl]^+$ ($C_{20}H_{23}N_4OCl$) required m/z 335.1872, found 335.1875

4.27 11-chloro-5-ethyl-10H-indolo[3,2-b]quinolin-5-ium chloride

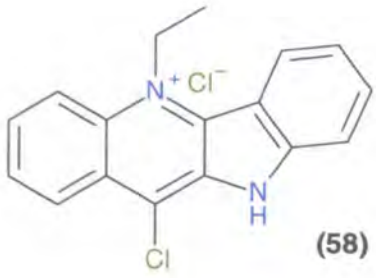

(58)

Figure 4.21 11-chloro-5-ethyl-10H-indolo[3,2-b]quinolin-5-ium chloride

According to the general procedure D, 11-chloro-10H-indolo[3,2-b]quinoline **(50)** (0.2 g, 0.8 mmol) and ethyltriflate (0.15 g, 0.8 mmol) were used to give 11-chloro-5-ethyl-10H-indolo[3,2-b]quinolin-5-ium chloride as brownish yellow solid **(58)** (0.142 g, 56%)

^{1}H NMR (400 MHz, DMSO- d_6) δ ppm 12.82 (s, NH), 8.49 (m, 1H), 8.24 (m, 1H) 8.16 (m, 1H) 8.09 (m, 1H), 7.68 (m, 1H), 7.64 (m, 1H), 7.48 (m, 1H), 7.24 (m, 1H), 5.2 (q, *J*=6.80, 2H, CH_2), 1.80 (t, *J*=6.80 Hz, 3H, CH_3).

^{13}C NMR (101 MHz, DMSO- d_6) δ ppm 147.5 (C-9a), 139.7 (C-5a), 138.1 (C-4a), 138.70 (C-Ar) 136.75 (C-Ar), 135.4 (C-Ar), 133.02 (C-Ar), 128.23 (C-Ar), 126.9 (C-Ar), 125 (C-Ar), 124.45 (C-Ar), 123 (C-Ar), 119.42 (C-Ar), 115.4 (C-5b), 114.1(C-9), 47.8 (N5-CH_2), 13.8 (N5-CH_3)

ESI-MS M/z (relative intensity, %) 281 (100, M^+) 263 (31)

HIRES-MS (ESI): calculated for $[M - Cl]^+$ ($C_{17}H_{14}N_2Cl_2$) required m/z 281.0846, found 281.0842

4.28 N-butyl-5-chloro-5-ethyl-10H-indolo[3,2-b]quinolin-11-amine

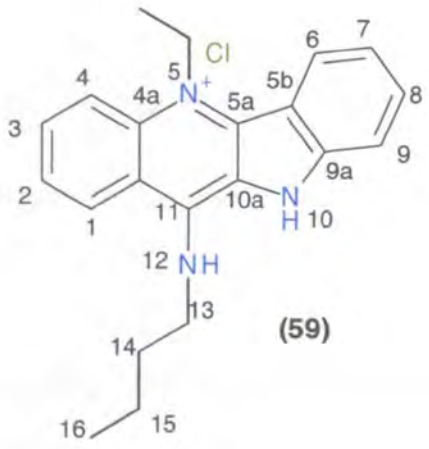

(59)

Figure 4.22 N-butyl-5-chloro-5-ethyl-10H-indolo[3,2-b]quinolin-11-amine

According to the general procedure C, 11-chloro-5-ethyl-10H-indolo[3,2-b]quinolin-5-ium chloride **(58)** (0.10 g, 0.3 mmol) and butylamine (0.044 g, 0.3 mmol) were used to give N-butyl-5-chloro-5-ethyl-10H-indolo[3,2-b]quinolin-11-amine (Figure 4.22) as yellow colour crystals **(59)** (0.037 g, 35%)

Melting point 296-298 °C

^{1}H NMR (400 MHz, methanol-d_4) δ ppm 8.65 (d, *J* = 8.53 Hz, 1H), 8.30 - 8.47 (m, 2H), 8.07 (t, *J* = 7.78 Hz, 1H), 7.83 - 7.93 (m, 1H), 7.67 - 7.82 (m, 2H), 7.49 (t, *J* = 7.65 Hz, 1H), 5.24 (q, *J* = 7.28 Hz, 2H, N-CH_2), 4.22 (t, *J* = 7.03 Hz, 2H), 2.85 - 3.01 (m, 3H), 1.94 (quin, *J* = 7.28 Hz, 2H), 1.81 (t, *J* = 7.15 Hz, 3H), 1.53 - 1.72 (m, 2H), 1.46 (sxt, *J* = 7.43 Hz, 2H), 1.03 (t, *J* = 7.22, Hz, 3H)

^{13}C NMR (101 MHz, methanol-d_4) δ ppm 144.08 (C-11), 143.73 (C-9a), 143.02(C-4a), 137.5,133.83, 131.95, 127.84, 125.93(C-Ar) , 124.52 (C-Ar),

123.04 (C-Ar) , 121.44 (C-Ar), 119.8 (C-Ar), 116.5 (C-Ar), 112.3 (C-4), 112 (C-9), 49.2 (C-13) 43.14 (N5-CH_2), 33.2 (C-14), 21.07 (C-15), 13.76 (N5-CH_3), 12.98 (C-C16)

ESI-MS M/z (relative intensity, %) 318 (100, M^+) 319 (20, M+1)

HIRES-MS (ESI): calculated for [M - Cl]- ($C_{21}H_{24}N_3Cl$) required m/z 318.1970, found 318.1961

4.29 5-methyl-N-pentyl-10H-indolo[3,2-b]quinolin-5-ium-11-amine chloride

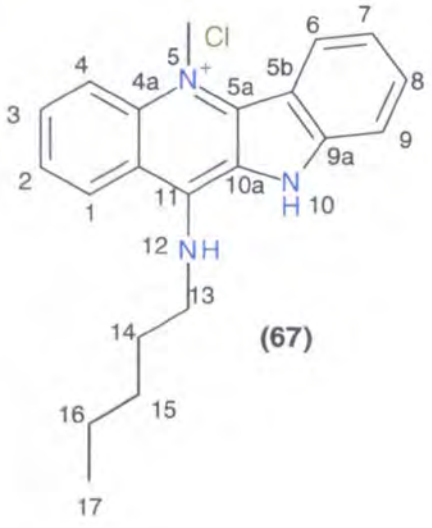

(67)

Figure 4.23 5-methyl-N-pentyl-10H-indolo[3,2-b]quinolin-5-ium-11-amine chloride

According to the general procedure E, 11-Chloro-5-methyl-10H-indolo[3,2-b]quinolin-5-ium chloride **(37)** (Figure 4.8) (0.1 g, 0.3 mmol) and pentylamine (0.523 g, 0.6 mmol) were used to give 5-methyl-N-pentyl-10H-indolo[3,2-b]quinolin-5-ium-11-amine chloride **(67)** (Figure 4.23) as yellow crystals (0.06 g, 67%).

Melting point 303-305 °C

1H NMR (400 MHz, DMSO- d6) δ ppm 8.79 (d, J = 8.28 Hz, 1H), 8.58 (d, J = 8.53 Hz, 1H), 8.36 (d, J = 8.78 Hz, 1H), 8.03 (t, J = 7.53 Hz, 1H), 7.90 (d, J = 8.28 Hz, 1H), 7.66 - 7.77 (m, 2H), 7.39 (t, J = 7.65 Hz, 1H), 4.63 (s, 3H), 4.17 (t, J = 7.03 Hz, 2H), 1.21 - 1.5 (m, 6H), 0.88 (m, J = 2.76, 6.90 Hz, 3H)

13C NMR (101 MHz, DMSO- d6) δ ppm 144.09 (C-11), 143.63(C-9a), 137.5 (C-4a), 133.83 (C-Ar), 131.95 (C-Ar), 127.84 (C-Ar), 127.65 (C-Ar), 125.93 (C-Ar), 124 (C-Ar), 123 (C-Ar), 121.44 (C-Ar), 119.8 (C-Ar), 116.5 (C-Ar), 113.1 (C-4), 112 (C-9), 47.92 (C-13) 38.22 (N5-CH_3), 32.4 (C-14), 28.34 (C-15), 22.31(C-16), 14 (C-17).

ESI-MS M/z (relative intensity, %) 318 (100, M^+) 319 (20, M+1)

HIRES-MS (ESI): calculated for [M - Cl]-($C_{21}H_{24}N_3Cl$) required m/z 318.1970 found 318.1966.

Chapter 5 Experimental: *In vitro* and Bio-physical Studies

5.1 MTT assay

5.1.1 Materials and equipment:

RPMI culture medium, DMEM culture medium, Foetal bovine serum(FBS), penicillin-streptomycin solution ((10,000 U/mL penicillin, 10 mg/mL streptomycin), L-glutamine (200 mM), Trypsin, Trypan blue solution, MTT, Doxorubicin, DMSO (biological grade) were obtained from Sigma Aldrich, UK. 96 well culture plates, T75ml flasks, and pipettes were purchased from Fischer Scientific, UK. Plate reader used to scan the 96 well plates was Labtech LT-4000. The Incubator used to grow the cells was from Thermo Scientific, UK.

5.1.2 Cell lines:

MCF-7, A549 and DLD-1 cells were obtained from the Institute of cancer therapeutics, Bradford University, Bradford, UK.

5.1.3 Growing conditions:

The three cell lines were grown in the presence of 95% humidified air mixed with 5% carbon dioxide at a fixed temperature of 37 °C. Exhausted growth medium was replaced with fresh growth medium every two days

5.1.4 Culture media Preparation:

FBS (50 ml) was heat inactivated at 60° C and added to incomplete RPMI medium (500 ml) then the frozen solution of penicillin–streptomycin-L-glutamine (mixture of 3, 5 ml) was warmed up (37 °C)and added to the mixture to form complete growth medium. Complete growth medium was always aliquoted and stored at 4°C.

5.1.5 Cell splitting:

T75 flasks with growing cells were taken out of the incubator and checked to see whether the cells were confluent enough to split. If the cells were 90% confluent, then they were ready to split. Firstly, in a laminar flow chamber, the media was removed and the cell were washed with 15 ml of PBS and then 2.5 ml of trypsin-EDTA solution was added then incubated for 5-7 min to allow the cell splitting to takes place. Then cells were observed under a light microscope (20x) to check if they were detached. If needed they were tapped gently to detach from each other. Fresh growth medium (10 ml) was added and the suspension was aspirated using a pasture pipette. For further culturing 2ml of that suspension was taken and added to 20 ml of fresh growth medium in a T75 flask and incubated.

5.1.6 Cell counting:

When the cells were 90% confluent, the medium was removed and the cells were washed with PBS and 2.5 ml of trypsin was added and incubated for further 5-7 min to allow cells to be detached. Then 7.5 ml of fresh growth medium was added and aspirated then centrifuged for 5 min at 1000g to form a cell pellet at the bottom of the centrifuge tube. Without disturbing the cell pellet supernant medium was discarded gently and the cells were re-

suspended with 10 ml of fresh growth medium. For counting purpose, 50 microliters of cell suspension was taken in an Eppendorf tube then an equal volume of trypan blue solution was added to it and mixed. Then this cell suspension was gently run on a haemocytometer using a micropipette and the microscope was focussed to count. Cells in the 4 corners of the haemocytometer are counted and total number of cells was calculated using the formula:

Number of cells = Total no. of cells $x10^4$ / number of squares counted x 2 (dilution factor)

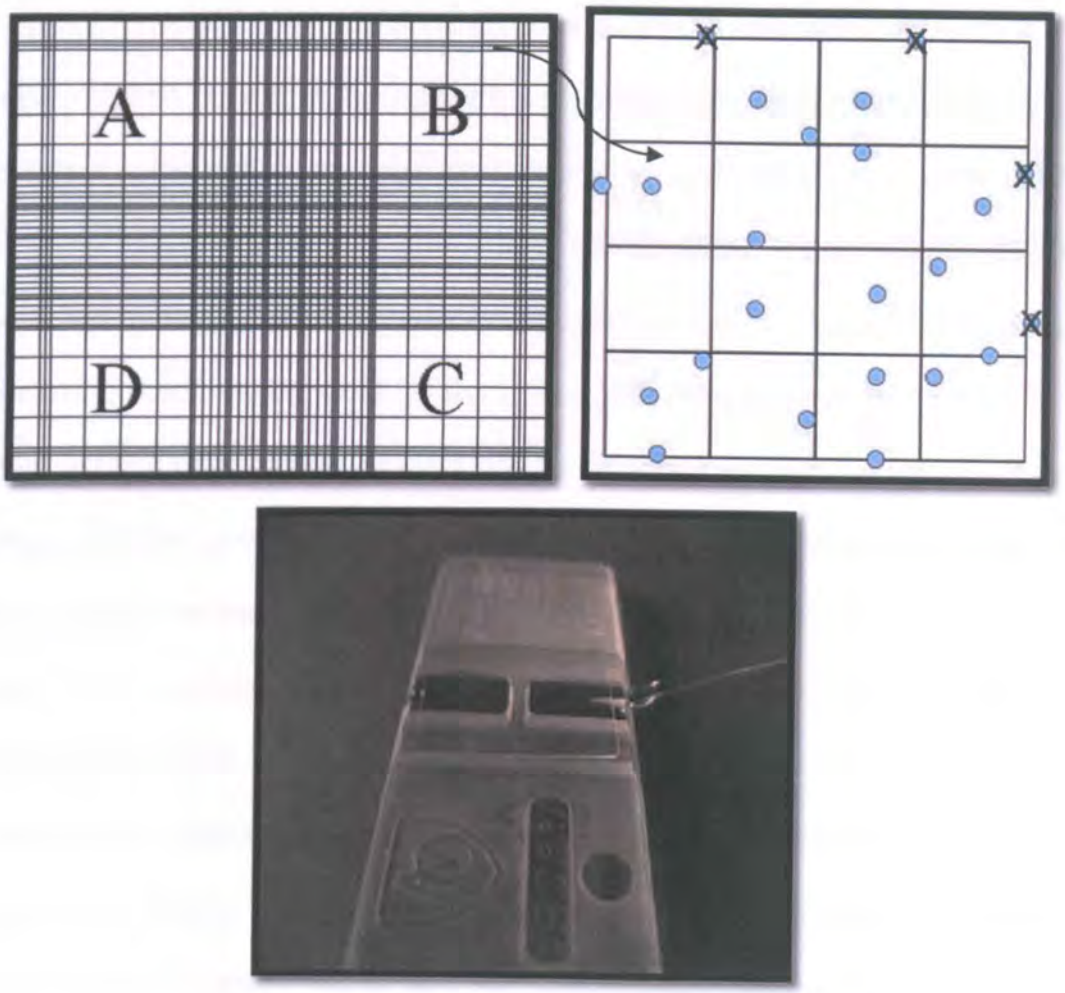

Figure 5.1. Modified: Microscopic and molecular methods for quantitative phytoplankton analysis, UNESCO - 2012

While counting cells in each squares A, B, C and D (figure 5.1), cells on the top and right lines of the square are ignored. Only live cells were visible shiny under the microscope whereas the dead cells were stained deep purple and are visible as a dark matter.

5.1.7 Growth curves

Growth curves were plotted on three cell lines MCF7, A549 and DLD-1 to observe the growth characteristics of the cells.

MTT assay was used to determine the growth of the cell over the course of time. After the treatment with trypsin, a single cell suspension was obtained in growth medium. Then cells were counted using a haemocytometer and the concentration of cells in the medium was calculated. Then, depending on the cell count, the cell suspension was diluted in such a way that wells of the multiwall plate will contain 500, 1000, 2000, 4000, 8000, 16000, 32000, 64000 in a series. While carrying out the dilution it was ensured that the total volume of each well should be the same. 200 Microliters of the growth medium without cells served as blank for the assay. After cell-plating the 96 well plates containing cells were incubated. After 96 hours the medium was removed from the wells using a micropipette and 25 µl of MTT reagent solution was added carefully without disturbing the cell layer this was then incubated for 3 hours. Once formation of purple colour precipitate occurred, 100 µl of DMSO were added to the wells and the plate was gently swirled. Plates were then left in the dark for an hour and were then scanned at 570nm using a plate reader. A graph was plotted with the average of absorbance on the Y-axis and cell count on the X-axis. This was replicated thrice on the same plate in three rows.

5.1.8 Solutions of cryptolepine and its derivatives

DMSO (biological grade) was used to dissolve cryptolepine and its analogues to get a drug solution of 10 mM (stock solution A). 100 µL of stock A was then added to 9.9 ml of growth medium to get a solution with a drug concentration of 100 µM. 1ml of this 100 µM solution was added to 9ml of media to get a solution of 10 µM. By following the previous step, serial dilutions were performed until a concentration of 0.001 was achieved. All of the drug solutions made were stored at -20°C and thawed when needed in the MTT assay experiment, the final concentration of DMSO in the working stocks was not more than 0.1% v/v.

5.1.9 The MTT assay

The first row of the 96 well plates was left unused. The second row was filled with 200µL of blank media which served as blank for the experiment. The rest of the wells were plated with 20,000 cells in each well. Then the plate was incubated for 24 hours.

After the incubation, cells were attached to the bottom surface of the wells so media was carefully removed from all the wells and the first row of the cells were again loaded with fresh media and the 3rd to 7th rows (from columns B, C and D) of the wells were filled with drug solutions (green) with different concentrations ranging 100 µM to 0.001µM and incubated for 96 hours (Figure 5.2).

Wells from Columns E to G rows 3 to 7 were filled with doxorubicin drug solution concentrations ranging from 100 µM to 0.001µM (Figure 5.2) which served as a positive control (red).

2nd row cells were filled with growth media, which served as a control (blue) (Figure 5.2).

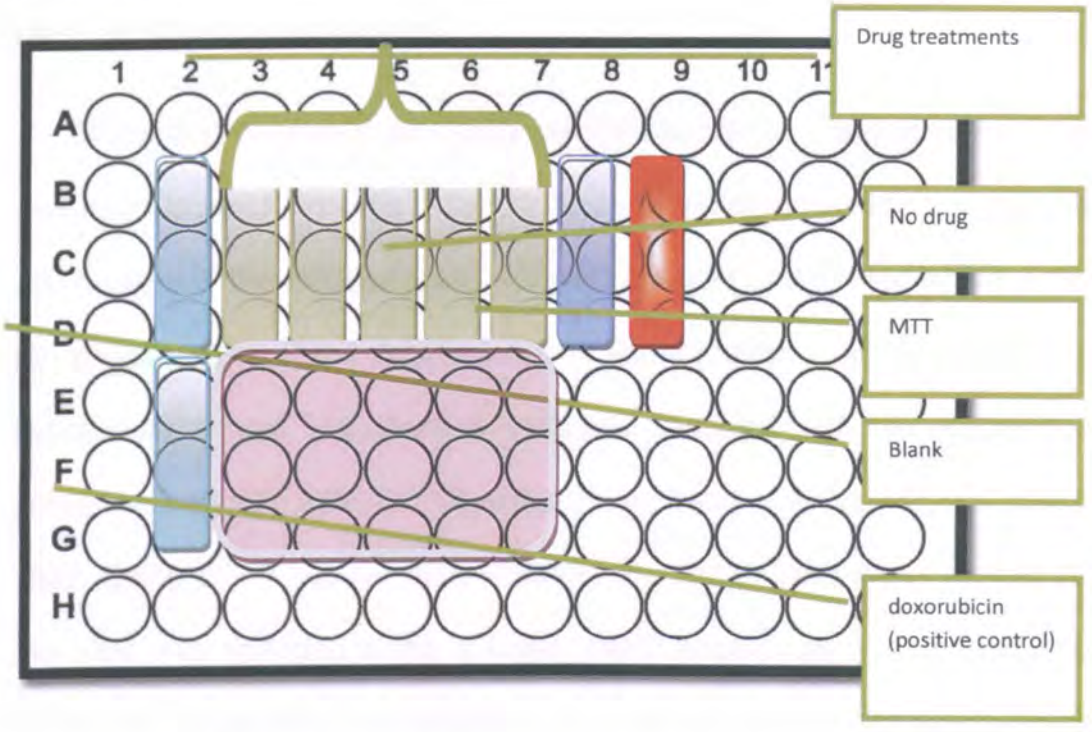

Figure 5.2 Showing the MTT assay design

Then the plate was taken out of the incubator and 50µL of MTT reagent was added to each well carefully and it was again incubated for another 4 hours. After MTT treatment purple colour crystals were observed under the microscope then medium from each well was carefully removed and 100µL of DMSO were added to dissolve the precipitate and the plate was left in the dark for an hour. In the next step plate was put in the UV-VIS plate reader which was prebuilt with auto plate shaker. The plate was gently shaken and then absorbance was read at 570nm.

The obtained raw data was then analysed using MS-Excel (2010) software and the IC50 values were calculated using GraphPad Prism software (ver. 6.0).

5.2 Microscopy

Using BD-Falcon 8 chambered culture slides A549 cells were grown in RPMI medium without any indicator.

A cell seeding density of 4000cells per well was determined as optimum and was used to seed the cells. After 17 hours of incubation camber slides were taken out and the medium was carefully removed and loaded with the desired concentration of the drug solution in RPMI medium then again it was incubated for 1 hour. The chamber slide was removed from the incubator and gently washed with PBS (37°C) and culture chamber was detached from the slide. Using DAPI nuclear stain solution (5 mg/ml), cells were stained then the slide was shielded using a fluoro-shield solution to protect from photo bleaching. A coverslip was placed on the slide ensuring no air bubble formed between the slide and coverslip. Finally the slide-coverslip junction was sealed using nail polish and it was observed under the microscope (40x) for drug localisation in the cells.

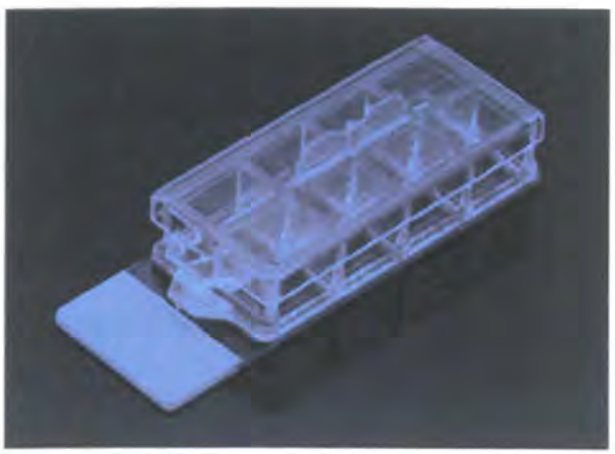

Figure 5.3 Showing a 8 well coated culture plate

Firstly pictures were taken using microscope (40x) under normal light then using fluorescent filters the nuclei of the cells were captured as they glow a blue colour. By changing the filter to green again the whole cells were observed to see the drug localisation. Finally both nuclei and the whole cell images were overlayed using Leica microscopy imaging software.

5.3 Drug uptake studies

Cryptolepine and its derivatives were dissolved in methanol and the solutions were scanned in UV spectrophotometer and the λ-max is recorded. Using these wavelength readings, samples were excited using a fluorescence spectrophotometer to record the emission wavelengths of the samples.

Cells were grown in a 96 well plate for 24 hours in RPMI medium without phenol red indicator at a seeding density of 20,000 cells per well. 7rows of 3 columns (7x3=21 wells) were loaded with cell suspension for incubation. The next day after 24 hours of incubation, media from the first row of the cells was removed and loaded with 100µL of drug solution (solvent = media) with a concentration of 10µM and the plate was placed back in to the incubator. After 30 min. plates was removed from the incubator and the media from the second row was removed and loaded with 100µL of drug solution (10µM). The same procedure was repeated for rest of the rows every half hour leaving the last row with no treatment (blank).

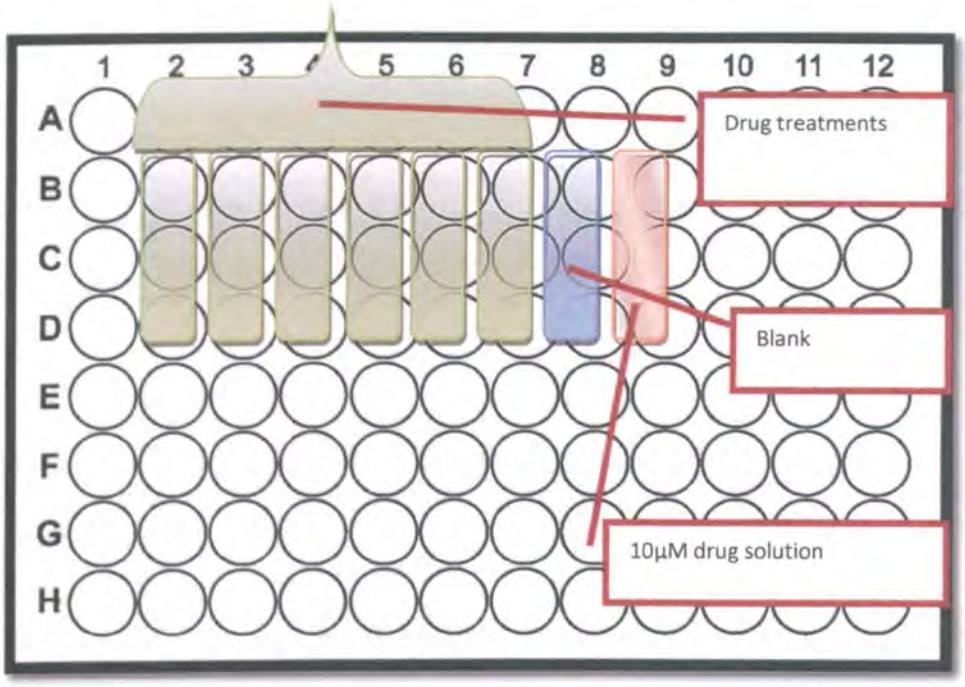

Figure 5.4 drug-uptake study design in a 96 well plate

After the treatments were finished, the drug solution was gently removed from all the wells and 100μL of DMSO was added to the wells and shaken gently for 30 minutes. The empty 8th row wells were filled with 100μL of 10μM drug solution.

Cells were lysed using Tritonx-100 (a non-ionic surfactant which increases the cell permeation) and extracted the drug using methanol. The plate was then scanned using a fluorescence plate reader measuring the intensity of the fluorescence from each well (25 scans for each well). As the 8th was filled with 10μM drug solution, which served as a positive control for the experiment. Using a positive control (100% drug solution) data was analysed and compared to generate the report of percentage drug uploaded in to the cells over the period of three hours.

5.4 Topoisomerase II assay

5.4.1 Materials

A topoisomerase II assay kit was purchased from Topogen, Florida, USA (Topogen, 2005)

5.4.2 Contents of the kit

kDNA, decatenated kDNA marker, Linear kDNA marker, gel loading buffer, protein kinase

BufferA: Mixture of Tris-HCl (pH-8) (0.5M), NaCl (1.50 M), MgCl2 (100 mM), Dithiothreitol (5mM), bovine serum albumin (BSA) (300ug /ml).

Buffer B : 20mM ATP in water

Drugs : Cryptolepine and its analogues

Eppendorf tubes, Micro pipettes and pipette tips, A grade glassware

5.4.3 Agarose gel

0.75 g of agarose was mixed with 75ml of TRIS buffer and microwaved for 3-5 min until all the agarose dissolved in the buffer. Once a clear solution is formed the agarose solution was taken out from the oven and ethidium bromide was added (0.5 µg/ml) to both gel and running buffer. Then the agarose solution was poured on to gel-tray and allowed to solidify at room temperature for an hour.

5.4.4 Running Buffer (TAE buffer)

50x concentration: Tris base (242 g), glacial acetic acid (57.1 ml) and of 0.5 M EDTA (100 ml). Diluted to 1x

5.4.5 Drug solutions

Cryptolepine and its analogues were dissolved in DMSO first and then diluted to get the desired concentration. Serial dilutions were carried out to produce a concentration range of 100 to 0.01μM. It was made sure that the concentration of DMSO in any solution was not more than 0.1% v/v

5.4.6 The topoisomerase II assay

Buffer (2 μl complete reaction buffer = buffer A + buffer B in 1:1 ratio), kDNA (0.25 μg/ml, 1μl), bovine serum albumin (30 μg/ml, 1 μl), distilled water (to make up to 20 μl), drug to be tested in desired concentration (1 μl) were pipetted out to a Eppendorf tube and incubated for 30 minutes at 37 °C

The reaction was then stopped by adding 4μl of stopping buffer and 2 μl of protein kinase. The mixture was then incubated for digestion for 30 minutes.

The reaction products were then loaded on to the ethidiumbromide-agarose gel and electrophoresis was carried out at 65V for 2.5 hours in TAE buffer. After the separation gel was visualised under UV illumination.

5.5 DNA binding studies (Thiozole orange displacement assay)

5.5.1 Materials

Duplex DNA (DS26) and quadruplex DNA (AG23) oligo-nucleotides were purchased from Eurogenetic, Belgium. Fluoremetric titrations were performed on Varian-Cary Eclipse fluorescence spectrometer (scans at 24,000 nm/min, radiation source is Xenon flash lamp with room light immunity) with carry eclipse spectrophotometric software.

5.5.2 Cacodylate Buffer

Sodium cacodylate was purchased from Sigma Aldrich, UK.

Made using 0.2M sodium cacodylate and 0.2M HC1

5.5.3 Ligands

Cryptolepine and its analogues.

Thiozole orange was purchased from sigma Aldrich, UK.

5.5.4 Preparation of Buffer

Cacodylate buffer was made by dissolving sodium cacodylate crystals (42.8 gm) in to distilled water (1L) and the pH was adjusted to 7.3 using aqueous HCl solution (0.2 M).

5.5.5 Preparation of oligonucleotides

5.5.5.1 22AG quadruplex

These G-quadruplexes were made by heating the 22AG nucleotide in the cacodylate buffer (10mM, pH 7.3), 100mM KCl at 90°C for five minutes and then the solution was cooled in ice to form G-quadruplxes by intermolecular folding.

5.5.5.2 DS26 duplex

This duplex nucleotide sequence was made by heating DS26 in the cacodylate buffer (10mM, pH 7.3), 100mM KCl at 90°C for five minutes and then slowly cooling over a period of 6 hours.

Once these DNA solutions were made the concentrations were measured using the UV-VIS spectrophotometer at 260nm using their extinction coefficient values

5.5.6 Fluorometric titarations

5.5.6.1 For DS26

Cacodylate buffer containing 100mM of KCl was used for all the dilutions to get desired concentrations. In a 3ml capacity cuvette 1ml of thiaozole orange solution and 1ml of DS26 solution were pipetted using a micropipette and then the volume was adjusted to 3ml using the blank buffer and the fluorescence was measured using the fluorimetry. This served as a control for the titration.

For the ligand experiments, first 1ml of thiozole orange and 1 ml of DS26 solution were put into a cuvette and then the total concentration of ligand was made 0.375μM adding desired ligand and the volume was made up using the cacodylate buffer. The solution was allowed to equilibrate for 3 min and then the fluorescence intensity was measured.

The same was repeated for each fluorometric titration by increasing the concentration of ligand to 0.75 μM, 1.5 μM, 3.0 μM, 4.5 μM, 7.5 μM in the cell and keeping the total volume of the cell constant 3ml.

5.5.6.2 For AG23

The same procedure was carried out for the G-qudruplex sequence with the only difference being the concentration of thiazole orange used which was compared to DS26. The reason for this is that quadruplex sequence has less number of binding sites compared to duplex sequence of DS26

During the titration, depending up on the activity of the ligand a gradual fall in the fluorescence was seen as the concentration of the ligand increases.

After the experiment for all the concentrations were recorded, using the Carry Eclipse software, the integrals graphs were measured for each ligand concentration was measured. The percentage fall in the fluorescence intensity was measured for each concentration of the ligand and hence the binding efficiency of the ligand was interpreted.

Chapter 6 Conclusions

The purpose of this study was to attach halogens (Cl, Br and I) and alkyl amino sidechains at the 11-position of cryptolepine and then investigate these molecules for anticancer activity using an *in vitro* cytotoxicity assay and biophysical studies including DNA binding assays, topo II assays, fluorescence microscopy and quantitative drug uptake studies.

Amongst all the molecules synthesised, the derivatives with the 11-amino linkages and the 11-halogenated compounds showed greater activity than compounds having the 11-amido side chains.

Overall, the 11-iodo and the 11-butylamino derivative showed the highest activity (Table 6.1 Summary of results). The reason behind the 11-butylamino compound could be because of its lipophilic alkyl sidechain which may have facilitated faster drug-uptake by the cells.

The derivative with the isopropylamino sidechain showed lower activity being less lipophilic than the butylamino compound. Another reason for this could be due to the structural difference between the butyl and isopropylamine. In this context, having a branched alkylamino sidechain at the 11 position reduced the activity significantly compared to a straight chain.

The same was seen in the drug-uptake studies, the intracellular concentration of 11-butylaminocryptolepine reached 40% within first 0.5 hours after drug treatment, then rose up to 60% in 1.5 hours.

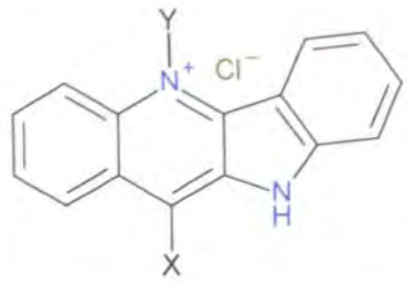		A549 cells IC_{50} values in µM	MCF-7 cells IC_{50} values in µM	DLD-1 cells IC_{50} values in µM	Topo II activity expressed as minimum inhibitory concentration (MIC) in µM	Kd values ± SD	
X	Y					DS26 duplex DNA	AG22 quadruplex DNA
H	CH_3	0.47±0.12	5.90±0.69	1.25±0.77	0.5	1.62 ± 0.62	2.45 ± 0.36
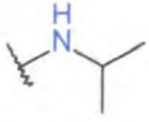	CH_3	20.38±2.01	17.92±2.31	37.05±2.36		2.51 ± 0.33	39.81 ± 5.17
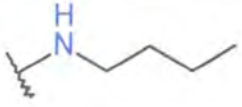	CH_3	1.05±0.15	0.63±0.51	2.85±0.87	0.25	0.79 ± 0.37	5.01 ± 1.85
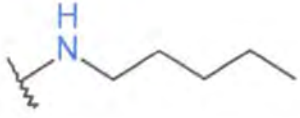	CH_3	0.83 ±0.28	4.253 ± 1.88	2.4±0.96		1.26 ± 0.26	6.31 ± 3.15

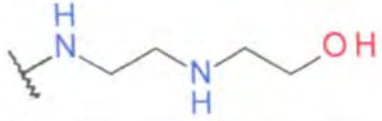	CH_3	10.41±0.75	6.77±2.03	12.23±1.20		2.51 ± 0.58	3.98 ± 1.53
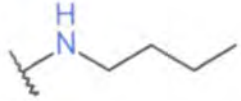	C_2H_5	12.58 ± 2.12	43.59±4.72	26.73±3.92		1.55 ± 0.55	26.92 ± 6.96
Br	CH_3	5.16±1.25	2.15±0.41	3.35±1.62			
I	CH_3	0.28 ± 0.1	0.1±0.02	0.34±0.05		0.10 ± 0.06	0.32 ± 0.10
Cl	CH_3	42.83± 3.74	62.87±2.71	81.58 ±2.61	0.25	0.40 ± 0.20	0.63 ± 0.002
Cl	C_2H_5	15.24± 2.2	21±3.62	31.84±3.86			
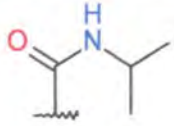	CH_3	42.64 ± 3.17	31.72±2.56	75.01±2.92	>100		
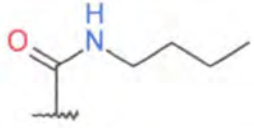	CH_3	21.41±1.76	7.26±1.24	4.14±0.891		2.00 ± 0.74	3.55 ± 1.04
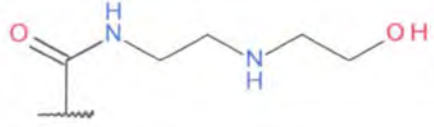	CH_3	12.38±2.16	9.15±1.56	15.21±3.23			

Table 6.1 Summary of results

Whereas the 11-isopropylamino compound gave a poor drug uptake profile with a percentage drug uptake of 8% in 0.5 hours and a maximum drug uptake of 18% seen at 2.5 hours

Topo II results reinforced the link between the cytotoxicity and topo II inhibition. Among the derivatives tested, derivatives with the 11-butylamino sidechain showed the highest topo II activity with a MIC value of 0.25 μM which is twofold higher than the parent compound.

Knowing the lower cytotoxicity of the 11-isopropylamido derivative, topo II assay was performed on this compound, and it gave a MIC value of >100 μM indicating that having a amido-linkage not only did not favoured the cytotoxicity but also reduced the topo II activity compared to the original compound (MIC = 0.5 μM). It may be the structural features of isopropyl sidechain have played a role in this context as well.

Surprisingly, despite its lower cytotoxicity, the 11-chloroderivative (Table 6.1) showed the highest topo II activity with an MIC value of 0.25 μM. When analysing its drug uptake profile, the percentage drug uptake was lower than both the 11-butylamino derivative and cryptolepine, reaching an intracellular concentration of only 25% in the first 30 minutes. In contrast to this despite its lower topo II activity, 11-iodocryptolepine (MIC = 0.5 μM) gave a higher cytotoxicity value compared to the11-chlorocryptolepine (Table 6.1).

Fluorescence microscopic images showed that, though 11-butylaminocryptolepine was dispersed throughout the cell, high concentrations were localised in the nucleus.

Altough this was also observed in 11-chlorocryptolepine, the amount of drug localised in the nucleus is dramatically lower than the 11- butylamino derivative and cryptolepine. This indicates that not only a lower amount of drug is being taken up by the cells but also the drug taken up is not reaching the nucleus effectively.

It is proposed that these molecules are cytotoxic through DNA intercalation and subsequent inhibition of topo II. DNA binding assays were performed to learn further reasons behind the activity of the derivatives.

Overall, the 11-alkylamino derivatives showed greater DNA binding thancryptolepine. Derivatives with the 11-butylamino and pentylamino sidechains showed higher binding constant activity than the 11-isopropylamino compounds, reinforcing the topo II and cytotoxcicity results.

The 11-chloro derivative showed a higher binding than the cryptolepine, further suggesting that pharmacokinetics of this molecule played a role in its lower cytotoxicity and supporting the topo II data.

11-Iodocryptolepine showed the highest DNA binding to both duplex and quadruplex structures, which is reflected by its high cytotoxic activity on all three cell lines.

Overall, in terms of selectivity, cryptolepine analogues preferred duplex DNA over G-quadruplex DNA, perhaps due to selectivity towards GC-rich sequences present in the duplex DNA.

In conclusion, these studies have shown that novel amino and halogenated cryptolepine analogues have greater *in vitro* cytotoxicity than the parent

compound and are important lead compounds in the development of novel potent and selective indoloquinone anti-neoplastic agents.

References

Ajayi, A. F., Akhigbe, R. E., Adewumi, O. M., Okeleji, L. O., Mujaidu, K. B. and Olaleye, S. B. (2012) 'Effect of ethanolic extract of Cryptolepis sanguinolenta stem on in vivo and in vitro glucose absorption and transport: Mechanism of its antidiabetic activity.', *Indian Journal of Endocrinology and Metabolism,* 16 (7), pp. 91-96.

Alberts, D. S., Peng, Y. M., Bowden, G. T., Dalton, W. S. and Mackel, C. (1985) 'Pharmacology of mitoxantrone: mode of action and pharmacokinetics', *Investigational New Drugs,* 3 (2), pp. 101-107.

Anand, P., Nair, H. B., Sung, B., Kunnumakkara, A. B., Yadav, V. R., Tekmal, R. R. and Aggarwal, B. B. (2010) 'Design of curcumin-loaded PLGA nanoparticles formulation with enhanced cellular uptake, and increased bioactivity i*n vitro* and superior bioavailability *in vivo*', *Biochemical Pharmacology,* 79 (3), pp. 330-338.

Anderson, D., Bishop, J. B., Garner, R. C., Ostrosky-Wegman, P. and Selby, P. B. (1995) 'Cyclophosphamide: Review of its mutagenicity for an assessment of potential germ cell risks', *Mutation Research/Fundamental and Molecular Mechanisms of Mutagenesis,* 330 (1–2), pp. 115-181.

Ansah, C., Khan, A. and Gooderham, N. J. (2005) 'In vitro genotoxicity of the West African anti-malarial herbal Cryptolepis sanguinolenta and its major alkaloid cryptolepine', *Toxicology,* 208 (1), pp. 141-147.

Arzel, E., Rocca, P., Grellier, P., Labaeid, M., Frappier, F., Gueritte, F., Gaspard, C., Marsais, F., Godard, A. and Queguiner, G. (2001) 'New synthesis of benzo-delta-carbolines, cryptolepines, and their salts: In vitro cytotoxic, antiplasmodial, and antitrypanosomal activities of delta-caribolines, benzo-delta-carbolines, and cryptolepines', *Journal of Medicinal Chemistry,* 44 (6), pp. 949-960.

Avendaño, C. and Menendez, J. C. (2008) *Medicinal chemistry of anticancer drugs (all chapters).* Elsevier.

AVRAMIS, V. I. (2012) 'Asparaginases: Biochemical Pharmacology and Modes of Drug Resistance', *Anticancer Research,* 32 (7), pp. 2423-2437.

Baguley, B. C. (1991) 'DNA intercalating anti-tumour agents', *Anti-Cancer Drug Design,* 6 (1), pp. 1-35.

Bailly, C. (2012) 'Contemporary challenges in the design of topoisomerase II inhibitors for cancer chemotherapy', *Chemical Reviews,* 112 (7), pp. 3611-3640.

Bailly, C., Laine, W., Baldeyrou, B., De Pauw-Gillet, M. C., Colson, P., Houssier, C., Cimanga, K., Van Miert, S., Vlietinck, A. J. and Pieters, L. (2000) 'DNA intercalation, topoisomerase II inhibition and cytotoxic activity of the plant alkaloid neocryptolepine', *Anti-Cancer Drug Design,* 15 (3), pp. 191-201.

Banerji, J., Lai, T. K., Basak, B., Neuman, A., Prange, T. and Chatterjee, A. (2005) 'A novel route to anticonvulsant imesatins and an approach to cryp-

tolepine, the alkaloid from Cryptolepis Sp.', *Indian Journal of Chemistry Section B-Organic Chemistry Including Medicinal Chemistry,* 44 (2), pp. 426-429.

Baraldi, P. G., Bovero, A., Fruttarolo, F., Preti, D., Tabrizi, M. A., Pavani, M. G. and Romagnoli, R. (2004) 'DNA minor groove binders as potential antitumor and antimicrobial agents', *Medicinal Research Reviews,* 24 (4), pp. 475-528.

Bardy, G. H., Lee, K. L., Mark, D. B., Poole, J. E., Packer, D. L., Boineau, R., Domanski, M., Troutman, C., Anderson, J. and Johnson, G. (2005) 'Amiodarone or an implantable cardioverter–defibrillator for congestive heart failure', *New England Journal of Medicine,* 352 (3), pp. 225-237.

Barth, H., Niemeyer, I. and Lorenz, W. (1973) 'Studies on the mode of action of histamine H1-and H2-receptor antagonists on gastric histamine methyltransferase', *Agents and Actions,* 3 (3), pp. 138-147.

Berger, J., Gamblin, S., Harrison, S. and Wang, J. (1996) 'Structure and mechanism of DNA topoisomerase II', *Nature,* 379 (6562), pp. 225-232.

Berthois, Y., Katzenellenbogen, J. A. and Katzenellenbogen, B. S. (1986) 'Phenol red in tissue culture media is a weak estrogen: implications concerning the study of estrogen-responsive cells in culture', *Proceedings of the National Academy of Sciences of the United States of America,* 83 (8), pp. 2496-2500.

Bierer, D. E. (1997) Cryptolepine analogs with hypoglycemic activity. U.S. Patent No.5,681,958.

Bierer, D. E., Dubenko, L. G., Zhang, P. S., Lu, Q., Imbach, P. A., Garofalo, A. W., Phuan, P. W., Fort, D. M., Litvak, J., Gerber, R. E., Sloan, B., Luo, J., Cooper, R. and Reaven, G. M. (1998) 'Antihyperglycemic activities of cryptolepine analogues: An ethnobotanical lead structure isolated from Cryptolepis sanguinolenta', *Journal of Medicinal Chemistry,* 41 (15), pp. 2754-2764.

Bierer, D. E., Fort, D. M., Dubenko, L. G., Mendez, C. D., Luo, J., Reed, M. J., PeterliRoth, P., Gerber, R. E., Litvak, J., Waldeck, N., Bruening, R. C., Noamesi, B. K., Hector, R. F., Carlson, T. J. and King, S. R. (1997) 'Ethnobotanical-directed discovery of the antihyperglycemic properties of cryptolepine: Its isolation from Cryptolepis sanguinolenta, synthesis, and in vitro and in vivo activities', *Abstracts of Papers of the American Chemical Society,* 213 pp. 131-135.

Bierer, D. E., Fort, D. M., Mendez, C. D., Luo, J., Imbach, P. A., Dubenko, L. G., Jolad, S. D., Gerber, R. E., Litvak, J., Lu, Q., Zhang, P. S., Reed, M. J., Waldeck, N., Bruening, R. C., Noamesi, B. K., Hector, R. F., Carlson, T. J. and King, S. R. (1998) 'Ethnobotanical-directed discovery of the antihyperglycemic properties of cryptolepine: Its isolation from Cryptolepis sanguinolenta, synthesis, and in vitro and in vivo activities', *Journal of Medicinal Chemistry,* 41 (6), pp. 894-901.

Bierer, D. E. (1999) Methods for use of cryptolepine analogs with hypoglycemic activity. U.S. Patent No. 5,925,647.

Blackburn, G. M. (2006) 'DNA and RNA structure', in 'DNA and RNA structure', in *Nucleic acids in chemistry and biology.* Royal Society of Chemistry, pp. 13-72.

Blackburn, E. H. (1991) 'Structure and function of telomeres', *Nature,* 350 (6319), pp. 569-573.

Bojanowski, K., Lelievre, S., Markovits, J., Couprie, J., Jacquemin-Sablon, A. and Larsen, A. K. (1992) 'Suramin is an inhibitor of DNA topoisomerase II in vitro and in Chinese hamster fibrosarcoma cells', *Proceedings of the National Academy of Sciences,* 89 (7), pp. 3025-3029.

Bonjean, K., De Pauw-Gillet, M. C., Defresne, M. P., Colson, P., Houssier, C., Dassonneville, L., Bailly, C., Greimers, R., Wright, C., Quetin-Leclercq, J., Tits, M. and Angenot, L. (1998) 'The DNA intercalating alkaloid cryptolepine interferes with topoisomerase II and inhibits primarily DNA synthesis in B16 melanoma cells', *Biochemistry,* 37 (15), pp. 5136-5146.

Bontenbal, M., Sieuwerts, A. M., Peters, H. A., Van Putten, W. L., Foekens, J. A. and Klijn, J. G. (1998) 'Uptake and distribution of doxorubicin in hormone-manipulated human breast cancer cells in vitro', *Breast Cancer Research and Treatment,* 51 (2), pp. 139-148.

Boye, G. L., Ampofo, O. (1983) 'Clinical uses of C. sanguinolenta. In: Proceedings of the First International Seminar on Cryp- tolepine,', (University of Science and Technology, Kumasi, Ghana,), pp. 37–40.

Brookes, P. and Lawley, P. D. (1961) 'The reaction of mono- and difunctional alkylating agents with nucleic acids.', *Biochemical Journal,* 80 (3), pp. 496-503.

Brookes, P. and Lawley, P. D. (1964) 'Alkylating Agents.', *British Medical Bulletin,* 20 (2), pp. 91-95.

Burden, D. A. and Osheroff, N. (1998) 'Mechanism of action of eukaryotic topoisomerase II and drugs targeted to the enzyme', *Biochimica Et Biophysica Acta (BBA)-Gene Structure and Expression,* 1400 (1), pp. 139-154.

Burger, A. M., Jenkins, T. C., Double, J. A. and Bibby, M. C. (1999) 'Cellular uptake, cytotoxicity and DNA-binding studies of the novel imidazoacridinone antineoplastic agent C1311', *British Journal of Cancer,* 81 (2), pp. 367-375.

Capizzi, R., Bertino, J. and Handschumacher, R. (1970) 'L-asparaginase', *Annual Review of Medicine,* 21 (1), pp. 433-444.

Cancer Research UK statistical reports, "Cancer in the UK: December, 2011"; internet <http://info.cancerresearchuk.org/prod_consump/groups/cr_common/@nre/@sta/documents/generalcontent/018070.pdf > (accessed on 17-jan-2013)

Chaires, J. B. (2005) 'Competition dialysis: an assay to measure the structural selectivity of drug-nucleic acid interactions', *Current Medicinal Chemistry-Anti-Cancer Agents,* 5 (4), pp. 339-352.

Champoux, J. J. (2001) 'DNA topoisomerases: structure, function, and mechanism', *Annual Review of Biochemistry,* 70 (1), pp. 369-413.

Chang, M., Takeuchi, Y., hashigaki, K. and null. (1992) 'Molecular modification and structure-activity relationship of antitumor active indoloquinoline derivatives', *Journal of Pharmacobio-Dynamics,* 15 (7), pp. Section-92.

Cheng, M. H., Yang, Y. C., Wong, Y. H., Chen, T. R., Lee, C. Y., Yang, C. C., Chen, S. H., Yang, I. N., Yang, Y. S., Huang, H. S., Yang, C. Y., Huang, M.

S. and Chiu, H. F. (2012) 'B1, a novel topoisomerase II inhibitor, induces apoptosis and cell cycle G1 arrest in lung adenocarcinoma A549 cells', *Anti-Cancer Drugs,* 23 (2), pp. 191-199.

Chhikara, B. S., Mandal, D. and Parang, K. (2012) 'Synthesis, anticancer activities, and cellular uptake studies of lipophilic derivatives of doxorubicin succinate', *Journal of Medicinal Chemistry,* 55 (4), pp. 1500-1510.

Chhikara, B. S., St. Jean, N., Mandal, D., Kumar, A. and Parang, K. (2011) 'Fatty acyl amide derivatives of doxorubicin: Synthesis and in vitro anticancer activities', *European Journal of Medicinal Chemistry,* 46 (6), pp. 2037-2042.

Cimanga, K., De Bruyne, T., Pieters, L., Totte, J., Tona, L., Kambu, K., Vanden Berghe, D. and Vlietinck, A. J. (1998) 'Antibacterial and antifungal activities of neocryptolepine, biscryptolepine and cryptoquindoline, alkaloids isolated from Cryptolepis sanguinolenta', *Phytomedicine,* 5 (3), pp. 209-214.

Cimanga, K., DeBruyne, T., Lasure, A., VanPoel, B., Pieters, L., Claeys, M., VandenBerghe, D., Kambu, K., Tona, L. and Vlietinck, A. J. (1996) 'In vitro biological activities of alkaloids from Cryptolepis sanguinolenta', *Planta Medica,* 62 (1), pp. 22-27.

Cimanga, K., DeBruyne, T., Pieters, L. and Vlietinck, A. J. (1997) 'In vitro and in vivo antiplasmodial activity of cryptolepine and related alkaloids from Cryptolepis sanguinolenta', *Journal of Natural Products,* 60 (7), pp. 688-691.

Clifford, B., Beljin, M., Stark, G. R. and Taylor, W. R. (2003) 'G2 arrest in response to topoisomerase II inhibitors: the role of p53', *Cancer Research,* 63 (14), pp. 4074-4081.

Comba, P. and Boeyens, J. C. A.(2010) 'On stacking, Structure and Function', in 'On stacking, Structure and Function', in *Structure and Function.* Springer, pp. 177-196.

Cooper, M. M., Lovell, J. M. and Joule, J. A. (1996a) 'Indole-β-nucleophilic substitution. Part 9 nitrogen nucleophiles. Syntheses of hydroxycryptolepine, cryptolepine, and quindoline', *Tetrahedron Letters,* 37 (24), pp. 4283-4286.

da Rocha, A. B., Lopes, R. M. and Schwartsmann, G. (2001) 'Natural products in anticancer therapy', *Current Opinion in Pharmacology,* 1 (4), pp. 364-369.

Dassonneville, L., Lansiaux, A., Wattelet, A., Wattez, N., Mahieu, C., Van Miert, S., Pieters, L. and Bailly, C. (2000) 'Cytotoxicity and cell cycle effects of the plant alkaloids cryptolepine and neocryptolepine: relation to drug-induced apoptosis', *European Journal of Pharmacology,* 409 (1), pp. 9-18.

Dassonneville, L., Bonjean, K., De Pauw-Gillet, M. C., Colson, P., Houssier, C., Quetin-Leclercq, J., Angenot, L. and Bailly, C. (1999) 'Stimulation of topoisomerase II-mediated DNA cleavage by three DNA-intercalating plant alkaloids: Cryptolepine, matadine, and serpentine', *Biochemistry,* 38 (24), pp. 7719-7726.

Dassonneville, L., Lansiaux, A., Wattelet, A., Wattez, N., Mahieu, C., Van Miert, S., Pieters, L. and Bailly, C. (2000) 'Cytotoxicity and cell cycle effects of the plant alkaloids cryptolepine and neocryptolepine: relation to drug-induced apoptosis', *European Journal of Pharmacology,* 409 (1), pp. 9-18.

De Cian, A., Guittat, L., Kaiser, M., Saccà, B., Amrane, S., Bourdoncle, A., Alberti, P., Teulade-Fichou, M., Lacroix, L. and Mergny, J. (2007) 'Fluorescence-based melting assays for studying quadruplex ligands', *Methods,* 42 (2), pp. 183-195.

Decker, T. and Lohmann-Matthes, M. (1988) 'A quick and simple method for the quantitation of lactate dehydrogenase release in measurements of cellular cytotoxicity and tumor necrosis factor (TNF) activity', *Journal of Immunological Methods,* 115 (1), pp. 61-69.

Desai, P. B. (1973) 'Preparation and stability of 4-fluoropyridine', *Journal of the Chemical Society, Perkin Transactions 1,* (0), pp. 1865-1866.

Dexter, D. L., Barbosa, J. A. and Calabresi, P. (1979) 'N, N-dimethylformamide-induced alteration of cell culture characteristics and loss of tumorigenicity in cultured human colon carcinoma cells', *Cancer Research,* 39 (3), pp. 1020-1025.

Dubenko, L. G., Gerber, R. E., Litvak, J., Peterli-Roth, P., Sloan, B., Waldeck, N., Luo, J., Reed, M. J. and Bierer, D. E. (1997) 'Antihyperglycemic activities of cryptolepine analogues: An ethnobotanical lead structure isolated from Cryptolepis', *Abstracts of Papers American Chemical Society,* 213 (1-3), pp. 132-MEDI 132.

Eastman, A. (1990) 'Activation of programmed cell death by anticancer agents: cisplatin as a model system.', *Cancer Cells (Cold Spring Harbor, NY: 1989),* 2 (8-9), pp. 275-280.

Elford, H. L., Wampler, G. L. and van't Riet, B. (1979) 'New ribonucleotide reductase inhibitors with antineoplastic activity', *Cancer Research,* 39 (3), pp. 844-851.

Erdelyi, M. (2012) 'Halogen bonding in solution', *Chemical Society Reviews,* 41 (9), pp. 3547-3557.

Eriksson, S., Kim, S. K., Kubista, M. and Norden, B. (1993) 'Binding of 4', 6-diamidino-2-phenylindole (DAPI) to AT regions of DNA: evidence for an allosteric conformational change', *Biochemistry,* 32 (12), pp. 2987-2998.

Fabry, W., Okemo, P. O. and Ansorg, R. (1998) 'Antibacterial activity of East African medicinal plants', *Journal of Ethnopharmacology,* 60 (1), pp. 79-84.

Falk, S. (2006) 'Principles of cancer treatment by radiotherapy', *Surgery (Oxford),* 24 (2), pp. 62-65.

Fan, P. and Ablordeppey, S. Y. (1997) 'An alternative synthesis of 10H-indolo[3,2-b]quinoline and its selective N-alkylation', *Journal of Heterocyclic Chemistry,* 34 (6), pp. 1789-1794.

Fang Bin, Tao Haisheng, Kan Xianwen and Shang Yongjia (2011) Selective electrochemical synthesis of 4-fluoropyridine using ET_3N-3HF. 10305-306.

Fedier, A. and Fink, D. (2004) 'Mutations in DNA mismatch repair genes: implications for DNA damage signaling and drug sensitivity (review).', *International Journal of Oncology,* 24 (4), pp. 1039-1047.

Fichter, F. and Boehringer, R. (1906) 'Ueber chindolin', *Berichte Der Deutschen Chemischen Gesellschaft,* 39 (4), pp. 3932-3942.

Fichter, F. and Rohner, F. (1910) 'Über einige derivate des chindolins', *Berichte Der Deutschen Chemischen Gesellschaft,* 43 (3), pp. 3489-3499.

Fortune, J. M. and Osheroff, N. (1998) 'Merbarone inhibits the catalytic activity of human topoisomerase IIa by blocking DNA cleavage', *Journal of Biological Chemistry,* 273 (28), pp. 17643-17650.

Foye, W. O., Lemke, T. L. and Williams, D. A.(2008) 'Foye's principles of medicinal chemistry (cancer and chemotherapy section)', in 'Foye's principles of medicinal chemistry (cancer and chemotherapy section)', in Lippincott Williams & Wilkins, pp. 1147-1191.

Fraga, H., Fernandes, D., Novotny, J., Fontes, R. and Esteves da Silva, Joaquim CG (2006) 'Firefly luciferase produces hydrogen peroxide as a coproduct in dehydroluciferyl adenylate formation', *ChemBioChem,* 7 (6), pp. 929-935.

Gascoigne, K. E. and Taylor, S. S. (2009) 'How do anti-mitotic drugs kill cancer cells?', *Journal of Cell Science,* 122 (Pt 15), pp. 2579-2585.

Gaucher, G., Marchessault, R. H. and Leroux, J. (2010) 'Polyester-based micelles and nanoparticles for the parenteral delivery of taxanes', *Journal of Controlled Release,* 143 (1), pp. 2-12.

Gelotte, K. O., Mason, D. N. and Meckler, H. (1990) 'An effective synthesis of the novel triazoloquinazoline adenosine antagonist', 27 pp. 1549-1552.

Genestier, L., Paillot, R., Quemeneur, L., Izeradjene, K. and Revillard, J. (2000) 'Mechanisms of action of methotrexate', *Immunopharmacology,* 47 (2–3), pp. 247-257.

Ghoshal, K. and Jacob, S. T. (1997) 'An alternative molecular mechanism of action of 5-fluorouracil, a potent anticancer drug', *Biochemical Pharmacology,* 53 (11), pp. 1569-1575.

Giard, D. J., Aaronson, S. A., Todaro, G. J., Arnstein, P., Kersey, J. H., Dosik, H. and Parks, W. P. (1973) 'In vitro cultivation of human tumors: establishment of cell lines derived from a series of solid tumors', *Journal of the National Cancer Institute,* 51 (5), pp. 1417-1423.

Gokcek, Y., Pollet, P. L., Wright, C. W. and Brown, J. E. (2000) 'In-vitro cytotoxicity and thermodenaturation studies for cryptolepine and analogues', *Journal of Pharmacy and Pharmacology,* 52 (Supplement), pp. 109-109.

Gong, Y., Firestone, G. L. and Bjeldanes, L. F. (2006) '3,3'-diindolylmethane is a novel topoisomerase IIalpha catalytic inhibitor that induces S-phase retardation and mitotic delay in human hepatoma HepG2 cells', *Molecular Pharmacology,* 69 (4), pp. 1320-1327.

Gormley, N. A., Orphanides, G., Meyer, A., Cullis, P. M. and Maxwell, A. (1996) 'The interaction of coumarin antibiotics with fragments of the DNA gyrase B protein', *Biochemistry,* 35 (15), pp. 5083-5092.

Goss, P. E. and Strasser, K. (2001) 'Aromatase inhibitors in the treatment and prevention of breast cancer', *Journal of Clinical Oncology,* 19 (3), pp. 881-894.

Gouni, S. R., Carrington, S. and Wright, C. W. (2006) 'Synthesis of novel halogenated cryptolepine analogues', *Journal of Heterocyclic Chemistry,* 43 (1), pp. 171-175.

Graves, D. E. and Velea, L. M. (2000) 'Intercalative binding of small molecules to nucleic acids', *Current Organic Chemistry,* 4 (9), pp. 915-929.

Gresh, N. and Kahn, P. H. (1990) 'Theoretical design of novel, 4 base pair selective derivatives of mitoxantrone', *Journal of Biomolecular Structure and Dynamics,* 7 (5), pp. 1141-1160.

Guittat, L., Alberti, P., Rosu, F., Van Miert, S., Thetiot, E., Pieters, L., Gabelica, V., De Pauw, E., Ottaviani, A., Riou, J. F. and Mergny, J. L. (2003a) 'Interactions of cryptolepine and neocryptolepine with unusual DNA structures', *Biochimie,* 85 (5), pp. 535-547.

Guittat, L., Alberti, P., Rosu, F., Van Miert, S., Thetiot, E., Pieters, L., Gabelica, V., De Pauw, E., Ottaviani, A., Riou, J. and Mergny, J. (2003b) 'Interactions of cryptolepine and neocryptolepine with unusual DNA structures', *Biochimie,* 85 (5), pp. 535-547.

Hagmann, W. K. (2008) 'The many roles for fluorine in medicinal chemistry', *Journal of Medicinal Chemistry,* 51 (15), pp. 4359-4369.

Halpern, R. M., Halpern, B. C., Clark, B. R., Ashe, H., Hardy, D. N., Jenkinson, P. Y., Chou, S. and Smith, R. A. (1975) 'New approach to antifolate treatment of certain cancers as demonstrated in tissue culture', *Proceedings of the National Academy of Sciences,* 72 (10), pp. 4018-4022.

Hamilton, P. L. and Arya, D. P. (2012) 'Natural product DNA major groove binders', *Natural Product Reports,* 29 (2), pp. 134-143.

Hande, K. R. (1998) 'Clinical applications of anticancer drugs targeted to topoisomerase II', *Biochimica Et Biophysica Acta (BBA)-Gene Structure and Expression,* 1400 (1), pp. 173-184.

Hawley, R. C., Kiessling, L. L. and Schreiber, S. L. (1989) 'Model of the interactions of calichemicin gamma 1 with a DNA fragment from pBR322', *Proceedings of the National Academy of Sciences of the United States of America,* 86 (4), pp. 1105-1109.

Hazra, S., Ghosh, S., Debnath, S., Seville, S., Prajapati, V. K., Wright, C. W., Sundar, S. and Hazra, B. (2012) 'Antileishmanial activity of cryptolepine analogues and apoptotic effects of 2,7-dibromocryptolepine against Leishmania donovani promastigotes', *Parasitology Research,* 111 (1), pp. 195-203.

Henderson, B. E. and Feigelson, H. S. (2000) 'Hormonal carcinogenesis', *Carcinogenesis,* 21 (3), pp. 427-433.

Hoffman, R. M. (1991) 'In vitro sensitivity assays in cancer: a review, analysis, and prognosis', *Journal of Clinical Laboratory Analysis,* 5 (2), pp. 133-143.

Holt, S. J. and Petrow, V. (1947) '111. Carbazoles, carbolines, and related compounds. Part I. Quindoline derivatives', *Journal of the Chemical Society (Resumed),* pp. 607-611.

Hopkins Jr, H. P. (1997) 'Calorimetric Techniques for Studying Drug–DNA Interactions', in 'Calorimetric Techniques for Studying Drug–DNA Interactions', in *Drug-DNA Interaction Protocols*. Springer, pp. 259-268.

Horwitz, K. B., Costlow, M. E. and McGuire, W. L. (1975) 'MCF-7: A human breast cancer cell line with estrogen, androgen, progesterone, and glucocorticoid receptors', *Steroids,* 26 (6), pp. 785-795.

Horwitz, S. B., Cohen, D., Rao, S., Ringel, I., Shen, H. J. and Yang, C. P. (1993) 'Taxol: mechanisms of action and resistance', *Journal of the National Cancer Institute.Monographs,* (15) (15), pp. 55-61.

Horwitz, S. B. and Horwitz, M. S. (1973) 'Effects of camptothecin on the breakage and repair of DNA during the cell cycle', *Cancer Research,* 33 (11), pp. 2834-2836.

Howerton, S. B., Nagpal, A. and Dean Williams, L. (2003) 'Surprising roles of electrostatic interactions in DNA?ligand complexes', *Biopolymers,* 69 (1), pp. 87-99.

Hsiang, Y. H., Lihou, M. G. and Liu, L. F. (1989) 'Arrest of replication forks by drug-stabilized topoisomerase I-DNA cleavable complexes as a mechanism of cell killing by camptothecin', *Cancer Research,* 49 (18), pp. 5077-5082.

Huang, K. C., Gao, H., Yamasaki, E. F., Grabowski, D. R., Liu, S., Shen, L. L., Chan, K. K., Ganapathi, R. and Snapka, R. M. (2001) 'Topoisomerase II poisoning by ICRF-193', *The Journal of Biological Chemistry,* 276 (48), pp. 44488-44494.

Hubbard, R. D. and Fidanze, S.(2007) '7.06 - Alkylating and Platinum Anti-tumor Compounds', in Editors-in-Chief: John B. Taylor &David J. Triggle (eds.) *Comprehensive Medicinal Chemistry II.* Oxford: Elsevier, pp. 129-148.

Jain, A. and Jain, S. K. (2008) 'In vitro and cell uptake studies for targeting of ligand anchored nanoparticles for colon tumors', *European Journal of Pharmaceutical Sciences,* 35 (5), pp. 404-416.

Jansen, B. A., Wielaard, P., Kalayda, G. V., Ferrari, M., Molenaar, C., Tanke, H. J., Brouwer, J. and Reedijk, J. (2004) 'Dinuclear platinum complexes with N, N'-bis (aminoalkyl)-1, 4-diaminoanthraquinones as linking ligands. Part I. Synthesis, cytotoxicity, and cellular studies in A2780 human ovarian carcinoma cells', *JBIC Journal of Biological Inorganic Chemistry,* 9 (4), pp. 403-413.

Jaskelioff, M., Muller, F. L., Paik, J., Thomas, E., Jiang, S., Adams, A. C., Sahin, E., Kost-Alimova, M., Protopopov, A. and Cadinanos, J. (2010) 'Telomerase reactivation reverses tissue degeneration in aged telomerase-deficient mice', *Nature,* 469 (7328), pp. 102-106.

Jerrum, P., Wright, C. W., Jewell, A., Brown, J. E. and Carrington, S. (2007) 'Synthesis and topoisomerase II activity of halogenated cryptolepine analogues', *Journal of Pharmacy and Pharmacology,* 59 pp. A2-A3.

Jerrum, P. W., Wright, C. W., Phillips, R. M., Gouni, S. R., Brown, J. E. and Carrington, S. (2006) 'Synthesis and in vitro cytotoxicity evaluation of novel iodocryptolepine analogues', *Journal of Pharmacy and Pharmacology,* 58 pp. A59-A59.

Jibodh, R. A., Lagas, J. S., Nuijen, B., Beijnen, J. H. and Schellens, J. H. M. (2013) 'Taxanes: Old drugs, new oral formulations', *European Journal of Pharmacology,* 717 (1), pp. 40-46.

Jordan, M. A. and Wilson, L. (2004) 'Microtubules as a target for anticancer drugs', *Nature Reviews Cancer,* 4 (4), pp. 253-265.

Jung, J., Park, S., Chung, H. K., Kang, H., Lee, S., Seo, M. H., Park, H. J., Song, S. Y., Jeong, S. and Choi, E. K. (2012) 'Polymeric Nanoparticles Containing Taxanes Enhance Chemoradiotherapeutic Efficacy in Non-small Cell Lung Cancer', *International Journal of Radiation Oncology*Biology*Physics,* 84 (1), pp. e77-e83.

Juskowiak, B. (2006) 'Analytical potential of the quadruplex DNA-based FRET probes', *Analytica Chimica Acta,* 568 (1), pp. 171-180.

Kaou, A. M., Mahiou-Leddet, V., Hutter, S., Aïnouddine, S., Hassani, S., Yahaya, I., Azas, N. and Ollivier, E. (2008) 'Antimalarial activity of crude extracts from nine African medicinal plants', *Journal of Ethnopharmacology,* 116 (1), pp. 74-83.

Kellner, U., Sehested, M., Jensen, P. B., Gieseler, F. and Rudolph, P. (2002) 'Culprit and victim - DNA topoisomerase II', *Lancet Oncology,* 3 (4), pp. 235-243.

King, A. T. and Primrose, J. (2003) 'Principles of cancer treatment by surgery', *Surgery (Oxford),* 21 (11), pp. 284-288.

Kobayashi, N., Muranaka, A. and Mack, J.(2012) 'Circular dichroism and magnetic circular dichroism spectroscopy for organic chemists (Circular dichroism of biomolecules section)', in 'Circular dichroism and magnetic circular dichroism spectroscopy for organic chemists (Circular dichroism of biomolecules section)', in Royal Society of Chemistry, pp. 142-149.

Kolonel, L. N., Altshuler, D. and Henderson, B. E. (2004) 'The multiethnic cohort study: exploring genes, lifestyle and cancer risk', *Nature Reviews Cancer,* 4 (7), pp. 519-527.

Korzeniewski, C. and Callewaert, D. M. (1983) 'An enzyme-release assay for natural cytotoxicity', *Journal of Immunological Methods,* 64 (3), pp. 313-320.

Kunwar, A., Barik, A., Mishra, B., Rathinasamy, K., Pandey, R. and Priyadarsini, K. I. (2008) 'Quantitative cellular uptake, localization and cytotoxicity of curcumin in normal and tumor cells', *Biochimica Et Biophysica Acta (BBA) - General Subjects,* 1780 (4), pp. 673-679.

Lai, T. K., Chatterjee, A., Banerji, J., Sarkar, D. and Chattopadhyay, N. (2008a) 'A Concise Synthesis of the DNA-Intercalating and Antimalarial Alkaloid Cryptolepine and Its Fluorescence Behaviour in Solvents of Different Polarities', *Helvetica Chimica Acta,* 91 (10), pp. 1975-1983.

Lai, T. K., Chatterjee, A., Banerji, J., Sarkar, D. and Chattopadhyay, N. (2008b) 'A Concise Synthesis of the DNA-Intercalating and Antimalarial Alkaloid Cryptolepine and Its Fluorescence Behaviour in Solvents of Different Polarities', *Helvetica Chimica Acta,* 91 (10), pp. 1975-1983.

Larsen, A. K., Escargueil, A. E. and Skladanowski, A. (2003) 'Catalytic topoisomerase II inhibitors in cancer therapy', *Pharmacology & Therapeutics,* 99 (2), pp. 167-181.

Laryea, D., Isaksson, A., Wright, C. W., Larsson, R. and Nygren, P. (2009) 'Characterization of the cytotoxic activity of the indoloquinoline alkaloid cryptolepine in human tumour cell lines and primary cultures of tumour cells from patients', *Investigational New Drugs,* 27 (5), pp. 402-411.

Lavrado, J., Paulo, A., Gut, J., Rosenthal, P. J. and Moreira, R. (2008a) 'Cryptolepine analogues containing basic aminoalkyl side-chains at C-11: Synthesis, antiplasmodial activity, and cytotoxicity', *Bioorganic & Medicinal Chemistry Letters,* 18 (4), pp. 1378-1381.

Lavrado, J., Reszka, A. P., Moreira, R., Neidle, S. and Paulo, A. (2010a) 'C-11 diamino cryptolepine derivatives NSC748392, NSC748393 and NSC748394: Anticancer profile and G-quadruplex stabilization', *Bioorganic & Medicinal Chemistry Letters,* 20 (23), pp. 7042-7045.

LePage, G. A. (1977) 'Purine Antagonists', in Becker, F. (ed.) Springer US, pp. 309-326.

Lerman, L. (1961) 'Structural considerations in the interaction of DNA and acridines', *Journal of Molecular Biology,* 3 (1), pp. 18-30.

Levenson, A. S. and Jordan, V. C. (1997) 'MCF-7: the first hormone-responsive breast cancer cell line', *Cancer Research,* 57 (15), pp. 3071-3078.

Li, T., Zeng, Z., Estevez, V. A., Baldenius, K. U., Nicolaou, K. and Joyce, G. F. (1994) 'Carbohydrate-Minor Groove Interactions in the Binding of Calicheamicin. gamma. 1I to Duplex DNA', *Journal of the American Chemical Society,* 116 (9), pp. 3709-3715.

Li, L. H., Fraser, T. J., Olin, E. J. and Bhuyan, B. K. (1972) 'Action of camptothecin on mammalian cells in culture', *Cancer Research,* 32 (12), pp. 2643-2650.

Lindsley, J. E. and Wang, J. C. (1991) 'Proteolysis patterns of epitopically labeled yeast DNA topoisomerase II suggest an allosteric transition in the enzyme induced by ATP binding', *Proceedings of the National Academy of Sciences of the United States of America,* 88 (23), pp. 10485-10489.

Lisgarten, J. N., Coll, M., Portugal, J., Wright, C. W. and Aymami, J. (2002a) 'The antimalarial and cytotoxic drug cryptolepine intercalates into DNA at cytosine-cytosine sites', *Nature Structural Biology,* 9 (1), pp. 57-60.

Lisgarten, J. N., Coll, M., Portugal, J., Wright, C. W. and Aymami, J. (2002b) 'The antimalarial and cytotoxic drug cryptolepine intercalates into DNA at cytosine-cytosine sites', 9 (1), pp. 57-60.

Longley, D. B., Harkin, D. P. and Johnston, P. G. (2003) '5-fluorouracil: mechanisms of action and clinical strategies', *Nature Reviews Cancer,* 3 (5), pp. 330-338.

Louie, A. C. and Issell, B. F. (1985) 'Amsacrine (AMSA)--a clinical review', *Journal of Clinical Oncology : Official Journal of the American Society of Clinical Oncology,* 3 (4), pp. 562-592.

Louvet, C., André, T., Lledo, G., Hammel, P., Bleiberg, H., Bouleuc, C., Gamelin, E., Flesch, M., Cvitkovic, E. and de Gramont, A. (2002) 'Gemcitabine combined with oxaliplatin in advanced pancreatic adenocarcinoma: final results of a GERCOR multicenter phase II study', *Journal of Clinical Oncology,* 20 (6), pp. 1512-1518.

Lu, W., Ding, J., Gao, H., Lin, L. and Chen, Y. (2014) Camptothecin derivatives and their use. U.S. Patent No. 8,685,997.

Luniewski, W., Wietrzyk, J., Godlewska, J., Switalska, M., Piskozub, M., Peczynska-Czoch, W. and Kaczmarek, L. (2012) 'New derivatives of 11-methyl-6-[2-(dimethylamino)ethyl]-6H-indolo[2,3-b]quinoline as cytotoxic DNA topoisomerase II inhibitors', *Bioorganic & Medicinal Chemistry Letters,* 22 (19), pp. 6103-6107.

Lv, J., Guo, N., Wen, S., Teng, Y., Ma, M. and Yu, P. (2013) 'Synthesis and antitumor activity evaluation of a novel series of camptothecin analogs', *Journal of Asian Natural Products Research,* 15 (8), pp. 867-874.

Maccari, L., Manetti, F., Corelli, F. and Botta, M. (2003) '3D QSAR studies for the β-tubulin binding site of microtubule-stabilizing anticancer agents (MSAAs): A pseudoreceptor model for taxanes based on the experimental structure of tubulin', *Il Farmaco,* 58 (9), pp. 659-668.

Maguire, C. A., Deliolanis, N. C., Pike, L., Niers, J. M., Tjon-Kon-Fat, L., Sena-Esteves, M. and Tannous, B. A. (2009) 'Gaussia luciferase variant for high-throughput functional screening applications', *Analytical Chemistry,* 81 (16), pp. 7102-7106.

Mardenborough, L. G., Zhu, X. Y., Fan, P. C., Jacob, M. R., Khan, S. I., Walker, L. A. and Ablordeppey, S. Y. (2005) 'Identification of bis-quindolines as new antiinfective agents', *Bioorganic & Medicinal Chemistry,* 13 (12), pp. 3955-3963.

Marini, J. C., Miller, K. G. and Englund, P. T. (1980) 'Decatenation of kinetoplast DNA by topoisomerases', *The Journal of Biological Chemistry,* 255 (11), pp. 4976-4979.

Martinez, R. and Chacon-Garcia, L. (2005) 'The search of DNA-intercalators as antitumoral drugs: what it worked and what did not work', *Current Medicinal Chemistry,* 12 (2), pp. 127-151.

Matsui, T., Sowa, Y., Murata, H., Takagi, K., Nakanishi, R., Aoki, S., Yoshikawa, M., Kobayashi, M., Sakabe, T., Kubo, T. and Sakai, T. (2007) 'The plant alkaloid cryptolepine induces p21(WAF1/C1P1) and cell cycle arrest in a human osteosarcoma cell line', *International Journal of Oncology,* 31 (4), pp. 915-922.

McCurrie, J., Albalawi, S., Wright, C. and Kuntworbe, N. (2009) 'Investigation of the absorption and vascular effects of the indoloquinoline alkaloid, cryptolepine', *Journal of Pharmacy and Pharmacology,* 61 pp. A67-A68.

McGrogan, B. T., Gilmartin, B., Carney, D. N. and McCann, A. (2008) 'Taxanes, microtubules and chemoresistant breast cancer', *Biochimica Et Biophysica Acta (BBA) - Reviews on Cancer,* 1785 (2), pp. 96-132.

Mergny, J. and Maurizot, J. (2001) 'Fluorescence resonance energy transfer as a probe for G-quartet formation by a telomeric repeat', *ChemBioChem,* 2 (2), pp. 124-132.

Mergny, J. -., Riou, J. -., Mailliet, P., Teulade-Fichou, M. -. and Gilson, E. (2002) 'Natural and pharmacological regulation of telomerase', *Nucleic Acids Research,* 30 (4), pp. 839-865.

Mewes, K., Blanz, J., Freund, S., Ehninger, G. and Zeller, K. (1994) 'Synthesis and structural elucidation of biliary excreted thioether derivatives of mitoxantrone', *Xenobiotica,* 24 (3), pp. 199-213.

Miller, K. G., Liu, L. F. and Englund, P. T. (1981) 'A homogeneous type II DNA topoisomerase from HeLa cell nuclei', *The Journal of Biological Chemistry,* 256 (17), pp. 9334-9339.

Molenaar, C., Teuben, J., Heetebrij, R. J., Tanke, H. J. and Reedijk, J. (2000) 'New insights in the cellular processing of platinum antitumor compounds, using fluorophore-labeled platinum complexes and digital fluorescence microscopy', *JBIC Journal of Biological Inorganic Chemistry,* 5 (5), pp. 655-665.

Monchaud, D., Allain, C. and Teulade-Fichou, M. (2006) 'Development of a fluorescent intercalator displacement assay (G4-FID) for establishing quadruplex-DNA affinity and selectivity of putative ligands', *Bioorganic & Medicinal Chemistry Letters,* 16 (18), pp. 4842-4845.

Monchaud, D., Allain, C., Bertrand, H., Smargiasso, N., Rosu, F., Gabelica, V., De Cian, A., Mergny, J. -. and Teulade-Fichou, M. -. (2008) 'Ligands playing musical chairs with G-quadruplex DNA: A rapid and simple displacement

assay for identifying selective G-quadruplex binders', *Biochimie,* 90 (8), pp. 1207-1223.

Mosmann, T. (1983) 'Rapid colorimetric assay for cellular growth and survival: Application to proliferation and cytotoxicity assays', *Journal of Immunological Methods,* 65 (1–2), pp. 55-63.

Mukherjee, A., Lavery, R., Bagchi, B. and Hynes, J. T. (2008) 'On the molecular mechanism of drug intercalation into DNA: a simulation study of the intercalation pathway, free energy, and DNA structural changes', *Journal of the American Chemical Society,* 130 (30), pp. 9747-9755.

Müller, W. and Crothers, D. M. (1968) 'Studies of the binding of actinomycin and related compounds to DNA', *Journal of Molecular Biology,* 35 (2), pp. 251-290.

Murdock, K., Child, R., Fabio, P., Angier, R. D., Wallace, R. E., Durr, F. E. and Citarella, R. (1979) 'Antitumor agents. 1. 1, 4-Bis [(aminoalkyl) amino]-9, 10-anthracenediones', *Journal of Medicinal Chemistry,* 22 (9), pp. 1024-1030.

Nagy, A., Armatis, P. and Schally, A. V. (1996) 'High yield conversion of doxorubicin to 2-pyrrolinodoxorubicin, an analog 500-1000 times more potent: structure-activity relationship of daunosamine-modified derivatives of doxorubicin', *Proceedings of the National Academy of Sciences of the United States of America,* 93 (6), pp. 2464-2469.

Narayana, N. and Weiss, M. A. (2009) 'Crystallographic analysis of a sex-specific enhancer element: sequence-dependent DNA structure, hydration, and dynamics', *Journal of Molecular Biology,* 385 (2), pp. 469-490.

Neidle, S. and Parkinson, G. (2002) 'Telomere maintenance as a target for anticancer drug discovery', *Nature Reviews Drug Discovery,* 1 (5), pp. 383-393.

Niles, A. L., Moravec, R. A. and Riss, T. L. (2008) 'Update on in vitro cytotoxicity assays for drug development', *Expert Opinion on Drug Discovery,* 3 (6), pp. 655-669.

Noamesi, B. K., Larsson, B. S., Laryea, D. L. and Ullberg, S. (1991) 'Whole-Body Autoradiographic Study on the Distribution of H-3 Cryptolepine in Mice', *Archives Internationales De Pharmacodynamie Et De Therapie,* 313 pp. 5-14.

O'Hagan, D. (2010) 'Fluorine in health care: Organofluorine containing blockbuster drugs', *Journal of Fluorine Chemistry,* 131 (11), pp. 1071-1081.

Ojima, I., Park, Y. H., Sun, C., Fenoglio, I., Appendino, G., Pera, P. and Bernacki, R. J. (1994) 'Structure-Activity Relationships of New Taxoids Derived from 14.beta.-Hydroxy-10-deacetylbaccatin III', *Journal of Medicinal Chemistry,* 37 (10), pp. 1408-1410.

Olajide, O. A., Ajayi, A. M. and Wright, C. W. (2009) 'Anti-inflammatory Properties of Cryptolepine', *Phytotherapy Research,* 23 (10), pp. 1421-1425.

Olajide, O. A., Bhatia, H. S., de Oliveira, A. C. P., Wright, C. W. and Fiebich, B. L. (2013) 'Anti-neuroinflammatory properties of synthetic cryptolepine in human neuroblastoma cells: Possible involvement of NF-κB and p38 MAPK inhibition', *European Journal of Medicinal Chemistry,* 63 (0), pp. 333-339.

Onyeibor, O., Croft, S. L., Dodson, H. I., Feiz-Haddad, M., Kendrick, H., Millington, N. J., Parapini, S., Phillips, R. M., Seville, S., Shnyder, S. D., Taramelli, D. and Wright, C. W. (2005) 'Synthesis of some cryptolepine analogues, assessment of their antimalarial and cytotoxic activities, and consideration of their antimalarial mode of action', *Journal of Medicinal Chemistry,* 48 (7), pp. 2701-2709.

Oyekan, A. O. (1995) 'Cryptolepine-induced vasodilation in the isolated perfused kidney of the rat: role of G-proteins, K+ and Ca2+ channels', *European Journal of Pharmacology,* 285 (1), pp. 1-9.

Palayoor, S. T., Macklis, R. M., Bump, E. A. and Coleman, C. N. (1995) 'Modulation of Radiation-Induced Apoptosis and G2/ M Block in Murine T-Lymphoma Cells', *Radiation Research,* 141 (3), pp. 235-243.

Palchaudhuri, R. and Hergenrother, P. J. (2007a) 'DNA as a target for anticancer compounds: methods to determine the mode of binding and the mechanism of action', *Current Opinion in Biotechnology,* 18 (6), pp. 497-503.

Palchaudhuri, R. and Hergenrother, P. J. (2007b) 'DNA as a target for anticancer compounds: methods to determine the mode of binding and the mechanism of action', *Current Opinion in Biotechnology,* 18 (6), pp. 497-503.

Parkinson, G. N., Lee, M. P. and Neidle, S. (2002) 'Crystal structure of parallel quadruplexes from human telomeric DNA', *Nature,* 417 (6891), pp. 876-880.

Parnell, C. and Woll, P. J. (2003) 'Principles of cancer treatment by chemotherapy', *Surgery (Oxford),* 21 (11), pp. 272-276.

Patrick, G. L. (2013) 'An introduction to medicinal chemistry (section 21. Anticancer agents)', in 'An introduction to medicinal chemistry (section 21. Anticancer agents)', in Oxford university press, pp. 519-575.

Patrick, T. B., Johri, K. K., White, D. H., Bertrand, W. S., Mokhtar, R., Kilbourn, M. R. and Welch, M. J. (1986) 'Replacement of the carboxylic acid function with fluorine', *Canadian Journal of Chemistry,* 64 (1), pp. 138-141.

Pei, R. and Stojanovic, M. N. (2008) 'Study of thiazole orange in aptamer-based dye-displacement assays', *Analytical and Bioanalytical Chemistry,* 390 (4), pp. 1093-1099.

Pinedo, H. M. and Peters, G. F. (1988) 'Fluorouracil: biochemistry and pharmacology.', *Journal of Clinical Oncology,* 6 (10), pp. 1653-1664.

Pogorelcnik, B., Perdih, A. and Solmajer, T. (2013) 'Recent Advances in the Development of Catalytic Inhibitors of Human DNA Topoisomerase II As Novel Anticancer Agents', *Current Medicinal Chemistry,* 20 (5), pp. 694-709.

R˘eha, D., Kabeláč, M., Ryjáček, F., Šponer, J., Šponer, J. E., Elstner, M., Suhai, S. and Hobza, P. (2002) 'Intercalators. 1. Nature of stacking interactions between intercalators (ethidium, daunomycin, ellipticine, and 4', 6-

diaminide-2-phenylindole) and DNA base pairs. Ab initio quantum chemical, density functional theory, and empirical potential study', *Journal of the American Chemical Society,* 124 (13), pp. 3366-3376.

Radl, S., Konvicka, P. and Vachal, P. (2001) 'ChemInform Abstract: A New Approach to the Synthesis of Benzofuro[3,2-b]quinolines, Benzothieno[3,2-b]quinolines and Indolo[3,2-b]quinolines.', *ChemInform,* 32 (2), pp. no-no.

Ragazzon, P. A., Garbett, N. C. and Chaires, J. B. (2007) 'Competition dialysis: A method for the study of structural selective nucleic acid binding', *Methods,* 42 (2), pp. 173-182.

Rai, S. S. and Wolff, J. (1997) 'Vinblastine-Induced Formation of Tubulin Polymers is Electrostatically Regulated and Nucleated', *European Journal of Biochemistry,* 250 (2), pp. 425-431.

Ray, P. and Gambhir, S. S.(2007) 'Noninvasive imaging of molecular events with bioluminescent reporter genes in living subjects', in 'Noninvasive imaging of molecular events with bioluminescent reporter genes in living subjects', in *Reporter genes.* Springer, pp. 131-144.

Reddy, B. S. P., Sondhi, S. M. and Lown, J. W. (1999) 'Synthetic DNA minor groove-binding drugs', *Pharmacology & Therapeutics,* 84 (1), pp. 1-111.

Redshaw, C., Elsegood, M. R., Frese, J. W., Ashby, S., Chao, Y. and Mueller, A. (2012) 'Cellular uptake studies of two hexanuclear, carboxylate bridged, zinc ring structures using fluorescence microscopy', *Chemical Communications,* 48 (53), pp. 6627-6629.

Rischin, D., Webster, L. K., Millward, M. J., Linahan, B. M., Toner, G. C., Woollett, A. M., Morton, C. G. and Bishop, J. F. (1996) 'Cremophor pharmacokinetics in patients receiving 3-, 6-, and 24-hour infusions of paclitaxel', *Journal of the National Cancer Institute,* 88 (18), pp. 1297-1301.

Riss, T., Moravec, R. and Niles, A. (2005) 'Selecting cell-based assays for drug discovery screening', *Cell Notes,* 13 pp. 16-21.

Rivory, L. P. and Robert, J. (1995) 'Molecular, cellular, and clinical aspects of the pharmacology of 20(S)camptothecin and its derivatives', *Pharmacology & Therapeutics,* 68 (2), pp. 269-296.

Roca, J., Ishida, R., Berger, J. M., Andoh, T. and Wang, J. C. (1994) 'Antitumor bisdioxopiperazines inhibit yeast DNA topoisomerase II by trapping the enzyme in the form of a closed protein clamp', *Proceedings of the National Academy of Sciences of the United States of America,* 91 (5), pp. 1781-1785.

Rogojina, A., Gajewski, S., Bahmed, K., Osheroff, N. and Nitiss, J. L.(2012) 'Topoisomerase II Inhibitors: Chemical Biology', in 'Topoisomerase II Inhibitors: Chemical Biology', in *DNA Topoisomerases and Cancer.* Springer, pp. 211-243.

Rubino, F. M. (2001) 'Separation methods for methotrexate, its structural analogues and metabolites', *Journal of Chromatography B: Biomedical Sciences and Applications,* 764 (1–2), pp. 217-254.

Rytting, M. E. (2012) 'Role of L-asparaginase in acute lymphoblastic leukemia: focus on adult patients.', *Blood & Lymphatic Cancer: Targets & Therapy,* 2 pp. 117-124.

Saceda, M., Lippman, M. E., Chambon, P., Lindsey, R. L., Ponglikitmongkol, M., Puente, M. and Martin, M. B. (1988) 'Regulation of the estrogen receptor in MCF-7 cells by estradiol', *Molecular Endocrinology,* 2 (12), pp. 1157-1162.

Salerno, S., Da Settimo, F., Taliani, S., Simorini, F., La Motta, C., Fornaciari, G. and M Marini, A. (2010) 'Recent advances in the development of dual topoisomerase I and II inhibitors as anticancer drugs', *Current Medicinal Chemistry,* 17 (35), pp. 4270-4290.

Sen, D. and Gilbert, W. (1991) 'The structure of telomeric DNA: DNA quadriplex formation', *Current Opinion in Structural Biology,* 1 (3), pp. 435-438.

Sen, D. and Gilbert, W. (1988) 'Formation of parallel four-stranded complexes by guanine-rich motifs in DNA and its implications for meiosis', *Nature,* 334 (6180), pp. 364-366.

Sergent, C., Franco, N., Chapusot, C., Lizard-Nacol, S., Isambert, N., Correia, M. and Chauffert, B. (2002) 'Human colon cancer cells surviving high doses of cisplatin or oxaliplatin in vitro are not defective in DNA mismatch repair proteins', *Cancer Chemotherapy and Pharmacology,* 49 (6), pp. 445-452.

Seville, S., Onyeibor, O., Feiz-haddad, M., Karodia, N., Phillips, R. M. and Wright, C. W. (2003) 'Synthesis, antiplasmodial and cytotoxic activities of some chlorinated cryptolepine analogues and 11-aminocryptolepine.', *Journal of Pharmacy and Pharmacology,* 55 (Supplement), pp. S.32-S.32.

Seville, S., Phillips, R. M., Shnyder, S. D. and Wright, C. W. (2007a) 'Synthesis of cryptolepine analogues as potential bioreducible anticancer agents', *Bioorganic & Medicinal Chemistry,* 15 (19), pp. 6353-6360.

Seville, S., Phillips, R. M., Shnyder, S. D. and Wright, C. W. (2007b) 'Synthesis of cryptolepine analogues as potential bioreducible anticancer agents', *Bioorganic & Medicinal Chemistry,* 15 (19), pp. 6353-6360.

Shao, J., Zhou, B., Chu, B. and Yen, Y. (2006) 'Ribonucleotide reductase inhibitors and future drug design', *Current Cancer Drug Targets,* 6 (5), pp. 409-431.

Silins, E., Copeland, J. and Dillon, P. (2007) 'Qualitative review of serotonin syndrome, ecstasy (MDMA) and the use of other serotonergic substances: hierarchy of risk', *The Australian and New Zealand Journal of Psychiatry,* 41 (8), pp. 649-655.

Sinclair, W. K. (1981) 'Hydroxyurea revisited: A decade of clinical effects studies', *International Journal of Radiation Oncology*Biology*Physics,* 7 (5), pp. 631-637.

Soule, H., Vazquez, J., Long, A., Albert, S. and Brennan, M. (1973) 'A human cell line from a pleural effusion derived from a breast carcinoma', *Journal of the National Cancer Institute,* 51 (5), pp. 1409-1416.

Stahl, S. M. and Felker, A. (2008) 'Monoamine oxidase inhibitors: a modern guide to an unrequited class of antidepressants', *CNS Spectr,* 13 (10), pp. 855-870.

Stuchinskaya, T., Mitchenall, L. A., Schoeffler, A. J., Corbett, K. D., Berger, J. M., Bates, A. D. and Maxwell, A. (2009) 'How Do Type II Topoisomerases Use ATP Hydrolysis to Simplify DNA Topology beyond Equilibrium? Investigating the Relaxation Reaction of Nonsupercoiling Type II Topoisomerases', *Journal of Molecular Biology*, 385 (5), pp. 1397-1408.

Sullivan, J. P. and Wong, J. L. (1977) 'Guanosine-methyldiazonium ion reaction: Variation of methylation product patterns with reaction variables', *Biochimica Et Biophysica Acta (BBA) - Nucleic Acids and Protein Synthesis*, 479 (1), pp. 1-15.

Takeuchi, Y., Chang, M. R., Hashigaki, K., Tashiro, T., Tsuruo, T., Tsukagoshi, S. and Yamato, M. (1992) 'Synthesis and antitumor activity of fused quinoline derivatives. III. Novel N-glycosylamino-indolo[3,2-b]quinolines', *Chemical & Pharmaceutical Bulletin*, 40 (6), pp. 1481-1485.

Tanious, F. A., Veal, J. M., Buczak, H., Ratmeyer, L. S. and Wilson, W. D. (1992) 'DAPI (4', 6-diamidino-2-phenylindole) binds differently to DNA and RNA: minor-groove binding at AT sites and intercalation at AU sites', *Biochemistry*, 31 (12), pp. 3103-3112.

The International Agency for Research on Cancer GLOBOCAN (WHO), 2008, http://www.iarc.fr/en/media-centre/iarcnews/2010/globocan2008.php> (accessed on 22-july-2010).

Tsukidate, K., Yamamoto, K., Snyder, J. and Farber, J. (1993) 'Microtubule antagonists activate programmed cell death (apoptosis) in cultured rat hepatocytes.', *The American Journal of Pathology*, 143 (3), pp. 918-925.

Valentini, A. M., Armentano, R., Pirrelli, M. and Caruso, M. L. (2006) 'Chemotherapeutic agents for colorectal cancer with a defective mismatch repair system: the state of the art.', *Cancer Treatment Reviews,* 32 (8), pp. 607-618.

Van Miert, S., Jonckers, T., Cimanga, K., Maes, L., Maes, B., Lemiere, G., Dommisse, R., Vlietinck, A. and Pieters, L. (2004) 'In vitro inhibition of beta-haematin formation, DNA interactions, antiplasmodial activity, and cytotoxicity of synthetic neocryptolepine derivatives', *Experimental Parasitology,* 108 (3-4), pp. 163-168.

Von Hoff, D. D., Coltman, C. A. and Forseth, B. (1981) 'Activity of mitoxantrone in a human tumor cloning system', *Cancer Research,* 41 (5), pp. 1853-1855.

Waring, M. (1965) 'Complex formation between ethidium bromide and nucleic acids', *Journal of Molecular Biology,* 13 (1), pp. 269-282.

Webster, L., Linsenmeyer, M., Millward, M., Morton, C., Bishop, J. and Woodcock, D. (1993) 'Measurement of cremophor EL following taxol: plasma levels sufficient to reverse drug exclusion mediated by the multidrug-resistant phenotype', *Journal of the National Cancer Institute,* 85 (20), pp. 1685-1690.

Weisenthal, L. and Lippman, M. E. (1985) 'Clonogenic and nonclonogenic in vitro chemosensitivity assays.', *Cancer Treatment Reports,* 69 (6), pp. 615-632.

Wermuth, C. G. (2011) *The practice of medicinal chemistry.* Academic Press.

Weyermann, J., Lochmann, D. and Zimmer, A. (2005) 'A practical note on the use of cytotoxicity assays', *International Journal of Pharmaceutics,* 288 (2), pp. 369-376.

Willcox, M., Bodeker, G., Rasoanaivo, P. and Addae-Kyereme, J. (2004) *Traditional medicinal plants and malaria.* pp 31–140 edn. CRC Press.

Williams, L. D., Egli, M., Gau, Q., Rich, A., Sarma, R. and Sarma, M. (1992) 'DNA intercalation: Helix unwinding and neighbor-exclusion', *Structure & Function,* 1 pp. 107-125.

Wood, A. J., Smith, I. E. and Dowsett, M. (2003) 'Aromatase inhibitors in breast cancer', *New England Journal of Medicine,* 348 (24), pp. 2431-2442.

Wright, C. W., Addae-Kyereme, J., Breen, A. G., Brown, J. E., Cox, M. F., Croft, S. L., Gokcek, Y., Kendrick, H., Phillips, R. M. and Pollet, P. L. (2001) 'Synthesis and evaluation of cryptolepine analogues for their potential as new antimalarial agents', *Journal of Medicinal Chemistry,* 44 (19), pp. 3187-3194.

Wright, C. W. (2007) 'Recent developments in naturally derived antimalarials: cryptolepine analogues', *Journal of Pharmacy and Pharmacology,* 59 (6), pp. 899-904.

Wurdinger, T., Badr, C., Pike, L., de Kleine, R., Weissleder, R., Breakefield, X. O. and Tannous, B. A. (2008) 'A secreted luciferase for ex vivo monitoring of in vivo processes', *Nature Methods,* 5 (2), pp. 171-173.

Xiong, Y. and Sundaralingam, M. (2001) 'Protein–nucleic acid interaction: major groove recognition determinants', *Encyclopedia of Life Sciences(eLS),* pp. 1-8.

Xu, W., Tan, J., Chen, S., Hou, J., Li, D., Huang, Z. and Gu, L. (2011) 'Studies on the binding of 5-N-methylated quindoline derivative to human telomeric G-quadruplex', *Biochemical and Biophysical Research Communications,* 406 (3), pp. 454-458.

Yamato, M., Takeuchi, Y., Chang, M. R., Hashigaki, K., Tsuruo, T., Tashiro, T. and Tsukagoshi, S. (1990) 'Synthesis and antitumor activity of fused quinoline derivatives', *Chemical & Pharmaceutical Bulletin,* 38 (11), pp. 3048-3052.

Yoneda, N. and Fukuhara, T. (1996) 'Facile preparation of aromatic fluorides by deaminative fluorination of aminoarenes using hydrogen fluoride combined with bases', *Tetrahedron,* 52 (1), pp. 23-36.

Zamble, D. B., Mu, D., Reardon, J. T., Sancar, A. and Lippard, S. J. (1996) 'Repair of cisplatin-DNA adducts by the mammalian excision nuclease', *Biochemistry,* 35 (31), pp. 10004-10013.

Zhao, H., Doyle, T. C., Wong, R. J., Cao, Y., Stevenson, D. K., Piwnica-Worms, D. and Contag, C. H. (2004) 'Characterization of coelenterazine analogs for measurements of Renilla luciferase activity in live cells and living animals.', *Molecular Imaging,* 3 (1), pp. 43-54.

Zhou, J. and Yuan, G. (2007) 'Specific Recognition of Human Telomeric G-Quadruplex DNA with Small Molecules and the Conformational Analysis by

ESI Mass Spectrometry and Circular Dichroism Spectropolarimetry', *Chemistry-A European Journal,* 13 (17), pp. 5018-5023.

Zhu, H. and Gooderham, N. J. (May 2006) 'Mechanisms of Induction of Cell Cycle Arrest and Cell Death by Cryptolepine in Human Lung Adenocarcinoma A549 Cells', *Toxicological Sciences,* 91 (1), pp. 132-139.

Zhu, X. Y., Mardenborough, L. G., Li, S., Khan, A., Zhang, W., Fan, P., Jacob, M., Khan, S., Walker, L. and Ablordeppey, S. Y. (2007) 'Synthesis and evaluation of isosteres of N-methyl indolo[3,2-b]-quinoline (cryptolepine) as new antfinfective', *Bioorganic & Medicinal Chemistry,* 15 (2), pp. 686-695.